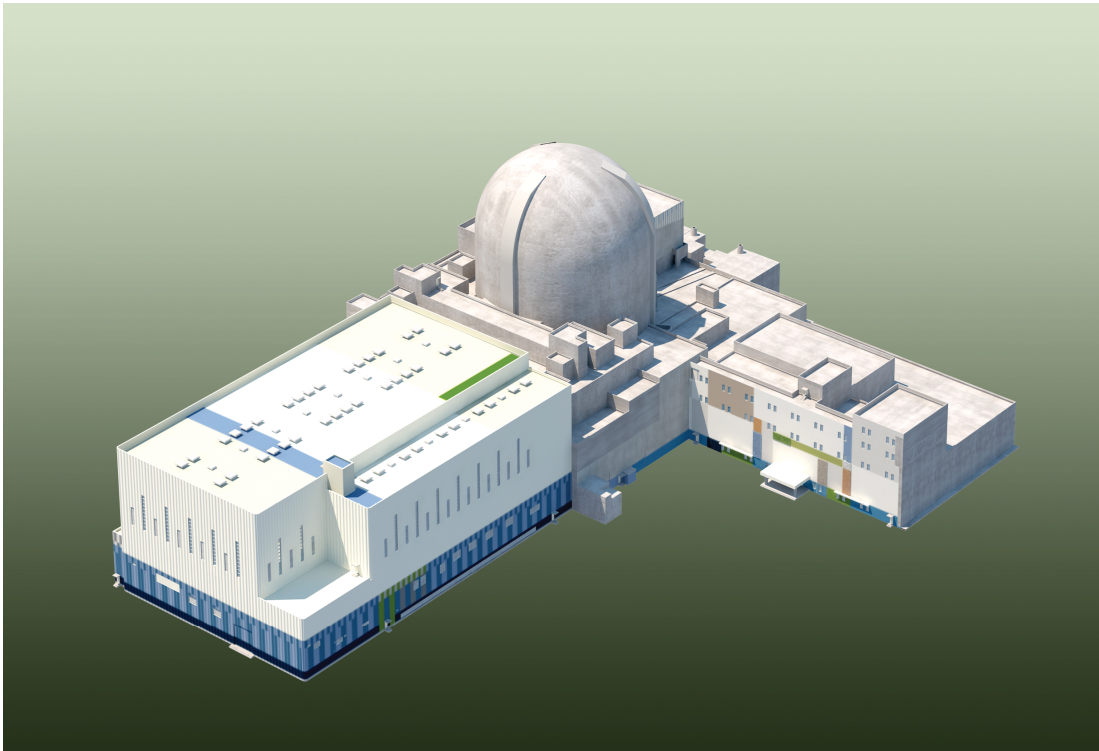


# **KCE-1 Critical Heat Flux Correlation for PLUS7 Thermal Design**

APR1400-F-C-TR-12002-NP-A

April 2017



**KOREA ELECTRIC POWER CORPORATION**



**KOREA HYDRO & NUCLEAR POWER CO., LTD**

Non-Proprietary

## CONTENTS

### SECTION DESCRIPTION

- A Letter from Jeffrey A. Ciocco (NRC) to Han-Gon KIM (KHNP),  
APR1400 FINAL SAFETY EVALUATION FOR TOPICAL REPORT  
APR1400-F-C-TR-12002-P, REVISION 0, "KCE-1 CRITICAL HEAT FLUX  
CORRELATION FOR PLUS7 THERMAL DESIGN," dated on March 22,  
2017.
- B KCE-1 CRITICAL HEAT FLUX CORRELATION FOR PLUS7 FUEL  
DESIGN Topical Report, APR1400-F-C-TR-12002-NP-A
- C Revised Response to 'Request for Additional Information 3-7443, dated March  
25, 2014,' dated on March 2, 2015
- D Revised Response to 'Request for Additional Information 3-7443, dated March  
25, 2014,' on Questions 6, 7, 9, and 17, dated on October 9, 2015

**Non-Proprietary**

**SECTION A**

**Non-Proprietary**

Page intentionally left blank

March 22, 2017

Dr. Han-Gon Kim, Project Manager  
APR1400 Design Certification  
Advanced Reactors Development Laboratory  
Korea Hydro and Nuclear Power Co., Ltd.  
70-1312-gil, Yuseong-daero  
Yuseong-Gu, Daejeon  
305-343 Korea (Republic of)

SUBJECT: APR1400 FINAL SAFETY EVALUATION FOR TOPICAL REPORT  
APR1400-F-C-TR-12002-P, REVISION 0, "KCE-1 CRITICAL HEAT FLUX  
CORRELATION FOR PLUS7 THERMAL DESIGN"

Dear Dr. Kim:

The U.S. Nuclear Regulatory Commission (NRC) staff has prepared a final Topical Report Safety Evaluation (TRSE) for Topical Report APR1400-F-C-TR-12002-P, Revision 0, "KCE-1 Critical Heat Flux Correlation for PLUS7 Thermal Design." This TRSE is also valid for the non-proprietary version of the topical report. This action is supported by the letter dated February 23, 2017 (ADAMS Accession No. ML17053A159), whereby the Advisory Committee on Reactor Safeguards agrees with the NRC staff's conclusions, within the limits and conditions that are specified in the TRSE. This evaluation is in support of the review of the APR1400 design certification application submitted by Korea Hydro and Nuclear Power (KHNP) on December 23, 2014.

The staff requests that KHNP publish the accepted proprietary and non-proprietary versions of this topical report within one month of receipt of this letter. The accepted versions shall incorporate this letter and the enclosed final TRSE after the title page. Also, they must contain historical review information, including NRC requests for additional information and your responses. The accepted versions of the topical report shall include an "-A" (designated accepted) following the report identification number.

If the NRC's criteria or regulations change such that its conclusion that the accepted topical report is invalidated, KHNP and/or the applicant referencing the topical report will be expected either to revise and resubmit its respective documentation or to submit justification for continued applicability of the topical report without revision of the respective documentation.

H. Kim

-2-

If you have any questions or comments concerning this matter, do not hesitate to call. I can be reached at (301) 415-6391 or via e-mail address at [Jeff.Ciocco@nrc.gov](mailto:Jeff.Ciocco@nrc.gov).

Sincerely,

***/RA/***

Jeffrey A. Ciocco, Senior Project Manager  
Licensing Branch 2  
Division of New Reactor Licensing  
Office of New Reactors

Docket No. 52-046

Enclosures:  
As stated

cc w/ encl.: See next page

APR1400 FINAL SAFETY EVALUATION FOR TOPICAL REPORT APR1400-F-C-TR-12002-P, REVISION 0, "KCE-1 CRITICAL HEAT FLUX CORRELATION FOR PLUS7 THERMAL DESIGN" DATE March 22, 2017

**DISTRIBUTION:**

D101	RidsNroLaCSmith	RidsOgcMailCenter Resource
Public	RidsNroLaCSmith	RidsAcrs_MailCTR, Resource
LB2 R/F	GWunder, NRO	RidsNroOd
RidsNroDnrl	JCiocco, NRO	RidsNroDnrlLb2
TechStaff	SHaider, DSRA	JMonninger, NRO
JKaizer, DSRA	RKaras, NRO	SVrahoretis, OGC

**ADAMS Accession Nos.**

**Package – ML17066A244**

**Letter – ML17066A307**

**TSER – ML17066A309**

via email\*

**NRO-002**

<b>OFFICE</b>	DNRL/LB2: PM	DEIA/ARPB: LA	DNRL/LB2: PM
<b>NAME</b>	GWunder	ARedden*	JCiocco
<b>DATE</b>	03 /17/ 2017	03 /13/ 2017	03 /22/ 2017

**OFFICIAL RECORD COPY**

**KHNP Mailing List**

**9/22/2015**

Daegeun Tony Ahn  
Director  
KHNP Washington DC Center  
8100 Boone Blvd, Suite 620  
Vienna, VA 22182

## Email

[kimhg1108@khnp.co.kr](mailto:kimhg1108@khnp.co.kr)  
[hansang.kim@khnp.co.kr](mailto:hansang.kim@khnp.co.kr)  
[dohwan.lee@khnp.co.kr](mailto:dohwan.lee@khnp.co.kr)  
[junghokim@khnp.co.kr](mailto:junghokim@khnp.co.kr)  
[yunho.kim@khnp.co.kr](mailto:yunho.kim@khnp.co.kr)  
[jiyong.oh@khnp.co.kr](mailto:jiyong.oh@khnp.co.kr)  
[ahn.daegeun@khnp.co.kr](mailto:ahn.daegeun@khnp.co.kr),  
[jksuh@khnp.co.kr](mailto:jksuh@khnp.co.kr)  
[hachewung@khnp.co.kr](mailto:hachewung@khnp.co.kr)  
[kang.deogji@khnp.co.kr](mailto:kang.deogji@khnp.co.kr)  
[sunguk.kwon@khnp.co.kr](mailto:sunguk.kwon@khnp.co.kr)  
[ptmaster300@kepco.co.kr](mailto:ptmaster300@kepco.co.kr)

[Han-Gon Kim]  
[Hansang Kim]  
[Do-Hwan Lee]  
[Jung-Ho Kim]  
[Yun Ho Kim]  
[Jiyong Andy Oh]  
[Daegeun Tony Ahn]  
[Jeong Kwan Suh]  
[Che Wung Ha]  
[Deog Ji Kang]  
[Sun Guk Kwon]  
[Hyun Chul Park]

SAFETY EVALUATION BY THE OFFICE OF NEW REACTORS  
LICENSING TOPICAL REPORT APR1400-F-C-TR-12002-P  
“KCE-1 CRITICAL HEAT FLUX CORRELATION FOR PLUS7 THERMAL DESIGN”  
KOREA HYDRO & NUCLEAR POWER CO., LTD.

## CONTENTS

1.0	INTRODUCTION .....	1
2.0	SUMMARY OF THE TOPICAL REPORT .....	2
3.0	REGULATORY BASIS .....	3
4.0	TECHNICAL EVALUATION .....	3
4.1	Background Information .....	3
4.1.1	Departure from Nucleate Boiling (DNB) and Critical Heat Flux (CHF) Correlation .....	3
4.1.2	KCE-1 CHF Correlation for PLUS7 Fuel Design .....	5
4.2	Critical Heat Flux Test Program and Procedures .....	5
4.3	Test Section Heat Losses .....	7
4.4	Spacer and Part-Length Heated Rod Effects .....	8
4.5	Axial Power Profile and Tong Factor.....	9
4.6	Uncertainties in CHF Measurements.....	10
4.7	Statistical Evaluation of 95/95 DNBR Limit.....	12
4.8	Challenges to the Statistical Evaluation of 95/95 DNBR Limit .....	13
4.8.1	Non-conservative Data Trend .....	13
4.8.2	Non-conservative Test Data Sub-region.....	15
4.8.3	Non-conservative Overfitting of the Test Data .....	16
4.8.4	Quantification of the Tong Factor Conservatism.....	17
4.8.5	Remaining Uncertainties in the KCE-1 CHF Correlation DNBR Limit.....	20

4.9	Applicability of the KCE-1 CHF Correlation .....	21
5.0	CONDITIONS AND LIMITATIONS .....	22
6.0	CONCLUSIONS .....	23
7.0	REFERENCES .....	24

**FINAL SAFETY EVALUATION REPORT  
BY THE OFFICE OF NEW REACTORS  
TOPICAL REPORT APR1400-F-C-TR-12002-P, REVISION 0,  
“KCE-1 CRITICAL HEAT FLUX CORRELATION FOR  
PLUS7 THERMAL DESIGN”  
KOREA HYDRO AND NUCLEAR POWER CO., LTD. (KHNP)  
PROJECT NO. 782**

**1.0      Introduction**

By letter dated January 7, 2013 (Ref. 1), Korea Hydro and Nuclear Power Co., Ltd. (KHNP) in conjunction with its affiliate company Korea Electric Power Corporation (KEPCO), submitted Topical Report (TR) Advanced Power Reactor 1400 (APR1400)-F-C-TR-12002-P/NP, Revision 0, “KCE-1 Critical Heat Flux Correlation for Plus7 Thermal Design,” (Ref. 2) to the U.S. Nuclear Regulatory Commission (NRC) for review and approval, in support of its application for design certification of the APR1400 reactor design. The purpose of this topical report is to justify the use of the KCE-1 Critical Heat Flux (CHF) correlation for PLUS7 fuel design for the pressurized water reactor (PWR) application. The TR presented the test data analysis and results for the KCE-1 CHF correlation development, and a description of the CHF test facility and test procedures. The KCE-1 CHF correlation can be applied to the thermal design and plant safety analyses for the PLUS7 fuel design within the approved range of operating parameters. The applicant applied the KCE-1 CHF correlation with the Thermal Hydraulics of a Reactor Core (TORC) subchannel computer code to perform the analyses and results presented in the TR.

The NRC staff started the review of the TR in August 2013, and issued a non-public proprietary request for additional information (RAI), RAI 3-7443 (Ref. 3), with 18 questions regarding the applicant’s analyses, computer codes, test procedures, assumptions, and uncertainties to support its safety review of the TR. A follow-up public meeting was held with the applicant on May 1, 2014 (Ref. 4), at the NRC offices in Rockville, MD, to discuss various proprietary and non-proprietary issues raised by the questions in RAI 3-7443. The non-proprietary meeting presentation made by the applicant is publicly available in the Agencywide Documents Access and Management System (ADAMS) (Ref. 5). The applicant submitted its responses to various RAI 3-7443 questions as Reference 6 (Questions 2, 3, and 5); Reference 7 (Questions 4, 10, 11, 12, and 18); and Reference 8 (Questions 1, 6, 7, 8, 9, 13, 14, 15, 16, and 17). The staff held numerous clarification public teleconferences throughout this process, but there were several issues that could not be resolved. In January 2015, the staff conducted a two-day regulatory audit (Ref. 9) to resolve the outstanding issues regarding the applicant’s RAI responses, and to establish the qualification status of Columbia University’s Heat Transfer Research Facility (HTRF), where the CHF tests were conducted. The audit allowed the staff to review the applicant’s data, calculations, and supporting documents to gain an in-depth understanding of the TR as well as the applicant’s responses to RAI 3-7443. The staff summarized the overall audit findings in an audit report (Ref. 10). As one of the fundamental

outcomes of the audit, the applicant updated and resubmitted its response to RAI 3-7443 (Ref. 11) in March 2015, which did not address several concerns iterated by the staff during the audit. For reasons explained later, the applicant's response to RAI 3-7443, Questions 6, 7, 9, and 17, were still not acceptable to the staff. The staff therefore conducted another public meeting with the applicant on September 3, 2015 (Ref. 12), where the applicant presented supplemental information regarding the KCE-1 CHF correlation to resolve the outstanding technical issues related to these four RAIs. Following the commitments made in the September 3, 2015, public meeting, the applicant revised and resubmitted its responses to the four open RAI questions (RAI 3-7443 Questions 6, 7, 9, and 17) (Ref. 13) in October 2015, to incorporate the supplemental information discussed during the meeting.

This safety evaluation report (SER) documents the NRC staff's review and findings regarding the TR, APR1400-F-C-TR-12002-P, Revision 0. Where appropriate, the staff discussed the response to the RAI 3-7443 questions in this SER. The aspects of the responses to the RAI questions not discussed in this SER were for the NRC staff's information or clarification and were found adequate. Based on its review of the TR, the NRC staff finds that the use of the KCE-1 CHF correlation is acceptable in calculating the CHF for the PLUS7 fuel design, provided that the conditions and limitations specified in Section 5.0 of this SER are met.

## **2.0 Summary of the Topical Report**

The applicant had the CHF tests conducted for PLUS7 fuel at the HTRF at Columbia University in New York, NY. The purpose of the testing was to collect data to develop an applicable CHF correlation for the PLUS7 fuel design. The PLUS7 fuel incorporates an advanced "R" mixing vane grid design. The split mixing vanes attached to the top of the grid strap are intended to improve the heat transfer between the coolant and fuel rods. The PLUS7 fuel CHF tests were performed with two test sections simulating configurations with and without a guide thimble tube. The TR uses the "TS101" designation for the thimble subchannel test section and "TS102" for the matrix subchannel test section without a guide thimble tube, as illustrated by Figures 2-3, "Mid-Grid of Thimble Subchannel Test Section TS101," and 2-4, "Mid-Grid of Matrix Subchannel Test Section TS102," in the TR, respectively. Each test section was composed of a 6x6 heater rod bundle with a fixed heated length of 381 cm (150 in.) and a fixed grid span of 39.9 cm (15.7 in.), which simulated the PLUS7 fuel geometry. All tests were performed with a non-uniform (chopped cosine) axial power distribution and an about [ ]radial power split between hot and cold rods.

The TR describes the CHF tests that the HTRF conducted to support the KCE-1 CHF correlation development. The functional formula of the KCE-1 CHF correlation is identical to the Westinghouse CE-1 CHF correlation. The coefficients of the KCE-1 CHF correlation were determined by a non-linear multiple-regression analysis of the measured CHF data with local fluid conditions in the test sections calculated by using the Westinghouse subchannel thermal-hydraulic analysis code TORC (Ref. 14). The KCE-1 CHF correlation departure from nucleate boiling ratio (DNBR) limit was determined with a 95 percent probability and at a 95 percent confidence level (95/95 DNBR limit). The CHF test data and the statistical methods applied to the correlation development and validation are described in appendices to the TR. The KCE-1

CHF correlation can be applied to the thermal design and plant safety analyses involving PLUS7 fuel.

### **3.0 Regulatory Basis**

General Design Criterion (GDC) 10, "Reactor Design," in Title 10 of the *Code of Federal Regulations* (10 CFR) Part 50, Appendix A "General Design Criteria for Nuclear Power Plants" (Ref. 15), requires that the reactor core and associated coolant, control, and protection systems shall be designed with an appropriate margin to ensure that the specified acceptable fuel design limits (SAFDLs) are not exceeded during any condition of normal operation, including anticipated operational occurrences (AOOs). GDC 10 is relevant to the CHF correlation, as it is used to establish safety-related margins for the fuel and cladding integrity. To ensure compliance with GDC 10, the staff confirmed that the thermal-hydraulic design of the core and the reactor coolant system was accomplished using acceptable analytical methods; is equivalent to or is a justified extrapolation from proven designs; provides adequate margins of safety from conditions that would lead to fuel damage during normal reactor operation and AOOs; and is not susceptible to thermal-hydraulic instability.

NUREG-0800, "Standard Review Plan for the Review of Safety Analysis Reports for Nuclear Power Plants" (Ref. 16) (henceforth, "SRP"), Section 4.4, "Thermal and Hydraulic Design," describes the staff's review process for thermal and hydraulic design applications. One of the acceptance criteria specified in SRP Section 4.4 for the evaluation of fuel design limits ensures that the hot fuel rod in the core does not experience departure from nucleate boiling (DNB) during normal operation or AOOs. This requires addressing the uncertainties in the values of process parameters, core design parameters, calculation methods, and instrumentation in the assessment of thermal margin with at least a 95 percent probability at a 95 percent confidence level. The origin of each uncertainty, such as fabrication uncertainty, computational uncertainty, and measurement uncertainty should be identified. According to Appendix B in SRP Section 4.2, "Fuel System Design," fuel cladding failure is presumed if local heat flux exceeds the thermal design limits.

The regulations in 10 CFR 50.34, "Contents of Applications; Technical Information," require that safety analysis reports (SARs) be submitted that analyze the design and performance of structures, systems, and components provided for the prevention of accidents and mitigation of consequences of accidents. As part of the core reload design process, licensees are responsible for reload safety evaluations to ensure that their safety analyses remain bounding for the design cycle. To confirm that the analyses are bounding, licensees confirm that those key inputs to the safety analyses (e.g., CHF) are conservative with respect to the design cycle.

## 4.0 Technical Evaluation

### 4.1 Background Information

#### 4.1.1 Departure from Nucleate Boiling (DNB) and Critical Heat Flux (CHF) Correlation

Departure from Nucleate Boiling (DNB) occurs when heat flux on a fuel rod surface is increased to the extent that the boiling water flowing past the fuel rod transitions from nucleate boiling to film boiling. This phenomenon causes a dramatic decrease in the heat transfer rate because of the generation of a vapor film on the fuel rod surface when the bubbles coalesce and prevent the water from reaching the surface of the fuel rod. The deterioration in heat transfer because of the DNB forces the fuel rod surface temperature to rise sharply, which may lead to fuel damage. The heat flux which causes the transition from nucleate boiling to film boiling at DNB is known as the Critical Heat Flux (CHF).

In PWRs, DNB is primarily a local phenomenon caused by the bubble crowding on the fuel rod surface. Fuel damage because of DNB is prevented by using rigorous correlations that conservatively predict the CHF to ensure that the peak heat flux in the core during normal reactor operation or an AOO will always remain below the predicted CHF. DNB is determined by CHF correlations that use the local fluid conditions as input. To prevent DNB at a location along the fuel rod, the departure from nucleate boiling ratio (DNBR) is used, which is the ratio of the calculated local CHF to the actual local heat flux during operation under the same fluid conditions, as defined below.

$$DNBR = \frac{q_{CHF|Same\ Location\ and\ Coolant\ Conditions}}{q_{Location}}$$

The DNBR is a measure of how close the actual heat flux is to the calculated CHF. For conservatism, the DNBR should always be greater than 1.0, so that the local heat flux is less than the CHF and the specific fuel rod will not undergo DNB. If the DNBR is greater than 1.0 for all locations in the core, DNB will not occur on any fuel rods, which provides assurance that there will be no fuel failure. If the DNBR is less than or equal to 1.0, the local heat flux is greater than or equal to the CHF, and the specific fuel rod will likely go through DNB. Because of the associated high surface temperatures, it is possible that the fuel rod experiencing the DNB may fail. Therefore, to produce a conservative safety analysis, any fuel rod that experiences DNB is assumed to have failed. When the fuel rod fails, the cladding ruptures and the first fission product barrier is breached. The radioactive nuclides, which were being contained by the cladding, will escape from the fuel rod and will be released into the reactor coolant system. Although fuel failures are undesirable, it is not possible to preclude all failures and therefore nuclear power plants have a cleanup system which can process a limited number of fuel failures.

To avoid the DNB occurrence in the bundle and to ensure that the number of fuel failures will be extremely small and limited to the “clean up” capability of the plant, a minimum DNBR value greater than 1.0 needs to be calculated by accounting for uncertainties and non-conservatism in the empirical CHF correlation, plant parameters, and AOOs. To account for any uncertainties and non-conservatism in the empirical CHF correlation, a one-sided 95/95 DNBR limit is used to bound the correlation’s prediction. The TR presents a statistical analysis to support a 95/95 DNBR limit of 1.124 for the PLUS7 fuel design.

#### **4.1.2 KCE-1 CHF Correlation for PLUS7 Fuel Design**

Many parameters can affect DNB or CHF such as pressure, mass flux, quality, heated length, heat flux distribution, rod bundle shape, grid spacers, wall superheat, flow memory, flow pattern, bubble size/population, bubble layer thickness, and flow instability (Ref. 17). Because of the complex nature of the DNB phenomenon, CHF correlations have empirical functional forms and are based on experimentally measured values of the CHF and CHF parameters for the specific fuel design. The functional formula of the KCE-1 CHF correlation for the PLUS7 fuel design is identical to the CE-1 CHF correlation. As presented by the applicant in the TR, the KCE-1 CHF correlation includes the following parameters: pressure, local mass flux, local quality, heated hydraulic diameter ratio of the subchannel to the subchannel matrix, latent heat of vaporization, and the Tong factor to account for the non-uniform axial power distribution. The application of the Tong factor additionally requires the knowledge of non-uniform axial heat flux distribution and heated length from the section inlet to the CHF location. The applicant determined the eight empirical coefficients in the KCE-1 CHF correlation by a non-linear multiple-regression analysis of the measured CHF data with local fluid conditions calculated by using the subchannel analysis code TORC.

#### **4.2 Critical Heat Flux Test Program and Procedures**

The CHF tests for the PLUS7 fuel geometry were conducted at Columbia University’s HTRF in New York, NY, which was in operation from 1951 to 2003, and collected an extensive amount of DNB data relevant to nuclear reactor fuel design. Over the years, several applicants used data from the HTRF facility and subjected the data to quality assurance (QA) review, and the NRC staff reviewed and certified the resulting CHF correlations. During the January 2015, audit (Ref. 10), the applicant provided a description of the QA Program (QAP) used at the HTRF test facility for the CHF tests for the PLUS7 fuel design. The documents (Refs. 18, 19, 20, and 21) furnished during the audit showed details of the [

]Reference 18 described [

] It confirmed that the facility

had mandated a QAP in conformance with applicable requirements of the latest edition of ANSI/ASME NQA-1, “Quality Assurance Program Requirements for Nuclear Facilities” with addenda, which was documented in the HTRF/QAP, Revision 5, issued March 1998. As the CHF tests were safety related, the HTRF qualified the engineering design and materials supplied to meet the necessary QA requirements to ensure that the CHF data conform to the applicable requirements of 10 CFR Part 50, Appendix B, “Quality Assurance Criteria for Nuclear Power Plants and Reprocessing Plants.” Reference 19 refers to a [

performed by [ (Ref. 20) that documents an audit of the HTRF

]10 CFR Part 50, Appendix B, and 10 CFR Part 21, "Reporting of Defects and Noncompliance." During the January 21–22, 2015 NRC audit, the staff was also informed that, as the Department of Energy (DOE) sponsored several HTRF research programs, DOE also conducted an audit of the facility on an annual basis.

The applicant did not describe in the TR whether or how frequently the instrumentation calibrations were performed at this test facility. In RAI 3-7443, Question 4, the staff asked the applicant about the test section flow measuring instrumentation details and calibration. Considering the significance of accurately measuring the mass flow rate and inlet/outlet conditions in the overall computation of the CHF and its subsequent design implications, it is important to establish that the calibration of related instruments were performed following an approved test procedure and QAP.

The staff noted that Reference 18 mentions that [

]water temperature measurements at both the inlet and outlet of the test sections by using calibrated platinum resistance temperature detectors (RTD) and calibrated iron-constantan thermocouple (Type J); and pressure measurements made at the beginning and the end of the heated length. No void fraction and quality measurements were made during the PLUS7 CHF tests. The reported local quality is based on the lumped parameter calculations using TORC. The applicant also provided a detailed description of a typical testing day that stressed the necessity to achieve steady state before the CHF data point was taken. The applicant explained how the water layer between outside the channels and the acrylic glass wall would help achieve steady state and curb the heat losses to the surroundings. Repeatability of the data was assured at the beginning and end of every day. In its updated response to RAI 3-7443, Question 4, (Ref. 11), along with the QA documents reviewed by the staff during the January 21–22, 2015 NRC audit, the applicant explained the instrumentation, redundancy and diversity applied to measurements. During the audit, the staff examined Reference 19, which showed that [

]Instrumentation and measuring devices were calibrated against devices traceable to the National Institute of Standards and Technology (NIST) at frequencies determined by the responsible engineers. The document also included the calibration records and calibration certificates of the measuring instruments used in the CHF test loop. Therefore, the staff concludes that **RAI 3-7443, Question 4, is resolved and closed.**

During the audit, the applicant explained that measurements of the thermocouples attached to the rods were only used to identify CHF occurrence qualitatively and were not used for any other purpose. As reported in the TR, the CHF point was confirmed to occur during the testing when incrementally increasing the total power led to a sudden temperature excursion of

5 to 15 °C (10 to 30 °F) inside the heater rods. When the temperature excursion was minimal, the HTRF obtained additional confirmation of the validity of the CHF point by observing a characteristic temperature decay with power reduction, as the CHF zone was rewetted. In its response to RAI 3-7443, Question 2 (Ref. 6), the applicant cited Reference 23 to corroborate the CHF point confirmation criteria. Based on the technical discussion during the audit, the information provided in the RAI response, and the supporting reference, the staff concluded that the applicant justified the CHF identification criteria, and considers **RAI 3-7443, Question 2, resolved and closed**. The applicant's response to RAI 3-7443, Question 3 (Ref. 6), clarified that the asymmetrical configuration of the seven thermocouples installed axially to measure the wall temperature along the 381 cm (150 in.) long heated length between the beginning of heated length (BOHL) and end of heated length (EOHL), posed no challenges to CHF identification. The applicant clarified that with a symmetric cosine axial power distribution applied to PLUS7 CHF tests, all CHF locations are downstream of the peak power for the test section with uniformly arranged spacer grids. That is why more thermocouples were installed in the upper part of the heated length. Figure 3-1, "As-measured CHF elevations for PLUS7 CHF test," in the RAI response shows that all CHF locations for PLUS7 fuel are at [ ] i.e., past the middle of the heated length. Since the CHF locations were at the thermocouples located past the middle of heated length, the asymmetrical configuration was appropriate as it gathered more information where CHF was expected. Therefore, the staff considers **RAI 3-7443, Question 3, resolved and closed**.

#### **4.3 Test Section Heat Losses**

In RAI 3-7443, Question 1, the staff asked the applicant to demonstrate that the heat losses from the CHF test section were duly accounted for in its CHF test data for the entire range of the tested bundle power. The applicant was expected to offer conservative estimates of the loss of generated heat that would fail to reflect in the local fluid conditions because of convection to the ambient or through axial conduction to the rod's end. Ignoring the heat losses from the test section would be non-conservative, as it would make CHF look higher than it actually is. The RAI response described, and the staff confirmed during the audit (Ref. 10), that a [ ] heat balance acceptance criterion was followed based on the [ ] (Ref. 18). However, this did not address the staff's concern that the overall heat balance was not performed for each CHF data point and was rather tested only under subcooled conditions at [ ]

[ ] conditions. The staff expected that these test conditions would involve much smaller heat losses than in the CHF test range used for the KCE-1 correlation development that involves bundle powers up to an order magnitude higher, inlet temperatures up to [ ] [ ] flow rates up to [ ] and pressures up to [ ]

During the audit, the applicant presented a bounding heat loss analysis that showed that even though the bundle power increased from [ ] in the PLUS7 test range, the inlet water temperature increased from [ ] Assuming a [ ] the resulting temperature difference

between the section inlet flow temperature and the ambient temperature increased by [ ]  
] The applicant stated that as the heat loss would conservatively be proportional to the temperature difference between the water flowing through the heated section and the ambient, the rise in input electrical power from the minimum to the maximum [ ] during testing outpaces the corresponding rise in heat losses. The staff concludes that this shows that as the electrical power input increases, even though the heat loss from the test section would increase, its proportion relative to the input power would actually decrease, which makes the [ ] heat loss acceptance criterion observed at the minimum bundle power to be bounding for the entire domain of KCE-1 CHF test conditions. The staff further notes that the maximum heat losses from the measured electrical power at the direct current (DC) generator terminals (Bbpwr) and at the test section inlet and outlet bus (Tspwr) were [ ]

] The mean values were [ ] respectively. The difference between the two heat losses corresponds to the loop components that are not a part of the heated test section. The applicant conservatively factored the heat loss from the test section into the CHF data reduction through a heat-input correction factor that was a function of the inlet water temperature, which allowed the measured CHF values to be based on the rise in fluid enthalpy through the test section. This eliminated the heat-loss related bias from the CHF test data. The applicant considered the deviation between the correction factor and the measured value in estimating the overall CHF measurement uncertainty, as addressed in its response to RAI 3-7443, Question 14 (Ref. 8). The applicant resubmitted the RAI response (Ref. 11) to justify the applicability of the [ ] heat loss acceptance criterion and to show that the heat losses measured at the lowest input power are bounding. Accordingly, the staff considers **RAI 3-7443, Question 1, to be resolved and closed.**

The staff issued RAI 3-7443, Question 5, to ask the applicant to describe how the overall bundle power was determined, as it was not clear from the TR. In its RAI 3-7443, Question 5, responses (Refs. 6 and 11), the applicant described that the HTRF obtained the bundle power (Tspwr) from the measured bus-to-bus power (Bbpwr) using a voltage correction factor that was derived from the measured bus-to-bus voltage and the test section voltage. Current metering/readouts for protection/control/test operation were provided by switchboard shunts and were recorded by the data acquisition system. Measurements of voltages were made between the two ends of heater rod (bus-to-bus voltage), and between the bottom end of the copper end pieces and the tip of the top nickel piece (connecting through top nickel plate) between the test section inlet and outlet (test section voltage). These voltages are conditioned through precision resistor divider networks and amplifiers for entry into the data acquisition system and readout in the control room. The HTRF maximum value of overall bundle power was 12 MW (240 Volt\*50,000 Ampere). Based on the description provided, the staff considers **RAI 3-7443, Question 5, to be resolved and closed.**

#### **4.4 Spacer and Part-Length Heated Rod Effects**

The HTRF conducted all CHF tests with a constant heated length of the rod (381 cm (150 in.)) and a constant grid spacing (39.9 cm (15.7 in.)). In RAI 3-7443, Question 12, the staff asked the applicant to explain whether the lack of heated length and grid spacing parameters in the

KCE-1 correlation would affect its applicability to the actual PLUS7 fuel bundle safety analyses. During the testing conducted for some other CHF correlations, heated length and grid spacing were also varied and duly accounted for in the resulting CHF correlation using additional terms. In its response to RAI 3-7443, Question 12 (Ref. 7), the applicant responded that the KCE-1 correlation was developed by using the CHF data from test sections with the same axial geometry as PLUS7 fuel as described in Table 2-1, "Characteristics of Geometrical Configuration of CHF Test Sections," and illustrated in Figure 2-9, "Axial Geometrical Configuration of Test Section," of the TR. This means that the effects of grid spacing and heated length on CHF were inherently included in the measured data, and thus were captured in the KCE-1 correlation. In addition, the KCE-1 correlation is limited to the PLUS7 geometry with fixed grid spacing and heated length. Based on these facts, there is no need for heated length and grid spacing parameters in the KCE-1 correlation, and the staff concludes that the response is acceptable and **RAI 3-7443, Question 12, is resolved and closed.**

#### **4.5 Axial Power Profile and Tong Factor**

The CHF test data for the PLUS7 fuel geometry were obtained by using a non-uniform axial power distribution (i.e., a symmetric chopped cosine power profile with a peak of 1.475 at the middle of the heated length). The test sections were also designed with a varying radial power distribution such that the highest power rods were in the middle of the bundle. In RAI 3-7443, Question 6, the staff asked the applicant to explain the appropriateness of testing a single axial profile and why the inlet/bottom or outlet/top peaked power profiles were not included in the test matrix. In its response to RAI 3-7443, Question 6 (Ref. 8), the applicant described the tested symmetric cosine axial power distribution as the typical axial power profile resulting from the two-dimensional neutron diffusion equation for the finite cylinder geometry (Ref. 24) representing the PLUS7 fuel design. The response additionally cited that the [

] The response also clarified the application of the Tong factor ( $F_c$ ), defined by the following equation,

$$F_c = \frac{q_{CHF,EU}}{q_{CHF,NU,measured}}$$

The Tong factor is meant to account for different axial power shapes. Table A-3, "Test Data Groups Excluded during KCE-1 CHF Correlation Development," in the updated RAI 3-7443, Question 6, response (Ref. 11), shows that [

] which is consistent with the response to RAI 3-7443, Question 3 (Ref. 6), which shows that all CHF points were observed at thermocouples that are downstream of the axial flux peak location. As no testing of the PLUS7 fuel geometry was conducted with a uniform axial power distribution, no Tong factor could be customized by the applicant for the KCE-1 CHF correlation. Such an optimization of the Tong factor for the PLUS7 fuel split vane mixing grid geometries would

require testing both uniform and non-uniform axial power distributions with and without the guide thimble tube, but it was not done for the tested PLUS7 fuel geometry. In RAI 3-7443, Question 7, the staff also asked the applicant to justify using the standard Tong factor with the KCE-1 correlation to predict the CHF for the PLUS7 fuel geometry. In its response to RAI 3-7443, Question 7 (Ref. 11), the applicant stated that the standard Tong factor was applicable to design and safety analyses of the PLUS7 core with the KCE-1 correlation based on its non-dependency on fuel design. The Tong factor does not have any terms related to fuel geometry and solely depends upon the axial flux distribution and the resulting local quality at the CHF location for the given mass flux. The applicant also provided citations (Refs. 26 and 27) to demonstrate that the standard Tong factor used by the KCE-1 correlation has been shown in previous CHF test programs to conservatively apply to various fuel designs and the corresponding CHF correlations under similar application environments as that of the KCE-1 CHF correlation. References 26 and 27 show that applying the standard Tong factor with the CE-1 CHF correlation had predicted CHF conservatively in several axially non-uniformly heated rod bundles. The staff, nevertheless, asked the applicant to qualify the statements by demonstrating additional conservatism in the KCE-1 correlation for the typical non-tested heat flux profiles to cover the actual axial power distribution experienced during the operation of PLUS7 fuel cores. In its final response to Question 6 (Ref. 13), the applicant stated that the

[ ] The range of Tong factor [ ] in the KCE-1 CHF correlation application using the PLUS7 tested cosine shape is shown in Figure 6-2, "Distribution of M/P versus Tong Factor Fc (Application Database)." The Tong factor range from the KCE-1 cosine tests is [ ] the range covered in previous CE-1 CHF tests with several different axial power shapes (Ref. 27).

The applicant further stated that while other shapes may produce more limiting DNBR, the Tong factor of the tested cosine shape is more limiting. The applicant demonstrated this by considering four classic power shapes: top-peaked, double-humped, symmetric cosine, and bottom-peaked. Figures 6-3, "Axial Behavior of KCE-1 DNBR for Each Power Shape," and 6-4, "Axial Behavior of Fc for Each Power Shape," in the response demonstrate that the double-humped and top-peaked shape could be more limiting for DNBR, but its Tong factors are [ ]

[ ] While the bottom-peaked shape has higher Tong factors than that of the cosine shape within the test range, the staff understands that it is rarely limiting as there is a high degree of sub-cooling and low quality which generally preclude CHF. Thus, the minimum DNBR from bottom-peaked shapes is typically much higher (i.e., more conservatively predicated than that from the top-peaked or cosine shapes). The staff recognizes that the likelihood of having a CHF at the start of the bundle is remote, and further believes that the KCE-1 correlation would conservatively predict the CHF in that region. Based on the information provided by the applicant, the staff concluded that using a symmetric cosine profile as the non-uniform axial power distribution of the PLUS7 fuel geometry was adequate for its CHF testing. Therefore, the applicant's response is acceptable, and **RAI 3-7443, Question 6, is resolved and closed.**

#### 4.6 Uncertainties in CHF Measurements

SRP Section 4.4, Acceptance Criterion 1, deals with various uncertainties involved in the CHF measurement and correlation development, such as fabrication uncertainty, computational uncertainty, and measurement uncertainty because of instrumentation. As the applicant supplied no discussion about these uncertainties in the TR, in RAI 3-7443, Question 14, the staff asked the applicant to provide the information. In its response to RAI 3-7443, Question 14 (Ref. 8), the applicant provided a detailed listing of the measurement uncertainties of the instrumentation employed in the CHF tests in Table 14-1, "Measurement Uncertainties for PLUS7 CHF Tests," extracted from Reference 28. However, the applicant did not provide any information about any computational uncertainties or the overall uncertainty in the measured CHF. During the audit, the applicant offered a detailed overview of the uncertainties involved in the CHF measurements. The applicant also explained that [

] During the audit, the applicant also explained that they also had accounted for an "operational" uncertainty in CHF measurement by keeping the maximum incremental rise in heat flux at [ ] The applicant explained that as the directly measured values of the electrical power input to the test section were used to normalize the heat flux profile and subchannel code TORC was not used for this purpose. The staff accepted that there are no computational uncertainties involved in the overall CHF measurement and data reduction.

In its updated response to RAI 3-7443, Question 14 (Ref. 11), the applicant also supplied an overall uncertainty analysis of the CHF measurement that accounted for the uncertainties involved in power measurement, temperature-dependent voltage correction, incremental heat flux stepping to approach CHF, tube wall thickness, and surface area. The applicant concluded that a maximum [ ] uncertainty in the measured CHF value based on [

] In its updated RAI response, the applicant also stated that the overall uncertainty in the measured CHF data is inherently captured in the 95/95 DNBR limit, which is determined by the measured-to-predicted (M/P) CHF values statistics. The staff concluded that the applicant provided sufficient information about the experimental uncertainties involved and established the overall uncertainty in CHF measurement, as requested by the staff. The staff found the applicant's treatment of the uncertainties, and the updated response to RAI 3-7443, Question 14 (Ref. 11), acceptable. The staff considers **RAI 3-7443, Question 14, to be resolved and closed.**

Using a CHF correlation for reactor core analysis requires nodalizing the core geometry to solve mass, momentum, and energy conservations across the core for the given heat flux profile and the inlet flow rate while accounting for the local transport properties of the coolant. This is done by using a subchannel analysis computer code such as TORC. Given the initial and boundary conditions of a transient from the system's code, the subchannel code can calculate the local

fluid conditions in the core to use with the correlation to calculate the CHF at those conditions. During reactor operation, the calculated CHF is divided by the local heat flux to calculate the operating DNBR value for technical specification monitoring purposes. The applicant determined the coefficients of the KCE-1 CHF correlation by a non-linear multiple regression analysis of the measured CHF data along with the local fluid conditions calculated by using TORC. The main input data used for TORC are summarized in Table 4-1, "Main Input Data of the TORC Model for CHF Test Data Analysis," of the TR but no discussion of the selection of inputs was provided by the applicant. In RAI 3-7443, Question 15, the staff asked the applicant to provide justifications and sources for its TORC input selections. In its final response to RAI 3-7443, Question 15 (Ref. 11), the applicant stated that the TORC input parameters given in Table 4-1 of the TR were [

]The response described various TORC input parameters and its adjustments to reflect the design characteristics of PLUS7 fuel. Table 15-1, "TORC Input Data Consistency with Design Constitutive Relations," in the response supplied justifications for using various TORC input parameters and its consistency with the design constitutive relations used in TORC to model various single-phase and two-phase heat transfer and fluid flow characteristics. Table 15-2, "TORC Design Constitutive Relations and Applicable Ranges," showed that the CHF data are taken at conditions that fall within the applicable range of the TORC design constitutive relations. Accordingly, the staff accepts the applicant's use of the TORC input data summarized in Table 4-1 of the TR. Therefore, **RAI 3-7443, Question 15, is resolved and closed.**

TORC is the only subchannel code that was used for the KCE-1 CHF correlation development. However, the TR mentioned that the KCE-1 CHF correlation can also be used with a different subchannel code, CETOP-D. The staff issued RAI 3-7443, Question 16, to inquire about the differences between the two codes, especially how they would calculate the local fluid conditions in the subchannels. According to the initial RAI 3-7443, Question 16, response (Ref. 8), the CETOP-D subchannel code used a different model to calculate the transport properties and a different numerical scheme to solve the conservation equations than the TORC code. During the audit, the staff asked for the justification of using the KCE-1 CHF correlation with CETOP-D code, as its different transport properties module and different numerical scheme may entail computational uncertainties potentially warranting additional non-conservatism in the 95/95 DNBR limit. The staff stressed that an application of the CETOP-D code for the design and safety analyses with the KCE-1 CHF correlation would require an assurance that the MDNBR calculated by CETOP-D shall always be bounded by the MDNBR calculated by TORC at the same boundary conditions. In its updated response to RAI 3-7443, Question 16 (Ref. 11), the applicant agreed to delete all references to CETOP-D from the TR and limit the application of the KCE-1 CHF correlation to TORC. As discussed during the audit and reflected by the updated response to RAI 3-7443, Question 16, the application of the KCE-1 CHF correlation is limited to the PLUS7 fuel geometry with the TORC subchannel computer code. The staff included a limitation in Section 5.0 of this safety evaluation to clarify that the use of the KCE-1 correlation with any other subchannel code will require additional review by the NRC. The staff considers **RAI 3-7443, Question 16, to be resolved and closed.**

#### **4.7 Statistical Evaluation of 95/95 DNBR Limit**

The applicant considered the following topics for the individual and collective statistical treatment of the M/P CHF ratios for various test data groups within and across TS101 (thimble subchannel test section) and TS102 (matrix subchannel test section) datasets: data groups comparison, treatment of outliers, normal distribution, homogeneity of variance and means, and the 95/95 DNBR limit. The applicant used standard statistical tests, including the D' Normality test at the 95-percent confidence level for groups with more than 50 data points. The applicant performed the Bartlett test (homogeneity of variance), and Unpaired *t* test (homogeneity of means) to test whether the data groups used for the correlation development could be pooled. The applicant performed the non-parametric Wilcoxon-Mann-Whitney test to test the null hypothesis that all the data of test sections TS101 and TS102 were sampled out of the same population. The results of these tests were provided in Tables 5-1 and 5-2, and the applicant provided brief descriptions of the statistical tests in TR Appendix B.

The DNBR limit which meets the 95/95 acceptance criterion, was determined by using Owen's one-sided tolerance limit method (Ref. 29). Use of this method has been previously approved by the NRC (Ref. 30). The general equation for Owen's method is as follows:

$$Limit_{95/95\_DNBR} = \frac{1}{\frac{\bar{M}}{P} - K_{95/95} \cdot \sigma}$$

Where

$\frac{\bar{M}}{P}$  is the test population mean of the measured-to-predicted CHF ratios.

$\sigma$  is the effective standard deviation of all the M/P data.

$K_{95/95}$  is a tolerance multiplier which provides the 95/95 probability/confidence level, and is a function of the effective degrees of freedom in the test series.

#### **4.8 Challenges to the Statistical Evaluation of 95/95 DNBR Limit**

During the review, the NRC staff identified multiple challenges to the applicant's proposed 95/95 DNBR limit of 1.124. These challenges included a non-conservative data trend at low pressures; the existence of a non-conservative sub-region around 12.07 MPa (1,750 psia); and the generation of the 95/95 DNBR limit using only training data but no validation data. The applicant had not accounted for these three non-conservatisms in the development of the KCE-1 CHF correlation. In addition, the applicant could not quantify the magnitude of the conservatism gained by its specific use of the Tong factor to possibly cover the three non-conservatisms. These staff concerns were expressed in RAI 3-7443, Questions 6, 7, 9, and 17 (Ref. 3). The issues could not be resolved by the earliest RAI responses (Ref. 8), audit (Ref. 10), and the post-audit response update (Ref. 11). A discussion to resolve these took

place in another public meeting with the applicant (Ref. 12). The issues were resolved with a subsequent RAI response revision (Ref. 13), as described in the following sections.

#### **4.8.1 Non-Conservative Data Trend**

SRP Section 4.4 outlines the DNB acceptance criterion to provide assurance that there is at least a 95-percent probability at a 95-percent confidence level that the hot fuel rod in the core does not experience a DNB or transition condition during normal operation or AOOs. The calculation of a single 95/95 DNBR limit to bound the overall uncertainty of a CHF correlation is predicated on three statistical assumptions: (1) normality, (2) homoscedasticity, and (3) independence. Of these three assumptions, the staff considered the assumption of independence the most important. Statistical independence implies that random sampling can represent the underlying population that comprises mutually independent and identically distributed random variables that have the same probability distribution. This means that an element in the sequence is independent of the random variables that came before it. In general, when the probability distribution of one observation is affected by the level of another, the observations are said to be statistically dependent (Ref. 31). Based on Figure 5-3, "95/95 DNBR Limits for Each Data Group," of the TR, the staff concluded that the assumption of independence may not hold as the KCE-1 CHF correlation does not behave consistently throughout the applied pressure range of 9.62–16.65 MPa (1,395–2,415 psia), and its uncertainty is sensitive to system pressure. The staff noted that the five pressure datasets in Figure 5-3 used in the correlation development seem to be from four different populations, and there is a distinct non-conservative trend of decreasing predictive capability with pressures from 15.17 MPa (2,200 psia) to 12.07 MPa (1,750 psia). While the trend in the M/P values has clearly reversed by the low pressures around 9.62 MPa (1,395 psia), it is not apparent how far the trend continued in the empty region between 9.62 to 12.07 MPa (1,395–1,750 psia) before reversing. The staff also noted that no data are available within the 9.62–12.07 MPa (1,395–1,750 psia) range to evaluate the magnitude of the non-conservatism associated with the non-conservative trend in the data at low pressures. In RAI 3-7443, Question 8, the staff asked the applicant to justify the use of a single statistical 95/95 DNBR limit to bound the KCE-1 CHF correlation over its entire application domain, primarily focusing on the non-conservative data trend between 9.62 and 12.07 MPa (1,395 and 1,750 psia). In its earlier response to RAI 3-7443, Question 8 (Ref. 8), the applicant did not offer any justification for the use of KCE-1 correlation in that range. The issue was discussed in detail at the audit and the applicant informed the staff that it planned to address the non-conservative data trend by excluding the low pressure region of 9.62-12.07 MPa (1395–1750 psia) from the applicable range of the KCE-1 CHF correlation and limiting the applicable range to 12.07–16.65 MPa (1750–2415 psia). The NRC staff would find this resolution acceptable, however, the applicant's post-audit response to RAI 3-7443, Question 8 (Ref. 11), did not reflect the commitment for reduced applicable pressure range. Table 18-1, "Range of AOO Design Analysis for APR1400," in the response to RAI 3-7443, Question 18 (Ref. 11), still showed the KCE-1 CHF correlation applicable pressure range to be 9.62–16.65 MPa (1,395–2,415 psia). Therefore, the NRC staff has formalized a limitation on the use of the KCE-1 CHF correlation that includes the modified pressure range of 12.1–16.7 MPa (1,750–2,415 psia), as documented in Section 5.0 of the present SER. The staff also concludes that there were no other significant non-conservative trends in the M/P CHF

data as a function of the KCE-1 correlation variables. The reduced pressure range has allowed the staff to consider **RAI 3-7443, Question 8, to be resolved and closed.**

The M/P CHF ratios of all test data were plotted for system pressure, local mass flux, local quality, and equivalent heated diameter ratio in Figure 5-3, "Distribution of M/P versus System Pressure," through Figure 5-6, "Distribution of M/P versus Equivalent Heated Diameter Ratio," of the TR, respectively. Figure 4-1, "System Pressure versus Average Heat Flux of Test Section," through Figure 4-3, "Inlet Mass Flux versus Average Heat Flux of Test Section," provide similar plots for bundle average heat flux data. However, the TR does not provide the corresponding plots of the measured CHF data. In RAI 3-7443, Question 11, the staff asked the applicant to supply the corresponding plots to identify any adverse and non-linear trends in the measured CHF data. In its response to RAI 3-7443, Question 11 (Ref. 11), the applicant provided the corresponding plots for pressure, local mass flux, and equivalent heated diameter ratio. The applicant supplied the plot for local quality as a part of its response to RAI 3-7443, Question 10. The staff did not observe any adverse or non-linear trends for these plots of the measured CHF data. Therefore, the staff considers **RAI 3-7443, Question 10 and Question 11, to be resolved and closed.**

#### **4.8.2 Non-Conservative Test Data Sub-Region**

One important assumption commonly made for CHF correlations is that the predictive behavior is consistent over the entire application domain when they are used in reactor safety analysis. The very notion of 95/95 statistics presumes that any error associated with the prediction of a CHF correlation must be random and uniformly distributed over the entire application domain of the correlation, which is defined by the limited ranges of their input predictor variables. The staff tested the validity of the assumption for the KCE-1 CHF correlation by identifying any non-conservative sub-regions in the application domain. As the correlation's predictive capability would be degraded in non-conservative sub-regions, its existence may impair the reactor safety analysis. The NRC staff used the method proposed by Kaizer (Ref. 32), and identified a non-conservative sub-region at pressures near 12.07 MPa (1,750 psia), qualities near 0.1, and local mass fluxes near 2  $\text{Mlb}_m/\text{hr-ft}^2$ , and this was the technical basis for RAI 3-7443, Question 9. The staff's method to identify the sub-region is a multidimensional approach capable of determining whether the CHF correlation's predictive behavior is likely to be because of random effects or because of degraded predictive capability. Because of a higher concentration of the non-conservative M/P CHF data points in the identified sub-region, mainly clustered around 12.07 MPa (1,750 psia), the KCE-1 correlation's predictive capability was degraded below what would have been justified by the 95/95 DNBR limit.

During the audit, the staff asked the applicant to quantify the margin in the 95/95 DNBR limit required to accommodate the non-conservative sub-region, so that the staff could understand how much of the margin gained in the DNBR limit by the Tong factor usage was consumed by the non-conservative sub-region. The non-conservative sub-region identified by the staff contains a higher than expected number of M/P points that fell below the 95/95 DNBR limit of 1.124 than can be explained by random chance. In Table A-2, "Test Data Groups Excluded during KCE-1 CHF Correlation Development," of the TR, seven points fall below M/P of [ ]

that corresponds to DNBR of 1.124. Six out of those seven points correspond to 12.07 MPa (1,750 psia) pressure. In its updated response to RAI 3-7443, Question 9 (Ref. 11), the applicant did not articulate a justification for the use of the KCE-1 correlation in this sub-region. However, during the September 3, 2015, public meeting (Ref. 12) and through the subsequent RAI response (Ref. 13), the applicant emphasized that the number of M/P values below the 95/95 DNBR limit in the identified non-conservative sub-region near 12.07 MPa (1,750 psia) was based on the correlation development database that [

] The upper part of Table 5-4, “KCE-1 CHF Correlation Statistical Data per Local Fluid Condition Extraction Method,” of the TR shows the DNBR limits of 1.124 and [ ] for the TS101 and TS102 datasets, respectively. Further, the staff noted that the number of M/P values below the 95/95 DNBR limit is reduced and the DNBR limit is reduced to [ ] when [ ] as shown in the lower part of Table 5-4 of the TR. This shows that [ ] as factored in the DNBR limit of 1.124 is conservative. Table 5-4 also shows that the DNBR limit of 1.124 for the TS101 dataset for thimble subchannel test section is at least [ ] more conservative than the DNBR limit of [ ] for the TS102 for the matrix subchannel test section. Because of the considerations noted above, the staff concludes that the effect of the thimble channel guide tube is conservative and has been factored into the KCE-1 CHF correlation.

In its revised response to RAI 3-7443 (Ref. 13), the applicant demonstrated that when a calculated  $F_c$  is used in the KCE-1 CHF predictions, the M/P versus pressure plot in Figure 9-1, “M/P versus Pressure with Tong factor  $F_c$ ,” shows no M/P data point below the M/P value associated with the DNBR limit of 1.124. Figure 9-1 in the RAI response, which is the plot of the M/P application database [ ] shows the lowest M/P value of [ ] corresponding to a DNBR of [ ] This point belongs to the TS101 dataset, which is more conservative than the TS102 dataset whose lowest M/P value of [ ] corresponds to a DNBR of [ ] The 95/95 DNBR of the entire correlation application database is [ ] which corresponds to an M/P value of [ ] The applicant thus demonstrated that the proposed DNBR limit of 1.124 has about [ ] conservative margin compared to the lowest M/P data point with a DNBR of [ ] and a [ ] margin compared with the 95/95 DNBR of [ ] of the entire application database. The staff finds that these margins and statistics appropriately accommodate the non-conservative sub-region; therefore, **RAI 3-7443, Question 9, is resolved and closed.**

#### **4.8.3 Non-Conservative Overfitting of the Test Data**

Best practices in fitting CHF correlations gathered from CHF topical reports reviewed by the NRC staff have suggested that a given CHF test database should be divided into a training dataset and a validation dataset (Ref. 33). Then, the applicant should fit correlation coefficients using the larger training dataset and independently validate it against the smaller validation dataset to ensure a consistent behavior of the correlation. This process helps the applicant assess whether the correlation lacks in predictive capability on data not used in the development of the correlation. In RAI 3-7443, Question 17, the staff inquired whether some test data were initially excluded from the KCE-1 correlation coefficient generation and were later

used for independent correlation validation. The staff was concerned about the potential for “overfitting,” which in this instance means that all available CHF data points in the database were used in the regression analysis to optimize the KCE-1 CHF correlation coefficients and no points were set aside to perform an independent validation of the correlation. The TR did not report any validation of the resulting correlation with an independent data set, so the correlation would likely be slightly non-conservative when applied at conditions for which it was not tested. As all the same CHF data that were used to generate the correlation were also used to evaluate its 95/95 DNBR limit, the staff determined there was a need to quantify the inherent non-conservatism. In its first response to RAI 3-7443 (Ref. 8), the applicant stated that the potential for overfitting is not expected in the KCE-1 CHF correlation, but did not elaborate.

During the audit, the applicant was asked again by the staff to address the potential for a decrease in the KCE-1 correlation’s predictive capability because of overfitting. The staff asked the applicant to estimate the non-conservatism in the 95/95 DNBR limit because of overfitting, by running a random-sub-samples analysis of the CHF database with a larger training (around 80 percent) and smaller validation (around 20 percent) datasets, and demonstrate that the conservative use of the Tong factor more than compensates for this. In its updated response to RAI 3-7443, Question 17 (Ref. 11), the applicant submitted results with a discrete k-folds cross-validation analysis of the correlation development database, which the staff expected to be less conservative than a continuous random-sub-samples analysis. The applicant’s 5-fold analysis shows a maximum 95/95 DNBR limit of [ ] for an 80 percent training-20 percent validation database distribution. Table 17-4, “M/P Statistics for Cases with Max. MAPE for Each k-folds,” showed an increasing trend in the 95/95 DNBR limit from 1.124 to [ ] as the number of k-folds increased from 2 to 5, which suggested an about [ ] non-conservatism in the DNBR limit because of overfitting. The NRC staff’s own random sub-samples confirmatory analysis of the applicant’s data, which is equivalent to repeating the applicant’s 5-folds analysis 10,000 times and generating a continuous probability density histogram, shows approximately a [ ] non-conservatism in the DNBR limit. After the September 3, 2015, public meeting, the applicant submitted a revised response to RAI 3-7443, Question 17 (Ref. 13), that showed a random sub-samples analysis that the applicant performed to quantify the non-conservatism because of using all available data as training data and leaving none for independent validation. Figure 17-4 shows the applicant’s results of a continuous probability density distribution of the M/P values for 1,000 runs. This analysis is consistent with the NRC staff’s own sub-sampling analysis that the correlation has a lower predictive capability on data that were not used in generating the correlation, and the NRC staff’s expectations based on previous experience. The information provided in various updates of the RAI 3-7443, Question 17, response, shows approximately a [ ] non-conservatism because of overfitting, which is consistent with the staff’s similar analysis. Thus, the demonstrated conservatism [ ] as explained in Section 4.8.4, more than accounts for the non-conservatism because of overfitting. The staff therefore considers **RAI 3-7443, Question 17, to be resolved and closed.**

#### 4.8.4 Quantification of the Tong Factor Conservatism

In RAI 3-7443, Questions 6 and 7, the staff inquired about the use of the Tong factor and the symmetric cosine axial power distribution with the KCE-1 correlation development and application. In its response to RAI 3-7443, Questions 6 and 7 (Ref. 8), the applicant provided more details of its treatment of the Tong factor in the KCE-1 correlation's development and subsequent use. The applicant argued during the first public meeting and through RAI responses as well as the audit, that it had treated the "Tong Factor" in a very conservative manner that would reduce the correlation's predicted CHF value. The applicant emphasized that the KCE-1 CHF correlation was developed based on [

] An application of [

] The applicant further explained that the CHF predicted by the resulting KCE-1 correlation is treated as if it was [

] The staff recognized that the conservatism at the correlation application stage is fundamentally caused [

] that appears in the denominator of the KCE-1 correlation.

The staff accepted the applicant's logic that such a treatment of [

] However, the applicant could neither quantify the conservatism inherent in the Tong factor treatment with the KCE-1 correlation nor demonstrate that it more than made up for the non-conservatisms that were identified by the staff. The staff was unable to understand the applicant's method for quantifying the Tong factor conservatism in the earlier RAI response (Ref. 8), and requested data in tables and plots during the audit. In its updated response to RAI 3-7443, Question 6 (Ref. 11), the applicant provided data, resubmitted after the audit, which was found to be inconsistent with the narrative, and did not reconcile with a Tong factor conservatism. The applicant argued in its response that [ ] the effect of axial power distribution on CHF through its Tong factor method has built about [ ] conservatism in the 95/95 DNBR limit (1.124) for its application in the design and safety analyses. However, when the staff more closely examined the eight figures and Table A-2, "Test Data Groups Excluded during KCE-1 CHF Correlation Development," in the RAI 3-7443, Question 6, response, the staff noted inconsistencies in the data that suggested that the actual margin created by the Tong factor conservatism was uncertain and may be much less than [ ]

The submitted information showed two different sets of Tong factors. The set that is documented in the modified Table A-3 and Figure 6-7, "Distribution of M/P versus Tong Factor  $F_c$  at MDNBR location without  $F_c$ ," of the response, is not the same as the one that has [ ] margin and is depicted in the remaining seven figures of the RAI response. The Tong factors' range documented in Table A-3 is [ ] which corresponds with Figure 6-7.

Figure 6-8, "Distribution of M/P versus Tong Factor Fc at MDNBR location with Fc," showing a plot of M/P values vs. Tong factor depicts much larger Tong factors, i.e., about [ ] Though Figure 6-8 is consistent with Figures 6-1, "KCE-1 CHF Correlation Predicted CHF vs. Measured CHF," through 6-6, "Distribution of M/P versus Tong Factor Fc at indicated CHF location," whose purpose is to demonstrate [ ] conservatism, the Tong factors used in these figures are much larger than the ones that are documented in Table A-3 and are likely to give a smaller conservatism. Essentially, the applicant could not demonstrate the magnitude of the conservatism because of [ ]

These difficulties in resolving the Tong factor conservatism and other outstanding issues despite the staff's repeated efforts through the audit and several rounds of the RAI response updates, led to the public meeting with the applicant at the NRC offices on September 3, 2015 (Ref. 12). During the meeting, the applicant agreed with the three non-conservatisms identified by the NRC staff and addressed them. They acknowledged that the conservative treatment of the Tong factor could not be demonstrated based on the information submitted thus far, and explained that the KCE-1 CHF database submitted as Table A-3 in the TR was the intermediate "correlation development database," and not the final "correlation application database." The applicant also provided, in the meeting package, the application version of the CHF database, correlation application results, revised statistics and figures that were previously not presented in the TR or RAI response updates. Contrary to the earlier RAI response (Ref. 11), the staff found the submitted information to be mutually consistent. In its revised response to RAI 3-7443, Question 7 (Ref. 13), the applicant also provided the correlation application database as Table 7-1, "KCE-1 CHF Correlation Database for Application," and explained its differences from the correlation development database. The application database accounted for the application of Tong factor with the KCE-1 correlation on the M/P and DNBR predictions as well as its effect on the subchannel local quantities calculated by using the TORC code. While analyzing the application database, the staff noted that as the minimum DNBR (MDNBR) always corresponds to one of the subchannels that surround the rod undergoing the CHF, applying the Tong factor and rerunning TORC may change the subchannel and node of MDNBR. So, even though all measured quantities and computed local fluid conditions remain the same throughout the TORC subchannel nodalization, the predicted MDNBR location in the application database may vary from the observed one in the development database because of factoring the Tong factor in the CHF prediction by the correlation.

In the TR, the applicant had provided the development database statistics from the comparison of the measured data to the KCE-1 predicted value [ ] In its revised response, the applicant reevaluated the statistics for the application database with the realistically calculated Tong factor to demonstrate its conservative margin. As a result, the DNBR limit dropped from 1.124 [ ] which shows that using a [ ] at the correlation development stage is equivalent to adding a [ ] conservatism to the DNBR. The [ ] "Tong factor conservatism" in the proposed DNBR limit of 1.124 is on top of using the most limiting CHF data point (M/P = [ ] or DNBR = [ ]) in the most bounding TS101 dataset, which is also about [ ] more conservative than the actual 95/95 DNBR of [ ] of the entire correlation application database. So, the [ ] margin

built by the Tong factor treatment is in addition to the [ ] that already covers the non-conservatism because of the non-conservative sub-region, as explained in Section 4.8.2. The staff concludes that the information presented in the public meeting and the later RAI response has adequately supported the applicant's proposed DNBR limit of 1.124 for the KCE-1 correlation by demonstrating that the KCE-1 correlation has an about [ ] conservative bias because of its Tong factor treatment. The staff also concludes that the demonstrated conservatism [ ] in the use of the Tong factor more than offsets the non-conservatism because of overfitting [ ]. The NRC staff has determined that the KCE-1 CHF correlation will accurately predict DNB occurrence with at least a 95-percent probability at the 95-percent confidence level when applied with the DNBR limit of 1.124. The staff considers **RAI 3-7443, Question 7, to be resolved and closed**. As the applicant relied on the conservatism derived from the application of the KCE-1 CHF correlation with the Tong factor being greater than one for the plant safety analyses, the staff has imposed a limitation in Section 5.0 of this SER, which will mandate the applicant's proposed use of the KCE-1 CHF correlation with [ ] as a requirement.

#### 4.8.5 Remaining Uncertainties in the KCE-1 CHF Correlation DNBR Limit

Based on the assessment of the non-conservative test data sub-region and overfitting as described above, the staff concluded that the KCE-1 correlation has at least [ ] margin after accommodating all major non-conservatisms. Not all the following uncertainties are non-conservatisms, and some of them actually are conservatisms.

- The RAI 3-7443, Question 14, response shows a maximum CHF measurement uncertainty of [ ] which was not explicitly factored into their correlation development or the 95/95 DNBR statistical analysis. The staff notes that as the measurement uncertainty is randomly distributed around the CHF data, the maximum non-conservatism it may incur to the 95/95 DNBR limit is about 1.7 percent.
- In Table 9-2, "The Detailed M/P Statistics of Test Section TS101 as the Application of Tong Factor Fc," of its updated response to RAI 3-7443, Question 9 (Ref. 11), the applicant showed that even a different assumption for the subchannel type associated with the CHF could lead to a slightly higher 95/95 DNBR limit of [ ] which exceeded the 1.124 value documented in the TR. So, there is an additional sensitivity to the choice of channel picked for data analysis that was not explored by the staff. Its potential non-conservatism is expected to be about 1 percent.
- As the KCE-1 correlation [ ] the data in the guide tube tests (Test 101) because of [ ] associated with the CHF, the correlation penalizes itself and provides excessively conservative M/P values. The staff found that each matrix subchannel in Test 101 has a higher predicted CHF than the guide thimble corner subchannel that is farther from CHF. Normally, one could ignore those subchannels and only consider the subchannels that are closest to CHF that have the lowest predicted CHF value. The applicant did not ignore them and rather used some data points, which makes the KCE-1 correlation's predictive capability

appear to be worse than it actually is. This conservative bias, which would have increased the [ ] demonstrated margin, was not investigated in the staff's review.

- As explained by the applicant in its response to RAI 3-7443, Question 7 (Ref. 13), the original Tong factor used by the KCE-1 correlation was developed based on single tube and annuli data, and has been shown to be excessively conservative in the CE-1 TR (Ref. 27) and in the WNG-1 TR (Ref. 34) for several axially non-uniformly heated rod bundle data. The NRC approved the WNG-1 correlation, which was developed with both uniform and non-uniform data, and its validation database also included data from a PLUS7 test (Test 102). In its response to RAI 3-7443, Question 7, the applicant showed that the KCE-1 correlation with the Tong factor applied is about [ ] more conservative than the WNG-1 correlation with a similar correction factor optimized with the WNG-1 uniform/non-uniform data. As no CHF tests with uniform axial power shape were conducted for the PLUS7 fuel design, the standard original Tong factor is applied to the KCE-1 correlation without any adjustment or optimization, which the staff considers to be another unquantified potential conservatism in the use of the KCE-1 correlation.

The staff concludes that the remaining quantified Tong factor conservatism in the 95/95 DNBR limit of 1.124 would more than make up for the above uncertainties associated with CHF measurement, testing, and the subchannel assumption. Therefore, a 95/95 DNBR limit of 1.124 would still be valid.

#### **4.9 Applicability of the KCE-1 CHF Correlation**

Section 6 of the TR implied that meeting the 95/95 DNBR limit would also mean meeting the DNB acceptance criterion in SRP Section 4.4 to provide 95/95 assurance that the hot fuel rod in the core would not experience a DNB or transition condition during AOOs. In RAI 3-7443, Question 13, the staff asked the applicant for a justification, emphasizing that the approval of the TR for a given 95/95 DNBR limit would not imply its direct applicability to AOOs that would be separately reviewed under the APR1400 design control document (DCD) review of the thermal design and safety analysis, and that would require additional DNBR margin to cover the limiting transient. In its response to RAI 3-7443, Question 13 (Ref. 8), the applicant committed to modifying the TR to reflect the results of the KCE-1 CHF correlation application to the AOO analysis of APR1400, which will also be included in the corresponding sub-section of the APR1400 DCD Section 4.4. The applicant made an additional commitment to include the supporting information in an updated version of Technical Report APR1400-F-C-NR-12001, "Thermal Design Methodology" (Ref. 35). The applicant maintained the same response in the updated response to RAI 3-7443, Question 13 (Ref. 11). Because the subject review of AOOs is performed under DCD Section 4.4, and because of the above commitments, the staff concludes that the applicant's response is acceptable, and **RAI 3-7443, Question 13, is resolved and closed.**

As identified in Figure 4-1, "System Pressure versus Average Heat Flux of Test Section," of the TR, [

] in Figure 4-3, "Inlet Mass Flux versus Average Heat Flux of Test Section," were also excluded by the applicant for the same reason. The staff considers that this has effectively reduced the application domain of the KCE-1 correlation to a maximum 2,415 psia (16.65 MPa) pressure and 3.15 Mlb<sub>m</sub>/hr-ft<sup>2</sup> (4,272 kg/s-m<sup>2</sup>) inlet mass flux. In RAI 3-7443, Question 18, the staff asked to inquire about the technical bases for selecting the applicable ranges, and whether the applicant envisions the actual PLUS7 design exceeding these ranges in any circumstances. In its response to RAI 3-7443, Question 18 (Ref. 11), the applicant provided the design analysis range of the APR1400 in Table 18-1 along with the applicable range of the KCE-1 correlation. The applicant stated that all APR1400 design/safety analyses are performed within the applicable range of the KCE-1 correlation at the MDNBR location. Among the variables included in Table 18-1, "Range of AOO Design Analysis for APR1400," the APR1400 design analysis range is within the applicable range of the KCE-1 correlation for pressure and local quality. For inlet mass flux, the upper limit of the KCE-1 correlation range is slightly lower than the APR1400 design analysis range. However, the local mass flux at the location of MDNBR in actual core analyses is still within the applicable range of the KCE-1 correlation. The higher pressure drop because of higher power and higher quality of the hot subchannel, where calculated DNBR is the minimum, reduces the flow by redistributing it from the hot subchannel to surrounding subchannels. Even though the excluded data were [

] Figures 18-1, "M/P Trend vs. System Pressure (with Excluded Data due to High Pressure and High Mass Flux)," and 18-2, "M/P Trend vs. Local Mass Flux (with Excluded Data due to High Pressure and High Mass Flux)," were reviewed by the staff and clearly show that the M/P behavior of the excluded points is comparable to the data within the applicable range, as shown in for pressure and mass flux, respectively. The staff considers **RAI 3-7443, Question 18, to be resolved and closed.**

## 5.0 Conditions and Limitations

Based on the foregoing technical and regulatory considerations, the NRC staff concludes that the use of the KCE-1 CHF correlation with a DNBR limit of 1.124 is acceptable for PLUS7 fuel thermal-hydraulic performance and plant safety analyses, provided that the following conditions are met:

1. The KCE-1 CHF correlation shall not be used outside its range of applicability defined by the range of the test data over which it was validated and found to behave in a consistent manner. The approved range for the KCE-1 CHF correlation is defined in the following table:

Parameter	British Units	SI Units
System Pressure	1,750–2,415 (psia)	12.07–16.65 (MPa)

Local Mass Flux	0.85–3.15 (Mlb <sub>m</sub> /hr-ft <sup>2</sup> )	1,153–4,272 (kg/s-m <sup>2</sup> )
Local Quality	-0.15–0.275	

The staff has modified the applicable pressure range from 9.62–16.65 MPa (1,395–2,415 psia) to 12.07–16.65 MPa (1,750–2,415 psia), because of non-conservative data at lower pressure ranges, as discussed in Section 4.8.1. Further application of any other CHF correlation within or outside the approved range tabulated above for the PLUS7 fuel design would have to be reviewed by the NRC as a part of a DCD or combined license application review, or revision of the TR.

2. The KCE-1 CHF correlation application is approved following the documented specific use of the correlation with Tong factor values that are [ ]
3. The KCE-1 CHF correlation shall be used with the TORC subchannel computer code using the models and parameters specified in the TR. The KCE-1 CHF correlation is dependent on local fluid conditions that shall be calculated by the version of the TORC computer code that was used for the TR. Further application of the KCE-1 CHF correlation with any other subchannel computer code would require additional NRC review and approval.
4. Modifications to the KCE-1 CHF correlation, its applicability range, or the associated DNBR limit of 1.124 would require additional NRC review and approval.

The NRC staff will require licensees and applicants referencing this TR in licensing applications to document how these conditions are met.

## **6.0 Conclusions**

Based on its review of Topical Report “KCE-1 Critical Heat Flux Correlation for PLUS7 Thermal Design,” APR1400-F-C-TR-12002-P, Revision 0, the NRC staff has reasonable assurance that the use of the KCE-1 CHF correlation is acceptable in calculating the CHF for PLUS7 fuel design, provided that the conditions and limitations specified in Section 5.0 of this SER are met. These conditions and limitations were identified by the staff to address all outstanding technical issues and to document their closure in this SER. Licensees referencing the TR will be required to ensure compliance with these conditions and limitations. Because of the staff’s review, all RAI questions are considered closed and resolved. The applicant is expected to update the TR to incorporate the mark-ups of the proposed changes submitted with various RAI responses.

When exercised appropriately, the staff finds the KCE-1 CHF correlation methods described in the TR to be applicable to the PLUS7 fuel thermal-hydraulic performance and plant safety analyses. Considering the overall quality of the data presented and analyses performed, the staff concludes that sufficient inherent conservatism is built into the KCE-1 CHF correlation to more than make up for all the non-conservatisms identified by the staff. The proposed DNBR limit of 1.124 for the KCE-1 CHF correlation provides reasonable assurance that GDC 10 and the SRP Section 4.4 acceptance criterion regarding the evaluation of fuel design limits have

been met, and there is at least a 95-percent probability at the 95-percent confidence level that the hot fuel rod in the core would not experience a DNB or transition condition during normal operation.

The NRC staff has reviewed the KCE-1 CHF correlation, and does not intend to review the associated TR when referenced in licensing evaluations. The NRC staff's review was based on the evaluation of the technical merit of the submittal and its compliance with the applicable regulations. If the NRC's regulations or acceptance criteria change such that the conclusions regarding the acceptability of the thermal-hydraulic methods or statistical analyses present in this TR are invalidated, the licensee or applicant referencing the TR will be expected to revise and resubmit its documentation, or submit justification for the continued effective applicability of these methods without revising the respective documentation.

## **7.0      References**

1. Submittal letter dated January 7, 2013, "Transmittal of Topical Report APR 1400-F-C-TR- 12002-P/-NP, Rev. 0, 'KCE-1 Critical Heat Flux Correlation for PLUS7 Thermal Design' for Safety Evaluation, dated November 2012," (Agencywide Documents Access and Management System (ADAMS) Accession No. ML13018A096).
2. Topical Report APR1400-F-C-TR-12002-P/NP, Revision 0, "KCE-1 Critical Heat Flux Correlation for PLUS7 Thermal Design," November 2012 (ADAMS Accession No. ML13018A147).
3. Non-Public Proprietary Request for Additional Information (RAI) RAI 3-7443 for the APR1400 Topical Report APR1400-F-C-TR-12002-P, "KCE-1 Critical Heat Flux Correlation for PLUS7 Thermal Design," to KHNP, March 25, 2014. Proprietary Information. Not publicly available.
4. "Summary of the April 30, 2014, through May 2, 2014, Public Meetings with Korea Hydro and Nuclear Power Co. Ltd. to Discuss Various Topics Related to the Advanced Power Reactor 1400 Design," June 16, 2014 (ADAMS Accession No. ML14154A030).
5. APR1400-F-C-RA-14001-NP, KEPCO/KHNP Presentation, "KCE-1 Critical Heat Flux Correlation for PLUS7 Thermal Design (APR1400-F-C-RT-12002)," May 1, 2014 (ADAMS Accession No. No. ML14132A133).
6. Enclosure 1, KHNP Response to RAI 3-7443 on Topical Report, "KCE-1 Critical Heat Flux Correlation for PLUS7 Thermal Design," APR1400-F-C-TR-12002-P, Rev. 0, Questions 2, 3, and 5; April 23, 2014 (ADAMS Accession No. ML14114A562).
7. Enclosure 3; KHNP Response to RAI 3-7443 on Topical Report "KCE-1 Critical Heat Flux Correlation for PLUS7 Thermal Design" APR1400-F-C-TR-12002-P, Rev. 0,

Questions 4, 10, 11, 12, and 18, May 23, 2014 (ADAMS Accession No. ML14143A115).

8. Enclosure 3; KHNP Response to RAI 3-7443 on Topical Report "KCE-1 Critical Heat Flux Correlation for PLUS7 Thermal Design" APR1400-F-C-TR-12002-P, Rev. 0; Questions 1, 6, 7, 8, 9, 13, 14, 15, 16, and 17, June 2014 (ADAMS Accession No. ML14176A792).
9. Audit Plan to Review Selected Documents Related to APR1400 KCE-1 Critical Heat Flux Correlation for PLUS7 Thermal Design (APR1400-F-C-TR-12002-P-Rev 0), December 11, 2014 (ADAMS Accession No. ML16228A411).
10. U.S. Nuclear Regulatory Commission's Audit Report for the January 21-22, 2015 Audit to Review Selected Documents Related to KEPCO/KHNP Topical Report on KCE-1 Critical Heat Flux Correlation for PLUS7 Thermal Design (APR1400-F-C-TR-12002-P, Rev 0); issued June 9, 2015 (ADAMS Accession No. ML16228A418).
11. Revised KHNP Response to RAI 3-7443 on Topical Report "KCE-1 Critical Heat Flux Correlation for PLUS7 Thermal Design," APR1400-F-C-TR-12002-P, Rev. 0, March 2, 2015 (ADAMS Accession No. ML15061A056).
12. Summary of Public Meeting With Korea Hydro and Nuclear Power Co. LTD. to Discuss Topics Related to the Advanced Power Reactor 1400 Design (ADAMS Accession No. ML15259A459).
13. Revised Response to RAI 3-7443 on Questions 6, 7, 9, and 17, October 9, 2015 (ADAMS Accession No. ML15282A603).
14. CENPD-161-P-A, "TORC Code, A Computer Code for Determining the Thermal Margin of a Reactor Core," April 1986. Proprietary Information. Not publicly available.
15. Title 10 of the *Code of Federal Regulations*, Part 50, "Domestic Licensing of Production and Utilization Facilities."
16. NUREG-0800, "Standard Review Plan for the Review of Safety Analysis Reports for Nuclear Power Plants." (ADAMS Accession No. ML070660036)
17. Tong, L.S., and Y.S. Tang, "Boiling Heat Transfer and Two-Phase Flow," Second Edition, Taylor & Francis, Washington D.C., 1997.
18. [ ]Proprietary Information.  
Not publicly available.

19. [ ]  
Proprietary Information. Not publicly available.
20. [ ] Proprietary Information.  
Not publicly available.
21. [ ] Proprietary Information. Not publicly  
available.
22. [ ] Proprietary Information. Not publicly available.
23. EPRI NP-2609, "Parametric Study of CHF Data, Volume 1: Compilation of Rod Bundle CHF Data Available at the Columbia University Heat Transfer Research Facility," September 1982.
24. Larmarsh, J.R., and A.J. Baratta, "Introduction to Nuclear Engineering 3 e/d," Prentice-Hall 2001.
25. WCAP-15025-P-A, "Modified WRB-2 Correlation, WRB-2M, for Predicting Critical Heat Flux in 17x17 Rod Bundles with Modified LPD Mixing Vane Grids," April 1999. Proprietary Information. Not publicly available.
26. CENPD-162-P-A, "C-E Critical Heat Flux, Critical Heat Flux Correlation for C-E Fuel Assemblies with Standard Spacer Grids, Part 1 Uniform Axial Power Distribution," September 1976. Proprietary Information. Not publicly available.
27. CENPD-207-P-A, "C-E Critical Heat Flux, Critical Heat Flux Correlation for C-E Fuel Assemblies with Standard Spacer Grids, Part 2 Non-uniform Axial Power Distribution," December 1984. Proprietary Information. Not publicly available.
28. [ ] Proprietary  
Information. Not publicly available.
29. Owen, D.B. "Factors for One-Sided Tolerance Limits and for Variable Sampling Plans," SC-R-607, Sandia Corporation, March 1963.
30. WCAP-12488-A, "Westinghouse Fuel Criteria Evaluation Process," October 1994. Proprietary Information. Not publicly available.

31. Box, G.E.P, W.G. Hunter, and J.S. Hunter, "Statistics for Experimenters," Chapter 3, John Wiley & Sons, 1978.
32. Kaizer, J. "Identification of Non-Conservative Sub-regions in Empirical Models Demonstrated using Critical Heat Flux Models," Nuclear Technology, Vol. 190, April 2015, pp 65-71.
33. Piepel, G.F., and J.M. Cuta, "Statistical concepts and techniques for developing, evaluating, and validating CHF correlations and corresponding fuel design limits," SKI Technical Report 93:46, December 1993.
34. WCAP-16766-P-A/WCAP-16766-NP-A, "Westinghouse Next Generation Correlation (WNG-1) for Predicting Critical Heat Flux in Rod Bundles with Split Vane Mixing Grids," February 2010. Proprietary Information. Not publicly available.
35. Korea Electric Power Corporation & Korea Hydro & Nuclear Power Co., Ltd, "Thermal Design Methodology," Technical Report APR1400-F-C-NR-12001-P, Rev. 0, July 2012 (ADAMS Accession No. ML13317A065).

**Non-Proprietary**

Page intentionally left blank

**Non-Proprietary**

**SECTION B**

**Non-Proprietary**

Page intentionally left blank

# **KCE-1 Critical Heat Flux Correlation for PLUS7 Thermal Design**

**(Approved Version)**

**Non-Proprietary**

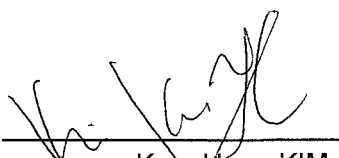
**April 2017**

**Copyright © 2017**

**Korea Electric Power Corporation &  
Korea Hydro & Nuclear Power Co., Ltd  
All Rights Reserved**

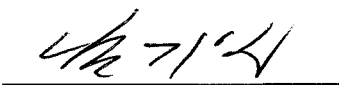
# KCE-1 Critical Heat Flux Correlation for PLUS7 Thermal Design

**(Approved Version)**

Prepared by: 

KangHoon KIM  
Principal Researcher  
Thermal-Hydraulic Design Team  
Core Engineering Department  
KEPCO Nuclear Fuel

04/11/2017  
Date (MM/DD/YYYY)

Prepared by: 

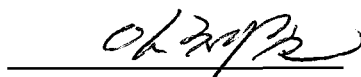
KeeYil NAHM  
General Manager  
Reload Core Project Management Team  
Plant Engineering Management Department  
KEPCO Nuclear Fuel

04/11/2017  
Date (MM/DD/YYYY)

Reviewed by: 

JongSeon LIM  
General Manager  
Thermal-Hydraulic Design Team  
Core Engineering Department  
KEPCO Nuclear Fuel

04/18/2017  
Date (MM/DD/YYYY)

Approved by: 

ChaeJoon LIM  
Vice President  
Core Engineering Department  
KEPCO Nuclear Fuel

04/19/2017  
Date (MM/DD/YYYY)

This document was prepared for the design certification application to the U.S. Nuclear Regulatory Commission and contains technological information that constitutes intellectual property.

Copying, using, or distributing the information in this document in whole or in part is permitted only by the U.S. Nuclear Regulatory Commission and its contractors for the purpose of reviewing design certification application materials. Other uses are strictly prohibited without the written permission of Korea Electric Power Corporation and Korea Hydro & Nuclear Power Co., Ltd.

## **ABSTRACT**

The Critical Heat Flux (CHF) tests for PLUS7 fuel were conducted at Columbia University's Heat Transfer Research Facility (HTRF) in New York City, New York. The objective of the tests was to obtain the data to develop an applicable CHF correlation for PLUS7 fuel.

The CHF tests were performed with two test sections simulating with and without a guide thimble tube, respectively. Each test section was composed of 6x6 heater rods with a heated length of 150 inches and a grid span of 15.7 inches, in accordance with the PLUS7 fuel geometry. The tests were performed with a cosine non-uniform axial power distribution and the radial power split between hot and cold rods was approximately 1 : 0.82.

The functional formula of the KCE-1 CHF correlation is identical to the Westinghouse CE-1 CHF correlation. The coefficients of the KCE-1 CHF correlation were determined by a non-linear multiple-regression analysis for the measured CHF data with local fluid conditions calculated by using the subchannel analysis code TORC (Thermal hydraulics Of a Reactor Core).

The correlation DNBR (Departure from Nucleate Boiling Ratio) limit was determined with a 95% probability and at a 95% confidence level (95/95 DNBR limit). The statistical results and the application ranges of parameters for the KCE-1 CHF correlation are given below.

- Statistical results

Number of Data	$\bar{x}_{(M/P)}$	$S_{(M/P)}$	Correlation DNBR Limit (95/95 DNBR Limit)
225	0.9866	0.05304	1.124

- Application ranges of parameters

Parameter	British Unit	SI Unit
System Pressure	1750 ~ 2415 <i>psia</i>	12.07 ~ 16.65 <i>MPa</i>
Local Mass Flux	0.85 ~ 3.15 <i>Mlbm/hr-ft<sup>2</sup></i>	1153 ~ 4272 <i>kg/s-m<sup>2</sup></i>
Local Quality	-0.150 ~ 0.275	

The test data analysis for the correlation development, its results, the CHF test facility and test procedure for the PLUS7 fuel are described in this report. The CHF test data, the statistical methods applied to the correlation development and verification are provided in the appendices.

The KCE-1 CHF correlation can be applied to the thermal design and safety analyses with TORC code for the OPR1000 and the APR1400, in which PLUS7 fuels are loaded.

## **TABLE OF CONTENTS**

ABSTRACT .....	II
LIST OF TABLES .....	IV
LIST OF FIGURES.....	IV
ACRONYMS AND ABBREVIATIONS .....	V
1. INTRODUCTION .....	1
2. TEST FACILITY AND TEST SECTION .....	2
2.1 TEST FACILITY.....	2
2.1.1 HEAT TRANSFER LOOP .....	2
2.1.2 CONTROL SYSTEM.....	3
2.1.3 ELECTRICAL SYSTEM .....	3
2.1.4 INSTRUMENTATION.....	3
2.2 TEST SECTION .....	4
3. TEST PROCEDURE AND CHF MEASUREMENTS .....	14
3.1 TEST PROCEDURE .....	14
3.2 CHF MEASUREMENTS.....	14
3.3 MEASUREMENTS UNCERTAINTIES .....	15
3.4 QUALITY ASSURANCE.....	15
4. CHF CORRELATION DEVELOPMENT .....	17
4.1 CHF TEST DATA .....	17
4.2 LOCAL FLUID CONDITION CALCULATION.....	17
4.3 CORRELATION FORMULA AND ASSUMPTIONS.....	18
4.4 CORRELATION COEFFICIENTS AND APPLICABLE RANGES OF PARAMETERS.....	19
5. CORRELATION DNBR LIMIT .....	33
5.1 STATISTICAL ANALYSIS FOR DEVELOPMENT DATABASE .....	33
5.2 ESTABLISHMENT OF CORRELATION DNBR LIMIT .....	33
5.3 VALIDATION AND VERIFICATION .....	33
5.3.1 VALIDITY FOR LOCAL FLUID CONDITION EXTRACTION.....	34
5.3.2 GRAPHICAL TEST FOR CORRELATION DNBR LIMIT .....	34
5.3.3 EVALUATION OF PREDICTION PERFORMANCE FOR AXIAL LOCATION OF CHF .....	34
5.3.4 EVALUATION FOR CONSERVATISM BASED ON APPLICATION DATABASE .....	34
5.3.5 EFFECT OF MEASUREMENT UNCERTAINTIES.....	35
6. CORRELATION APPLICATION .....	56
7. CONCLUSION .....	57
8. REFERENCES .....	58
APPENDIX A. DATA FOR KCE-1 CHF CORRELATION DEVELOPMENT/APPLICATION .....	A-1
APPENDIX B. STATISTICAL ANALYSIS.....	B-1

## **LIST OF TABLES**

Table 2-1	Characteristics of Geometrical Configuration of CHF Test Sections .....	5
Table 3-1	Measurement Uncertainties for PLUS7 CHF Tests.....	16
Table 4-1	Main Input Data of the TORC Model for CHF Test Data Analysis .....	22
Table 4-2	Statistical Tests for Data Group Comparison for Test Sections TS102.0 & TS102.1 .....	23
Table 4-3	Treatment of Outliers .....	24
Table 4-4	KCE-1 CHF Correlation Coefficients and Application Ranges of Parameters .....	25
Table 5-1	D' Normality Test (Development Database).....	36
Table 5-2	Statistical Tests for Each Data Group (Development Database).....	37
Table 5-3	95/95 DNBR Limits for Each Data Group (Development Database).....	38
Table 5-4	KCE-1 CHF Correlation Statistical Data per Local Fluid Condition Extraction Method (Development Database) .....	39
Table 5-5	KCE-1 CHF Correlation Conservatism based on Application Database.....	40

## **LIST OF FIGURES**

Figure 2-1	Schematic of Heat Transfer Research Facility (HTRF).....	6
Figure 2-2	Instrumentation Arrangement.....	7
Figure 2-3	Mid-Grid of Thimble Subchannel Test Section TS101 .....	8
Figure 2-4	Mid-Grid of Matrix Subchannel Test Section TS102 .....	8
Figure 2-5	Radial Power Distribution for Thimble Subchannel Test Section TS101 .....	9
Figure 2-6	Radial Power Distribution for Matrix Subchannel Test Section TS102.0.....	10
Figure 2-7	Radial Power Distribution for Matrix Subchannel Test Section TS102.1 .....	11
Figure 2-8	Axial Power Distribution for Test Section .....	12
Figure 2-9	Axial Geometrical Configuration of Test Section.....	13
Figure 4-1	System Pressure versus Average Heat Flux of Test Section .....	26
Figure 4-2	Inlet Temperature versus Average Heat Flux of Test Section .....	27
Figure 4-3	Inlet Mass Flux versus Average Heat Flux of Test Section .....	28
Figure 4-4	System Pressure versus Measured CHF at CHF Location.....	29
Figure 4-5	Local Mass Flux versus Measured CHF at CHF Location .....	30
Figure 4-6	Local Quality versus Measured CHF at CHF Location .....	31
Figure 4-7	Equivalent Heated Diameter Ratio versus Measured CHF at CHF Location .....	32
Figure 5-1	Frequency Diagram of M/P for Test Section TS101 (Development Database).....	41
Figure 5-2	KCE-1 CHF Correlation Predicted CHF versus Measured CHF (Development Database)....	42
Figure 5-3	Distribution of M/P versus System Pressure (Development Database).....	43
Figure 5-4	Distribution of M/P versus Local Mass Flux (Development Database).....	44
Figure 5-5	Distribution of M/P versus Local Quality (Development Database) .....	45
Figure 5-6	Distribution of M/P versus Equivalent Heated Diameter Ratio (Development Database) .....	46
Figure 5-7	Prediction Accuracy of KCE-1 CHF Correlation for CHF Axial Location (Development Database).....	47
Figure 5-8	Frequency Diagram of M/P for Test Section TS101 for Application Database .....	48
Figure 5-9	KCE-1 CHF Correlation Predicted CHF versus Measured CHF for Application Database ...	49
Figure 5-10	Distribution of M/P versus System Pressure for Application Database .....	50
Figure 5-11	Distribution of M/P versus Local Mass Flux for Application Database.....	51
Figure 5-12	Distribution of M/P versus Local Quality for Application Database .....	52
Figure 5-13	Distribution of M/P versus Equivalent Heated Diameter Ratio for Application Database .....	53
Figure 5-14	Distribution of M/P versus Tong Factor for Application Database .....	54
Figure 5-15	Prediction Accuracy of KCE-1 CHF Correlation for CHF Axial Location for Application Database.....	55

## **ACRONYMS AND ABBREVIATIONS**

10CFR21	The Code of Federal Regulations Title 10, Part 21
95/95	95% Probability at a 95% Confidence Level
AOOs	Anticipated Operational Occurrences
APR1400	Advanced Power Reactor 1400
BOHL	Beginning of Heated Length
CHF	Critical Heat Flux
$d, DH$	Equivalent heated diameter of subchannel of interest
$d_m, DHM$	Equivalent heated diameter of matrix subchannel
DCD	Design Control Document
$DNBR$	Departure from Nucleate Boiling Ratio
EOHL	End of Heated Length
$F_C$	Tong Factor
$G$	Local mass flux at the CHF location
$h_{fg}$	Latent heat of vaporization
HTRF	Columbia University's Heat Transfer Research Facility
KGrid	Spacer Grid Loss Coefficients
$l_{DNB}$	CHF axial location
$MDNBR$	Minimum DNBR
MV	Mixing Vain Grid
$M/P$	Measured to Predicted CHF ratio
NMV	Non-Mixing Vane Grid
OPR1000	Optimized Power Reactor 1000
$P$	Pressure
PWR	Pressurized Water Reactor
$q_{CHF,NU}''$	CHF for non-uniform axial power distribution
$q_{CHF,U}''$	CHF for uniform axial power distribution
QA	Quality Assurance
QAP	QA Procedure
QMS	Quality Management System
SAFDL	Specified Acceptable Fuel Design Limit
SER	Safety Evaluation Report
SRP	Standard Review Plan
TC, T/C	Thermocouple
$TDC$	Thermal Diffusion Coefficient
$\chi$	Local quality at the CHF location

## 1. INTRODUCTION

The PLUS7 fuel has been developed with the advanced “R” mixing vane grid design<sup>(1)</sup>. The split mixing vanes attached to the top of the grid strap improve the heat transfer between the coolant and fuel rods and increase the thermal margin. To verify the thermal performance of the PLUS7 fuel, critical heat flux (CHF) tests were conducted at Columbia University’s Heat Transfer Research Facility (HTRF) in New York City, New York and the KCE-1 CHF correlation was developed by using the measured CHF data. This report describes the test data analysis for the correlation development, its results, the CHF test facility and test procedure for the PLUS7 fuel including configurations of the test section.

A description of CHF tests supporting KCE-1 CHF correlation is described in Chapters 2 and 3. Chapter 4 describes the test data evaluation and development of the KCE-1 CHF correlation. The test data were evaluated by using Westinghouse thermal-hydraulic code, TORC<sup>(2),(3)</sup>. TORC code was used to calculate the local fluid condition for the CHF test sections. Chapter 5 summarizes the statistical analysis to determine the 95/95 DNBR limit and the results of verification and validation of the KCE-1 CHF correlation. Discussion on the correlation application to thermal design and safety analyses is described in Chapter 6.

The CHF test data, correlation database and the statistical methods applied to the correlation development are described in the appendices.

## **2. TEST FACILITY AND TEST SECTION**

The CHF tests for the PLUS7 fuel were conducted at Columbia University's Heat Transfer Research Facility (HTRF) in New York City, New York. The test facility and the test sections used for the CHF tests are described in this Chapter. The HTRF has been shut down and closed in the end of 2004.

### **2.1 TEST FACILITY**

The following components of the HTRF of Columbia University are presented in this Chapter; the heat transfer loop, the control system, the electric system, and the instrumentation. The schematic of HTRF is shown in Figure 2-1.

#### **2.1.1 Heat Transfer Loop**

The major components of the loop were the circulating pumps, the flow control, measuring spool piping section, the test section housing, the heat exchangers and mixing tee, the water purification system, the feed water supply, make-up, and bleed system.

The loop was constructed of Series 300 stainless steel with the main piping of 4-inch nominal diameter on the discharge side and 6-inch diameter on the suction side of the main pumps.

Water flow in the loop was provided by two centrifugal pumps connected in parallel. Each pump of 100 HP delivered a maximum flow of 650 gpm (33kg/sec) against a head of 550 ft (168 m) of water. The total flow supplied by the pumps split with the main part going through the measuring spool piping and into the test section housing and the remainder through a series of heat exchangers. The flow through the measuring spool was controlled by a flow control valve electrically operated from the control room.

The test section flow was measured by two (2) Venturi flow meters and a turbine meter prior to the entrance to the test section flow housing. The cooling water passing through the test section housing merged with the flow from the heat exchanger system in a mixing tee. The mixing tee provided a stable coolant temperature at the test section inlet.

Flow through the heat exchangers was also controlled by a series of valves operated from the control room. The heat exchangers were of the shell and tube type and had 500 ft<sup>2</sup> (46 m<sup>2</sup>) total heat transfer area. These units could be operated solely or in any combination to provide wide range of achievable sub-cooling. The secondary side of the heat exchangers was a once-through open loop with approximately 800 gpm (45 kg/sec) of cooling water obtained from wells on site.

The test section flow housing consisted of five (5) major components: a pressure housing, grid plate, top adapter, shroud box and bottom adapter.

Water from the measuring spool pipe entered near the bottom of the pressure housing, flowed down between the annulus formed by the shrouds and the pressure housing inner wall, passed through the bottom adapter holes and turned upwards into the test section. The cooling water extracting the heat from the heater rods passed upwards through the test section and flowed through the enlarged top adapter plate and through the grid plate into the upper spool section and into the mixing tee.

The grid plate, machined from a nickel plate, positioned the rod bundle and held the shroud box in place, and transferred the DC power to the individual rods. The top adaptor located the shroud box with reference to the heated geometry and offered the transition between the heater rods and unheated calming length.

The shroud box was constructed of Series 400 stainless steel bolted together to form a rigid square housing to fit the ceramic flow liners. This type of stainless steel material was chosen to closely match the expansion coefficient of the ceramic, thereby eliminating potential bypass flow.

The ceramic flow liners were made of 99.5% dense Aluminum Oxide ( $Al_2O_3$ ) in 15-inch (38.1 cm) long sections. The ceramic channel extended beyond the rod bundle heated length ensuring a constant geometry to prevent adverse flow effects. Several pressure tap holes were drilled at selected locations along the axial length of the shroud box and flow liners to monitor the differential pressures during the test. The lines of the pressure taps installed at such tap holes were brought outside of the pressure housing through an instrument flange and were connected to pressure transducers.

The bottom adapter located the inlet end of the shroud box in the center of the bottom flange and was isolated from the flange by solid ceramic cylinders. It had eight (8) 1-inch diameter holes equally spaced circumferentially to distribute the inlet flow evenly.

### **2.1.2 Control System**

The control room contained instrumentation and control to perform the following functions:

- Control primary loop temperature to 650 °F, (345 °C)
- Control primary loop pressure to 2500 psia, (17.2 MPa)
- Control primary loop flow rate to 650 gpm, (33 kg/s)
- Control flow rates, temperatures, and pressure to the secondary side of the heat exchangers,
- Control, monitor, and protect the performance of the D.C. motor generator sets,
- Provide temperature protection for the primary and secondary flow pumps,
- Provide over-pressure protection for the primary and secondary systems,
- Monitor water supply tanks for high and low water level conditions,
- Monitor the rod thermocouples and provide protection for over temperatures.

Loop pressure was controlled by electrically operated make-up pumps and back-pressure regulators. The test section outlet pressure was measured with several precision Bourdon type pressure gages and several absolute pressure transducers. The test section inlet flow was adjusted by an electrically operated 4-inch valve.

### **2.1.3 Electrical System**

Heater rods of the test section were heated by a D.C. power system. This power system was composed of six (6) D.C. generators, the motors that derived them, the motor generator protective system, the control panel in the control room for remote operation and the protective and interlocking system. The A.C. power system included two (2) 13.2 KV, 7 MW feeders with interlocks to prevent feedback from one feeder to the other in the event of a fault or ground. The entire system functioned at an overall maximum voltage of 240 volts which was generated by all six (6) D.C. generators.

The output voltage from the all D.C. generators was controlled from the two (2) potentiometers which provide a continuously variable output from the two (2) SCR power supplies. The system voltage could be varied continuously from zero (0) to full power at 240 volts.

### **2.1.4 Instrumentation**

The instrumentation required to perform CHF experiments successfully as well as the instrumentation needed to operate the heat transfer loop were as follows:

- test section inlet mass flow rate,
- water temperature at the inlet and outlet of the test section,

- total pressure at the inlet and outlet of the test section,
- differential pressures between axial points in the test section,
- temperatures in different sections of the loop,
- total D.C. power to the test section,
- wall temperature of heater rod.

Typical arrangement of the loop instrumentation is shown in Figure 2-2.

## **2.2 TEST SECTION**

Two types of test sections, which simulate the PLUS7 fuel, were fabricated to conduct the CHF tests. Test section No. 101 (TS101) was the thimble subchannel test section simulating the guide thimble tube and the flow channels around it. Test section No. 102 (TS102) was the matrix subchannel test section simulating a square flow channel surrounded by four heater rods only. The main geometrical configuration features are summarized in Table 2-1.

The mid-grids with split mixing vanes ("R" mixing vane grid design) used in the individual test section are shown in Figure 2-3 and Figure 2-4.

Test sections with a 5x5 rod array were used by ABB-CE/Westinghouse for the CE-1 CHF correlation while test sections with a 6x6 rod array were used in CHF tests for the PLUS7 fuel. The 6x6 rod array of the test section was introduced to minimize the effect of the shroud inner wall on thermal hydraulic behaviors during the CHF tests and to prevent onset of CHF at peripheral heater rods.

The radial power distributions for each test section were non-uniform as shown in Figure 2-5 through Figure 2-7. Figure 2-5 represents the radial power distribution for the thimble subchannel test section TS101 while Figure 2-6 and Figure 2-7 provide those for the matrix subchannel test sections TS102.0 and TS102.1, respectively. Since heater rods were damaged during the CHF tests with the matrix subchannel test section TS102, the test was resumed after replacing thirteen (13) heater rods. Therefore, there were two (2) radial power distributions for the matrix subchannel test sections, TS102.0 and TS102.1.

The axial power distribution used in the tests had a cosine shape with a peak of 1.475 as shown in Figure 2-8.

Figure 2-9 shows the axial geometrical configuration of the test section. Each axial geometrical configuration simulated the actual PLUS7 fuel dimension identically. For instance, the heated length of the heater rods was 150 inches, and eleven (11) spacer grids were attached to the test section including nine (9) mixing vane mid-grids spaced by 15.7 inches equally. Seven (7) thermocouples were installed axially to measure the wall temperature of the heater rods.

**Table 2-1 Characteristics of Geometrical Configuration of CHF Test Sections**  
(unit: inch)

Test Section No.	Bundle Array	Rod Diameter	Rod Pitch	Heated Length	Grid Spacing	Guide Thimble	Guide Thimble Diameter	Axial Power Distribution
TS101	6x6	0.374	0.506	150.0	15.7	Yes	0.980	1.475 cosine
TS102	6x6	0.374	0.506	150.0	15.7	No	N/A	1.475 cosine

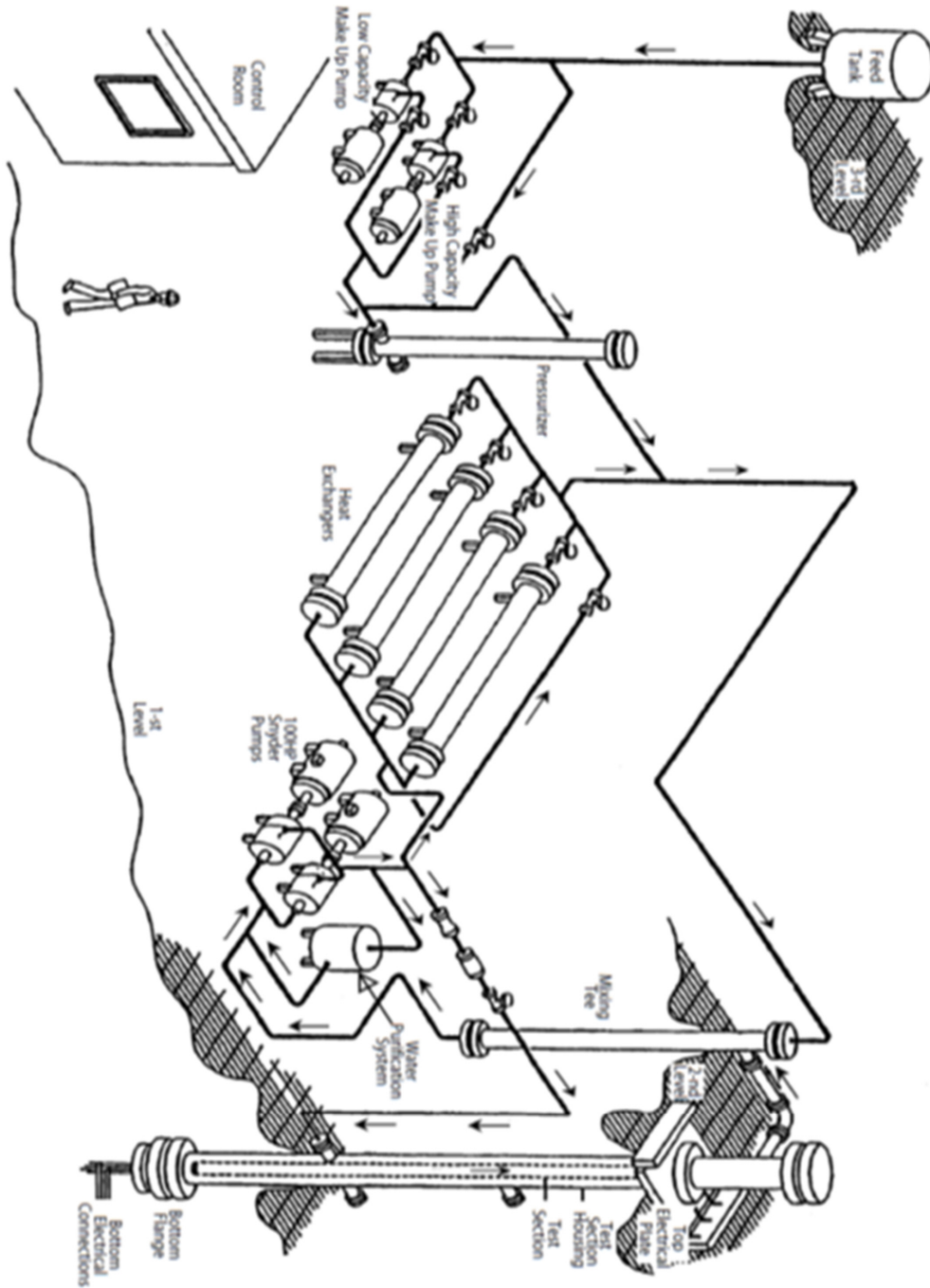


Figure 2-1 Schematic of Heat Transfer Research Facility (HTRF)

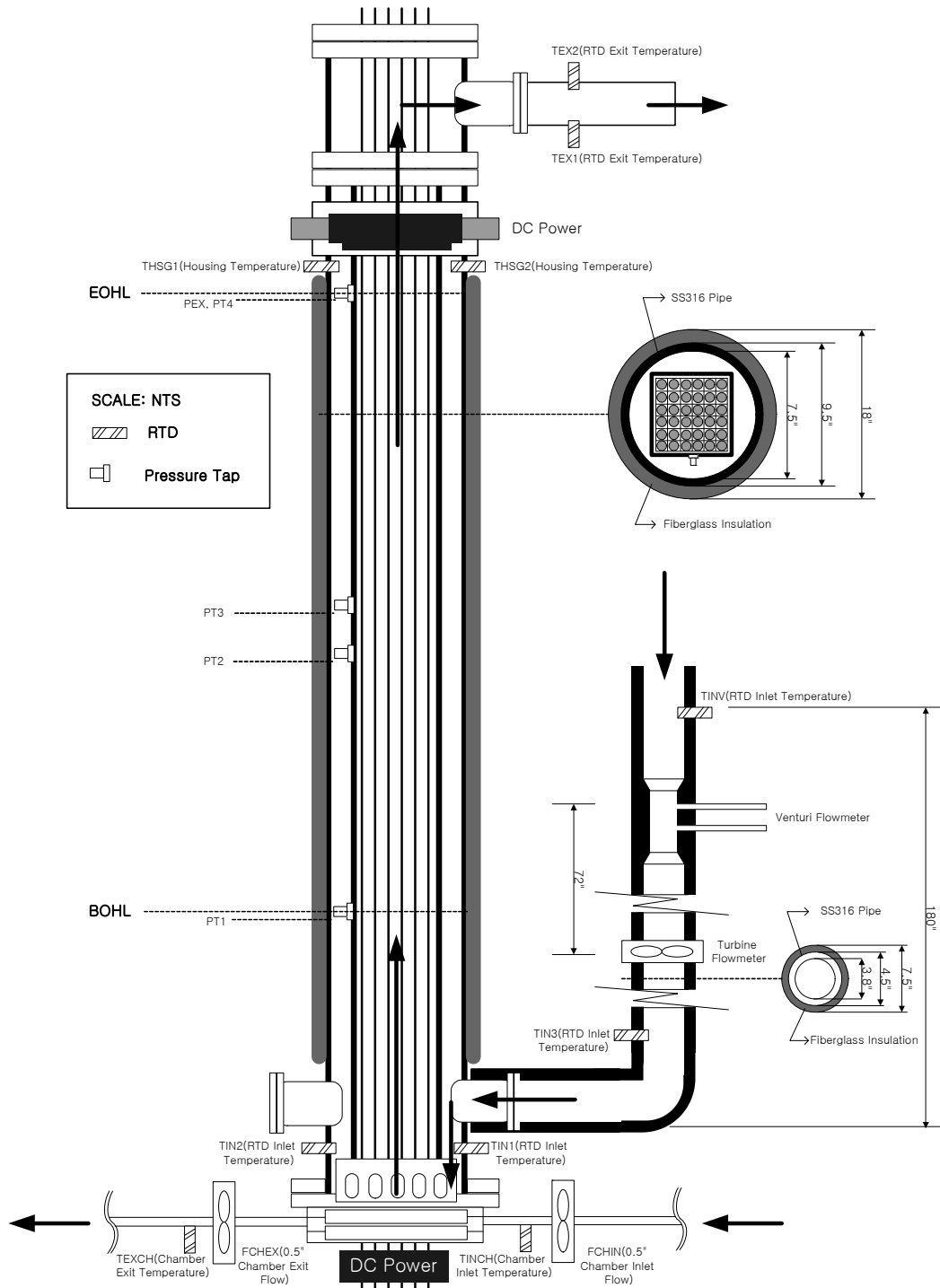


Figure 2-2 Instrumentation Arrangement

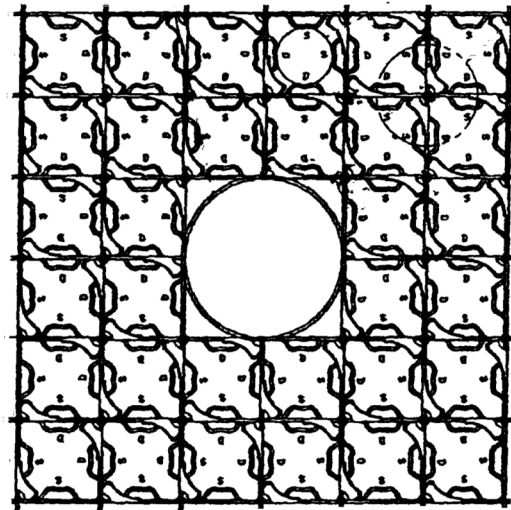


Figure 2-3 Mid-Grid of Thimble Subchannel Test Section TS101

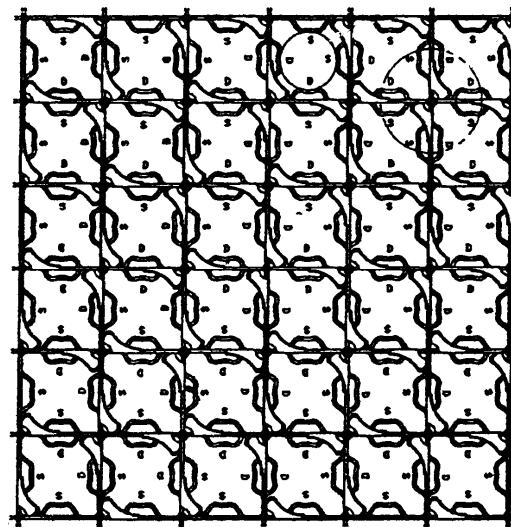
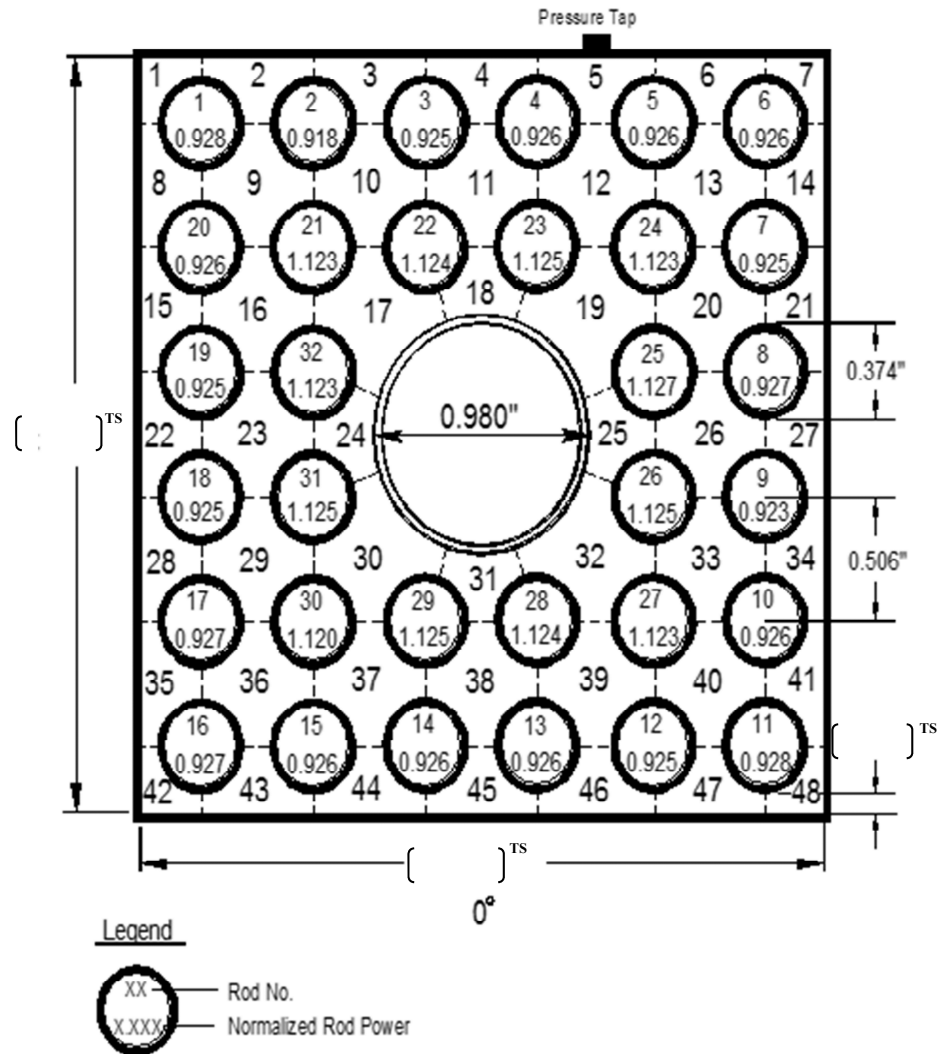
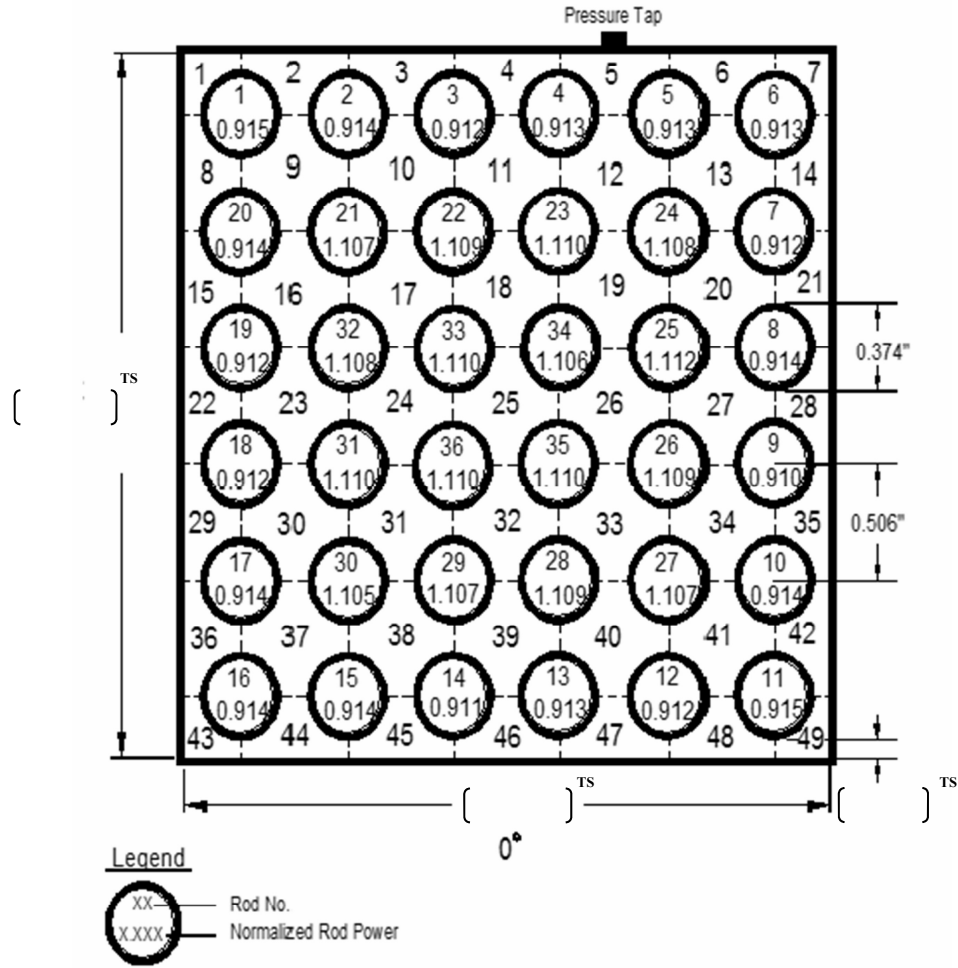


Figure 2-4 Mid-Grid of Matrix Subchannel Test Section TS102



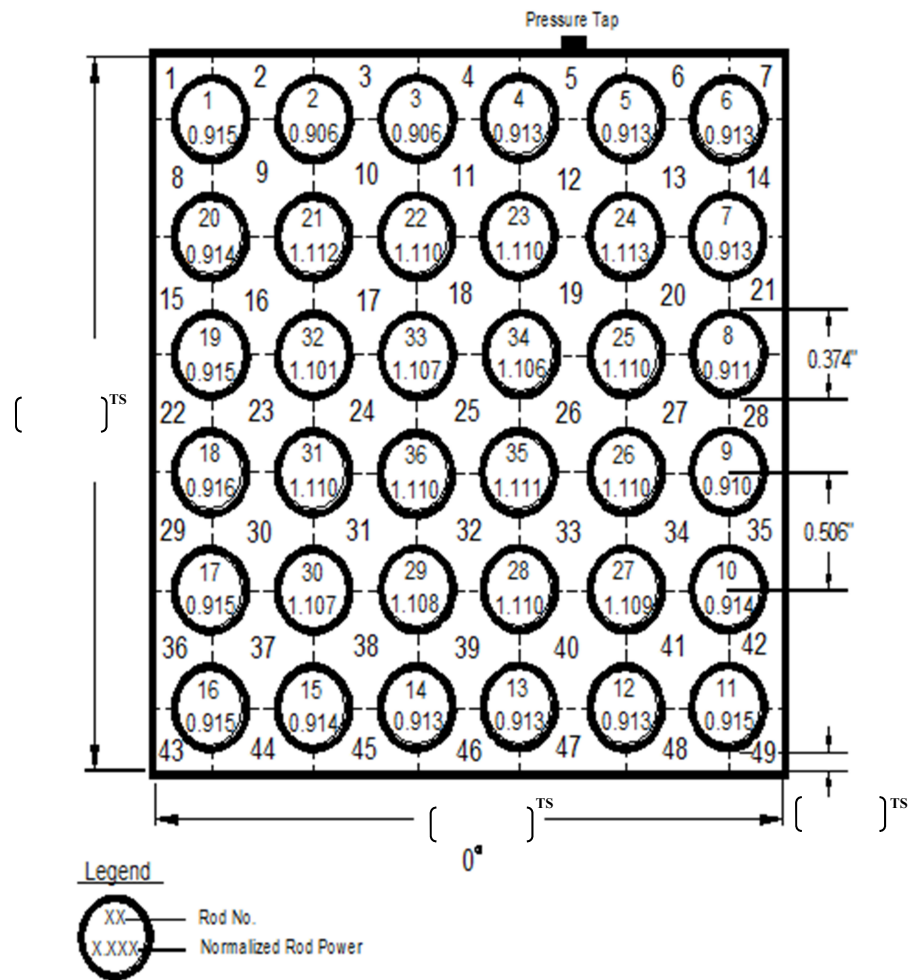
(Numbers inside dashed lines are the subchannel number of TORC model)

**Figure 2-5 Radial Power Distribution for Thimble Subchannel Test Section TS101**



(Numbers inside dashed lines are the subchannel number of TORC model)

**Figure 2-6 Radial Power Distribution for Matrix Subchannel Test Section TS102.0**



(Numbers inside dashed lines are the subchannel number of TORC model)

**Figure 2-7 Radial Power Distribution for Matrix Subchannel Test Section TS102.1**

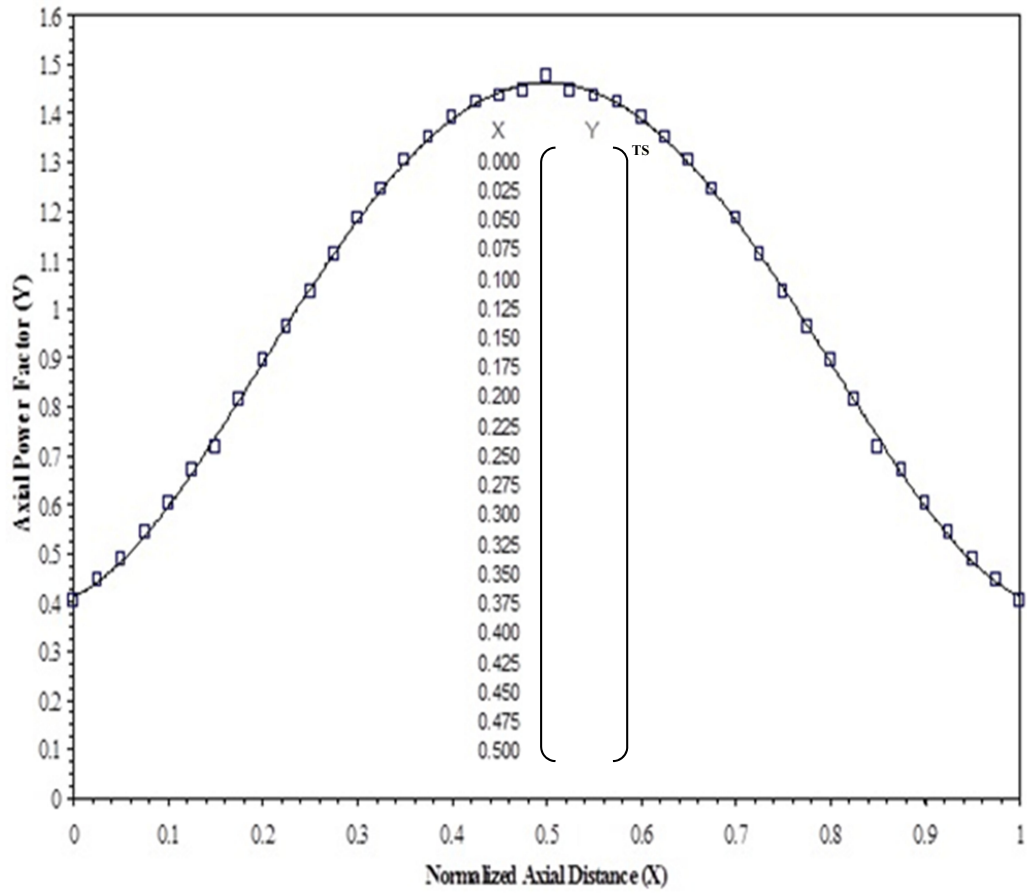


Figure 2-8 Axial Power Distribution for Test Section

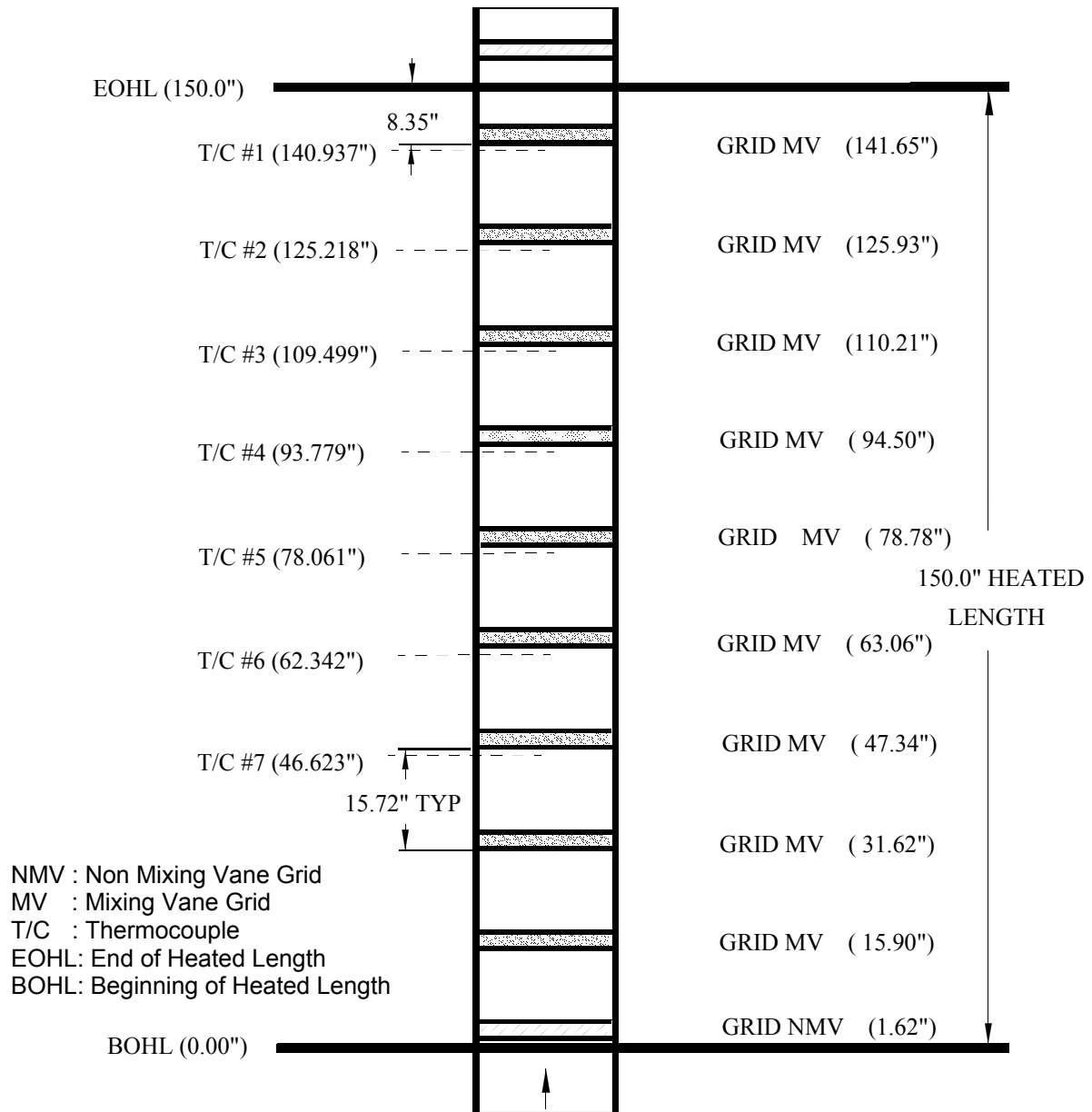


Figure 2-9 Axial Geometrical Configuration of Test Section

### 3. TEST PROCEDURE AND CHF MEASUREMENTS

This chapter describes the procedure to confirm the integrity of the test sections and the system prior to the test as well as the CHF measurement method.

#### 3.1 TEST PROCEDURE

The experimental data to be obtained included cold flow pressure drop at isothermal condition, heat balance at single-phase heated condition and CHF data.

At the beginning of each test, cold flow pressure drop points were obtained over a range of flow conditions. At the start of each day of testing, a repeat pressure drop point was taken for comparison with earlier data. These data provided isothermal grid span pressure drop values to compare with the prediction and also established a base for comparison in case of a malfunction of the rod bundle during the tests. Pressure drop measurements were obtained for each test at the following conditions:

- Pressure: 1000 psi (6.89 MPa)
- Isothermal Temperature: 80 °F (26.7 °C)
- Mass Velocity: 1.0 to 3.5 Mlbm/hr-ft<sup>2</sup> (1356 to 4747 kg/s-m<sup>2</sup>)

Heat balances were performed on the test section to check all loop and bundle instrumentation at high temperature and power and to check heat losses. These runs were accomplished at subcooled conditions before CHF data were obtained at the beginning of each day of operation. The ( )<sup>15</sup> of heat loss acceptance criterion was applied on heat balance test. Heat balances were obtained for each test at the following condition:

- Pressure: 1500 psi (10.34 MPa)
- Inlet Temperature: 400 °F (204.4 °C)
- Mass Velocity: 1.5 Mlbm/hr-ft<sup>2</sup> (2034 kg/s-m<sup>2</sup>)
- Bundle Power: 1.6 MW

The CHF test data were obtained after the heat loss was confirmed to be within the acceptable tolerance range from the heat balance test.

#### 3.2 CHF MEASUREMENTS

The CHF tests were performed by maintaining the following loop parameters constant:

- test section outlet pressure
- inlet temperature
- inlet mass flux (mass velocity)

The total power to the test section was then increased until a temperature excursion was observed by one or more thermocouples installed inside of the heater rods. The amount of the excursion was approximately 10 to 30 °F and varied depending on system conditions. The power was decreased if the temperature excursion was sufficient. When the temperature indication was minimal, confirmation of the validity of a CHF point was obtained by observing the temperature decay with power reduction. There was characteristic temperature decay with time as the CHF zone was rewetted. This evidence was considered confirming in cases where the temperature decay pattern was typical. Otherwise, the test would be repeated<sup>(5)</sup>.

When a CHF point was observed, the following measurements were recorded:

- test section outlet pressure from Heise gauge
- identification number of heater rod experiencing CHF and relevant thermocouple
- test section voltage
- bus-to-bus voltage
- D.C. generator electric current
- inlet temperature
- exit temperature
- exit pressure transducers
- inlet pressure transducers
- turbine flow meter transducer
- Venturi flow meters transducers
- test section pressure drop transducers
- heater rod temperatures

For the above recordings, the first two measurements were recorded manually while other measurements were recorded by the data acquisition system with a HP3852A data acquisition/ control unit.

### **3.3 MEASUREMENTS UNCERTAINTIES**

Measurement uncertainties of CHF test data are subject to any inaccuracy of instrumentations and of the techniques for obtaining and processing the data. The uncertainties had been estimated on the basis of instrument specifications, calibration data, electronics of the data acquisition systems, testing procedures, and variations in test section dimensions from specification. Uncertainties of each measured variable of the CHF test are listed in Table 3-1<sup>(6)</sup>.

### **3.4 QUALITY ASSURANCE**

The engineering design, materials supplied, and all experimental operations satisfy the Columbia University QAP requirements governed by Quality Management System (QMS) to ensure that the CHF data conform to the requirements of ANSI/ASME NQA-1-1989 with addenda, and the Code of Federal Regulations Title 10, Part 21 (10CFR21). All QA related activities performed during the test are reported in Reference 7.

**Table 3-1 Measurement Uncertainties for PLUS7 CHF Tests**

Variable	Unit	Range	Uncertainty
Pressure	<i>psi</i>		<sup>TS</sup>
Mass flux	<i>Mlbm/hr-ft<sup>2</sup></i>		
Inlet Temperature	<i>°F</i>		
Power	<i>MW</i>		

## 4. CHF CORRELATION DEVELOPMENT

The KCE-1 CHF correlation was developed using the CHF test data for the PLUS7 fuel obtained from HTRF. This chapter describes the CHF test data, local fluid condition calculation method, the correlation coefficient optimization procedure and applicable range of parameters to the correlation.

### 4.1 CHF TEST DATA

{ }<sup>TS</sup> test data for the thimble subchannel test section TS101 and one { }<sup>TS</sup> data for the matrix subchannel test section TS102 were obtained, respectively. The entire { }<sup>TS</sup> test data are listed in Table A-1 of APPENDIX A.

Figure 4-1 through Figure 4-3 show average heat fluxes (hence powers) of the test section versus system pressure, inlet temperature and inlet mass flux, respectively. As identified in Figure 4-1, { }<sup>TS</sup>

### 4.2 LOCAL FLUID CONDITION CALCULATION

Using the subchannel analysis code, TORC, local fluid conditions for the CHF test data were computed. The TORC code is an adaptation of the COBRA-IIIC code with modifications including an improved lateral momentum equation and lateral boundary condition capability to simulate actual core behaviors for all flow channels in the core. It is a detailed model code predicting the steady-state thermal hydraulic characteristics of the nuclear reactor cores. The TORC code divides the core into a series of control volumes and solves 3-dimensional conservation equations for each control volume thereby predicting fluid thermal hydraulic local conditions at every position in the core.

The verification of TORC code includes a comparison of subchannel coolant temperature rise and overall pressure drop for CHF test bundles, and full size open core effects of actual operating reactor data.

The TORC code has been approved for use in licensing application of reactor core analyses for steady-state calculations involving unblocked flow channels or subchannels (other than the minimal blockage offered by intact spacer grids). The spacer grid with split type "R" mixing vanes, which was adopted in PLUS7 fuel, did not affect the TORC code applicability to thermal hydraulic analyses of reactor cores as approved by USNRC.

The TORC code models were generated by using subchannel arrangements, radial and axial power distributions and spacer grid locations of each test sections as shown in Figure 2-5 through Figure 2-9. Other main input data are summarized in Table 4-1.

The TORC input parameters, given in Table 4-1, were { }<sup>TS</sup> Among them, { }<sup>TS</sup>

TDC of { }<sup>TS</sup> or the inverse Peclet number of { }<sup>TS</sup> was applied to PLUS7 CHF data analysis. Assessment on the applicability had been performed based on { }<sup>TS</sup> Generally, { }<sup>TS</sup>

{ }<sup>TS</sup> The TDC value for grid spacing of 26 inches was { }<sup>TS</sup> It would be conservatively applicable to PLUS7 CHF data analysis. The mid grid of PLUS7 fuel is an R-type split mixing vane design. The grid spacing of PLUS7 fuel and the CHF test section is 15.7 inches as described in Figure 2-9 of the topical report. A lower value of TDC or an inverse Peclet number would be applied to design and safety analyses, as described in Section 6 of the topical report.

KGrid's were determined by the analytical prediction method for 6x6 CHF test grids (mid grid with mixing vane and non-mixing vane grid, MV and NMV in Figure 2-9 of the topical report) { }<sup>TS</sup> Figure 15-1 shows analytically derived KGrid for a mid grid with mixing vanes of Test Sections TS101 and TS102 (TS102.0 and TS102.1 were the test sections with the same geometry as described in Subsection 2.2 of the topical report).

The turbulent momentum factor is the weighting factor that allows the user to account for uncertainties associated with the formulation of the axial momentum carried by turbulent interchange. For PLUS7 CHF data analysis, the value of { }<sup>TS</sup> was used rather than { }<sup>TS</sup> The deviation induced from the turbulent momentum factor is implicitly included in M/P statistics. In design application, the momentum factor of { }<sup>TS</sup> would be consistently applied to APR1400 design and safety analyses.

For CHF tests using a uniform axial power distribution, such as the CHF test cases for the CE-1 correlation<sup>(9)</sup> development, CHF always occurs in the upper exit region of the heater rods (end-of-heated-length, EOHL). Hence, surface temperatures of heater rods and subchannels experiencing CHF can be detected by thermocouples installed azimuthally in the EOHL four (4) subchannels surrounding a heater rod.

For CHF tests using a non-uniform axial power distribution, as in the CHF tests for PLUS7 and for Reference 10, the axial location of CHF occurrence depends on the shape of the axial power distribution and local fluid conditions. Moreover, the surface temperatures of heater rods are measured with ring-typed junction thermocouples installed at various axial positions. In this case, the axial location of a heater rod where CHF occurs can be detected but the subchannel experiencing CHF cannot be identified exactly. Thus, the local fluid conditions for the KCE-1 CHF correlation were extracted with the following basic assumptions:



Therefore, { }<sup>TS</sup> were extracted per each individual datum from TS101 while { }<sup>TS</sup> per datum from TS102.

Figure 4-4 through 4-7 show measured CHF at CHF indication location versus system pressure, local mass flux, local quality and equivalent heated diameter ratio.

**4.3 CORRELATION FORMULA AND ASSUMPTIONS**

The functional formula of the KCE-1 CHF correlation is identical to the CE-1 CHF correlation, and is given as follow:

$$q''_{CHF,U} = \frac{B_1(d/d_m)^{B_2} [(B_3 + B_4P)(G/10^6)^{(B_5+B_6P)} - (G/10^6)\chi h_{fg}]}{(G/10^6)^{(B_7P+B_8(G/10^6))}}$$

where,  $q''_{CHF,U}$  CHF for uniform axial power distribution,  $MBtu/hr-ft^2$   
 $P$  Pressure,  $psia$   
 $d$  Equivalent heated diameter of subchannel of interest,  $inch$   
 $d_m$  Equivalent heated diameter of matrix subchannel,  $inch$   
 $G$  Local mass flux at the CHF location,  $lbm/hr-ft^2$   
 $\chi$  Local quality at the CHF location  
 $h_{fg}$  Latent heat of vaporization,  $Btu/lbm$ .

The coefficients of the CE-1 CHF correlation were determined based on the CHF test data with a uniform axial power distribution. Through subsequent CHF tests with a non-uniform axial power distribution, the non-uniform axial power distribution correction factor, Tong factor  $F_C^{(10),(11)}$ , was combined with the CE-1 CHF correlation as follow, and was proven to predict the CHF values conservatively:

$$q''_{CHF,NU} = q''_{CHF,U} / F_C$$

where,  $q''_{CHF,NU}$  CHF for non-uniform axial power distribution,  $MBtu/hr-ft^2$   
 $q''_{CHF,U}$  CHF for uniform axial power distribution,  $MBtu/hr-ft^2$   
 $F_C$  Non-uniform axial power distribution correction factor

The Tong factor  $F_C$  was defined as follow :

$$F_C = \frac{C}{q''_{CHF,NU} (1 - e^{-Cl_{DNB}})} \int_0^{l_{DNB}} q''(z) e^{-C(l_{DNB}-z)} dz$$

$$C = 1.8 (1 - \chi_{DNB})^{4.31} / (G/10^6)^{0.478} ft^{-1}$$

where,  $l_{DNB}$  CHF axial location  
 $\chi_{DNB}$  Local quality at the CHF location

According to the SER issued by USNRC shown in the enclosure of Reference 10, the 95/95 DNBR (Departure from Nucleate Boiling Ratio) limit of the CE-1 CHF correlation established for the uniform axial power distribution was allowed to be applied to the non-uniform axial power distribution since the CE-1 CHF correlation combined with the Tong factor  $F_C$  predicts the CHF conservatively for the non-uniform axial power distribution.

The CHF test data for the PLUS7 fuel were obtained with a non-uniform axial power distribution, a symmetric cosine with a peak of 1.475. For a conservatism, [

#### 4.4 CORRELATION COEFFICIENTS AND APPLICABLE RANGES OF PARAMETERS

The applicable ranges of parameters for the KCE-1 CHF correlation were determined based on the local fluid conditions at the location of the predicted minimum DNBR. The coefficients of KCE-1 CHF correlation were developed by an iterative process to optimize the coefficients as given below:

1) As the first step in the iterative process, the local fluid conditions at the { }<sup>TS</sup> elevation were used to determine the initial coefficients for the correlation and to estimate the range of applicability for the correlation. The selected range used in the initial runs was based upon the range of data at the { }<sup>TS</sup> elevation. The initial dataset is listed in Table A-2 of APPENDIX A.

2) The second step was to determine the initial estimate of the eight coefficients of the CE-1 CHF correlation formula by using a nonlinear regression code. To obtain convergence, the initial guesses were based upon the values for the CE-1 CHF correlation, Reference 9. The resulting applicable ranges of parameters for the initial KCE-1 CHF correlation were as follows:

- System pressure { }<sup>TS</sup>
- Local mass flux { }<sup>TS</sup>
- Local quality { }<sup>TS</sup>

3) As the third step, statistical tests were performed for the indicated CHF elevation data with the CHF statistics for the initial KCE-1 CHF correlation. An outlier test was applied to identify potential test data which could be removed. There was no outlier for the { }<sup>TS</sup> elevation data.

{ }<sup>TS</sup>

4) As the fourth step, an iterative process was then applied by using the initial coefficients of the KCE-1 CHF correlation from the { }<sup>TS</sup> elevation for each test section with { }<sup>TS</sup>.

5) As the fifth step, local fluid conditions were extracted at the minimum DNBR elevation in a channel { }<sup>TS</sup> rod. The local fluid conditions at the { }<sup>TS</sup> { }<sup>TS</sup> rod, if applicable, were extracted for TS101. As stated in section 4.3 and Reference 9 { }<sup>TS</sup> { }<sup>TS</sup>

6) Step 2 was repeated several times with the minimum DNBR data to determine the eight coefficients of the CE-1 CHF correlation formula. After the initial run at the minimum DNBR elevation, the data were examined for outliers. Based upon this outlier test, { }<sup>TS</sup> was eliminated, as shown in Table 4-3. It was

( )<sup>TS</sup>

- 7) Steps 4 ~ 6 were repeated until the correlation statistics were unchanged with update of the coefficients. Although there is a change in the minimum DNBR elevation for a small number of runs between previous and current runs, if the coefficient change results in essentially no change in the final statistics, the iteration process was completed and the coefficients from the previous run were considered the final.

The data rejected during the correlation development process from the entire ( )<sup>TS</sup> test data are listed in Table A-3 of APPENDIX A.

The final coefficients determined and the application ranges of parameters for the KCE-1 CHF correlation are presented in Table 4-4. Corresponding development database of KCE-1 CHF correlation is given in Table A-4 of APPENDIX A.

**Table 4-1 Main Input Data of the TORC Model for CHF Test Data Analysis**

Supplementary output file selected  
 Single phase friction factor  
 Two-phase pressure drop  
 Forced flow diversion  
 Axial power distribution  
 Crossflow resistance relationship  
 Diversion crossflow resistance factor ( $K_{ij}$ )  
 The turbulent momentum factor  
 The traverse momentum parameter ( $s/l$ )  
 The number of axial nodes  
 The allowable fractional error in flow convergence  
 The flow damping factor  
 Thermal conduction in the coolant  
 Two-phase flow model  
 Inlet flow option  
 Thermal diffusion coefficient  
 Tong factor  $F_c$   
 Loss coefficients of spacer grid ( $K_{Grid}$ )  
     NMV  
     MV  
  
 Re = Reynolds Number  
 1/Pe = Inverse Peclet Number

TS

**Table 4-2 Statistical Tests for Data Group Comparison for Test Sections TS102.0 & TS102.1**

- Bartlett Test Results

TS	$n$	$\bar{x}_{(M/P)}$	$s_{(M/P)}$	$K$	$M/C$	$\chi^2_{0.95}$	Test
102.0	{						} TS
102.1							
All							

- Unpaired  $t$  Test Results

TS	$n$	$\bar{x}_{(M/P)}$	$s_{(M/P)}$	$\bar{x}_1 - \bar{x}_2$	$s_0$	$t$	$t_{0.025/95}$	Test
102.0	{							} TS
102.1								
All								

- Wilcoxon-Mann-Whitney Test Results

TS	$n$	$W$	$\mu_w$	$\sigma_w^2$	$z$	$z_{0.95}$	Test
102.0	{						} TS
102.1							
All							

**Table 4-3 Treatment of Outliers**

- Treatment of outliers for each test section test data group

TS	Run No.	Channel Type	M/P	$n$	$\bar{x}_{(M/P)}$	$S_{(M/P)}$	$\alpha'$	$z$	$b$	Test
101										
101										
102.1										

- Treatment of outliers for the entire test data groups

TS	Run No.	Channel Type	M/P	$n$	$\bar{x}_{(M/P)}$	$S_{(M/P)}$	$\alpha'$	$z$	$b$	Test
101										
101										
102.1										

**Table 4-4 KCE-1 CHF Correlation Coefficients and Application Ranges of Parameters**

- $DNBR = \frac{q''_{KCE-1}}{q''_{measured}}$

- $q''_{KCE-1} = q''_{KCE-1,U} / F_C$

- KCE-1 CHF Correlation

$$q''_{KCE-1,U} = \frac{B_1 (d/d_m)^{B_2} [(B_3 + B_4 P)(G/10^6)^{(B_5 + B_6 P)} - (G/10^6)\chi h_{fg}]}{(G/10^6)^{(B_7 P + B_8 (G/10^6))}}$$

where,  $q''_{KCE-1,U}$  Predicted CHF by KCE-1 correlation for uniform axial power distribution, *MBtu/hr-ft<sup>2</sup>*

$q''_{measured}$  Actual measured CHF, *MBtu/hr-ft<sup>2</sup>*

$P$  Pressure, *psia*

$d$  Equivalent heated diameter of subchannel of interest, *inch*

$d_m$  Equivalent heated diameter of matrix subchannel, *inch*

$G$  Local mass flux, *lbm/hr-ft<sup>2</sup>*

$\chi$  Local quality

$h_{fg}$  Latent heat of vaporization, *Btu/lbm*.

$F_C$  Tong's non-uniform axial power distribution correction factor.

- KCE-1 CHF Correlation Coefficients

B <sub>1</sub>	( ) <sup>TS</sup>	B <sub>5</sub>	( ) <sup>TS</sup>
B <sub>2</sub>	( )	B <sub>6</sub>	( )
B <sub>3</sub>	( )	B <sub>7</sub>	( )
B <sub>4</sub>	( )	B <sub>8</sub>	( )

- Application Ranges of Parameters for KCE-1 CHF Correlation

Parameter	British Unit	SI Unit
System Pressure	1750 ~ 2415 <i>psia</i>	12.07 ~ 16.65 <i>MPa</i>
Local Mass Flux	0.85 ~ 3.15 <i>Mlbm/hr-ft<sup>2</sup></i>	1153 ~ 4272 <i>kg/s-m<sup>2</sup></i>
Local Quality	-0.150 ~ 0.275	

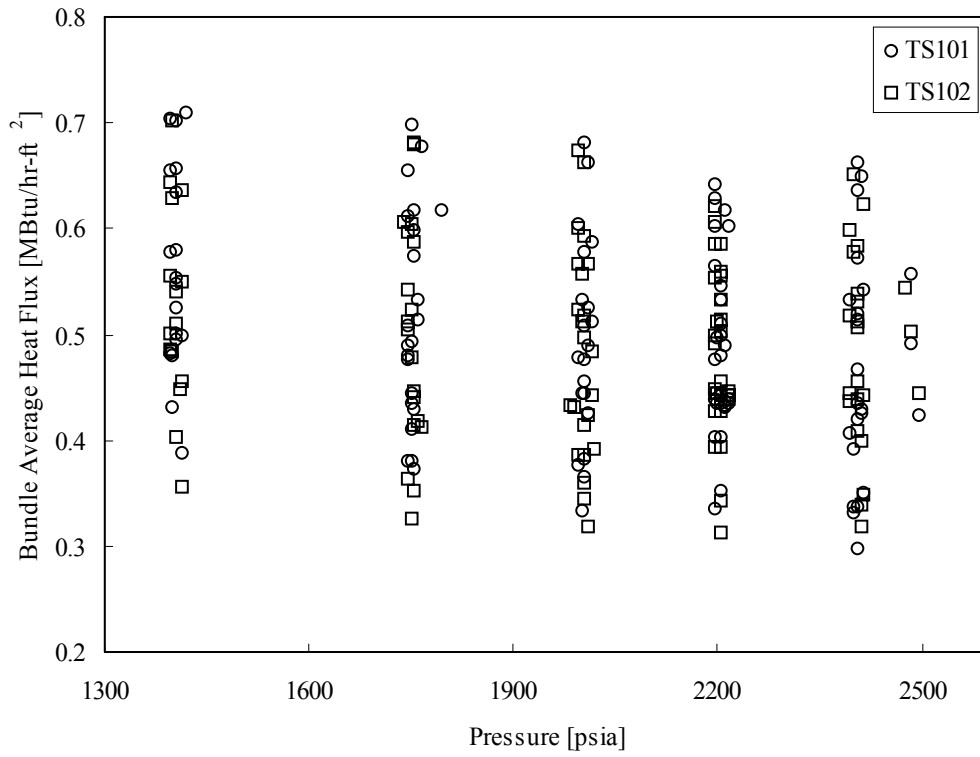
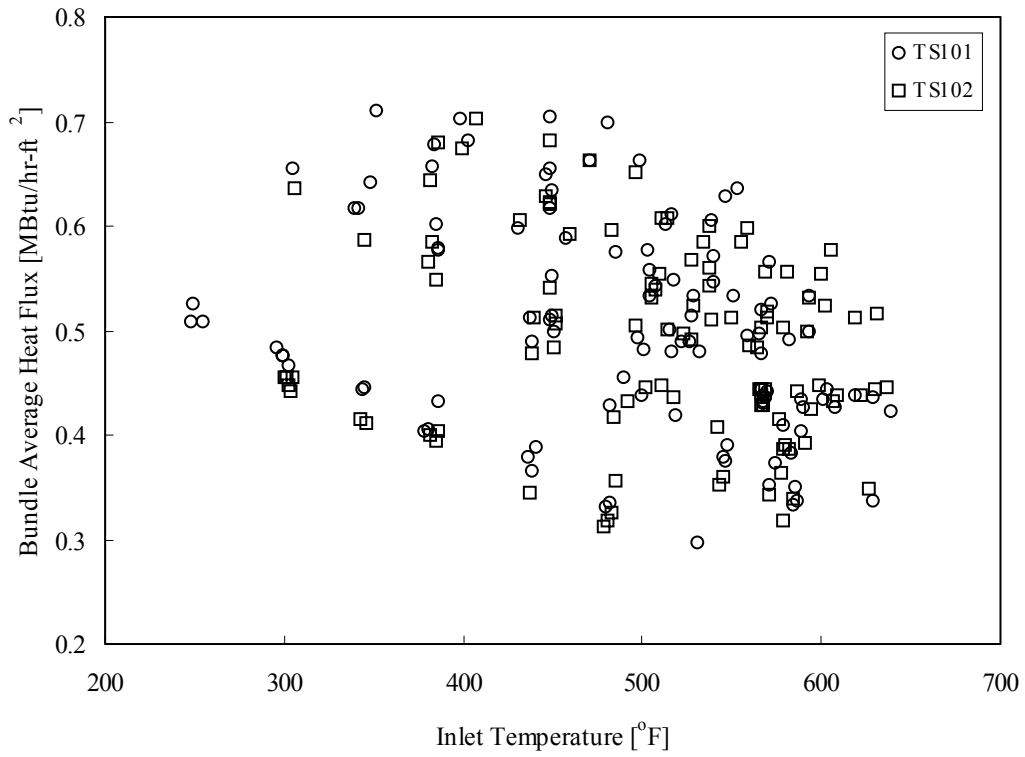


Figure 4-1 System Pressure versus Average Heat Flux of Test Section



**Figure 4-2 Inlet Temperature versus Average Heat Flux of Test Section**

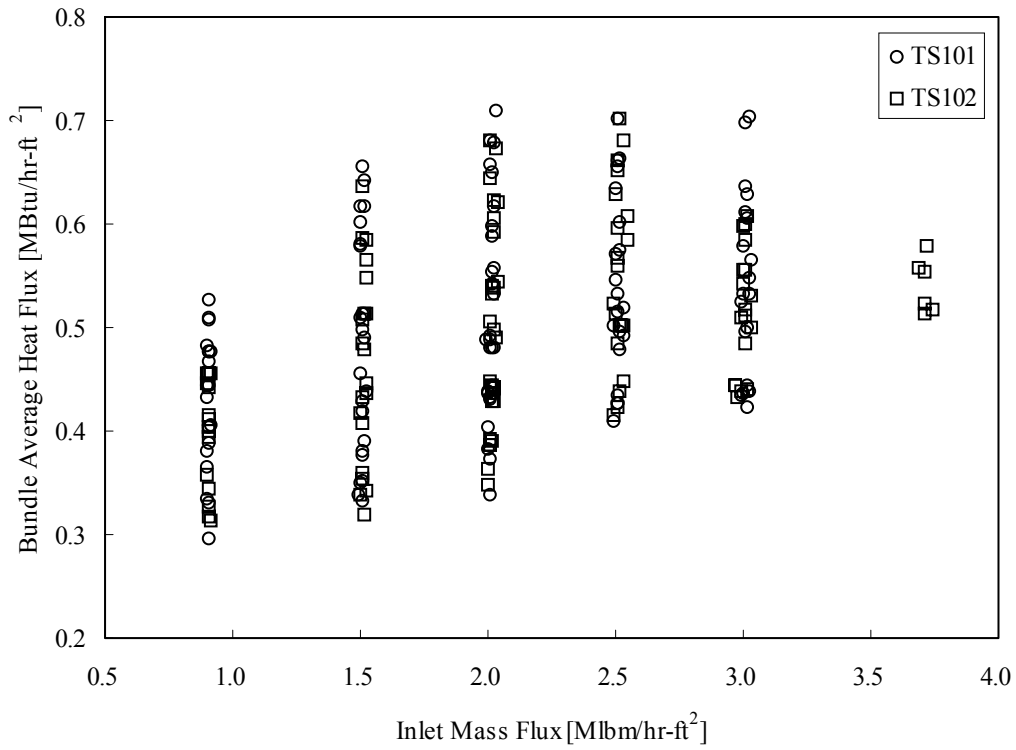
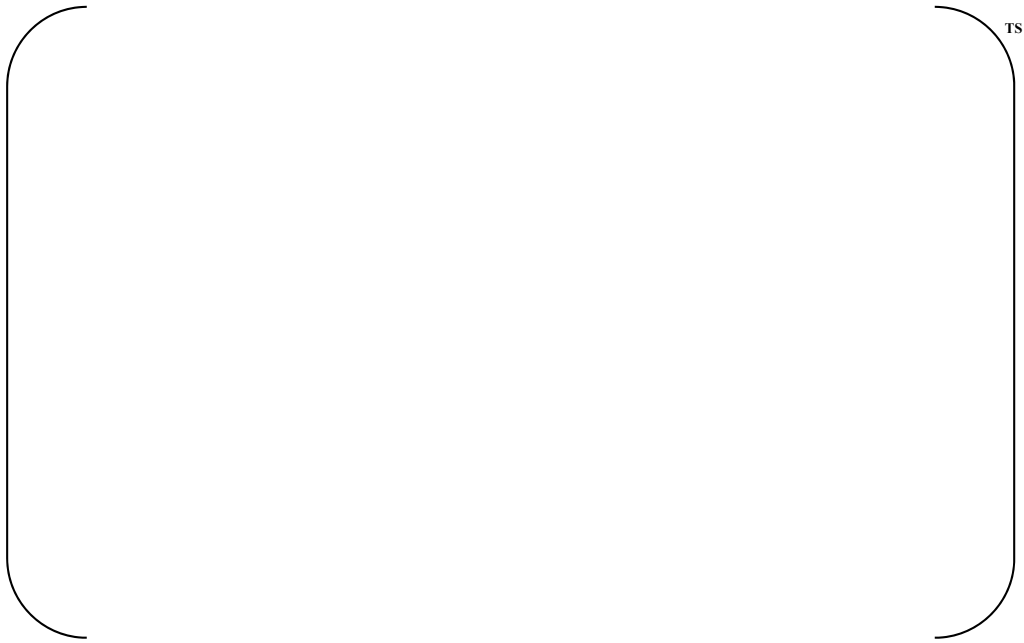


Figure 4-3 Inlet Mass Flux versus Average Heat Flux of Test Section



**Figure 4-4 System Pressure versus Measured CHF at CHF Location**



**Figure 4-5 Local Mass Flux versus Measured CHF at CHF Location**



**Figure 4-6 Local Quality versus Measured CHF at CHF Location**



**Figure 4-7 Equivalent Heated Diameter Ratio versus Measured CHF at CHF Location**

**5. CORRELATION DNBR LIMIT**

This chapter describes the process for determining the 95/95 DNBR limit (DNBR limit with a 95% probability and a 95% confidence interval) of the KCE-1 CHF correlation developed in Chapter 4 and the statistical tests applied to the process.

**5.1 STATISTICAL ANALYSIS FOR DEVELOPMENT DATABASE**

To determine the 95/95 correlation DNBR limit, each data group used for the correlation development must be checked whether these groups could be pooled. For this purpose, a normality test and homogeneity tests for variances and means were performed. The brief description of these statistical tests is provided in sections B.2 and B.3 of APPENDIX B.

The normality test was performed using the D' test and the test results are provided in Table 5-1 for development database. } <sup>TS</sup>


**5.2 ESTABLISHMENT OF CORRELATION DNBR LIMIT**


Number of Data	$\bar{x}_{(M/P)}$	$S_{(M/P)}$	Correlation DNBR Limit (95/95 DNBR Limit)
225	0.9866	0.05304	1.124

**5.3 VALIDATION AND VERIFICATION**

The validities of the local condition extraction method, which was used to generate the test data groups for the correlation development, and the conservatism of the 95/95 DNBR limit were verified as follows.

### 5.3.1 Validity for Local Fluid Condition Extraction

The validity of the method for extracting the local fluid conditions, described in section 4.2, was verified via comparison of the M/P statistics between the cases with and without the assumption of  $\left\{ \begin{array}{l} \text{ } \\ \text{ } \end{array} \right\}^{\text{TS}}$ . For the case without the assumption,  $\left\{ \begin{array}{l} \text{ } \\ \text{ } \end{array} \right\}^{\text{TS}}$  was considered where calculated DNBR was the minimum regardless of  $\left\{ \begin{array}{l} \text{ } \\ \text{ } \end{array} \right\}^{\text{TS}}$ .

As shown in Table 5-4, the former (with the assumption) led to more conservative results than the latter (without assumption) with respect to the 95/95 DNBR limit. Hence, the assumption for extracting the local fluid conditions applied to develop the KCE-1 CHF correlation is valid.

### 5.3.2 Graphical Test for Correlation DNBR Limit

After the determination of the 95/95 DNBR limit for the correlation, scatter plots were then generated for all of the variables in the correlation to examine the correlation for trends or regions of non-conservatism. The Measured-to-Predicted CHF ratio (M/P) was plotted as a function of fluid parameters such as pressure, local mass flux, local quality and geometric parameter (equivalent heated diameter ratio,  $d/d_m$ ) for development database. The 95/95 DNBR limit ( $\text{DNBR}_{95}$ ) is also shown on these plots to show the number of tests points that fall below the limit and the location of those points.

Figure 5-2 shows the predicted and measured values for each test point. The M/Ps of all test data were plotted for system pressure, local mass flux, local quality and equivalent heated diameter ratio in Figure 5-3 through Figure 5-6, respectively. When the lines of each figure corresponding to the correlation DNBR limit are compared with those M/Ps, any adverse trend is not observed against them.

The numbers of data out of 95/95 DNBR limit are  $\left\{ \begin{array}{l} \text{ } \\ \text{ } \end{array} \right\}^{\text{TS}}$  for test sections TS101 and TS102, respectively, which correspond to less than  $\left\{ \begin{array}{l} \text{ } \\ \text{ } \end{array} \right\}^{\text{TS}}$  of the total number of data for each group (development database).

### 5.3.3 Evaluation of Prediction Performance for Axial Location of CHF

To evaluate the accuracy of the KCE-1 CHF correlation in predicting the axial location (or elevation) of indicated CHF, the actual indicated CHF elevation were compared with the elevations of the minimum DNBR predicted by the KCE-1 CHF correlation for development database. As shown in Figure 5-7, approximately  $\left\{ \begin{array}{l} \text{ } \\ \text{ } \end{array} \right\}^{\text{TS}}$  of the entire test data are included within  $\left\{ \begin{array}{l} \text{ } \\ \text{ } \end{array} \right\}^{\text{TS}}$  of the heated length with respect to the indicated CHF elevation. Thus the prediction performance for the elevation of CHF is acceptable.

### 5.3.4 Evaluation for Conservatism based on Application Database

During the KCE-1 CHF correlation development process, the CHF test data for the non-uniform axial power distribution were not  $\left\{ \begin{array}{l} \text{ } \\ \text{ } \end{array} \right\}^{\text{TS}}$ . However, the non-uniform axial power distribution correction factor (Tong factor  $F_c$ ) should be applied to the actual design calculation. Therefore, the conservatism of the correlation could be evaluated by comparing M/P statistics of the development database and the results with application of Tong factor  $F_c$   $\left\{ \begin{array}{l} \text{ } \\ \text{ } \end{array} \right\}^{\text{TS}}$ , application database.

The average M/P value is  $\left\{ \begin{array}{l} \text{ } \\ \text{ } \end{array} \right\}^{\text{TS}}$ , as given in Table 5-5. For the application database,  $\left\{ \begin{array}{l} \text{ } \\ \text{ } \end{array} \right\}^{\text{TS}}$ .

{ }<sup>TS</sup>. Corresponding application database is given in Table A-6 of APPENDIX A with excluded data in Table A-5 of APPENDIX A. Frequency diagram of M/P for the application database is similar to that for the development database, as shown in Figure 5-8.

Graphical tests, corresponding Figures 5-2 to 5-6 for the development database, show no adverse trend { }<sup>TS</sup> current 95/95 DNBR limit (1.124 based on development database), as shown in Figures 5-9 to 5-13 for the application database. No adverse trend shows with respect to Tong factor  $F_c$  as shown in Figure 5-14 for the application database.

Prediction performance for axial location of CHF, corresponding to Figure 5-7 for the development database, shows that similar results as shown in Figure 5-15 for the application database.

This proves that the KCE-1 CHF correlation, which was developed under the assumption of the measured CHF for the non-uniform axial power distribution as that for the { }<sup>TS</sup>, has conservatism more than { }<sup>TS</sup> for 95/95 DNBR limit in the database and/or more than { }<sup>TS</sup> for DNBR in actual design application, respectively.

### 5.3.5 Effect of Measurement Uncertainties

Uncertainties of each measured variable of the CHF test are inherently captured in the 95/95 DNBR limit, which is described in Section 5.2. Also, the conservatism that derives from the application of Tong factor  $F_c$  in design analysis can offset the effect of measurement uncertainties.

**Table 5-1 D' Normality Test (Development Database)**

TS	$n$	$\bar{x}_{(M/P)}$	$S_{(M/P)}$	S	T	D' Calculated	D' P=0.025	D' P=0.975	Test
101									) TS
102									
All									

**Table 5-2 Statistical Tests for Each Data Group (Development Database)**

• KCE-1 CHF Correlation Data Groups

Test Section	Bundle Array	Rod Diam. [ in ]	Heated Length [ in ]	Grid Spacing [ in ]	Guide Thimble	Axial Power Distribution	$n$	$\bar{x}_{(M/P)}$	$S_{(M/P)}$
101	6x6	0.374	150.0	15.7	Yes	1.475 Cosine	[		]
102	6x6	0.374	150.0	15.7	No	1.475 Cosine			
All									

• Bartlett Test Results

TS	$n$	$\bar{x}_{(M/P)}$	$S_{(M/P)}$	$K$	$M/C$	$\chi^2_{0.95}$	Test
101	[						]
102							
All							

• Unpaired  $t$  Test Results

TS	$n$	$\bar{x}_{(M/P)}$	$S_{(M/P)}$	$\bar{x}_1 - \bar{x}_2$	$s_0$	$t$	$t_{0.025,319}$	Test
101	[							]
102								
All								

• Wilcoxon-Mann-Whitney Test Results

TS	$N$	$W$	$\mu_{W_1}$	$\sigma^2_{W_1}$	$z$	$z_{0.95}$	Test
101	[						]
102							
All							

**Table 5-3 95/95 DNBR Limits for Each Data Group (Development Database)**

- 95/95 DNBR Limit calculated with  $\left[ \begin{array}{c} \text{TS} \\ \bar{x}_{(M/P)} \\ s_{(M/P)} \\ n \\ K \end{array} \right]^{\text{TS}}$ 

TS	$\bar{x}_{(M/P)}$	$s_{(M/P)}$	$n$	$K$	95/95 DNBR Limit (DNBR <sub>95</sub> )
- $\left[ \begin{array}{c} \text{TS} \\ \gamma \\ P \\ n \\ m^* \\ \text{Value} \end{array} \right]^{\text{TS}}$  95/95 DNBR Limit
 

TS	$\gamma$	$P$	$n$	$m^*$	Value	95/95 DNBR Limit (DNBR <sub>95</sub> )

\* Ranking of Data

Run	M/P	Rank( $m$ )
		1
		2
		3
		4
		5
		6
		7
		8

**Table 5-4 KCE-1 CHF Correlation Statistical Data per Local Fluid Condition Extraction Method (Development Database)**

- | [ ] <sup>TS</sup> (minimum DNBR per each [ ] <sup>TS</sup> ) |          |                   |             |  |
|--|----------|-------------------|-------------|--|
| TS   | <i>n</i> | $\bar{x}_{(M/P)}$ | $S_{(M/P)}$ | 95/95 DNBR Limit (DNBR <sub>95</sub> ) |
| 101  |          |                   |             |  |
| 102  |          |                   |             |  |
| All  |          |                   |             |  |

- | Regardless of [ ] <sup>TS</sup> (minimum DNBR [ ] <sup>TS</sup> ) |          |                   |             |  |
|---|----------|-------------------|-------------|--|
| TS  | <i>n</i> | $\bar{x}_{(M/P)}$ | $S_{(M/P)}$ | 95/95 DNBR Limit (DNBR <sub>95</sub> ) |
| 101   |          |                   |             |  |
| 102   |          |                   |             |  |
| All   |          |                   |             |  |

**Table 5-5 KCE-1 CHF Correlation Conservatism based on Application Database**

Test Section	M/P Statistics				95/95 DNBR	Remark
	N	Average	Standard Deviation	Minimum M/P		
101						*)
102						
All					*	

\*)

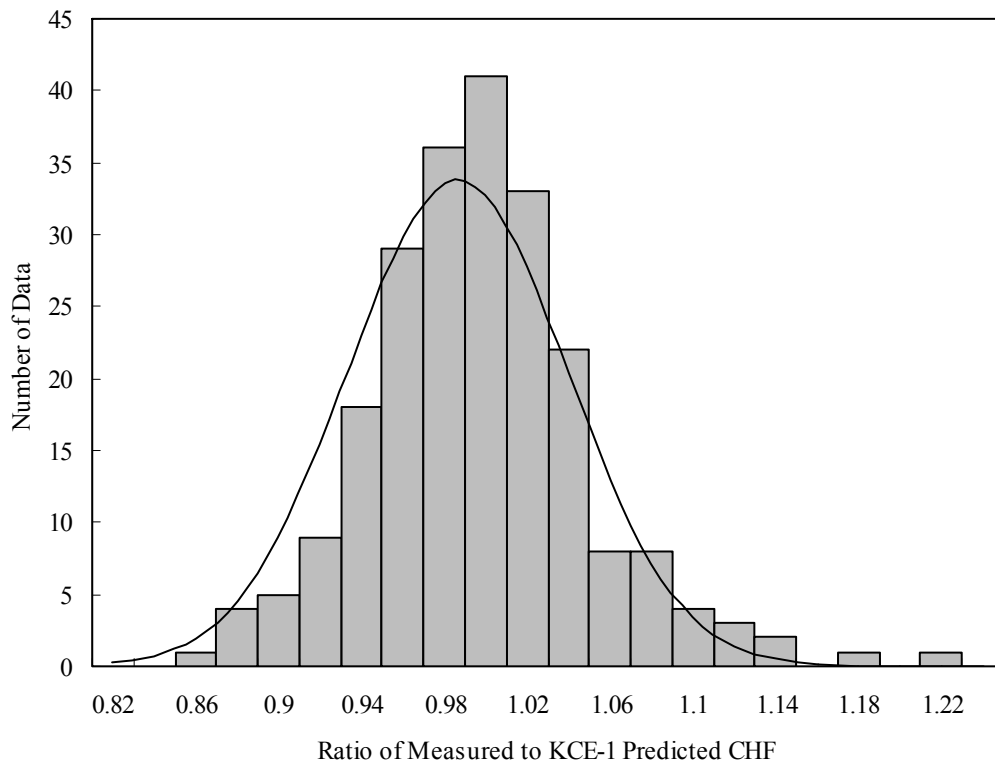


**Figure 5-1 Frequency Diagram of M/P for Test Section TS101 (Development Database)**

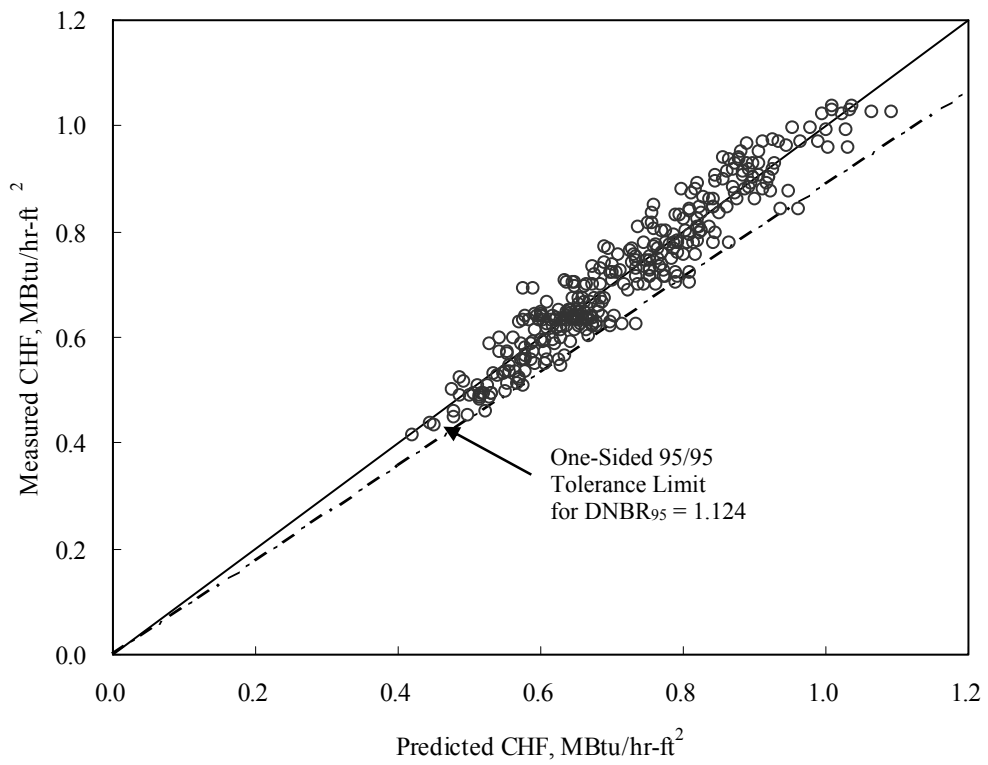


**Figure 5-2 KCE-1 CHF Correlation Predicted CHF versus Measured CHF (Development Database)**

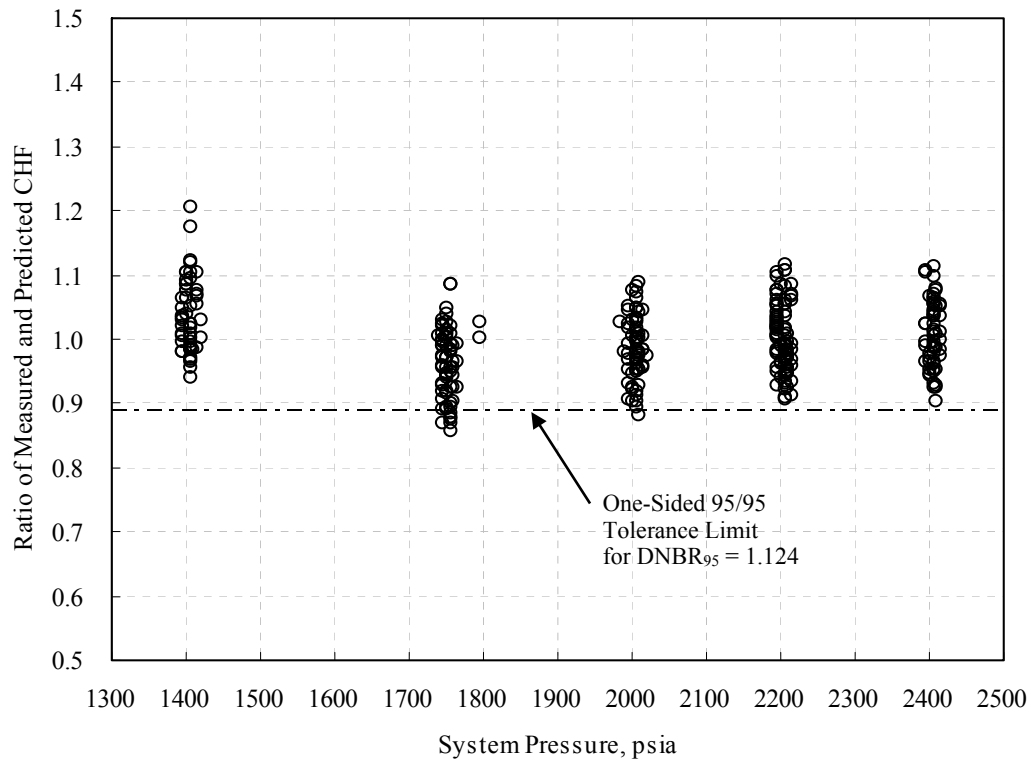


**Figure 5-3 Distribution of M/P versus System Pressure (Development Database)**

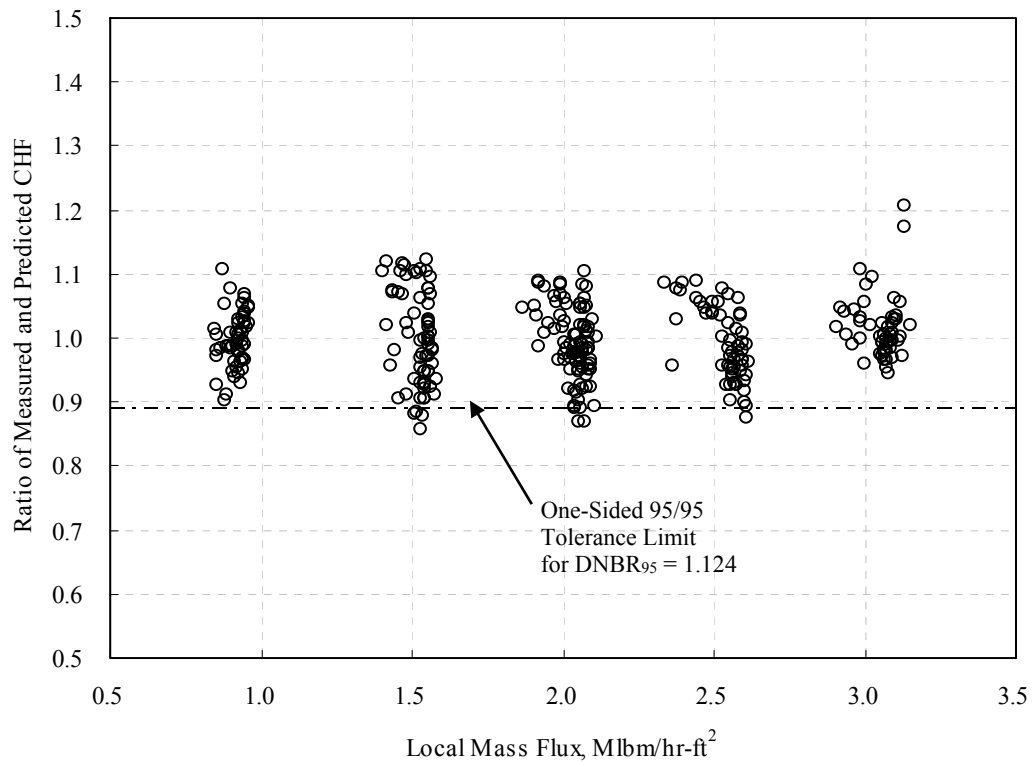


**Figure 5-4 Distribution of M/P versus Local Mass Flux (Development Database)**

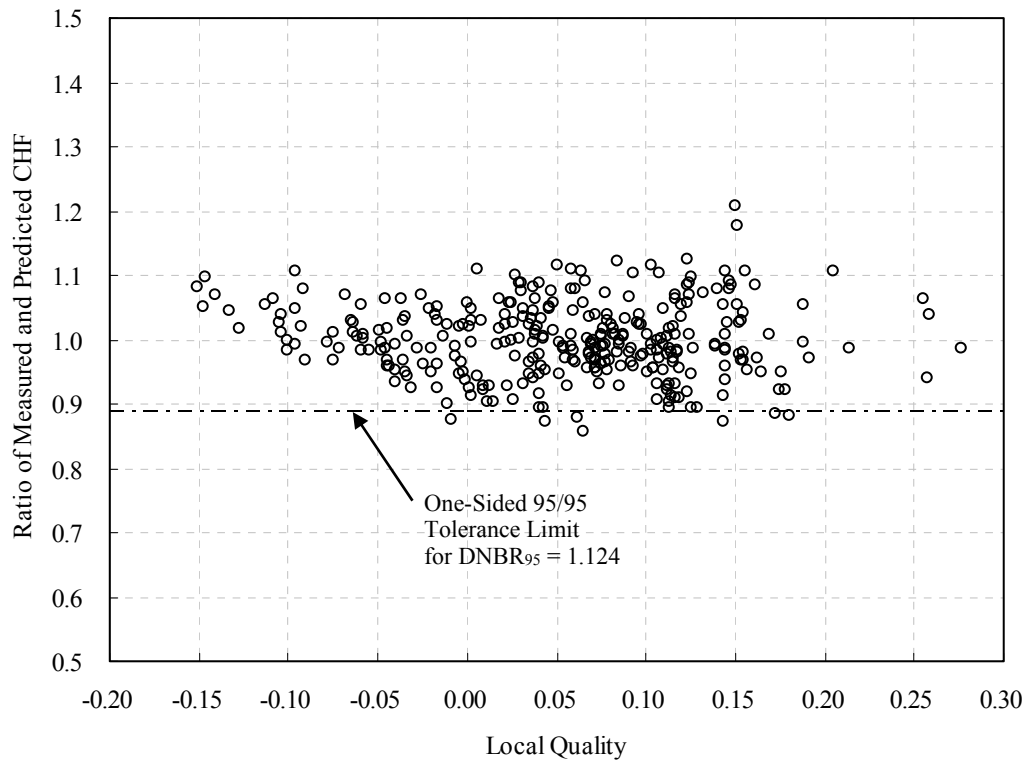
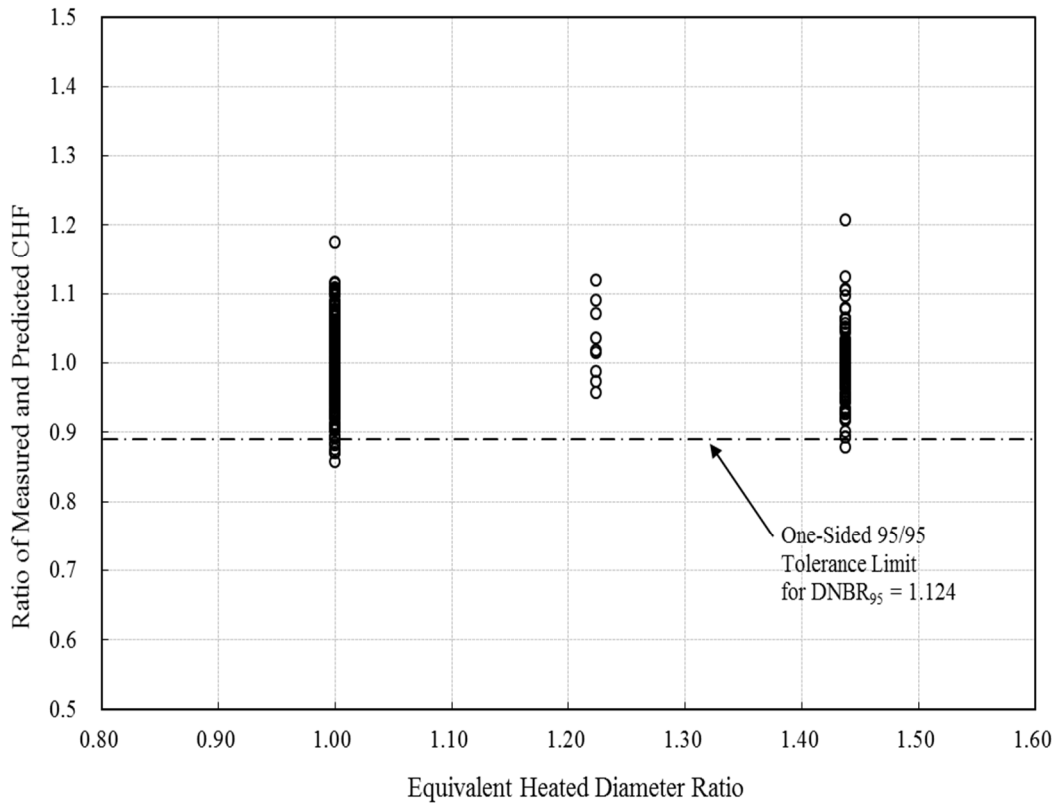
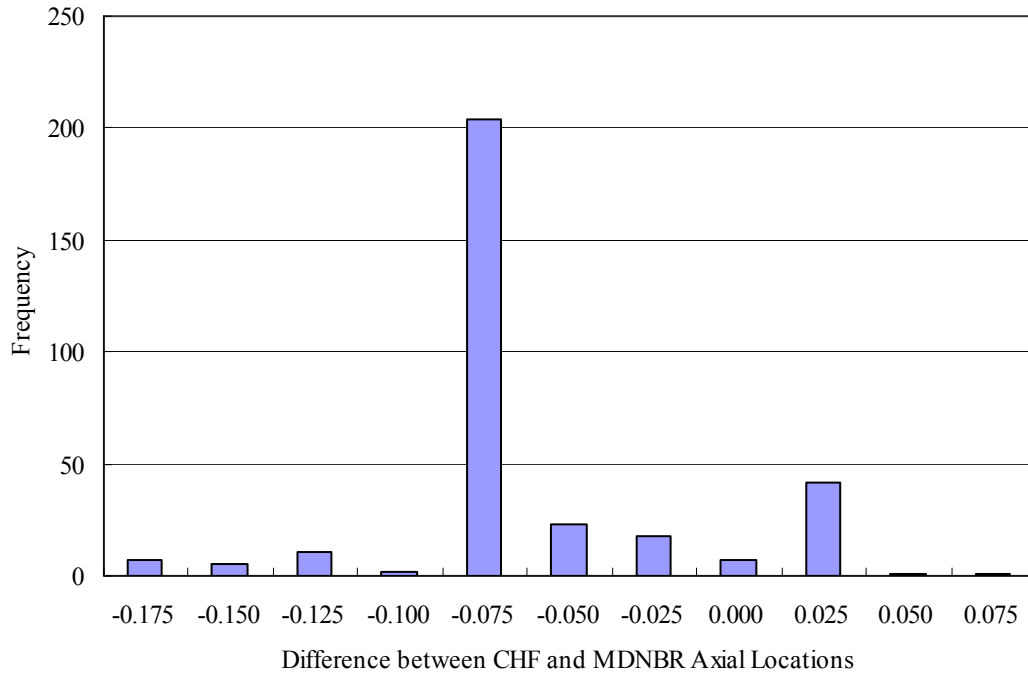


Figure 5-5 Distribution of M/P versus Local Quality (Development Database)



**Figure 5-6 Distribution of M/P versus Equivalent Heated Diameter Ratio (Development Database)**



$$Difference = \frac{(MDNBR \text{ Axial Location}) - (CHF \text{ Axial Location})}{Heated \text{ Length}}$$

**Figure 5-7 Prediction Accuracy of KCE-1 CHF Correlation for CHF Axial Location (Development Database)**



**Figure 5-8 Frequency Diagram of M/P for Test Section TS101 for Application Database**



**Figure 5-9 KCE-1 CHF Correlation Predicted CHF versus Measured CHF for Application Database**



**Figure 5-10 Distribution of M/P versus System Pressure for Application Database**



**Figure 5-11 Distribution of M/P versus Local Mass Flux for Application Database**



**Figure 5-12 Distribution of M/P versus Local Quality for Application Database**



**Figure 5-13 Distribution of M/P versus Equivalent Heated Diameter Ratio for Application Database**



**Figure 5-14 Distribution of M/P versus Tong Factor for Application Database**



**Figure 5-15 Prediction Accuracy of KCE-1 CHF Correlation for CHF Axial Location for Application Database**

## 6. CORRELATION APPLICATION

KEPCO Nuclear Fuel uses the KCE-1 CHF correlation for evaluating thermal design of the PLUS7 fuel assembly and the reactor core of APR1400 and OPR1000 in accordance with the CHF or DNB acceptance criteria defined in the Standard Review Plan (SRP)<sup>(12)</sup>.

Sections 4.2 and 4.4 of SRP state that the DNB acceptance criterion provides assurance that there be at least a 95% probability at the 95% confidence level that the hot fuel rod in the core does not experience a DNB or transition condition during normal operation or AOOs (Anticipated Operational Occurrences). The acceptance criterion is met in thermal design and safety analysis when the MDNBR of the hot rod in the hot channel is above appropriate DNBR limit (Specified Acceptable Fuel Design Limit, SAFDL) which includes 95/95 DNBR limit of the KCE-1 correlation. The results of KCE-1 CHF correlation applying to AOO analysis of APR1400 would be included corresponding subsection of the APR1400 Design Control Document (DCD) Section 4.4. Establishment of the KCE-1 correlation 95/95 DNBR limit was presented in Chapter 5. The KCE-1 CHF correlation was used only with a computer code that has been used for the correlation development and has been qualified with the 95/95 DNBR limit.

The KCE-1 CHF correlation 95/95 DNBR limit and its supporting M/P statistics with the TORC code is 1.124. The application ranges of the parameters, based on database, are given in Table 4.4. Note that the Tong factor  $F_c$  is [ ]<sup>TS</sup> are applied to MDNBR calculation for the design application and safety analyses. The value of Tong factor  $F_c$  depends on the various axial power distribution and local fluid conditions but it is conservatively limited to [ ]<sup>TS</sup>. The application of the KCE-1 CHF correlation with TORC code is in full compliance with the conditions of the Safety Evaluation Report (SER) on the TORC code and modeling for CE-PWRs. The OPR1000 and the APR1400 are CE-PWRs.

The TORC code is used in thermal design and safety analyses to perform detailed modeling of the core and hot assembly and to determine MDNBR in the hot assembly.

The KCE-1 CHF correlation is implemented to TORC code by modifying correlation coefficients only. Note that the functional formula is identical for both KCE-1 and CE-1 CHF correlations, as described in Section 4.3.

Thus, the topical reports described in References 2 and 3 for TORC code will remain valid with the application of KCE-1 CHF correlation.

Even though a higher value of inverse Peclet number based on the empirically determined thermal diffusion coefficient was used in the TORC model for CHF data analysis and correlation development, the reactor analysis is to be performed with the design inverse Peclet number ( $1/Pe = 0.0101$ ). This is equivalent to the value of the thermal diffusion coefficient ( $TDC = 0.038$ ) applied to the Westinghouse PWR for fuel assembly with "R" mixing vane grid design<sup>(13)</sup>.

## 7. CONCLUSION

The CHF tests were performed with two test sections simulating with and without a guide thimble tube, respectively. Each test section was composed of 6x6 heater rods with a heated length of 150 inches and a grid span of 15.7 inches, in accordance with the PLUS7 fuel geometry. The tests were performed with a non-uniform cosine axial power shape and the radial power split between hot and cold rods was approximately 1 : 0.82.

The KCE-1 CHF correlation was developed based on the CHF test data of the PLUS7 fuel. The functional formula of the KCE-1 CHF correlation is the same as the CE-1 CHF correlation. The correlation coefficients were optimized by performing a non-linear multiple-regression analysis for the measured CHF data along the local fluid conditions calculated by a subchannel analysis code, TORC. During the development stage, the non-uniform axial power distribution correction factor, the Tong factor  $F_C$ , was {  $\left[ \frac{1}{1 + 0.0001 \left( \frac{P}{P_{ref}} \right)^{1.5}} \right]^{TS}$  } of nuclear power plants. The optimized correlation coefficients are presented in Table 4-4.

Based on the statistical analysis of the test data groups used for the correlation development and for the correlation DNBR limit establishment, the most conservative DNBR limit for the test sections was established as the 95/95 DNBR limit of the KCE-1 CHF correlation. Based on the local fluid conditions used for the correlation development, the applicable ranges of parameters for the KCE-1 CHF correlation were determined. The results are summarized in the following table.

- Statistical results for KCE-1 CHF Correlation

Number of Data	$\bar{x}_{(M/P)}$	$S_{(M/P)}$	Correlation DNBR Limit (95/95 Limit)
225	0.9866	0.05304	1.124

- Application ranges of parameters for KCE-1 CHF Correlation

Parameter	British Unit	SI Unit
System Pressure	1750 ~ 2415 <i>psia</i>	12.07 ~ 16.65 <i>MPa</i>
Local Mass Flux	0.85 ~ 3.15 <i>Mlbm/hr-ft<sup>2</sup></i>	1153 ~ 4272 <i>kg/s-m<sup>2</sup></i>
Local Quality	-0.150 ~ 0.275	

The data groups used for the correlation development were generated conservatively and any adverse trend was not observed against the correlation DNBR limit (95/95 DNBR limit). Thus, the validity of the CHF correlation and the established correlation DNBR limit were confirmed.

The KCE-1 CHF correlation can be applied to the thermal design and safety analysis with the Westinghouse thermal hydraulic design code TORC for the OPR1000 and the APR1400, which PLUS7 fuels are loaded.

## 8. REFERENCES

- (1) APR1400-F-M-TR-12001-P Rev.0, "PLUS7 Fuel Design for the APR1400," November 2012.
- (2) CENPD-161-P-A, "TORC Code, A Computer Code for Determining the Thermal Margin of a Reactor Core," April 1986.
- (3) CENPD-206-P-A, "TORC Code, A Verification and Simplified Modeling Methods," June 1981.
- (4) { }<sup>TS</sup>
- (5) EPRI NP-2609, "Parametric Study of CHF Data, Volume 1 : Compilation of Rod Bundle CHF Data Available at the Columbia University Heat Transfer Research Facility", September 1982.
- (6) { }<sup>TS</sup>
- (7) { }<sup>TS</sup>
- (8) { }<sup>TS</sup>
- (9) CENPD-162-P-A, "C-E Critical Heat Flux, Critical Heat Flux Correlation for C-E Fuel Assemblies with Standard Spacer Grids, Part 1 Uniform Axial Power Distribution," September 1976.
- (10) CENPD-207-P-A, "C-E Critical Heat Flux, Critical Heat Flux Correlation for C-E Fuel Assemblies with Standard Spacer Grids, Part 2 Nonuniform Axial Power Distribution," December 1984.
- (11) Tong, L. S., Boiling Crisis and Critical Heat Flux, U. S. Atomic Energy Commission, 1972.
- (12) NUREG-0800, "Standard Review Plan Section 4.2, 'Fuel System Design' Revision 3, and Section 4.4, 'Thermal and Hydraulic Design' Revision 2," March 2007.
- (13) ML071580898 - Westinghouse AP1000 Design Control Document Rev.16 – Tier 2 "Chapter 4 – Reactor – Section 4.4 Thermal and Hydraulic Design," May 2007.

## APPENDIX A. DATA FOR KCE-1 CHF CORRELATION DEVELOPMENT/APPLICATION

The raw test data, { }<sup>TS</sup> in total, collected from the PLUS7 fuel CHF tests are listed in Table A-1. The initial dataset, { }<sup>TS</sup> in total, extracted from the measured CHF location is presented in Table A-2 of APPENDIX A. The { }<sup>TS</sup> local fluid conditions excluded during the correlation development process from the local fluid conditions for each test data calculated by the TORC code are listed along with the reason for exclusion in Table A-3. The KCE-1 CHF correlation development database, { }<sup>TS</sup> in total, is presented in Table A-4.

Application database of the KCE-1 CHF correlation, { }<sup>TS</sup>, is presented in Table A-6 with excluded data in Table A-5.

Acronyms presented in the subsequent tables:

TS	:	test section number
RUN	:	run number
PR	:	system pressure, <i>psia</i>
TIN	:	inlet temperature, °F
GIN	:	inlet mass flux (inlet mass velocity), <i>Mlbm/hr-ft<sup>2</sup></i>
BAP	:	bundle average power, <i>MW</i>
HFX	:	heat flux (BAP/bundle heat transfer area*unit conversion factor), <i>MBtu/hr-ft<sup>2</sup></i>
TC	:	primary CHF rod and thermocouple number (XX.x)*
CT	:	CHF subchannel type
M	:	matrix subchannel
C	:	guide thimble corner subchannel
S	:	guide thimble side subchannel
GL	:	local mass flux (local mass velocity), <i>Mlbm/hr-ft<sup>2</sup></i>
XL	:	local quality
DH	:	equivalent heated diameter of CHF subchannel (4 * flow area / heated perimeter of the subchannel of interest), <i>in.</i>
DHM	:	equivalent heated diameter of matrix subchannel(4 * flow area / heated perimeter of the matrix subchannel), <i>in.</i>
CHFM	:	measured CHF (HFX * rod power factor * axial power factor at the elevation of interest), <i>MBtu/hr-ft<sup>2</sup></i>
CHFP	:	KCE-1 correlation predicted CHF, <i>MBtu/hr-ft<sup>2</sup></i>
Fc	:	Tong factor
HL	:	length from BOHL, <i>in.</i>
CH	:	subchannel number
hfg	:	latent heat of vaporization, <i>Btu/lbm</i>
DNBR	:	departure from nucleate boiling ratio
M/P	:	ratio of measured CHF to predicted CHF

\* XX = Rod number, x = T/C number  
(See Figure 2-5 through Figure 2-7 and Figure 2-9.)

**Table A-1 PLUS7 CHF Test Data ( 1/5 )**

TS	RUN	PR	TIN	GIN	BAP	HFX	TC

**Table A-1 PLUS7 CHF Test Data ( 2/5 )**

TS	RUN	PR	TIN	GIN	BAP	HFX	TC

**Table A-1 PLUS7 CHF Test Data ( 3/5 )**

TS	RUN	PR	TIN	GIN	BAP	HFX	TC

**Table A-1 PLUS7 CHF Test Data ( 4/5 )**

TS	RUN	PR	TIN	GIN	BAP	HFX	TC

**Table A-1 PLUS7 CHF Test Data ( 5/5 )**

TS	RUN	PR	TIN	GIN	BAP	HFX	TC

**Table A-2 KCE-1 CHF Correlation Initial Dataset (1/7)**

TS	CT	RUN	PR	GL	XL	hfg	DH	DHM	CHFM

**Table A-2 KCE-1 CHF Correlation Initial Dataset (2/7)**

TS	CT	RUN	PR	GL	XL	hfg	DH	DHM	CHFM

**Table A-2 KCE-1 CHF Correlation Initial Dataset (3/7)**

TS	CT	RUN	PR	GL	XL	hfg	DH	DHM	CHFM

TS

**Table A-2 KCE-1 CHF Correlation Initial Dataset (4/7)**

TS	CT	RUN	PR	GL	XL	hfg	DH	DHM	CHFM

TS

**Table A-2 KCE-1 CHF Correlation Initial Dataset (5/7)**

TS	CT	RUN	PR	GL	XL	hfg	DH	DHM	CHFM

**Table A-2 KCE-1 CHF Correlation Initial Dataset (6/7)**

TS	CT	RUN	PR	GL	XL	hfg	DH	DHM	CHFM

TS

**Table A-2 KCE-1 CHF Correlation Initial Dataset (7/7)**

TS	CT	RUN	PR	GL	XL	hfg	DH	DHM	CHFM

TS

**Table A-3 Test Data Groups Excluded during KCE-1 CHF Correlation Development**

TS	CT	RUN	PR	GL	XL	hfg	DH	DHM	CHFM	CHFP	M/P	Remark

**Table A-4 KCE-1 CHF Correlation Database (1/8)**

TS	CT	RUN	PR	GL	XL	hfg	DH	DHM	CHFM	CHFP	M/P

**Table A-4 KCE-1 CHF Correlation Database (2/8)**

TS	CT	RUN	PR	GL	XL	hfg	DH	DHM	CHFM	CHFP	M/P

**Table A-4 KCE-1 CHF Correlation Database (3/8)**

TS	CT	RUN	PR	GL	XL	hfg	DH	DHM	CHFM	CHFP	M/P

**Table A-4 KCE-1 CHF Correlation Database (4/8)**

TS	CT	RUN	PR	GL	XL	hfg	DH	DHM	CHFM	CHFP	M/P

**Table A-4 KCE-1 CHF Correlation Database (5/8)**

TS	CT	RUN	PR	GL	XL	hfg	DH	DHM	CHFM	CHFP	M/P

**Table A-4 KCE-1 CHF Correlation Database (6/8)**

TS	CT	RUN	PR	GL	XL	hfg	DH	DHM	CHFM	CHFP	M/P

**Table A-4 KCE-1 CHF Correlation Database (7/8)**

TS	CT	RUN	PR	GL	XL	hfg	DH	DHM	CHFM	CHFP	M/P

**Table A-4 KCE-1 CHF Correlation Database (8/8)**

TS	CT	RUN	PR	GL	XL	hfg	DH	DHM	CHFM	CHFP	M/P

**Table A-5 Data Excluded from Application Database**

TS	RUN	PR	CHFM	HL	GL	XL	CH.	hfg	Fc	DH	DHM	DNBR	M/P	Remark

**Table A-6 KCE-1 CHF Correlation Application Database (1/5)**

TS	RUN	PR	CHFM	HL	GL	XL	CH.	hfg	Fc	DH	DHM	DNBR	M/P

TS

**Table A-6 KCE-1 CHF Correlation Application Database (2/5)**

TS	RUN	PR	CHFM	HL	GL	XL	CH.	hfg	Fc	DH	DHM	DNBR	M/P

**Table A-6 KCE-1 CHF Correlation Application Database (3/5)**

TS	RUN	PR	CHFM	HL	GL	XL	CH.	hfg	Fc	DH	DHM	DNBR	M/P

**Table A-6 KCE-1 CHF Correlation Application Database (4/5)**

TS	RUN	PR	CHFM	HL	GL	XL	CH.	hfg	Fc	DH	DHM	DNBR	M/P

TS

**Table A-6 KCE-1 CHF Correlation Application Database (5/5)**

TS	RUN	PR	CHFM	HL	GL	XL	CH.	hfg	Fc	DH	DHM	DNBR	M/P

TS

## APPENDIX B. STATISTICAL ANALYSIS

To develop the CHF correlation and establish the correlation DNBR limit (95/95 DNBR limit), a series of statistical analyses were conducted for each CHF test data group and combined data group. The statistical tests applied to these processes are explained briefly in APPENDIX B.

### B.1 Treatment of Outliers <sup>(B-1)</sup>

The objective of this statistical test is to statistically evaluate whether a specific datum (suspected observation) is excluded from a certain data group or not. To do this, the symbols 'a' and 'b' are defined as follows:

$$a = \bar{x} - s \cdot z_{1-\alpha'/2}$$

$$b = \bar{x} + s \cdot z_{1-\alpha'/2}$$

where,  $\bar{x}$  sample mean,  
 $s$  sample standard deviation,  
 $z$  normal distribution index  
 $\alpha'$   $\alpha' = 1 - (1 - \alpha)^{1/n}$   
 $\alpha$  significance probability,  
 $n$  sample size.

Any observation that does not lie in the interval a to b is rejected. The method assumes a normal distribution and the values of the population mean and the population standard deviation of the data are reasonable estimates of those of the sample. Therefore, care must be taken to ensure the fact that the elimination of outliers is justifiable.

### B.2 Normality Tests <sup>(B-2)</sup>

The assumption of a normal distribution is evaluated for a data group comprising more than fifty (50) data with the D' test. D' is defined as:

$$D' = T/S$$

where,

$$S = \left[ \sum_{i=1}^n (x_i - \bar{x})^2 \right]^{1/2},$$

$$T = \sum_{i=1}^n \left[ i - \frac{(n+1)}{2} \right] \cdot x_i, \quad x_i \text{ in ascending order.}$$

The hypothesis of a normal distribution is rejected if the calculated value of D' falls outside of the range established from of the D' distribution table for the probability or risk intended to be tested. The D' test is a more rigorous method compared to other tests such as the Kolomogorov-Smirnov test, etc.

### B.3 Statistical Test for Comparison of Data Groups <sup>(B-1), (B-3), (B-4), (B-5)</sup>

Statistical tests were performed to determine whether data groups could be considered to come from the same population or not, in order to be combined for the evaluation of the 95/95 DNBR tolerance limit of the CHF correlation. For normally distributed data groups, the assumption of the same population could be examined via tests for the homogeneity of variances by Bartlett's test and the homogeneity of means by a t-test or a one-way ANOVA. The unpaired t-test is used to examine the homogeneity of means between two (2) data groups while the one-way ANOVA (analysis of variance)

test is widely used to examine the homogeneity of means among multiple data groups of more than or equal to three (3).

For the data groups that failed to pass the normality test, the Wilcoxon-Mann-Whitney test is performed to check the null hypotheses that the data from two (2) independent data groups were sampled from the same population. For multiple data groups, the Kruskal-Wallis One Way Analysis of Variance by Ranks test is performed.

Considering that there were two (2) data groups for the KCE-1 CHF correlation development, statistical test methods for comparison of two (2) data groups are described in this APPENDIX B.3.

### B.3.1 Bartlett's Test <sup>(B-3)</sup>

For a set of variances ( $s^2$ ) estimated from  $K$  independent samples extracted from normal distribution having a common variance ( $\chi^2$ ), Bartlett showed that a quantity  $M/C$  would have a distribution satisfactorily approximated by the distribution defined the symbols of  $M$  and  $C$  as follows;

$$M = N \ln \left( N^{-1} \sum_{i=1}^K v_i s_i^2 \right) - \sum_{i=1}^K v_i \ln s_i^2$$

$$C = 1 + \frac{1}{3(K-1)} \left( \sum_{i=1}^K \frac{1}{v_i} - \frac{1}{N} \right)$$

where,  $s_i^2$  estimated variance of the  $i$ -th group with  $v_i$  degree of freedom,  
 $K$  number of data groups,

$$N = \sum_{i=1}^K v_i$$

If the value of  $M/C$  is within the range of the  $\chi^2$  distribution table with  $(K-1)$  degree of freedom and probability or risk to be tested, then it could be assumed that the data groups are sampled from the same population.

### B.3.2 Unpaired $t$ Test <sup>(B-4)</sup>

If data from two groups with normal distribution passed the Bartlett statistical test for the homogeneity of variances, the unpaired  $t$  test, which evaluates the hypothesis of homogeneity of the means that  $\bar{x}_1 - \bar{x}_2 = 0$  or  $\bar{x}_1 = \bar{x}_2$  was employed. Here,  $\bar{x}_1$  and  $\bar{x}_2$  represent the mean of data groups 1 and 2, respectively.

$$t = \frac{\bar{x}_1 - \bar{x}_2}{s_o \left( \frac{1}{n_1} + \frac{1}{n_2} \right)^{1/2}}$$

$$s_o^2 = \frac{\sum_{j=1}^{n_1} (x_{1,j} - \bar{x}_1)^2 + \sum_{j=1}^{n_2} (x_{2,j} - \bar{x}_2)^2}{n_1 + n_2 - 2}, \quad \text{pooled estimate}$$

where,  $x_{i,j}$   $j$ th variation for the data group  $i$ ,  
 $n_j$  number of data for the data group  $i$ .

If the calculated  $t$  value is less than ( $t_{\alpha/2, n_1+n_2-2}$ ) of the  $t$ -distribution table with probability or risk to be tested, the hypothesis is accepted.

### B.3.3 Wilcoxon-Mann-Whitney test <sup>(B-1), (B-5)</sup>

For combinations where one or both tests fail the normality, the Wilcoxon-Mann-Whitney test is used to examine whether data from two groups were extracted from the same population or not. The test could be applied to a data comparison regardless of the normality and/or homogeneity of variances where one of the data group comprises more than ten (10) data. The data of two groups should be mixed and sorted in ascending order.

$$\mu_{W_1} = \frac{n_1(N+1)}{2}$$

$$\sigma_{W_1}^2 = \frac{n_1 \cdot n_2 (N+1)}{12}$$

where,  $W_1$  sum of the ranks of data in a small data group,  
 $n_1$  number of data for a small data group,  
 $n_2$  number of data for a large data group,  
 $N$  total number of data ( $N = n_1 + n_2$ )

Accordingly, if the  $z$  value defined below is less than the value  $Z_{1-\alpha}$  of for the standard normal distribution table with probability or risk to be tested, the hypothesis that the two data groups are sampled from the same population is passed or accepted.

$$z = \frac{W_1 \pm 0.5 - \mu_{W_1}}{\sigma_{W_1}}$$

### B.4 Statistical Limit Establishment <sup>(B-1), (B-6)</sup>

For the selection of data groups used for the correlation 95/95 DNBR tolerance limit calculations, the statistical test for the data group comparison described in section B.3 is performed. If the normality test is passed, the correlation DNBR limit is calculated with Owen's one-sided tolerance limit factor for the data group(s). If not, it is determined with the distribution-free one-sided limit or the non-parametric limit for the data group(s).

#### B.4.1 95/95 DNBR Tolerance Limit for Normal Distribution Data Group

For the data groups that passed the D' normality test, the 95/95 DNBR limit was calculated as follows:

$$DNBR_{95/95} = \frac{1}{\bar{x} - K \cdot s}$$

where,  $\bar{x}$  mean of the ratio of measured CHF to predicted one  
 $s$  standard deviation of the ratio of measured CHF to predicted one  
 $K$  confidence multiplication factor<sup>(B-6)</sup>

The confidence multiplication factor for the 95/95 probability/confidence is given as:

$$K = \frac{1.645 + 1.645 \left[ 1 - \left( 1 - \frac{2.706}{2(N-1)} \right) \left( 1 - \frac{1}{N} \right) \right]^{1/2}}{1 - \frac{2.706}{2(N-1)}}$$

where,  $N$  = number of data

#### **B.4.2 95/95 DNBR Tolerance Limit for Distribution-Free Data Group**

The distribution-free one-sided limit was established for the data groups that did not pass the D' normality test. The largest value of rank ( $m$ ) from Table A-31 of Reference B-1 is used such that one can assert with a 95% confidence ( $\gamma$ ) that 95% of the probability ( $P$ ) lies above the  $m$ -th smallest value of  $x_i$ , an individual datum. The inverse of this value is the 95/95 DNBR limit.

#### **B.5 References**

- (B-1) Natrella, M. G., "Experimental Statistics," National Bureau of Standards Handbook 91, Issued August 1963, Reprinted October, 1966 with corrections.
- (B-2) ANSI N15.15-1974, "American National Standard Assessment of the Assumption of Normality (Employing Individual Observed Values)," October 3, 1973.
- (B-3) Pearson, E. S. and Hartley, H. O., "Biometrika Tables for Statisticians," Vol. I, Third Edition, Cambridge, 1966, pp. 63-66 and table 7.
- (B-4) Crow, E. L., Davis, F. A., and Maxfield, M. W., "Statistics Manual," Dover Publications, 1960.
- (B-5) Siegal, S., and Castellan, Jr., N. J., "Nonparametric Statistics for the Behavioral Sciences," 2nd Edition, McGraw-Hill, 1988, pp. 128-137 & 206-216.
- (B-6) Owen, D. B., "Factors for One-sided Tolerance Limits and for Variable Sampling Plans," SC-R-607, March 1963.

**Non-Proprietary**

Page intentionally left blank

**Non-Proprietary**

**SECTION C**

Non-Proprietary

Page intentionally left blank

**KHNP****KOREA HYDRO & NUCLEAR POWER CO., LTD**

70-1312-gil, Yuseong-daero, Yuseong-gu, Daejeon, 305-343, KOREA

Tel: +82-42-870-5740 / Fax: +82-42-870-5779

<http://www.khnp.co.kr>

March 2, 2015  
Document Control Desk  
U.S. Nuclear Regulatory Commission  
Washington, DC 20555-0001

Attention: Mr. Jeff Ciocco  
Division of New Reactor Licensing

Project No.0782  
MKD/NW-15-0002L

**Subject: Revised Response to RAI 3-7443**

**Reference: 1) NRC Request for Additional Information 3-7443, dated March 25, 2014**

KHNP is hereby submitting revised response to the Request for Additional Information (RAI) 3-7443, dated March 25, 2014 as discussed with the NRC staff during the audit held on 21-22 January, 2015. This RAI response addresses questions 1 through 18 of the RAI 3-7443.

Enclosure 1 contains one copy of the associated affidavit. Enclosure 2 provides Revised Response to RAI 3-7443 on Topical Report "KCE-1 Critical Heat Flux Correlation for PLUS7 Thermal Design" APR1400-F-C-TR-12002-P, Rev.0 (Proprietary), and Enclosure 3 provides Revised Response to RAI 3-7443 on Topical Report "KCE-1 Critical Heat Flux Correlation for PLUS7 Thermal Design" APR1400-F-C-TR-12002-NP, Rev.0 (Non-proprietary).

If additional information or clarification is required, please contact Yunho Kim, director of KHNP Washington DC center at [yunho.kim@khnp.co.kr](mailto:yunho.kim@khnp.co.kr) or 703-388-0592.

Sincerely,

Myung-Ki Kim  
Project Manager  
Advanced Reactors Development Laboratory  
Central Research Institute  
Korea Hydro and Nuclear Power Co., Ltd  
70 Yuseong-daero 1312 Beon-gil, Yuseong-gu, Daejeon 305-353, Korea  
Office: 82-42-870-5700/Cell: 82-10-2737-8915  
Email: [kimmkcri@khnp.co.kr](mailto:kimmkcri@khnp.co.kr)

Enclosures:

1. Affidavit KAW-15-0002
2. Revised Response to RAI 3-7443 on Topical Report "KCE-1 Critical Heat Flux Correlation for PLUS7 Thermal Design" APR1400-F-C-TR-12002-P, Rev.0 (Proprietary)



**KHNP**  
KOREA HYDRO & NUCLEAR POWER CO., LTD

3. Revised Response to RAI 3-7443 on Topical Report “KCE-1 Critical Heat Flux Correlation for PLUS7 Thermal Design” APR1400-F-C-TR-12002-NP, Rev.0 (Non-proprietary)

Cc: Mr. Samuel S. Lee

**Non-Proprietary**

Page intentionally left blank

**Non-Proprietary**

Page intentionally left blank

Enclosure 3

Docket No. PROJ 0782

Revised Response to RAI 3-7443 on Topical Report  
“KCE-1 Critical Heat Flux Correlation for PLUS7 Thermal Design”  
APR1400-F-C-TR-12002-NP, Rev.0

February 2015

Non-Proprietary Version

## RESPONSE TO REQUEST FOR ADDITIONAL INFORMATION

### APR1400 Topical Reports

Korea Electric Power Corporation / Korea Hydro & Nuclear Power Co., LTD

Docket No. PROJ 0782

RAI No.: 3-7443 Question 1

SRP Section: N/A

Application Section: KCE-1 Critical Heat Flux Correlation for PLUS7 Thermal Design  
(APR1400-F-C-TR-12002-NP, Rev.0)

Date of RAI Issued: 03/25/2014

Response Date: 02/25/2015

### Question 1

According to the KCE-1 CHF topical report (APR1400-F-C-TR-12002-P Rev.0), an overall heat balance was not performed for each CHF data point or for the entire range of the tested bundle power. Rather, the heat balance was typically tested at the beginning of each day of operation under sub-cooled conditions at the test section pressure (1500 psi), inlet temperature (400 °F), mass velocity (1.5 M lbm/hr-ft<sup>2</sup>), and bundle power 1.6 MW. These test conditions are expected to involve much smaller heat losses than the typical CHF measurements reported in the KCE-1 correlation database that involve inlet temperatures as high as 650 °F and 10 MW facility bundle power. The applicant should include the acceptable heat loss tolerance in the topical report, and justify the validity of the heat balance observed at low power and temperature conditions on the entire domain of KCE-1 CHF measurements.

### Response

*The purposes of heat balances were to check the integrity of all loops and bundle instrumentation, and to check the heat losses, if any, before starting/finishing the CHF tests.*

*The [ ]<sup>TS</sup> heat loss (heat balance) acceptance criterion will be included in an appropriate subsection of the topical report (APR1400-F-C-TR-12002), as shown in the attached markup. This value was based on HTRF standard procedure and acceptance criteria (Reference:*

[

]<sup>TS</sup>).

*The heat balance was automatically calculated by DAS (Data Acquisition System) using the energy balance equation below (Reference: [*

]<sup>TS</sup>).

$$H_{loss} = [ \quad ]^{TS} \quad (\text{equation 1-1})$$

where,

$H_{loss}$  = heat loss (%)

[

$]^{TS}$

During the test, two kinds of voltages were measured as presented in section 3.2 of the topical report (APR1400-F-C-TR-12002). The first measurement was the bus to bus voltage (independent and redundant measurements), which was measured between two extreme ends of the heater rods connecting through the bottom of the bottom copper end piece and the tip of the top nickel end piece. It was used to calculate the Bbpwr as described in the response to Question 5 of RAI 3-7443. Bus to bus voltage was considered as the reference voltage to evaluate the heat balance and voltage correction factor. The second measurement was the test section voltage, which was measured at the test section inlet and outlet (active heated region), and was used to calculate the test section power (Tspwr). This Tspwr was considered as [

$]^{TS}$ . For the test section voltage measurement, its measurement line was welded to the inner surface of a specific heater rod. Since the measurement line can break due to thermal stress during the test, the voltage correction factor, defined as [

$]^{TS}$ . The deviation between this correction factor and the measured value was considered in a calculation of overall CHF measurement uncertainty, as addressed in the response to Question 14 of RAI 3-7443.

As described above, bus to bus power (Bbpwr) was applied to evaluate the heat balance. Thus, the calculated heat loss value was not the actual heat loss from the test section but the total heat loss value, which includes all the possible losses, as presented below, and measurement uncertainties. Because the calculation was based on the measured parameters (inlet/exit temperatures, pressure, flow rate, voltage, and current), measurement uncertainties were included implicitly.

There were four (4) main heat loss sources based on Bbpwr, as depicted in Figure 1-1.

- Heat loss through upper/lower parts, including extensions
  - Heat loss through bottom O-ring cooling chambers
  - Heat loss from annulus to environment
  - Heat loss from test section to annulus
- where, annulus is formed by shrouds and the pressure vessel inner wall

[

]TS.

*The impact of heat loss on data quality was also minimized, as shown below.*

- *Optimize test sequence → minimize thermal hydraulic disturbance between data points  
→ minimize disturbance due to temperature fluctuation inside the annulus*
- *Perform CHF test in the sequence of high temperature to low temperature → minimize natural circulation in annulus → reduce heat loss*

*As justified below, the heat balance observed at low power and temperature conditions is valid for the entire domain of KCE-1 CHF measurements.*

[

]TS, as given in Table 1-2.

*In reality, as long as natural circulation disappears and the annulus temperature reaches steady state, heat loss into the annulus will be very small and even a slight heat gain might occur, depending on the prior operating condition. Therefore, a heat balance estimated at the tested condition for PLUS7 CHF Test Program is valid for the entire domain of KCE-1 CHF measurements.*

Note: KAFD was the project name for PLUS7 development (joint program between Westinghouse Electric Company and KEPCO Nuclear Fuel Company)

*Table 1-1 Heat Balance Measurements for PLUS7 CHF Tests (WH101 and WH102)*

TS

*Table 1-2 Heat Loss Calculation*

TS



**Impact on DCD**

N/A

**Impact on Technical/Topical/Environmental Report**

Topical Report APR1400-F-C-TR-12002-NP will be revised as indicated on the attached markups.

- Document Mark-up Cover Sheet : 1 page
- Mark-up for Q1 of RAI 3-7443 : 7 pages

※Remark: Minor formatting, such as numbering figures, tables and references, etc., will be cleaned up before finalizing the topical report.

# Document Mark-up Cover Sheet

1. **Project ID:** *APR1400 NRC DC*
2. **Type of Corresponding Document:**  
 DCD     Topical Report     Technical Report     Other(s) \_\_\_\_\_
3. **Title of Corresponding Document:** *KCE-1 CHF Correlation for PLUS7 Thermal Design  
(APR1400-F-C-TR-12002-NP)*
4. **RAI ID/Question ID:** *3-7443 / Q1*
5. **Page(s) attached:** *7 (Seven)*

### 3. TEST PROCEDURE AND CHF MEASUREMENTS

This chapter describes the procedure to confirm the integrity of the test sections and the system prior to the test as well as the CHF measurement method.

#### 3.1 TEST PROCEDURE

The experimental data to be obtained included cold flow pressure drop at isothermal condition, heat balance at single-phase heated condition and CHF data.

At the beginning of each test, cold flow pressure drop points were obtained over a range of flow conditions. At the start of each day of testing, a repeat pressure drop point was taken for comparison with earlier data. These data provided isothermal grid span pressure drop values to compare with the prediction and also established a base for comparison in case of a malfunction of the rod bundle during the tests. Pressure drop measurements were obtained for each test at the following conditions:

- Pressure: 1000 psi (6.89 MPa)
- Isothermal Temperature: 80 °F (26.7 °C)
- Mass Velocity: 1.0 to 3.5 Mlbm/hr-ft<sup>2</sup> (1356 to 4747 kg/s-m<sup>2</sup>)

Heat balances were performed on the test section to check all loop and bundle instrumentation at high temperature and power and to check heat losses. These runs were accomplished at subcooled conditions before CHF data were obtained at the beginning of each day of operation. Heat balances were obtained for each test at the following condition:

- Pressure: 1500 psi (10.34 MPa)
- Inlet Temperature: 400 °F (204.4 °C)
- Mass Velocity: 1.5 Mlbm/hr-ft<sup>2</sup> (2034 kg/s-m<sup>2</sup>)
- Bundle Power: 1.6 MW

The CHF test data were obtained after the heat loss was confirmed to be within the acceptable tolerance range from the heat balance test.

The [ ]<sup>TS</sup> of heat loss acceptance criterion was applied on heat balance test.

#### 3.2 CHF MEASUREMENTS

The CHF tests were performed by maintaining the following loop parameters constant:

- test section outlet pressure
- inlet temperature
- inlet mass flux (mass velocity)

INSERT

The total power to the test section was then increased until a temperature excursion was observed by one or more thermocouples installed inside of the heater rods. The amount of the excursion was approximately 10 to 30 °F and varied depending on system conditions. The power was decreased if the temperature excursion was sufficient. When the temperature indication was

**4. CHF CORRELATION DEVELOPMENT**

The KCE-1 CHF correlation was developed using the CHF test data for the PLUS7 fuel obtained from HTRF. This chapter describes the CHF test data, local fluid condition calculation method, the correlation coefficient optimization procedure and applicable range of parameters to the correlation.

**4.1 CHF TEST DATA**

[ ]<sup>TS</sup> test data for the thimble subchannel test section TS101 and [ ]<sup>TS</sup> data for the matrix subchannel test section TS102 were obtained, respectively. The entire [ ]<sup>TS</sup> test data are listed in Table A-1 of APPENDIX A.

Figure 4-1 through Figure 4-3 show average heat fluxes (hence powers) of the test section versus system pressure, inlet temperature and inlet mass flux, respectively. As identified in Figure 4-1, [ ]<sup>TS</sup>

[ ]<sup>TS</sup>

**4.2 LOCAL FLUID CONDITION CALCULATION**

Using the subchannel analysis code, TORC, local fluid conditions for the CHF test data were computed.

The TORC code is an adaptation of the COBRA-IIIC code with modifications including an improved lateral momentum equation and lateral boundary condition capability to simulate actual core behaviors for all flow channels in the core. It is a detailed model code predicting the steady-state thermal hydraulic characteristics of the nuclear reactor cores. The TORC code divides the core into a series of control volumes and solves 3-dimensional conservation equations for each control volume thereby predicting fluid thermal hydraulic local conditions at every position in the core.

The verification of TORC code includes a comparison of subchannel coolant temperature rise and overall pressure drop for CHF test bundles, and full size open core effects of actual operating reactor data.

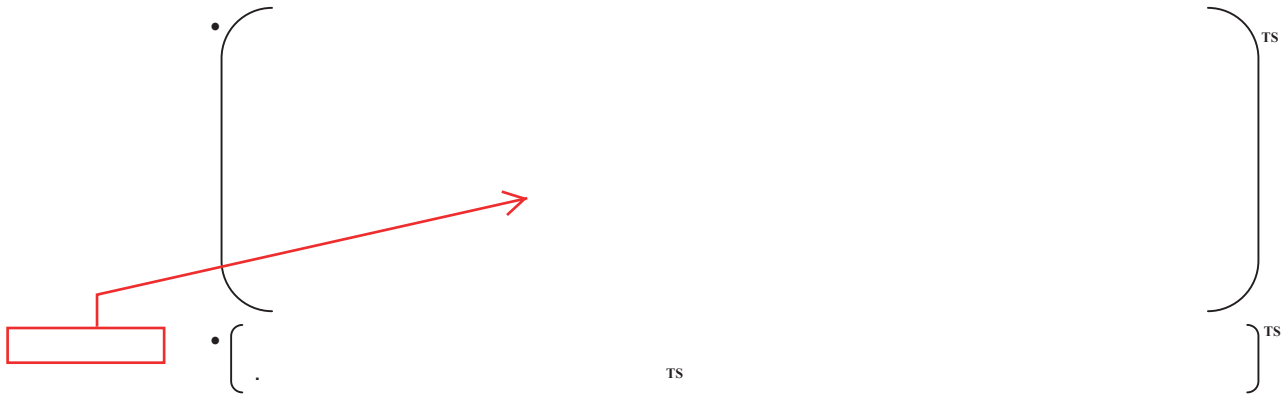
The TORC code has been approved for use in licensing application of reactor core analyses for steady-state calculations involving unblocked flow channels or subchannels (other than the minimal blockage offered by intact spacer grids). The spacer grid with split type “R” mixing vanes, which was adopted in PLUS7 fuel, did not affect the TORC code applicability to thermal hydraulic analyses of reactor cores as approved by USNRC.

The TORC code models were generated by using subchannel arrangements, radial and axial power distributions and spacer grid locations of each test sections as shown in Figure 2-5 through Figure 2-9. Other main input data are summarized in Table 4-1.

correlation<sup>(5)</sup>

For CHF tests using a uniform axial power distribution, such as the CHF test cases for the CE-1 correlation<sup>(4)</sup> development, CHF always occurs in the upper exit region of the heater rods (end-of-heated-length, EOHL). Hence, surface temperatures of heater rods and subchannels experiencing CHF can be detected by thermocouples installed azimuthally in the EOHL four (4) subchannels surrounding a heater rod.

For CHF tests using a non-uniform axial power distribution, as in the CHF tests for PLUS7 and for Reference 5, the axial location of CHF occurrence depends on the shape of the axial power distribution and local fluid conditions. Moreover, the surface temperatures of heater rods are measured with ring-typed junction thermocouples installed at various axial positions. In this case, the axial location of a heater rod where CHF occurs can be detected but the subchannel experiencing CHF cannot be identified exactly. Thus, the local fluid conditions for the KCE-1 CHF correlation were extracted with the following basic assumptions:



Therefore, [ ] were extracted per each individual datum from TS101 while [ ]<sup>TS</sup> per datum from TS102.

**4.3 CORRELATION FORMULA AND ASSUMPTIONS**

The functional formula of the KCE-1 CHF correlation is identical to the CE-1 CHF correlation, and is given as follow:

$$q_{CHF,U}'' = \frac{B_1(d / d_m)^{B_2} [(B_3 + B_4 P)(G / 10^6)^{(B_5 + B_6 P)} - (G / 10^6) \chi h_{fg}]}{(G / 10^6)^{(B_7 P + B_8 (G / 10^6))}}$$

- where,  $q_{CHF,U}''$  CHF for uniform axial power distribution, *MBtu/hr-ft<sup>2</sup>*
- $P$  Pressure, *psia*
- $d$  Equivalent heated diameter of subchannel of interest, *inch*
- $d_m$  Equivalent heated diameter of matrix subchannel, *inch*
- $G$  Local mass flux at the CHF location, *lbm / hr-ft<sup>2</sup>*
- $\chi$  Local quality at the CHF location
- $h_{fg}$  Latent heat of vaporization, *Btu/lbm*.

The coefficients of the CE-1 CHF correlation were determined based on the CHF test data with a uniform axial power distribution. Through subsequent CHF tests with a non-uniform axial power distribution, the non-uniform axial power distribution correction factor, Tong factor  $F_c^{(6),(6)}$ , was

$F_c^{(6),(7)}$

combined with the CE-1 CHF correlation as follow, and was proven to predict the CHF values conservatively:

$$q''_{CHF,NU} = q''_{CHF,U} / F_C$$

where,  $q''_{CHF,NU}$  CHF for non-uniform axial power distribution,  $MBtu/hr-ft^2$   
 $q''_{CHF,U}$  CHF for uniform axial power distribution,  $MBtu/hr-ft^2$   
 $F_C$  Non-uniform axial power distribution correction factor

The Tong factor  $F_C$  was defined as follow :

$$F_C = \frac{C}{q''_{CHF,NU} (1 - e^{-Cl_{DNB}})} \int_0^{l_{DNB}} q''(z) e^{-C(l_{DNB}-z)} dz$$

$$C = 1.8 (1 - \chi_{DNB})^{4.31} / (G/10^6)^{0.478} ft^{-1}$$

where,  $l_{DNB}$  CHF axial location  
 $\chi_{DNB}$  Local quality at the CHF location

Reference 6

According to the SER issued by USNRC shown in the enclosure of ~~Reference 5~~, the 95/95 DNBR (Departure from Nucleate Boiling Ratio) limit of the CE-1 CHF correlation established for the uniform axial power distribution was allowed to be applied to the non-uniform axial power distribution since the CE-1 CHF correlation combined with the Tong factor  $F_C$  predicts the CHF conservatively for the non-uniform axial power distribution.

The CHF test data for the PLUS7 fuel were obtained with a non-uniform axial power distribution, a symmetric cosine with a peak of 1.475. For a conservatism, [

#### 4.4 CORRELATION COEFFICIENTS AND APPLICABLE RANGES OF PARAMETERS

The applicable ranges of parameters for the KCE-1 CHF correlation were determined based on the local fluid conditions at the location of the predicted minimum DNBR. The coefficients of KCE-1 CHF correlation were developed by an iterative process to optimize the coefficients as given below:

- 1) As the first step in the iterative process, the local fluid conditions at the [ ]<sup>TS</sup> elevation were used to determine the initial coefficients for the correlation and to estimate the range of applicability for the correlation. The

selected range used in the initial runs was based upon the range of data at the [ ] elevation.

- 2) The second step was to determine the initial estimate of the eight coefficients of the CE-1 CHF correlation formula by using a nonlinear regression code. To obtain convergence, the initial guesses were based upon the values for the CE-1 CHF correlation, Reference 4. The resulting applicable ranges of parameters for the initial KCE-1 CHF correlation were as follows:

- System pressure
  - Local mass flux
  - Local quality
- } <sup>TS</sup>

Reference 5

- 3) As the third step, statistical tests were performed for the indicated CHF elevation data with the CHF statistics for the initial KCE-1 CHF correlation. An outlier test was applied to identify potential test data which could be removed. There was no outlier for the [ ] <sup>TS</sup> elevation data.

[ ] <sup>TS</sup>

- 4) As the fourth step, an iterative process was then applied by using the initial coefficients of the KCE-1 CHF correlation from the [ ] <sup>TS</sup> elevation for each test section with [ ] <sup>TS</sup>

- 5) As the fifth step, local fluid conditions were extracted at the minimum DNBR elevation in a channel [ ] <sup>TS</sup> rod. The local fluid conditions at the [ ] <sup>TS</sup> rod, if applicable, were extracted for TS101. As stated in section 4.3 and Reference 4,

[ ] <sup>TS</sup>

Reference 5

- 6) Step 2 was repeated several times with the minimum DNBR data to determine the eight coefficients of the CE-1 CHF correlation formula. After the initial run at the minimum DNBR elevation, the data were examined for outliers. Based upon this outlier test, [ ] <sup>TS</sup> was eliminated, as shown in Table 4-3. [ ] <sup>TS</sup>

[ ] <sup>TS</sup>

## 6. CORRELATION APPLICATION

KEPCO Nuclear Fuel uses the KCE-1 CHF correlation for evaluating thermal design of the PLUS7 fuel assembly and the reactor core of APR1400 and OPR1000 in accordance with the CHF or DNB acceptance criteria defined in the Standard Review Plan (SRP)<sup>(7)</sup>. (SRP)<sup>(8)</sup>

Sections 4.2 and 4.4 of SRP state that the DNB acceptance criterion provides assurance that there be at least a 95% probability at the 95% confidence level that the hot fuel rod in the core does not experience a DNB or transition condition during normal operation or AOOs (Anticipated Operational Occurrences). The acceptance criterion is met in thermal design and safety analysis when the MDNBR of the hot rod in the hot channel is above 95/95 DNBR limit of the correlation. Establishment of the KCE-1 correlation 95/95 DNBR limit was presented in Chapter 5. The KCE-1 CHF correlation was used only with a computer code that has been used for the correlation development and has been qualified with the 95/95 DNBR limit.

The KCE-1 CHF correlation 95/95 DNBR limit and its supporting M/P statistics with the TORC code is 1.124. The applicable ranges of the parameters, based on database, are given in Table 4.4. Note that the Tong factor  $F_C$  is [ ]<sup>TS</sup> are applied to MDNBR calculation for the design application and safety analyses. The value of Tong factor  $F_C$  depends on the various axial power distribution and local fluid conditions but it is conservatively limited to [ ]<sup>TS</sup>. The application of the KCE-1 CHF correlation with TORC code is in full compliance with the conditions of the Safety Evaluation Report (SER) on the TORC code and modeling for CE-PWRs. The OPR1000 and the APR1400 are CE-PWRs.

The TORC code is used in thermal design and safety analyses to perform detailed modeling of the core and hot assembly and to determine MDNBR in the hot assembly. The CETOP-D code<sup>(8)</sup> is a fast running tool which is used in thermal design and safety analyses to calculate MDNBR in the hot subchannel. code<sup>(9)</sup>

While the TORC code can be applied directly in the thermal analysis and safety analyses, typically the TORC code is used to benchmark the MDNBR results of CETOP-D code such that the CETOP-D results are conservative relative to those of TORC code. The KCE-1 CHF correlation is implemented to both TORC and CETOP-D codes by modifying correlation coefficients only. Note that the functional formula is identical for both KCE-1 and CE-1 CHF correlations, as described in Section 4.3. Reference 9

Thus, the topical reports described in References 2 and 3 for TORC code and ~~Reference 8~~ for CETOP-D code will remain valid with the application of KCE-1 CHF correlation. Therefore, the application of KCE-1 CHF correlation with CETOP-D code for OPR1000 and APR1400 is equivalent to its application with TORC code.

Even though a higher value of inverse Peclet number based on the empirically determined thermal diffusion coefficient was used in the TORC model for CHF data analysis and correlation development, the reactor analysis is to be performed with the design inverse Peclet number ( $1/Pe = 0.0101$ ). This is equivalent to the value of the thermal diffusion coefficient (TDC = 0.038) applied to the Westinghouse PWR for fuel assembly with "R" mixing vane grid design<sup>(9)</sup>. design<sup>(10)</sup>

**8. REFERENCES**

- (1) APR1400-F-M-TR-12001-P Rev.0, "PLUS7 Fuel Design," November 2012.
- (2) CENPD-161-P-A, "TORC Code, A Computer Code for Determining the Thermal Margin of a Reactor Core," April 1986.
- (3) CENPD-206-P-A, "TORC Code, A Verification and Simplified Modeling Methods," June 1981.

(5) → (4) CENPD-162-P-A, "C-E Critical Heat Flux, Critical Heat Flux Correlation for C-E Fuel Assemblies with Standard Spacer Grids, Part 1 Uniform Axial Power Distribution," September 1976.

(6) → (5) CENPD-207-P-A, "C-E Critical Heat Flux, Critical Heat Flux Correlation for C-E Fuel Assemblies with Standard Spacer Grids, Part 2 Nonuniform Axial Power Distribution," December 1984.

(7) → (6) Tong, L. S., Boiling Crisis and Critical Heat Flux, U. S. Atomic Energy Commission, 1972.

(8) → (7) NUREG-0800, "Standard Review Plan Section 4.2, 'Fuel System Design' Revision 3, and Section 4.4, 'Thermal and Hydraulic Design' Revision 2," March 2007.

(9) → (8) CEN-139(A)-P, "Response to First Round Questions on the Statistical Combination of Uncertainties Program : CETOP-D Code Structure and Modeling Methods," March 1981 and CEN-214(A)-NP, "CETOP-D Code Structure and Modeling Methods for Arkansas Nuclear One –Unit 2," July 1982.

(10) → (9) ML071580898 - Westinghouse AP1000 Design Control Document Rev.16 – Tier 2 "Chapter 4 – Reactor – Section 4.4 Thermal and Hydraulic Design," May 2007.

(4) [ ]<sup>TS</sup>.

↑  
INSERT

## RESPONSE TO REQUEST FOR ADDITIONAL INFORMATION

### APR1400 Topical Reports

Korea Electric Power Corporation / Korea Hydro & Nuclear Power Co., LTD

Docket No. PROJ 0782

RAI No.: 3-7443 Question 2  
SRP Section: N/A  
Application Section: KCE-1 Critical Heat Flux Correlation for PLUS7 Thermal Design  
(APR1400-F-C-TR-12002-NP, Rev.0)  
Date of RAI Issued: 03/25/2014  
Response Date: 02/25/2015

---

### **Question 2**

The topical report described that the CHF point was confirmed when increasing the total power led to a temperature excursion of 10 to 30OF inside the heater rods. When the temperature indication was minimal, confirmation of the validity of a CHF point was obtained by observing a characteristic temperature decay with power reduction, as the CHF zone was rewetted. The applicant is asked to justify the above-mentioned CHF point confirmation technique, possibly by including a citation in the report that corroborates it.

### **Response**

*The CHF identification criteria described in the topical report (APR1400-F-C-TR-12002) are generally accepted ones and had been applied since the early phase of HTRF operation (Reference: EPRI-NP 2609 Vol. 1, Sep. 1982). The typical shape of characteristic temperature decay can be identified in Figure 2-1 (largest red circle on the right-side, but temperature excursion of this case is sufficient: time flows from top to bottom of the plot). This is due to the retarded recovery of heat transfer after CHF occurred ( $D \rightarrow D'$ ) from post-dryout film boiling to transition boiling ( $D' \rightarrow E \rightarrow D$ ) or subcooled boiling( $D' \rightarrow E \rightarrow E'$ ), similar to hysteresis, inferred from a typical boiling curve as shown in Figure 2-2 and heat transfer mechanism in the corresponding boiling regime.*

*A citation to the reference will be added to the topical report as shown in the attached markup.*

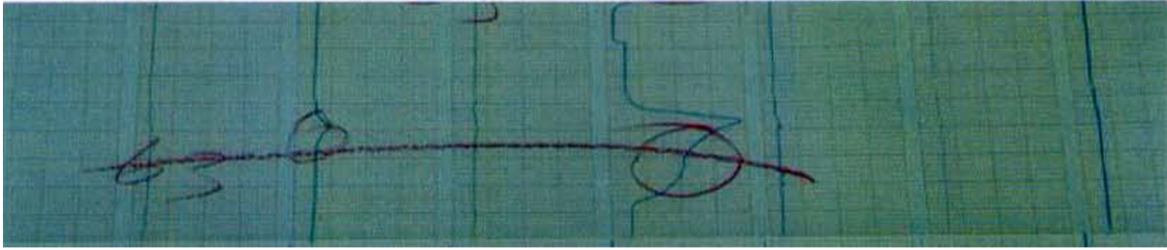


Figure 2-1 Typical Example of Characteristic Temperature Decay

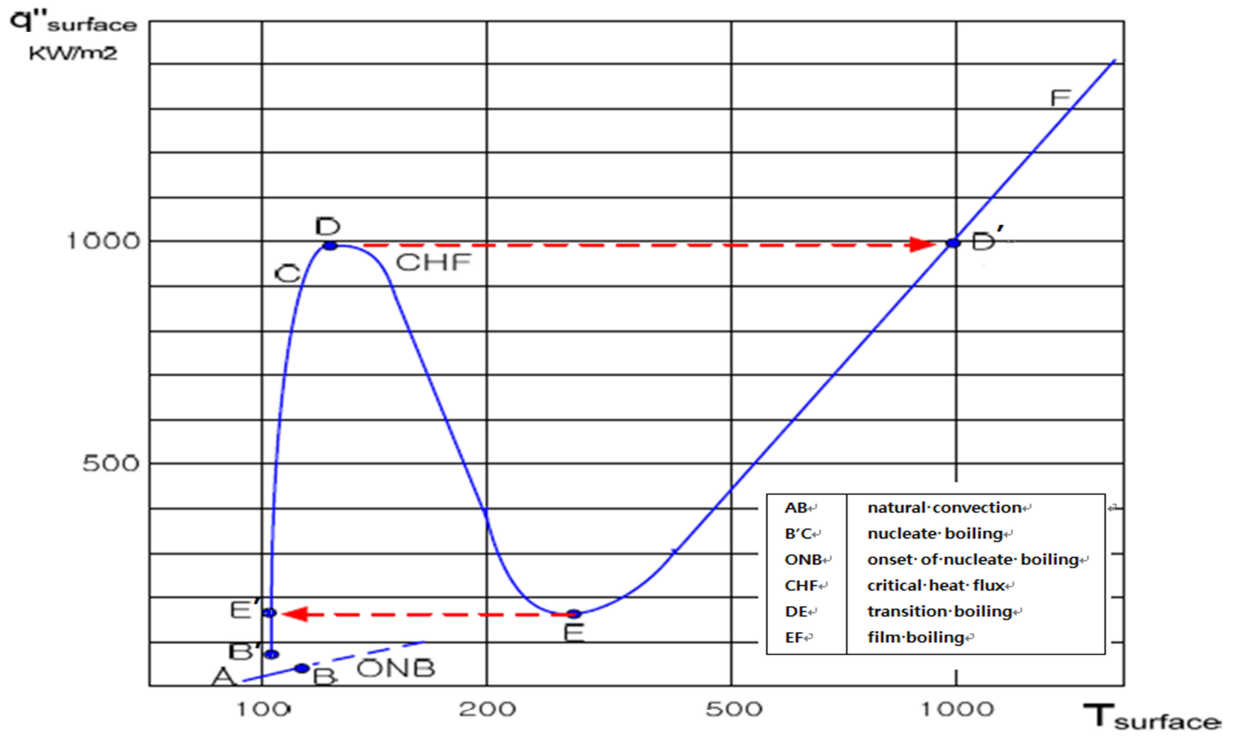


Figure 2-2 Typical Boiling Curve of the Water

**Impact on DCD**

N/A

**Impact on Technical/Topical/Environmental Report**

Topical Report APR1400-F-C-TR-12002-NP will be revised as indicated on the attached markups.

- Document Mark-up Cover Sheet : 1 page
- Mark-up for Q2 of RAI 3-7443 : 7 pages

※Remark: Minor formatting, such as numbering figures, tables and references, etc., will be cleaned up before finalizing the topical report.

# Document Mark-up Cover Sheet

1. **Project ID:** *APRI400 NRC DC*
2. **Type of Corresponding Document:**  
 DCD     Topical Report     Technical Report     Other(s) \_\_\_\_\_
3. **Title of Corresponding Document:** *KCE-1 CHF Correlation for PLUS7 Thermal Design  
(APRI400-F-C-TR-12002-P)*
4. **RAI ID/Question ID:** *3-7443 / Q2*
5. **Page(s) attached:** *7 (Seven)*

minimal, confirmation of the validity of a CHF point was obtained by observing the temperature decay with power reduction. There was characteristic temperature decay with time as the CHF zone was rewetted. This evidence was considered confirming in cases where the temperature decay pattern was typical. Otherwise, the test would be repeated.

When a CHF point was observed, the following measurements were recorded:

- test section outlet pressure from Heise gauge repeated<sup>(4)</sup>
- identification number of heater rod experiencing CHF and relevant thermocouple
- test section voltage
- bus-to-bus voltage
- D.C. generator electric current
- inlet temperature
- exit temperature
- exit pressure transducers
- inlet pressure transducers
- turbine flow meter transducer
- Venturi flow meters transducers
- test section pressure drop transducers
- heater rod temperatures

For the above recordings, the first two measurements were recorded manually while other measurements were recorded by the data acquisition system with a HP3852A data acquisition/control unit.

## 4. CHF CORRELATION DEVELOPMENT

The KCE-1 CHF correlation was developed using the CHF test data for the PLUS7 fuel obtained from HTRF. This chapter describes the CHF test data, local fluid condition calculation method, the correlation coefficient optimization procedure and applicable range of parameters to the correlation.

### 4.1 CHF TEST DATA

[ ]<sup>TS</sup> test data for the thimble subchannel test section TS101 and [ ]<sup>TS</sup> data for the matrix subchannel test section TS102 were obtained, respectively. The entire [ ]<sup>TS</sup> test data are listed in Table A-1 of APPENDIX A.

Figure 4-1 through Figure 4-3 show average heat fluxes (hence powers) of the test section versus system pressure, inlet temperature and inlet mass flux, respectively. As identified in Figure 4-1, [ ]<sup>TS</sup>

[ ]<sup>TS</sup>

### 4.2 LOCAL FLUID CONDITION CALCULATION

Using the subchannel analysis code, TORC, local fluid conditions for the CHF test data were computed.

The TORC code is an adaptation of the COBRA-IIIC code with modifications including an improved lateral momentum equation and lateral boundary condition capability to simulate actual core behaviors for all flow channels in the core. It is a detailed model code predicting the steady-state thermal hydraulic characteristics of the nuclear reactor cores. The TORC code divides the core into a series of control volumes and solves 3-dimensional conservation equations for each control volume thereby predicting fluid thermal hydraulic local conditions at every position in the core.

The verification of TORC code includes a comparison of subchannel coolant temperature rise and overall pressure drop for CHF test bundles, and full size open core effects of actual operating reactor data.

The TORC code has been approved for use in licensing application of reactor core analyses for steady-state calculations involving unblocked flow channels or subchannels (other than the minimal blockage offered by intact spacer grids). The spacer grid with split type "R" mixing vanes, which was adopted in PLUS7 fuel, did not affect the TORC code applicability to thermal hydraulic analyses of reactor cores as approved by USNRC.

The TORC code models were generated by using subchannel arrangements, radial and axial power distributions and spacer grid locations of each test sections as shown in Figure 2-5 through Figure 2-9. Other main input data are summarized in Table 4-1.

correlation<sup>(5)</sup>

For CHF tests using a uniform axial power distribution, such as the CHF test cases for the CE-1 correlation<sup>(4)</sup> development, CHF always occurs in the upper exit region of the heater rods (end-of-heated-length, EOHL). Hence, surface temperatures of heater rods and subchannels experiencing CHF can be detected by thermocouples installed azimuthally in the EOHL four (4) subchannels surrounding a heater rod.

For CHF tests using a non-uniform axial power distribution, as in the CHF tests for PLUS7 and for Reference 5, the axial location of CHF occurrence depends on the shape of the axial power distribution and local fluid conditions. Moreover, the surface temperatures of heater rods are measured with ring-typed junction thermocouples installed at various axial positions. In this case, the axial location of a heater rod where CHF occurs can be detected but the subchannel experiencing CHF cannot be identified exactly. Thus, the local fluid conditions for the KCE-1 CHF correlation were extracted with the following basic assumptions:



Therefore, [ ] were extracted per each individual datum from TS101 while [ ]<sup>TS</sup> per datum from TS102.

**4.3 CORRELATION FORMULA AND ASSUMPTIONS**

The functional formula of the KCE-1 CHF correlation is identical to the CE-1 CHF correlation, and is given as follow:

$$q''_{CHF,U} = \frac{B_1(d/d_m)^{B_2} [(B_3 + B_4P)(G/10^6)^{(B_5+B_6P)} - (G/10^6)\chi h_{fg}]}{(G/10^6)^{(B_7P+B_8(G/10^6))}}$$

- where,  $q''_{CHF,U}$  CHF for uniform axial power distribution, *MBtu/hr-ft<sup>2</sup>*
- $P$  Pressure, *psia*
- $d$  Equivalent heated diameter of subchannel of interest, *inch*
- $d_m$  Equivalent heated diameter of matrix subchannel, *inch*
- $G$  Local mass flux at the CHF location, *lbm / hr-ft<sup>2</sup>*
- $\chi$  Local quality at the CHF location
- $h_{fg}$  Latent heat of vaporization, *Btu/lbm*.

The coefficients of the CE-1 CHF correlation were determined based on the CHF test data with a uniform axial power distribution. Through subsequent CHF tests with a non-uniform axial power distribution, the non-uniform axial power distribution correction factor, Tong factor  $F_C^{(6),(6)}$ , was

$F_C^{(6),(7)}$

combined with the CE-1 CHF correlation as follow, and was proven to predict the CHF values conservatively:

$$q''_{CHF,NU} = q''_{CHF,U} / F_C$$

where,  $q''_{CHF,NU}$  CHF for non-uniform axial power distribution,  $MBtu/hr-ft^2$   
 $q''_{CHF,U}$  CHF for uniform axial power distribution,  $MBtu/hr-ft^2$   
 $F_C$  Non-uniform axial power distribution correction factor

The Tong factor  $F_C$  was defined as follow :

$$F_C = \frac{C}{q''_{CHF,NU} (1 - e^{-Cl_{DNB}})} \int_0^{l_{DNB}} q''(z) e^{-C(l_{DNB}-z)} dz$$

$$C = 1.8 (1 - \chi_{DNB})^{4.31} / (G/10^6)^{0.478} f^{-1}$$

where,  $l_{DNB}$  CHF axial location  
 $\chi_{DNB}$  Local quality at the CHF location

Reference 6

According to the SER issued by USNRC shown in the enclosure of ~~Reference 5~~, the 95/95 DNBR (Departure from Nucleate Boiling Ratio) limit of the CE-1 CHF correlation established for the uniform axial power distribution was allowed to be applied to the non-uniform axial power distribution since the CE-1 CHF correlation combined with the Tong factor  $F_C$  predicts the CHF conservatively for the non-uniform axial power distribution.

The CHF test data for the PLUS7 fuel were obtained with a non-uniform axial power distribution, a symmetric cosine with a peak of 1.475. For a conservatism, [

#### 4.4 CORRELATION COEFFICIENTS AND APPLICABLE RANGES OF PARAMETERS

The applicable ranges of parameters for the KCE-1 CHF correlation were determined based on the local fluid conditions at the location of the predicted minimum DNBR. The coefficients of KCE-1 CHF correlation were developed by an iterative process to optimize the coefficients as given below:

- 1) As the first step in the iterative process, the local fluid conditions at the [ ]<sup>TS</sup> elevation were used to determine the initial coefficients for the correlation and to estimate the range of applicability for the correlation. The

selected range used in the initial runs was based upon the range of data at the [ ] elevation.

- 2) The second step was to determine the initial estimate of the eight coefficients of the CE-1 CHF correlation formula by using a nonlinear regression code. To obtain convergence, the initial guesses were based upon the values for the CE-1 CHF correlation, Reference 4. The resulting applicable ranges of parameters for the initial KCE-1 CHF correlation were as follows:

- System pressure
    - Local mass flux
    - Local quality
- } <sup>TS</sup>

- 3) As the third step, statistical tests were performed for the indicated CHF elevation data with the CHF statistics for the initial KCE-1 CHF correlation. An outlier test was applied to identify potential test data which could be removed. There was no outlier for the [ ] <sup>TS</sup> elevation data.

[ ] <sup>TS</sup>

- 4) As the fourth step, an iterative process was then applied by using the initial coefficients of the KCE-1 CHF correlation from the [ ] <sup>TS</sup> elevation for each test section with [ ] <sup>TS</sup>

- 5) As the fifth step, local fluid conditions were extracted at the minimum DNBR elevation in a channel [ ] <sup>TS</sup> rod. The local fluid conditions at the [ ] <sup>TS</sup> rod, if applicable, were extracted for TS101. As stated in section 4.3 and Reference 4,

[ ] <sup>TS</sup>

- 6) Step 2 was repeated several times with the minimum DNBR data to determine the eight coefficients of the CE-1 CHF correlation formula. After the initial run at the minimum DNBR elevation, the data were examined for outliers. Based upon this outlier test, [ ] <sup>TS</sup> was eliminated, as shown in Table 4-3. [ ] <sup>TS</sup>

[ ] <sup>TS</sup>

## 6. CORRELATION APPLICATION

KEPCO Nuclear Fuel uses the KCE-1 CHF correlation for evaluating thermal design of the PLUS7 fuel assembly and the reactor core of APR1400 and OPR1000 in accordance with the CHF or DNB acceptance criteria defined in the Standard Review Plan (SRP)<sup>(7)</sup>.

(SRP)<sup>(8)</sup>

Sections 4.2 and 4.4 of SRP state that the DNB acceptance criterion provides assurance that there be at least a 95% probability at the 95% confidence level that the hot fuel rod in the core does not experience a DNB or transition condition during normal operation or AOOs (Anticipated Operational Occurrences). The acceptance criterion is met in thermal design and safety analysis when the MDNBR of the hot rod in the hot channel is above 95/95 DNBR limit of the correlation. Establishment of the KCE-1 correlation 95/95 DNBR limit was presented in Chapter 5. The KCE-1 CHF correlation was used only with a computer code that has been used for the correlation development and has been qualified with the 95/95 DNBR limit.

The KCE-1 CHF correlation 95/95 DNBR limit and its supporting M/P statistics with the TORC code is 1.124. The applicable ranges of the parameters, based on database, are given in Table 4.4. Note that the Tong factor  $F_C$  is [ ]<sup>TS</sup> are applied to MDNBR calculation for the design application and safety analyses. The value of Tong factor  $F_C$  depends on the various axial power distribution and local fluid conditions but it is conservatively limited to [ ]<sup>TS</sup>. The application of the KCE-1 CHF correlation with TORC code is in full compliance with the conditions of the Safety Evaluation Report (SER) on the TORC code and modeling for CE-PWRs. The OPR1000 and the APR1400 are CE-PWRs.

code<sup>(9)</sup>

The TORC code is used in thermal design and safety analyses to perform detailed modeling of the core and hot assembly and to determine MDNBR in the hot assembly. The CETOP-D code<sup>(8)</sup> is a fast running tool which is used in thermal design and safety analyses to calculate MDNBR in the hot subchannel.

While the TORC code can be applied directly in the thermal analysis and safety analyses, typically the TORC code is used to benchmark the MDNBR results of CETOP-D code such that the CETOP-D results are conservative relative to those of TORC code. The KCE-1 CHF correlation is implemented to both TORC and CETOP-D codes by modifying correlation coefficients only. Note that the functional formula is identical for both KCE-1 and CE-1 CHF correlations, as described in Section 4.3.

Reference 9

Thus, the topical reports described in References 2 and 3 for TORC code and Reference 8 for CETOP-D code will remain valid with the application of KCE-1 CHF correlation. Therefore, the application of KCE-1 CHF correlation with CETOP-D code for OPR1000 and APR1400 is equivalent to its application with TORC code.

Even though a higher value of inverse Peclet number based on the empirically determined thermal diffusion coefficient was used in the TORC model for CHF data analysis and correlation development, the reactor analysis is to be performed with the design inverse Peclet number ( $1/Pe = 0.0101$ ). This is equivalent to the value of the thermal diffusion coefficient (TDC = 0.038) applied to the Westinghouse PWR for fuel assembly with "R" mixing vane grid design<sup>(9)</sup>.

design<sup>(10)</sup>

## 8. REFERENCES

- (1) APR1400-F-M-TR-12001-P Rev.0, "PLUS7 Fuel Design," November 2012.
- (2) CENPD-161-P-A, "TORC Code, A Computer Code for Determining the Thermal Margin of a Reactor Core," April 1986.
- (3) CENPD-206-P-A, "TORC Code, A Verification and Simplified Modeling Methods," June 1981.

(5) → (4) CENPD-162-P-A, "C-E Critical Heat Flux, Critical Heat Flux Correlation for C-E Fuel Assemblies with Standard Spacer Grids, Part 1 Uniform Axial Power Distribution," September 1976.

(6) → (5) CENPD-207-P-A, "C-E Critical Heat Flux, Critical Heat Flux Correlation for C-E Fuel Assemblies with Standard Spacer Grids, Part 2 Nonuniform Axial Power Distribution," December 1984.

(7) → (6) Tong, L. S., Boiling Crisis and Critical Heat Flux, U. S. Atomic Energy Commission, 1972.

(8) → (7) NUREG-0800, "Standard Review Plan Section 4.2, 'Fuel System Design' Revision 3, and Section 4.4, 'Thermal and Hydraulic Design' Revision 2," March 2007.

(9) → (8) CEN-139(A)-P, "Response to First Round Questions on the Statistical Combination of Uncertainties Program : CETOP-D Code Structure and Modeling Methods," March 1981 and CEN-214(A)-NP, "CETOP-D Code Structure and Modeling Methods for Arkansas Nuclear One –Unit 2," July 1982.

(10) → (9) ML071580898 - Westinghouse AP1000 Design Control Document Rev.16 – Tier 2 "Chapter 4 – Reactor – Section 4.4 Thermal and Hydraulic Design," May 2007.

(4) EPRI NP-2609, "Parametric Study of CHF Data, Volume 1 : Compilation of Rod Bundle CHF Data Available at the Columbia University Heat Transfer Research Facility", September 1982.

INSERT

## RESPONSE TO REQUEST FOR ADDITIONAL INFORMATION

### APR1400 Topical Reports

Korea Electric Power Corporation / Korea Hydro & Nuclear Power Co., LTD

Docket No. PROJ 0782

RAI No.: 3-7443 Question 3

SRP Section: N/A

Application Section: KCE-1 Critical Heat Flux Correlation for PLUS7 Thermal Design  
(APR1400-F-C-TR-12002-NP, Rev.0)

Date of RAI Issued: 03/25/2014

Response Date: 02/25/2015

---

### **Question 3**

Figure 2-9 depicts seven thermocouples installed axially to measure the wall temperature of the heater rods. However, the thermocouple grid is asymmetrical between the BOHL (Beginning of Heated Length) and EOHL (End of Heated Length). Justify the temperature measurements made by using the asymmetrical thermocouples grid to be conservative with reference to the overall data reduction to compute CHF.

### **Response**

*With axially non-uniform axial power distribution (uniformly spaced grids), the locations of CHF indication are the downstream of peak power and underneath the grid. For the cosine power shape (peak at middle of heated length and symmetry) applied to the PLUS7 CHF test, possible CHF locations would be thermocouple (T/C) ID 1 through 5.*

*According to actual test data, the CHF elevations are limited to [ ]<sup>TS</sup> as summarized in Figure 3-1 below, and Table A-1 of the topical report. No CHF is indicated at other locations including BOHL and EOHL.*

*Therefore, no impact on CHF measurement and data reduction due to axial T/C configuration applied to the PLUS7 CHF test.*



*Figure 3-1 As-measured CHF elevations for PLUS7 CHF tests*

---

**Impact on DCD**

N/A

**Impact on Technical/Topical/Environmental Report**

N/A

---

## RESPONSE TO REQUEST FOR ADDITIONAL INFORMATION

### APR1400 Topical Reports

Korea Electric Power Corporation / Korea Hydro & Nuclear Power Co., LTD

Docket No. PROJ 0782

**RAI No.:** 3-7443 Question 4

**SRP Section:** N/A

**Application Section:** KCE-1 Critical Heat Flux Correlation for PLUS7 Thermal Design  
(APR1400-F-C-TR-12002-NP, Rev.0)

**Date of RAI Issued:** 03/25/2014

**Response Date:** 02/25/2015

---

### **Question 4**

The TR reports that the test section flow was measured by two (2) Venturi flow meters and a turbine meter prior to the entrance to the test section flow housing. However, Figure 2-2 shows only one Venturi flow meter, and not the two. Describe the logic behind using this flow rate measurement arrangement. Was there any parallel arrangement made to manually measure the pressure drops across the Venturi flow meter as well as the test section using manometers, as has been the methodology used in other CHF test programs?

### **Response**

*Figure 2-2 of the topical report is not a detailed drawing but an overall schematic sketch of instrumentation arrangement. Thus, some components are not depicted in the sketch.*

*The flow rate was primarily measured by the first Venturi flow meter, and the second Venturi flow meter provided redundancy in case of primary flow meter failure. The turbine flow meter provided the diversity for flow measurement verification. The pressure drop at the throat of each Venturi flow meter was measured by two independent differential pressure transducers, and the measured pressure drops were automatically recorded by the data acquisition system. The differential pressure transducers were periodically/properly calibrated against certified devices traceable to NIST standards, or themselves were certified prior to the tests.*

*Calibration records for differential pressure transducers were provided in the QA report for PLUS7 CHF tests (Reference: [*

]TS).

*A manometer was not used in PLUS7 CHF test.*

*The following measurements were considered as the primary parameters to satisfy all QA requirements. Thus, independent and redundant measurements were performed during the test program.*

- test section inlet mass flow rate*
- water temperature at the inlet and outlet of the test section,*
- total pressure at the inlet and outlet of the test section,*
- total D.C. power to the test section*

*The engineering design, materials supplied, and all experimental operations satisfy the Columbia University QAP requirements governed by Quality Management System (QMS) to ensure that the CHF data conform to the requirements of ANSI/ASME NQA-1-1989 with addenda, and the Code of Federal Regulations Title 10, Part 21 (10CFR21).*

*QA related statements and reference will be included in the appropriate subsection of the topical report, as shown in attached markup.*

Note: KAFD was the project name for PLUS7 development (joint program between Westinghouse Electric Company and KEPCO Nuclear Fuel Company)

**Impact on DCD**

N/A

**Impact on Technical/Topical/Environmental Report**

Topical Report APR1400-F-C-TR-12002-NP will be revised as indicated on the attached markups.

- Document Mark-up Cover Sheet : 1 page
- Mark-up for Q4 of RAI 3-7443 : 7 pages

※Remark: Minor formatting, such as numbering figures, tables and references, etc., will be cleaned up before finalizing the topical report.

# Document Mark-up Cover Sheet

1. **Project ID:** *APRI400 NRC DC*
2. **Type of Corresponding Document:**  
 DCD     Topical Report     Technical Report     Other(s) \_\_\_\_\_
3. **Title of Corresponding Document:** *KCE-1 CHF Correlation for PLUS7 Thermal Design  
(APRI400-F-C-TR-12002-NP)*
4. **RAI ID/Question ID:** *3-7443 / Q4*
5. **Page(s) attached:** *7 (Seven)*

minimal, confirmation of the validity of a CHF point was obtained by observing the temperature decay with power reduction. There was characteristic temperature decay with time as the CHF zone was rewetted. This evidence was considered confirming in cases where the temperature decay pattern was typical. Otherwise, the test would be repeated.

When a CHF point was observed, the following measurements were recorded:

- test section outlet pressure from Heise gauge
- identification number of heater rod experiencing CHF and relevant thermocouple
- test section voltage
- bus-to-bus voltage
- D.C. generator electric current
- inlet temperature
- exit temperature
- exit pressure transducers
- inlet pressure transducers
- turbine flow meter transducer
- Venturi flow meters transducers
- test section pressure drop transducers
- heater rod temperatures

For the above recordings, the first two measurements were recorded manually while other measurements were recorded by the data acquisition system with a HP3852A data acquisition/control unit.

### **3.3 QUALITY ASSURANCE**

The engineering design, materials supplied, and all experimental operations satisfy the Columbia University QAP requirements governed by Quality Management System (QMS) to ensure that the CHF data conform to the requirements of ANSI/ASME NQA-1-1989 with addenda, and the Code of Federal Regulations Title 10, Part 21 (10CFR21). All QA related activities performed during the test are reported in Reference 4.



INSERT

## 4. CHF CORRELATION DEVELOPMENT

The KCE-1 CHF correlation was developed using the CHF test data for the PLUS7 fuel obtained from HTRF. This chapter describes the CHF test data, local fluid condition calculation method, the correlation coefficient optimization procedure and applicable range of parameters to the correlation.

### 4.1 CHF TEST DATA

[ ]<sup>TS</sup> test data for the thimble subchannel test section TS101 and [ ]<sup>TS</sup> data for the matrix subchannel test section TS102 were obtained, respectively. The entire [ ]<sup>TS</sup> test data are listed in Table A-1 of APPENDIX A.

Figure 4-1 through Figure 4-3 show average heat fluxes (hence powers) of the test section versus system pressure, inlet temperature and inlet mass flux, respectively. As identified in Figure 4-1, [ ]<sup>TS</sup>

[ ]<sup>TS</sup>

### 4.2 LOCAL FLUID CONDITION CALCULATION

Using the subchannel analysis code, TORC, local fluid conditions for the CHF test data were computed.

The TORC code is an adaptation of the COBRA-IIIC code with modifications including an improved lateral momentum equation and lateral boundary condition capability to simulate actual core behaviors for all flow channels in the core. It is a detailed model code predicting the steady-state thermal hydraulic characteristics of the nuclear reactor cores. The TORC code divides the core into a series of control volumes and solves 3-dimensional conservation equations for each control volume thereby predicting fluid thermal hydraulic local conditions at every position in the core.

The verification of TORC code includes a comparison of subchannel coolant temperature rise and overall pressure drop for CHF test bundles, and full size open core effects of actual operating reactor data.

The TORC code has been approved for use in licensing application of reactor core analyses for steady-state calculations involving unblocked flow channels or subchannels (other than the minimal blockage offered by intact spacer grids). The spacer grid with split type "R" mixing vanes, which was adopted in PLUS7 fuel, did not affect the TORC code applicability to thermal hydraulic analyses of reactor cores as approved by USNRC.

The TORC code models were generated by using subchannel arrangements, radial and axial power distributions and spacer grid locations of each test sections as shown in Figure 2-5 through Figure 2-9. Other main input data are summarized in Table 4-1.

correlation<sup>(5)</sup>

For CHF tests using a uniform axial power distribution, such as the CHF test cases for the CE-1 correlation<sup>(4)</sup> development, CHF always occurs in the upper exit region of the heater rods (end-of-heated-length, EOHL). Hence, surface temperatures of heater rods and subchannels experiencing CHF can be detected by thermocouples installed azimuthally in the EOHL four (4) subchannels surrounding a heater rod.

For CHF tests using a non-uniform axial power distribution, as in the CHF tests for PLUS7 and for Reference 5, the axial location of CHF occurrence depends on the shape of the axial power distribution and local fluid conditions. Moreover, the surface temperatures of heater rods are measured with ring-typed junction thermocouples installed at various axial positions. In this case, the axial location of a heater rod where CHF occurs can be detected but the subchannel experiencing CHF cannot be identified exactly. Thus, the local fluid conditions for the KCE-1 CHF correlation were extracted with the following basic assumptions:



Therefore, [ ] were extracted per each individual datum from TS101 while [ ]<sup>TS</sup> per datum from TS102.

**4.3 CORRELATION FORMULA AND ASSUMPTIONS**

The functional formula of the KCE-1 CHF correlation is identical to the CE-1 CHF correlation, and is given as follow:

$$q''_{CHF,U} = \frac{B_1(d/d_m)^{B_2} [(B_3 + B_4P)(G/10^6)^{(B_5+B_6P)} - (G/10^6)\chi h_{fg}]}{(G/10^6)^{(B_7P+B_8(G/10^6))}}$$

- where,  $q''_{CHF,U}$  CHF for uniform axial power distribution, *MBtu/hr-ft<sup>2</sup>*
- $P$  Pressure, *psia*
- $d$  Equivalent heated diameter of subchannel of interest, *inch*
- $d_m$  Equivalent heated diameter of matrix subchannel, *inch*
- $G$  Local mass flux at the CHF location, *lbm / hr-ft<sup>2</sup>*
- $\chi$  Local quality at the CHF location
- $h_{fg}$  Latent heat of vaporization, *Btu/lbm*.

The coefficients of the CE-1 CHF correlation were determined based on the CHF test data with a uniform axial power distribution. Through subsequent CHF tests with a non-uniform axial power distribution, the non-uniform axial power distribution correction factor, Tong factor  $F_C^{(6),(6)}$ , was

$F_C^{(6),(7)}$

combined with the CE-1 CHF correlation as follow, and was proven to predict the CHF values conservatively:

$$q''_{CHF,NU} = q''_{CHF,U} / F_C$$

where,  $q''_{CHF,NU}$  CHF for non-uniform axial power distribution,  $MBtu/hr-ft^2$   
 $q''_{CHF,U}$  CHF for uniform axial power distribution,  $MBtu/hr-ft^2$   
 $F_C$  Non-uniform axial power distribution correction factor

The Tong factor  $F_C$  was defined as follow :

$$F_C = \frac{C}{q''_{CHF,NU} (1 - e^{-Cl_{DNB}})} \int_0^{l_{DNB}} q''(z) e^{-C(l_{DNB}-z)} dz$$

$$C = 1.8 (1 - \chi_{DNB})^{4.31} / (G/10^6)^{0.478} f^{-1}$$

where,  $l_{DNB}$  CHF axial location  
 $\chi_{DNB}$  Local quality at the CHF location

Reference 6

According to the SER issued by USNRC shown in the enclosure of ~~Reference 5~~, the 95/95 DNBR (Departure from Nucleate Boiling Ratio) limit of the CE-1 CHF correlation established for the uniform axial power distribution was allowed to be applied to the non-uniform axial power distribution since the CE-1 CHF correlation combined with the Tong factor  $F_C$  predicts the CHF conservatively for the non-uniform axial power distribution.

The CHF test data for the PLUS7 fuel were obtained with a non-uniform axial power distribution, a symmetric cosine with a peak of 1.475. For a conservatism, [

#### 4.4 CORRELATION COEFFICIENTS AND APPLICABLE RANGES OF PARAMETERS

The applicable ranges of parameters for the KCE-1 CHF correlation were determined based on the local fluid conditions at the location of the predicted minimum DNBR. The coefficients of KCE-1 CHF correlation were developed by an iterative process to optimize the coefficients as given below:

- 1) As the first step in the iterative process, the local fluid conditions at the [ ]<sup>TS</sup> elevation were used to determine the initial coefficients for the correlation and to estimate the range of applicability for the correlation. The

selected range used in the initial runs was based upon the range of data at the [ ] elevation.

- 2) The second step was to determine the initial estimate of the eight coefficients of the CE-1 CHF correlation formula by using a nonlinear regression code. To obtain convergence, the initial guesses were based upon the values for the CE-1 CHF correlation, Reference 4. The resulting applicable ranges of parameters for the initial KCE-1 CHF correlation were as follows:

- System pressure
  - Local mass flux
  - Local quality
- } TS

Reference 5

- 3) As the third step, statistical tests were performed for the indicated CHF elevation data with the CHF statistics for the initial KCE-1 CHF correlation. An outlier test was applied to identify potential test data which could be removed. There was no outlier for the [ ]<sup>TS</sup> elevation data.

[ ]<sup>TS</sup>

- 4) As the fourth step, an iterative process was then applied by using the initial coefficients of the KCE-1 CHF correlation from the [ ]<sup>TS</sup> elevation for each test section with [ ]<sup>TS</sup>

- 5) As the fifth step, local fluid conditions were extracted at the minimum DNBR elevation in a channel [ ]<sup>TS</sup> rod. The local fluid conditions at the [ ]<sup>TS</sup> rod, if applicable, were extracted for TS101. As stated in section 4.3 and Reference 4,

[ ]<sup>TS</sup>

Reference 5

- 6) Step 2 was repeated several times with the minimum DNBR data to determine the eight coefficients of the CE-1 CHF correlation formula. After the initial run at the minimum DNBR elevation, the data were examined for outliers. Based upon this outlier test, [ ]<sup>TS</sup> was eliminated, as shown in Table 4-3. [ ]<sup>TS</sup>

[ ]<sup>TS</sup>

## 6. CORRELATION APPLICATION

KEPCO Nuclear Fuel uses the KCE-1 CHF correlation for evaluating thermal design of the PLUS7 fuel assembly and the reactor core of APR1400 and OPR1000 in accordance with the CHF or DNB acceptance criteria defined in the Standard Review Plan (SRP)<sup>(7)</sup>.

(SRP)<sup>(8)</sup>

Sections 4.2 and 4.4 of SRP state that the DNB acceptance criterion provides assurance that there be at least a 95% probability at the 95% confidence level that the hot fuel rod in the core does not experience a DNB or transition condition during normal operation or AOOs (Anticipated Operational Occurrences). The acceptance criterion is met in thermal design and safety analysis when the MDNBR of the hot rod in the hot channel is above 95/95 DNBR limit of the correlation. Establishment of the KCE-1 correlation 95/95 DNBR limit was presented in Chapter 5. The KCE-1 CHF correlation was used only with a computer code that has been used for the correlation development and has been qualified with the 95/95 DNBR limit.

The KCE-1 CHF correlation 95/95 DNBR limit and its supporting M/P statistics with the TORC code is 1.124. The applicable ranges of the parameters, based on database, are given in Table 4.4. Note that the Tong factor  $F_C$  is [ ]<sup>TS</sup> are applied to MDNBR calculation for the design application and safety analyses. The value of Tong factor  $F_C$  depends on the various axial power distribution and local fluid conditions but it is conservatively limited to [ ]<sup>TS</sup>. The application of the KCE-1 CHF correlation with TORC code is in full compliance with the conditions of the Safety Evaluation Report (SER) on the TORC code and modeling for CE-PWRs. The OPR1000 and the APR1400 are CE-PWRs.

code<sup>(9)</sup>

The TORC code is used in thermal design and safety analyses to perform detailed modeling of the core and hot assembly and to determine MDNBR in the hot assembly. The CETOP-D code<sup>(8)</sup> is a fast running tool which is used in thermal design and safety analyses to calculate MDNBR in the hot subchannel.

While the TORC code can be applied directly in the thermal analysis and safety analyses, typically the TORC code is used to benchmark the MDNBR results of CETOP-D code such that the CETOP-D results are conservative relative to those of TORC code. The KCE-1 CHF correlation is implemented to both TORC and CETOP-D codes by modifying correlation coefficients only. Note that the functional formula is identical for both KCE-1 and CE-1 CHF correlations, as described in Section 4.3.

Reference 9

Thus, the topical reports described in References 2 and 3 for TORC code and Reference 8 for CETOP-D code will remain valid with the application of KCE-1 CHF correlation. Therefore, the application of KCE-1 CHF correlation with CETOP-D code for OPR1000 and APR1400 is equivalent to its application with TORC code.

Even though a higher value of inverse Peclet number based on the empirically determined thermal diffusion coefficient was used in the TORC model for CHF data analysis and correlation development, the reactor analysis is to be performed with the design inverse Peclet number ( $1/Pe = 0.0101$ ). This is equivalent to the value of the thermal diffusion coefficient (TDC = 0.038) applied to the Westinghouse PWR for fuel assembly with "R" mixing vane grid design<sup>(9)</sup>.

design<sup>(10)</sup>

**8. REFERENCES**

- (1) APR1400-F-M-TR-12001-P Rev.0, "PLUS7 Fuel Design," November 2012.
- (2) CENPD-161-P-A, "TORC Code, A Computer Code for Determining the Thermal Margin of a Reactor Core," April 1986.
- (3) CENPD-206-P-A, "TORC Code, A Verification and Simplified Modeling Methods," June 1981.

(5) → (4) CENPD-162-P-A, "C-E Critical Heat Flux, Critical Heat Flux Correlation for C-E Fuel Assemblies with Standard Spacer Grids, Part 1 Uniform Axial Power Distribution," September 1976.

(6) → (5) CENPD-207-P-A, "C-E Critical Heat Flux, Critical Heat Flux Correlation for C-E Fuel Assemblies with Standard Spacer Grids, Part 2 Nonuniform Axial Power Distribution," December 1984.

(7) → (6) Tong, L. S., Boiling Crisis and Critical Heat Flux, U. S. Atomic Energy Commission, 1972.

(8) → (7) NUREG-0800, "Standard Review Plan Section 4.2, 'Fuel System Design' Revision 3, and Section 4.4, 'Thermal and Hydraulic Design' Revision 2," March 2007.

(9) → (8) CEN-139(A)-P, "Response to First Round Questions on the Statistical Combination of Uncertainties Program : CETOP-D Code Structure and Modeling Methods," March 1981 and CEN-214(A)-NP, "CETOP-D Code Structure and Modeling Methods for Arkansas Nuclear One –Unit 2," July 1982.

(10) → (9) ML071580898 - Westinghouse AP1000 Design Control Document Rev.16 – Tier 2 "Chapter 4 – Reactor – Section 4.4 Thermal and Hydraulic Design," May 2007.

(4) [ ]<sup>TS.</sup>

INSERT

## RESPONSE TO REQUEST FOR ADDITIONAL INFORMATION

### APR1400 Topical Reports

Korea Electric Power Corporation / Korea Hydro & Nuclear Power Co., LTD

Docket No. PROJ 0782

RAI No.: 3-7443 Question 5  
SRP Section: N/A  
Application Section: KCE-1 Critical Heat Flux Correlation for PLUS7 Thermal Design  
(APR1400-F-C-TR-12002-NP, Rev.0)  
Date of RAI Issued: 03/25/2014  
Response Date: 02/25/2015

---

### **Question 5**

Please describe how the overall bundle power was measured or calculated? It is not clear from the topical report.

### **Response**

*As described in the response to Question 1 of RAI 3-7443, bundle power ( $Tspwr$ ) was reduced from the measured bus to bus power ( $Bbpwr$ ) using the voltage correction factor. And this correction factor was derived from the measured bus to bus voltage and test section voltage. Finally, bundle power was calculated as below,*

*Bundle power = (Measured bus to bus voltage) / (voltage correction factor) x (Measured current)*

*Current metering/readouts for protection/control/test operation are provided by switchboard shunts and are recorded by the data acquisition system. Measurements of voltages are made:*

- between the two ends of heater rod (bus to bus voltage): between the bottom end of the copper end pieces and the tip of the top nickel piece (connecting through top nickel plate)*
- between the test section inlet and outlet (test section voltage).*

*These voltages are conditioned through precision resistor divider networks and amplifiers for entry into the data acquisition system and readout in the control room.*

---

**Impact on DCD**

N/A

**Impact on Technical/Topical/Environmental Report**

N/A

## RESPONSE TO REQUEST FOR ADDITIONAL INFORMATION

### APR1400 Topical Reports

Korea Electric Power Corporation / Korea Hydro & Nuclear Power Co., LTD

Docket No. PROJ 0782

RAI No.: 3-7443 Question 6

SRP Section: N/A

Application Section: KCE-1 Critical Heat Flux Correlation for PLUS7 Thermal Design  
(APR1400-F-C-TR-12002-NP, Rev.0)

Date of RAI Issued: 03/25/2014

Response Date: 02/25/2015

---

### **Question 6**

The CHF test data for the PLUS7 fuel geometry were obtained by using a non-uniform axial power distribution, a symmetric cosine power profile shape with a peak of 1.475. The applicant should explain the appropriateness of testing a single axial profile and why the inlet/bottom or outlet/top peaked power profiles were not included in the test matrix. The applicant should describe how well the tested power distribution represents the actual profile experienced during the operation of the PLUS7 fuel.

### **Response**

*A symmetric cosine axial power distribution is a typical axial power shape resulting from two (2) dimensional neutron diffusion equation for finite cylinder geometry in Table 6-2 of the corresponding reference (Reference : J.R. Larmarsh & A.J. Baratta, "Introduction to Nuclear Engineering 3 e/d," Prentice-Hall 2001).*

*Considering conservatism described below and applicability of the standard Tong factor  $F_c$  to the KCE-1 prediction, which is addressed in the response to Question 7 of RAI 3-7443, the KCE-1 prediction is conservatively valid, not only to tested axial power distribution but also to non-tested ones including top/bottom peaked. Non-tested axial power distributions include the actual axial power distribution that is expected to be experienced during the operation of PLUS7 fuel cores.*

*The effect of non-uniform axial power distribution on CHF was inherently included in the KCE-1 correlation prediction because the KCE-1 CHF correlation was developed using [*

By applying the Tong factor  $F_c$  in the design analysis [ ], the KCE-1 prediction would be more conservative than previous correlations developed with equivalent uniform heat flux from [ ]

By comparing [ ], the effects of axial power distribution are [ ]

With this approach, conservatism is up to [ ] as given in Table 5-5 of the topical report. Figures 6-1 to 6-5 show that no data fall below the current 95/95 limit if the Tong factor  $F_c$  is applied to the KCE-1 prediction. Also, the figures show consistency and reasonable M/P behaviors with respect to variables in the KCE-1 correlation, such as pressure, local mass flux, quality, and heated diameter ratio, respectively.

The background for the above conclusion is as follows.

[ ]  
[ ] is defined as;

$$[ ]^{TS} \quad \text{(Equation 6-1)}$$

where,

$$[ ]^{TS}$$

The physical basis and definition of the Tong factor  $F_c$  implied that the Tong factor  $F_c$  would be lower than one (1.0) for the upstream of the peaked elevation. [ ]

[ ], the CHF prediction for the region of interest resulted in lower DNBR than expected in real phenomenon.

By applying [ ] of the Tong factor  $F_c$ , conservatism given in Table 5-5 of the topical report was evaluated as an [ ]

[ ]. The conservatism was evaluated as approximately [ ]

[ ]. In actual design and safety analyses, the as-calculated Tong factor  $F_c$  is applied when predicting MDNBR. Thus, conservatism in design and safety analyses would be approximately [ ]. M/P trends/distributions are reasonable and/or conservative with respect to the Tong factor  $F_c$  for all cases in Table 5-5 of the topical report, as shown in Figures 6-6 to 6-8.

*The Tong factor  $F_c$  for the KCE-1 correlation database will be included in A-3 of the topical report, as shown in the attached markup. All values of the Tong factor  $F_c$  for the KCE-1 correlation database based on the MDNBR location are [ ]<sup>TS</sup>.*



*Figure 6-1 KCE-1 CHF Correlation Predicted CHF vs. Measured CHF  
(ref. to Figure 5-2 of topical report)*



*Figure 6-2 Distribution of M/P vs. System Pressure  
(ref. to Figure 5-3 of topical report)*



*Figure 6-3 Distribution of M/P vs. Local Mass Flux  
(ref. to Figure 5-4 of topical report)*



*Figure 6-4 Distribution of M/P vs. Local Quality  
(ref. to Figure 5-5 of topical report)*



*Figure 6-5 Distribution of M/P vs. equivalent Heated Diameter Ratio  
(ref. to Figure 5-6 of topical report)*



*Figure 6-6 Distribution of M/P versus Tong Factor  $F_c$  [*

*]*<sup>TS</sup>



Figure 6-7 Distribution of M/P versus Tong Factor Fc [

TS

] <sup>TS</sup>

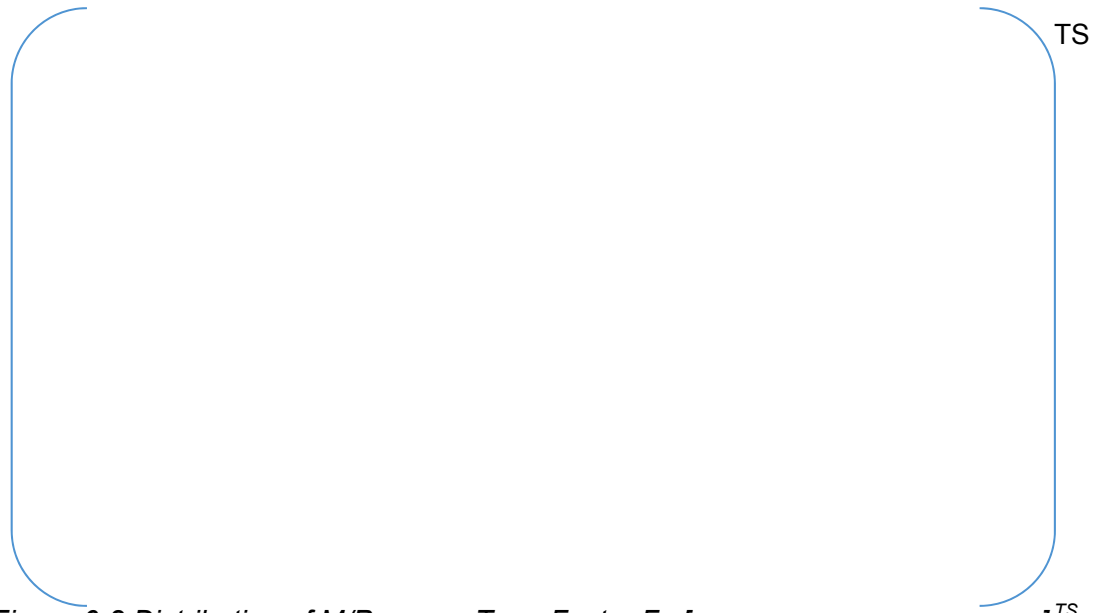


Figure 6-8 Distribution of M/P versus Tong Factor Fc [

TS

] <sup>TS</sup>

**Impact on DCD**

N/A

**Impact on Technical/Topical/Environmental Report**

Topical Report APR1400-F-C-TR-12002-NP will be revised as indicated on the attached markups.

- Document Mark-up Cover Sheet : 1 page
- Mark-up for Q6 of RAI 3-7443 : 17 pages

※Remark: Minor formatting, such as numbering figures, tables and references, etc., will be cleaned up before finalizing the topical report.

# Document Mark-up Cover Sheet

1. **Project ID:** *APRI400 NRC DC*
2. **Type of Corresponding Document:**  
 DCD     Topical Report     Technical Report     Other(s) \_\_\_\_\_
3. **Title of Corresponding Document:** *KCE-1 CHF Correlation for PLUS7 Thermal Design  
(APRI400-F-C-TR-12002-NP)*
4. **RAI ID/Question ID:** *3-7443 / Q6*
5. **Page(s) attached:** *17 (Seventeen)*

## APPENDIX A. DATA FOR KCE-1 CHF CORRELATION DEVELOPMENT

The raw test data, [ ]<sup>TS</sup> in total, collected from the PLUS7 fuel CHF tests are listed in Table A-1. The [ ]<sup>TS</sup> local fluid conditions excluded during the correlation development process from the local fluid conditions for each test data calculated by the TORC code are listed along with the reason for exclusion in Table A-2. Finally, the KCE-1 CHF correlation database, [ ]<sup>TS</sup> in total, is presented in Table A-3.

Acronyms presented in the subsequent tables:

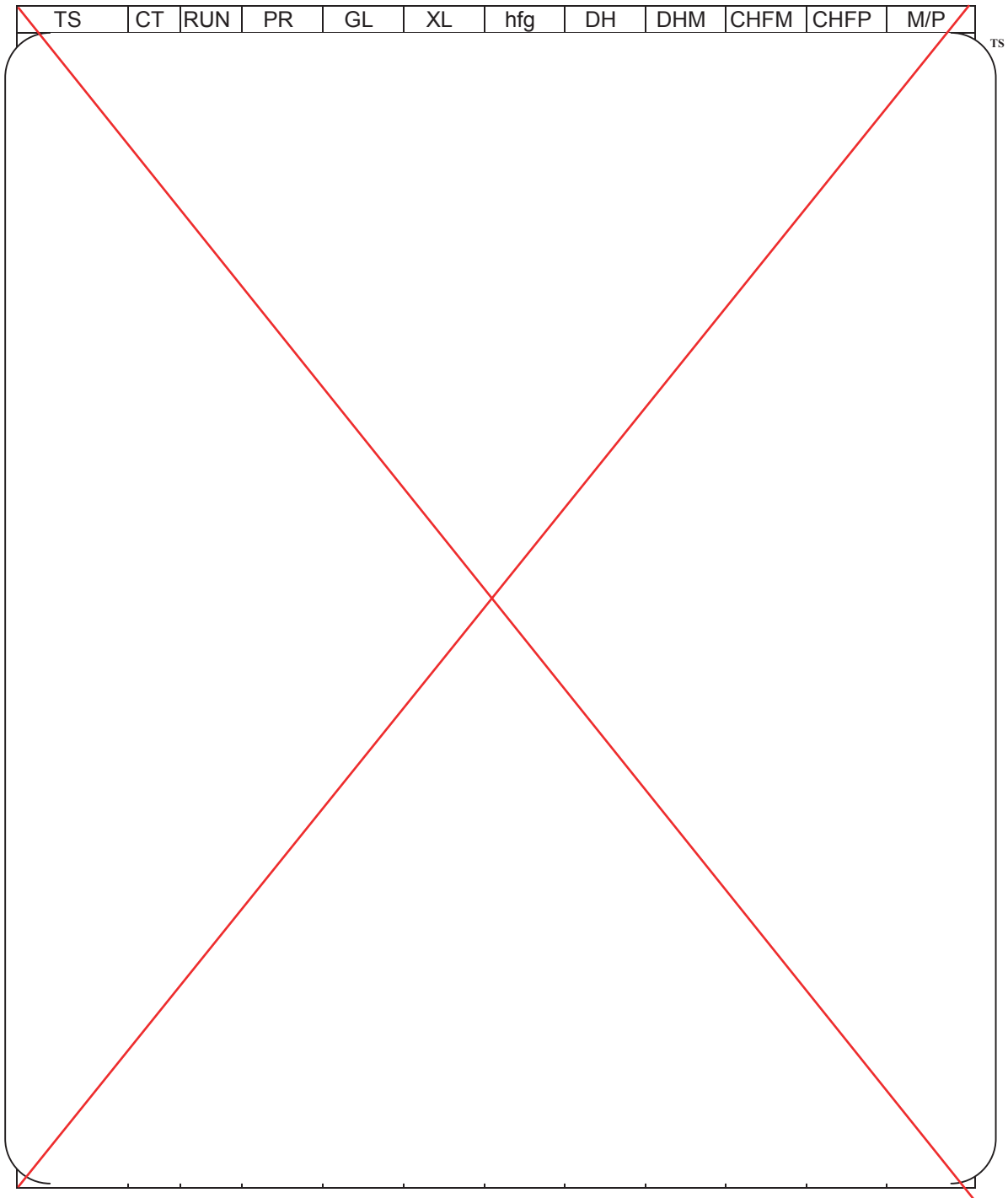
TS	:	test section number
RUN	:	run number
PR	:	system pressure, <i>psia</i>
TIN	:	inlet temperature, <i>°F</i>
GIN	:	inlet mass flux (inlet mass velocity), <i>Mlbm/hr-ft<sup>2</sup></i>
BAP	:	bundle average power, <i>MW</i>
HFX	:	heat flux, <i>MBtu/hr-ft<sup>2</sup></i>
TC	:	primary CHF rod and thermocouple number (XX.x)*
CT	:	CHF subchannel type
M	:	matrix subchannel
C	:	guide thimble corner subchannel
S	:	guide thimble side subchannel
GL	:	local mass flux (local mass velocity), <i>Mlbm/hr-ft<sup>2</sup></i>
XL	:	local quality
DH	:	equivalent heated diameter of CHF subchannel, <i>in.</i>
DHM	:	equivalent heated diameter of matrix subchannel, <i>in.</i>
CHFM	:	measured CHF, <i>MBtu/hr-ft<sup>2</sup></i>
CHFP	:	KCE-1 correlation predicted CHF, <i>MBtu/hr-ft<sup>2</sup></i>

**F<sub>c</sub>** : Tong factor

\* XX = Rod number, x = T/C number  
(See Figure 2-5 through Figure 2-7 and Figure 2-9.)

INSERT

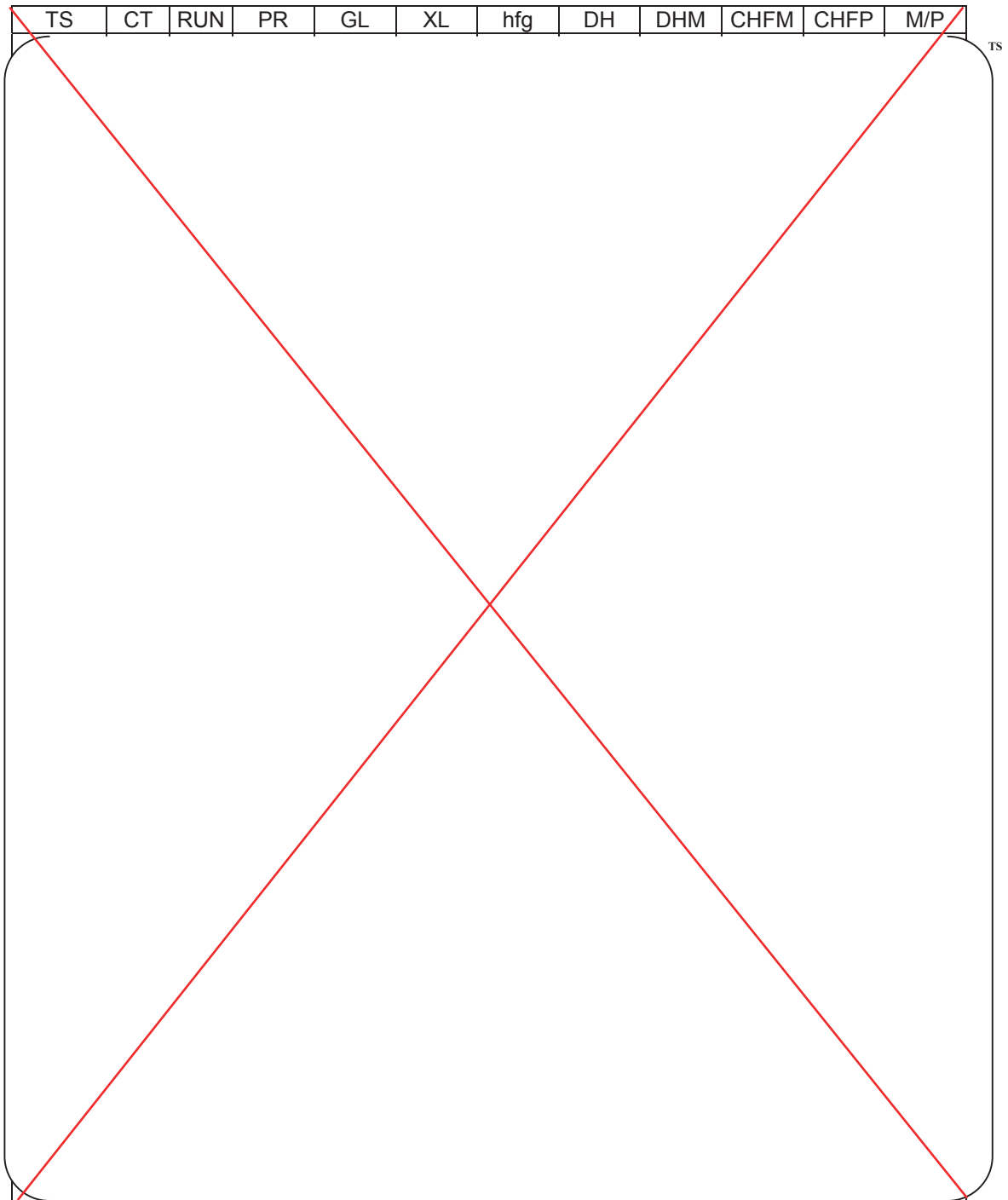
**Table A-3 KCE-1 CHF Correlation Database (1/8)**

TS	CT	RUN	PR	GL	XL	hfg	DH	DHM	CHFM	CHFP	M/P
											

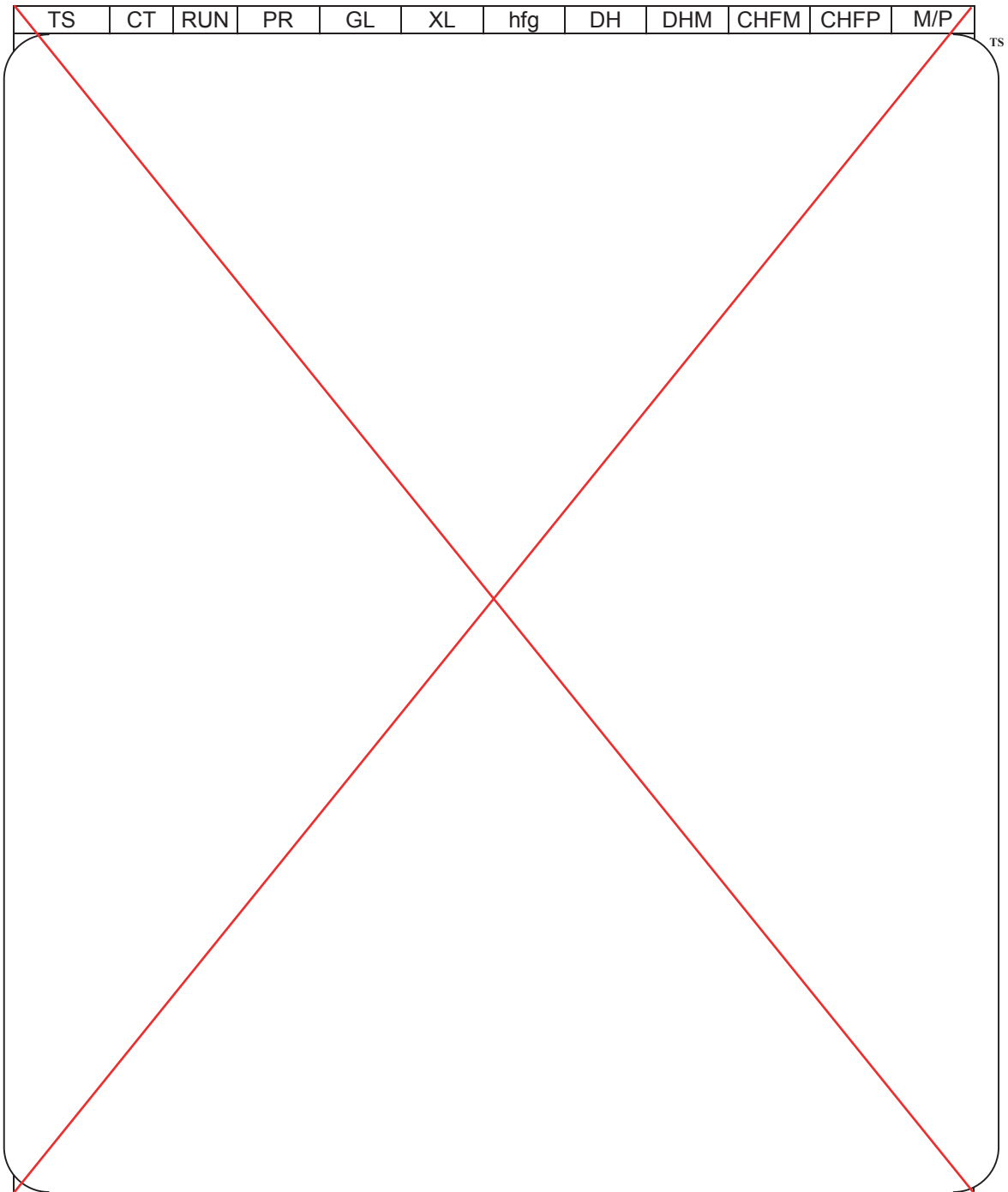
**Table A-3 KCE-1 CHF Correlation Database (2/8)**

TS	CT	RUN	PR	GL	XL	hfg	DH	DHM	CHFM	CHFP	M/P

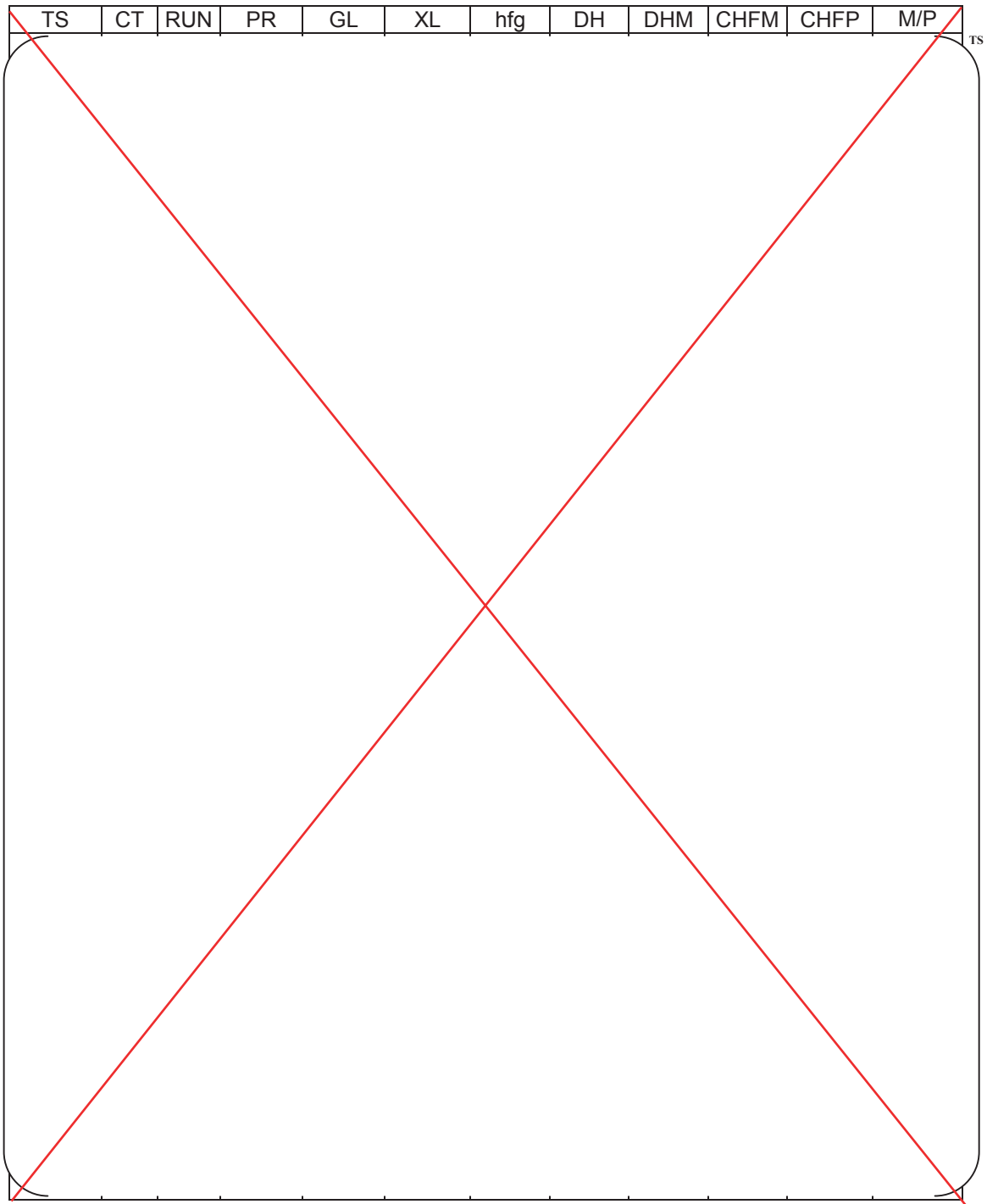
**Table A-3 KCE-1 CHF Correlation Database (3/8)**

TS	CT	RUN	PR	GL	XL	hfg	DH	DHM	CHFM	CHFP	M/P
											

**Table A-3 KCE-1 CHF Correlation Database (4/8)**

TS	CT	RUN	PR	GL	XL	hfg	DH	DHM	CHFM	CHFP	M/P
											

**Table A-3 KCE-1 CHF Correlation Database (5/8)**

TS	CT	RUN	PR	GL	XL	hfg	DH	DHM	CHFM	CHFP	M/P
											

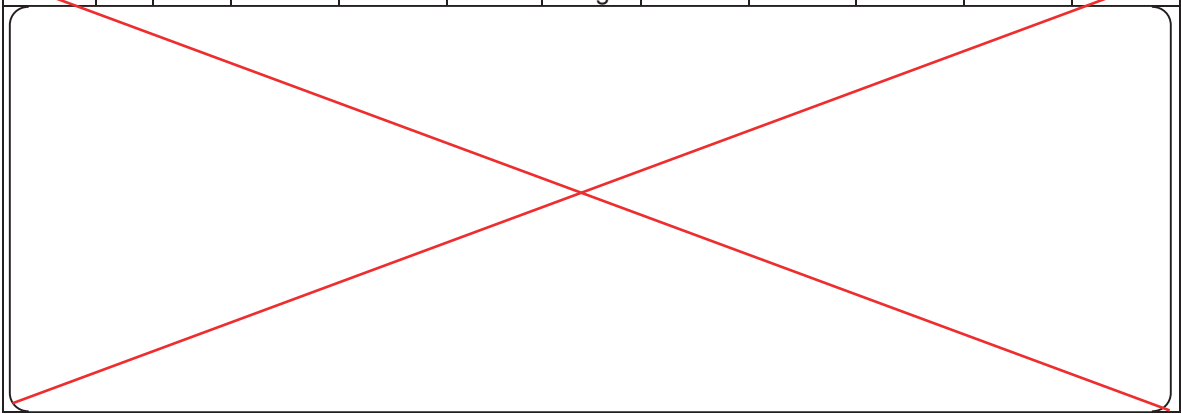
**Table A-3 KCE-1 CHF Correlation Database (6/8)**

TS	CT	RUN	PR	GL	XL	hfg	DH	DHM	CHFM	CHFP	M/P

**Table A-3 KCE-1 CHF Correlation Database (7/8)**

TS	CT	RUN	PR	GL	XL	hfg	DH	DHM	CHFM	CHFP	M/P

**Table A-3 KCE-1 CHF Correlation Database (8/8)**

TS	CT	RUN	PR	GL	XL	hfg	DH	DHM	CHFM	CHFP	MP
											

**Table A-3 KCE-1 CHF Correlation Database (1/8)**

TS	CT	RUN	PR	GL	XL	hfg	DH	DHM	CHFM	CHFP	M/P	F <sub>c</sub>

**Table A-3 KCE-1 CHF Correlation Database (2/8)**

TS	CT	RUN	PR	GL	XL	hfg	DH	DHM	CHFM	CHFP	M/P	F <sub>c</sub>

**Table A-3 KCE-1 CHF Correlation Database (3/8)**

TS	CT	RUN	PR	GL	XL	hfg	DH	DHM	CHFM	CHFP	M/P	F <sub>c</sub>
[Empty table body]												

Table A-3 KCE-1 CHF Correlation Database (4/8)

TS	CT	RUN	PR	GL	XL	hfg	DH	DHM	CHFM	CHFP	M/P	Fc

**Table A-3 KCE-1 CHF Correlation Database (5/8)**

TS	CT	RUN	PR	GL	XL	hfg	DH	DHM	CHFM	CHFP	M/P	F <sub>c</sub>

**Table A-3 KCE-1 CHF Correlation Database (6/8)**

TS	CT	RUN	PR	GL	XL	hfg	DH	DHM	CHFM	CHFP	M/P	F <sub>c</sub>

**Table A-3 KCE-1 CHF Correlation Database (7/8)**

TS	CT	RUN	PR	GL	XL	hfg	DH	DHM	CHFM	CHFP	M/P	F <sub>c</sub>
----	----	-----	----	----	----	-----	----	-----	------	------	-----	----------------

**Table A-3 KCE-1 CHF Correlation Database (8/8)**

TS	CT	RUN	PR	GL	XL	hfg	DH	DHM	CHFM	CHFP	M/P	F <sub>c</sub>

## RESPONSE TO REQUEST FOR ADDITIONAL INFORMATION

### APR1400 Topical Reports

Korea Electric Power Corporation / Korea Hydro & Nuclear Power Co., LTD

Docket No. PROJ 0782

RAI No.: 3-7443 Question 7

SRP Section: N/A

Application Section: KCE-1 Critical Heat Flux Correlation for PLUS7 Thermal Design  
(APR1400-F-C-TR-12002-NP, Rev.0)

Date of RAI Issued: 03/25/2014

Response Date: 02/25/2015

### **Question 7**

As no testing was conducted with uniform axial power distribution, no “non-uniform axial power distribution correction factor, Tong factor  $FC$ ,” could be developed for the KCE-1 CHF correlation for the tested PLUS7 fuel geometry. Such an optimization of Tong factor for the PLUS7 fuel split vane mixing grid geometries would require testing both uniform and non-uniform axial power distributions with and without guide thimbles, but it was not done for the tested PLUS7 fuel geometry. However, the applicant plans to conservatively use the Tong factor along with the KCE-1 correlation to predict the CHF in the design analyses. The applicant should justify using the CE-1 Correlation Tong factor not developed for the tested PLUS7 fuel geometry. Other CHF correlations generally use Tong factor developed by the test data taken with both uniform and non-uniform axial power profiles.

### **Response**

*Applying the standard Tong factor  $F_c$  to PLUS7 CHF data analysis with KCE-1 CHF correlation is conservative as discussed in the response to Question 6 of RAI 3-7443. It is applicable to design and safety analyses on PLUS7 cores with KCE-1 prediction based on the technical background of non-dependency to fuel design (note that Tong factor  $F_c$  did not have any terms related to geometric variables) and to correlation under the assumption described in subsection 4.3 of the topical report.*

*The effect of Tong factor  $F_c$  application to design and safety analyses is addressed in the response to Question 6 of RAI 3-7443 including [*

*]<sup>TS</sup>.*

As shown below, the standard Tong factor  $F_c$  has been applied successfully to various fuel designs and corresponding CHF correlations under similar application environments with KCE-1 CHF correlation.

- Standard Tong factor  $F_c$  for rod bundles applied to W-3 CHF correlation (Reference: Rosal, E.R. et al., "High Pressure Rod Bundle DNB Data with Axially Non-Uniform Heat Flux," Nuclear Engineering and Design 31, pp 1-20, 1975)

*Effects on CHF due to non-uniform axial power distribution had been investigated for the spacer grid design (with and without mixing vane), grid spacing, heated length, and pitch to rod diameter ratio. Applying standard the Tong factor  $F_c$  to W-3 CHF correlation with spacer factor had predicted CHF accurately in axially non-uniformly heated rod bundles.*

- Standard Tong factor  $F_c$  for rod bundles applied to CE-1 CHF correlation (Reference: CENPD-162-P-A & CENPD-207-P-A, references 4 & 5 of topical report)

*Applying the standard Tong factor  $F_c$  to the CE-1 CHF correlation had predicted CHF conservatively in axially non-uniformly heated rod bundles. The CE-1 CHF correlation was developed with CHF data from axially uniformly heated rod bundles for various spacer grid designs and pitch to rod diameter ratios.*

- Standard Tong factor  $F_c$  for rod bundles applied to WRB-1 CHF correlation (Reference: WCAP-8763-A, "New Westinghouse Correlation WRB-1 for Predicting Critical Heat Flux in Rod Bundles with Mixing Vane Grids," July 1984 )

*The confirmation process for existing non-uniform F factor (standard Tong factor  $F_c$ ) had been performed with respect to the CHF correlation developed with CHF data from axially uniformly heated rod bundles. The results of applying the standard Tong factor  $F_c$  to WRB-1 prediction for non-uniform data showed that no modification to either the constant or the form of F factor was necessary for application.*

- The geometries of CHF test data for the above included design characteristics of PLUS7 fuel. The data for CE-1 correlation (2nd circle above) included data with rod pitch (0.506 inch) and guide tube diameter (0.980 inch) of PLUS7 fuel. Data for W-3 and/or WRB-1 correlation (1st and/or 3rd circle above) included data with mixing vane design (R-type split vane) and range of grid spacing (15.72 inch), and rod diameter (0.374 inch) of PLUS7 fuel.

---

**Impact on DCD**

N/A

**Impact on Technical/Topical/Environmental Report**

N/A

---

## RESPONSE TO REQUEST FOR ADDITIONAL INFORMATION

### APR1400 Topical Reports

Korea Electric Power Corporation / Korea Hydro & Nuclear Power Co., LTD

Docket No. PROJ 0782

**RAI No.:** 3-7443 Question 8

**SRP Section:** N/A

**Application Section:** KCE-1 Critical Heat Flux Correlation for PLUS7 Thermal Design  
(APR1400-F-C-TR-12002-NP, Rev.0)

**Date of RAI Issued:** 03/25/2014

**Response Date:** 02/25/2015

---

### **Question 8**

SRP Section 4.4 outlines the DNB acceptance criterion to provide assurance that there be at least a 95-percent probability at a 95-percent confidence level that the hot fuel rod in the core does not experience a DNB or transition condition during normal operation or AOOs. The use of a single 95/95 DNBR limit to bound the uncertainty of the KCE-1 correlation is predicated on the assumption that the correlation behaves consistently and its uncertainty is independent of location throughout the application domain. Figure 5-3 of the topical report suggests that this assumption may not be true. The five (5) pressure datasets in the figure used in the correlation development seem to be from four different populations. Additionally, there is a trend of decreasing predictive capability with pressures from 2200 to 1750 psia. While that trend has clearly reversed by the low pressures around 1400 psia, it is not apparent how far the trend would continue in the empty region of pressures between 1400–1750 psia before reversing, and what causes the reversal. Provide justification for the use of a single uncertainty to bound the KCE-1 correlation over its intended application domain, focusing specifically on the regions which demonstrated a trend in decreasing predictive capability. Further provide justification for the application of the uncertainty in the empty region around pressures between 1400–1750 psia. To a less extent, a similar concern pertains to Figure 5-4, where a more conservative dataset of local mass flux at about 0.85 Mlbm/hr-ft<sup>2</sup> is included in the correlation development after a similar reversal in the predictive capability of the KCE-1 correlation.

### **Response**

*The 95/95 DNBR limit of KCE-1 CHF correlation, 1.124, is the most limiting value among cases considered in Table 5-3 of the topical report with the assumption described in subsection 4.2 of the topical report. Corresponding M/P plots to the 95/95 DNBR limit of 1.124 were given in Figures 5-3 and 5-4 of the topical report for pressure and mass flux, respectively. However the*

assumption to consider the type of subchannel would not be applied to design and safety analyses with KCE-1 CHF correlation. M/P statistics without the assumption led to a lower 95/95 limit value, as given in Table 5-4 of the topical report. Corresponding M/P plots without the assumption are given in Figures 8-1 and 8-2 for pressure and mass flux, respectively. Even though M/Ps of pressure [

] <sup>TS</sup>. The dataset used to plot the Figures 8-1 and 8-2 was already provided in Table A-3 of the topical report. Especially, selecting the maximum M/P for each data point of Test Section TS101 led to the dataset used for Figures 8-1 and 8-2. It means that the data with maximum M/P were just selected for the same "RUN" regardless of the sub-channel type of "CT". For the NRC staff's verification analysis, normalized data is provided in Table 8-1. This dataset is composed of [ ] <sup>TS</sup> data, which corresponds to the second table in Table 5-4 of the topical report.

[

] <sup>TS</sup>.

Therefore, the KCE-1 CHF correlation, with the 95/95 DNBR limit of 1.124, is applicable to the design analysis range (AOO) of APR1400 for pressure (1,785 - 2,415 psia, as addressed in the response to Question 18 of RAI 3-7443).

*Table 8-1. Normalized Dataset for Figures 8-1 and 8-2 (1/4)*

TS

*Table 8-1. Normalized Dataset for Figures 8-1 and 8-2 (2/4)*

TS

*Table 8-1. Normalized Dataset for Figures 8-1 and 8-2 (3/4)*

TS

*Table 8-1. Normalized Dataset for Figures 8-1 and 8-2 (4/4)*

TS

*Table 8-2. Comparison of 95/95 DNBR limit*

TS

*Table 8-3. D' Normality Test*

TS



*Figure 8-1 Distribution of M/P versus System Pressure (without the assumption: relaxation)*



*Figure 8-2 Distribution of M/P versus Local Mass Flux (without the assumption: relaxation)*

---

**Impact on DCD**

N/A

**Impact on Technical/Topical/Environmental Report**

N/A

## RESPONSE TO REQUEST FOR ADDITIONAL INFORMATION

### APR1400 Topical Reports

Korea Electric Power Corporation / Korea Hydro & Nuclear Power Co., LTD

Docket No. PROJ 0782

RAI No.: 3-7443 Question 9  
SRP Section: N/A  
Application Section: KCE-1 Critical Heat Flux Correlation for PLUS7 Thermal Design  
(APR1400-F-C-TR-12002-NP, Rev.0)  
Date of RAI Issued: 03/25/2014  
Response Date: 02/25/2015

---

### **Question 9**

Detailed investigation of the test data, conducted by the staff, has revealed a potentially nonconservative subregion at pressures near 1750 psia, qualities near 0.1, and local mass fluxes near 2 Mlbm/hr-ft<sup>2</sup>. This subregion contains a higher than expected number of M/P values which were below the 95/95 statistic than can be explained by random chance. Provide justification for the use of the KCE-1 correlation in this subregion, and the surrounding empty subregions.

### **Response**

*As pointed out in Question 9 of RAI 3-7443, a relatively large number of M/P points fell below the 95/95 DNBR limit in pressure near 1750 psia, but it would not be critical for applying the KCE-1 CHF correlation to APR1400 cores within applicable ranges of parameters given in Section 7 of the topical report because;*

- *A number of M/Ps less than the 95/95 DNBR limit were small and randomly distributed over the range of variables, except for the pressure.*

*Seven (7) out of 321 M/Ps in the database of KCE-1 CHF correlation fell below the 95/95 DNBR limit, 1.124. In case of pressure, six (6) out of 7 were in near 1,750 psia and one (1) out of 7 was near 2,200 psia. In case of local mass flux, four (4) out of 7 were near 1.5 Mlbm/hr-ft<sup>2</sup>, two (2) out of 7 were near 2.0 Mlbm/hr-ft<sup>2</sup>, and one (1) out of 7 was near 2.5 Mlbm/hr-ft<sup>2</sup>. In case of local quality, one (1) out of 7 was below 0.0, one (1) out of 7 was near/below 0.05, two (2) out of 7 were near/above 0.05, one (1) out of 7 was near 0.15 and two (2) out of 7 were near 0.17.*

- *The number of M/Ps that fell below 95/95 DNBR limit reduced when the assumption*

*described in subsection 4.2 of the topical report was not considered.*

*As shown in Figure 8-1 of the response to Question 8 of RAI 3-7443, distribution of M/P versus pressure was improved (to a more appropriate trend) without the assumption. And it resulted in [*

*]TS. The assumption led to a conservatively higher 95/95 DNBR limit value of KCE-1 correlation, as given in Table 5-4 of the topical report.*

- *The Tong factor  $F_c$  was applied to the [ ]TS data, which were used to obtain the results in Table 8-2 of the response to Question 8 of RAI 3-7443, to calculate the 95/95 DNBR limit values when the Tong factor  $F_c$  is applied. The results are shown in Table 9-1. Compared to the results in Table 8-2, the mean M/P increased over [ ]TS and the 95/95 DNBR limit decreased over [ ]TS with Tong factor  $F_c$  application in all three data groups.*

*Especially, M/P statistics analyses were performed using 187 data for the same pressure range from only Test Section TS101.*

*The purpose of these analyses were to compare the differences among the M/P statistics and the 95/95 DNBR limit specifically in “All M/P”, “Min. M/P”, and “Max. M/P”. The descriptions and results of each case are presented in Table 9-2. When the 95/95 DNBR limit of the three cases with Tong factor  $F_c$  application was determined, the current DNBR limit value of the KCE-1 correlation, 1.124 was still conservative and no data fell below 1.124, as shown in Figure 9-1.*

- *For the application of KCE-1 CHF correlation to the design analysis range of APR1400, DNBRs are calculated in all locations of cores with Tong Factor  $F_c$  and MDNBR is determined regardless of [ ]TS among all DNBRs. Therefore, determining correlation statistics or the 95/95 DNBR limit based on MDNBR (Max. M/P) is consistent with actual design application.*

*Table 9-1. The comparison of M/P statistics as the application of Tong Factor  $F_c$*  TS

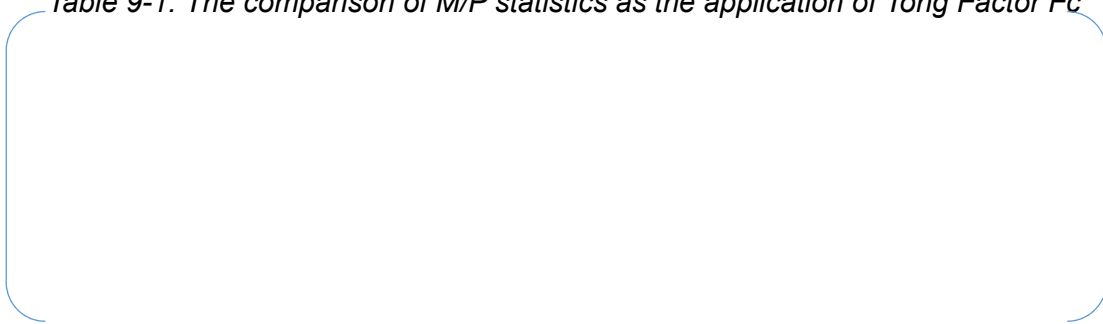


*Table 9-2. The detailed M/P statistics of Test Section TS101 as the application of Tong Factor  $F_c$*  TS

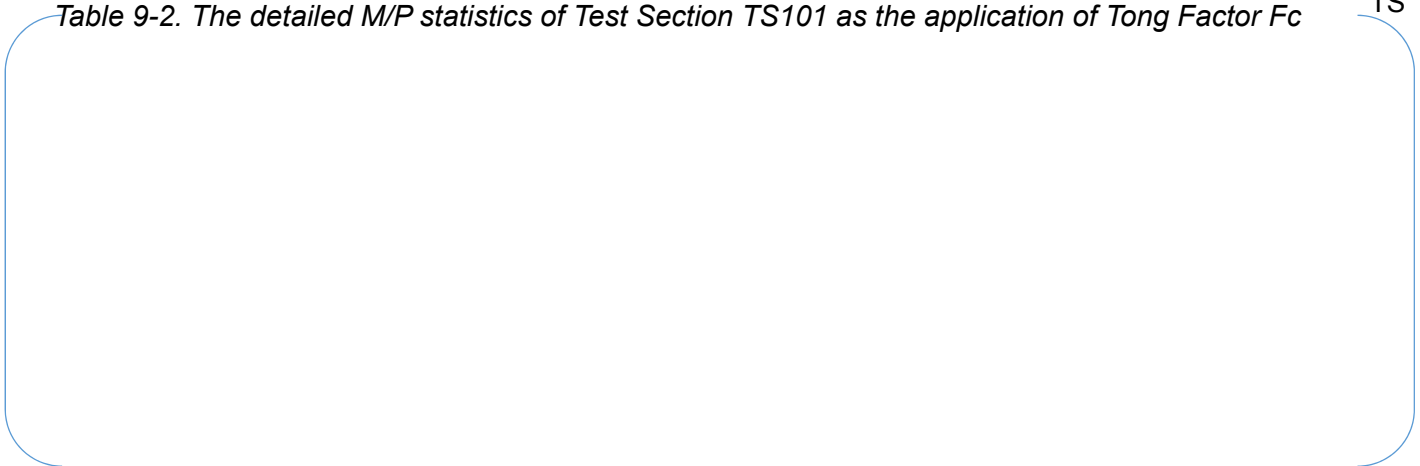




*Figure 9-1 M/P versus Pressure of Test Section TS101 with Tong factor  $F_c$  at 95/95 DNBR limit of "Min. M/P" (Refer to Table 9-2)*

---

**Impact on DCD**

N/A

**Impact on Technical/Topical/Environmental Report**

N/A

## RESPONSE TO REQUEST FOR ADDITIONAL INFORMATION

### APR1400 Topical Reports

Korea Electric Power Corporation / Korea Hydro & Nuclear Power Co., LTD

Docket No. PROJ 0782

**RAI No.:** 3-7443 Question 10  
**SRP Section:** N/A  
**Application Section:** KCE-1 Critical Heat Flux Correlation for PLUS7 Thermal Design  
(APR1400-F-C-TR-12002-NP, Rev.0)  
**Date of RAI Issued:** 03/25/2014  
**Response Date:** 02/25/2015

---

### **Question 10**

The applicant should explain the technical basis for using 0.275 as the upper limit of the tested local quality range (-0.150~0.275) applicable to the PLUS7 fuel design. Other fuel bundle designs have used higher upper limits of quality range. Does the applicant envision exceeding the quality range in any circumstances, e.g., future power uprate, etc.? Please include the measured CHF vs. local quality data in the present topical report for the staff to ensure that there were no adverse trends in the data.

### **Response**

*The applicable range of local quality is determined based on the quality at the predicted MDNBR location by KCE-1 CHF correlation. All design/safety analysis activities will be limited to meet the current applicable range of the quality of KCE-1 CHF correlation at the location of MDNBR.*

*The measured CHF versus local quality data at the CHF location (where CHF occurred during the CHF test) was part of the initial data set at the beginning of KCE-1 CHF correlation development. Those are shown in Figure 10-1 for all data sets (including excluded data, tabulated in Table A-2 of the topical report).*

*Initial data given in Table 10-1 represent local fluid conditions extracted from measured CHF location during the test. In detail, as presented in Table A-1 of the topical report, all test points*

have their own test conditions, such as pressure, inlet temperature, inlet mass flux, and heat flux, and also have information on occurred/indicated CHF location.

Subchannel code TORC calculated the local fluid conditions using the above test condition as code input. Then, local fluid conditions at the measured CHF location were extracted per each test point. This dataset is called the initial data set.

The initial dataset was a start point of determining the correlation coefficients. An iterative process was used to optimize the coefficients as below. This process is also described in Subsection 4.4 of the topical report.

- 1) First step, as described above, the initial data set is extracted from TORC output files.
- 2) Second step, set the initial estimate of the eight coefficients as same as the CE-1 CHF correlation and this is the initial KCE-1 CHF correlation.
- 3) Third step, M/P analyses are performed for the initial data set using the initial KCE-1 CHF correlation.
- 4) Fourth step, extract the local fluid conditions at the location with MDNBR(Maximum M/P).
- 5) Fifth step, by using the local fluid condition extracted in the fourth step, revise KCE-1 CHF correlation and re-extract the local fluid conditions at MDNBR using the revised KCE-1 CHF correlation. This process is repeated until the correlation statistics are not changed by revising KCE-1 CHF correlation.

By an iterative process, final coefficients of the correlation were determined. Table A-3 of the topical report shows the local fluid conditions and relevant information at the location with MDNBR, among the DNBR values calculated with the final coefficient of the KCE-1 CHF correlation

As explained above, Table 10-1 shows the local fluid conditions at the CHF location. However, Table A-3 of the topical report shows the local fluid conditions and relevant information at the location with MDNBR after the final coefficients of the KCE-1 CHF correlation determined by an iterative process.

The initial data set is a starting point to fit the correlation, so no correlation is available at that moment. That is why the predicted CHF and M/P values are not included in Table 10-1.

The trend of measured CHF with respect to local quality was typical, meaning that [ ]<sup>TS</sup> without any adverse behavior. This information is listed in Table 10-1 and will be included in an appropriate section of the topical report as shown in the attached markup.

Additionally, the reason why KCE-1 CHF Correlation Database was selected at the MDNBR location is as follows.

- The major design criterion for thermal design was established to “Provide assurance that there be at least a 95-percent probability at 95-percent confidence level that the hot fuel rod in the core does not experience a CHF during normal operation or AOOs”. KCE-1 CHF correlation applies to the thermal design of the APR1400 reactor core loaded with PLUS7 fuel assembly, in accordance with CHF or DNB acceptance criteria. From the design criterion, “the hot fuel” means the limiting location where the thermal margin is minimum in the core and it is the same meaning with subchannels adjacent to the rod having the MDNBR. So, in accordance with CHF acceptance criteria for thermal design, the KCE-1 CHF correlation database is composed with local fluid conditions where the KCE-1 correlation predicted MDNBR.
- As shown below, the same data selection method was applied to WRB-1 and WRB-2 correlations to compose the correlation database.

*From subsection 3-3 of the WRB-1 correlation topical report,*

*(Reference: WCAP 8763-A, “New Westinghouse Correlation WRB-1 for Predicting Critical Heat Flux in Rod Bundles with Mixing Vane Grids”)*

*“Table 3-1 gives the result of applying the WRB-1 correlation to each of the various rod bundle sets, in the form of an average measured-to-predicted critical heat flux ratio,  $(M/P)_{AV}$  and sample standard deviation,  $s$ , for each data set. **The individual M/P’s were evaluated at the point of minimum DNBR**, which is defined as~”*

*From subsection A.2.3.1 of Reference Core Report (VANTAGE 5 Fuel Assembly)*

*(Reference: WCAP 10444-P-A, “Reference Core Report Vantage 5 Fuel Assembly”)*

*“Table A-1 gives the WRB-2 CHF correlations statistics (average measured-to-predicted critical heat flux ratio and sample standard deviation) for each data set in the WRB-2 database. **The individual M/P’s were evaluated at the point of minimum DNBR in the rod bundle**, where~”*

Note :

○ MDNBR elevation/location

- where DNBR was minimum among all the locations within the test sections
- $DNBR = \text{heat flux predicted by KCE-1 correlation} / \text{actual heat flux at the location of interest}$
- Table A-3 (KCE-1 correlation database) of the topical report listed the information at the MDNBR elevation/location

○ CHF elevation/location

- where CHF was indicated (measured) by temperature excursion on corresponding TC(s) of test sections
- Table A-1 (PLUS7 CHF Test Data) of topical report listed the information at the CHF elevation/location
- Table 10-1 listed corresponding information to Table A-3 of topical report at CHF location (including excluded data given in Table A-2 of the topical report)

○ The legend in Table 10-1 is the same as given in page A-1 of the topical report

*Table 10-1 KCE-1 CHF Correlation Initial Dataset (1/7)*

TS

*Table 10-1 KCE-1 CHF Correlation Initial Dataset (2/7)*

TS

*Table 10-1 KCE-1 CHF Correlation Initial Dataset (3/7)*

TS

*Table 10-1 KCE-1 CHF Correlation Initial Dataset (4/7)*

TS

*Table 10-1 KCE-1 CHF Correlation Initial Dataset (5/7)*

TS

*Table 10-1 KCE-1 CHF Correlation Initial Dataset (6/7)*

TS

*Table 10-1 KCE-1 CHF Correlation Initial Dataset (7/7)*

TS



*Figure 10-1 Measured CHF vs. Local Quality (at CHF location)*

**Impact on DCD**

N/A

**Impact on Technical/Topical/Environmental Report**

Topical Report APR1400-F-C-TR-12002-NP will be revised as indicated on the attached markups.

- Document Mark-up Cover Sheet : 1 page
- Mark-up for Q10 of RAI 3-7443 : 21 pages

※Remark: Minor formatting, such as numbering figures, tables and references, etc., will be cleaned up before finalizing the topical report.

# Document Mark-up Cover Sheet

1. **Project ID:** *APR1400 NRC DC*
2. **Type of Corresponding Document:**  
 DCD     Topical Report     Technical Report     Other(s) \_\_\_\_\_
3. **Title of Corresponding Document:** *KCE-1 CHF Correlation for PLUS7 Thermal Design  
(APR1400-F-C-TR-12002-NP)*
4. **RAI ID/Question ID:** *3-7443 / Q10*
5. **Page(s) attached:** *21 (Twenty One)*

selected range used in the initial runs was based upon the range of data at the [ ] elevation.

The initial dataset is listed in Table A-2 of APPENDIX A.

2) The second step was to determine the initial estimate of the eight coefficients of the CE-1 CHF correlation formula by using a nonlinear regression code. To obtain convergence, the initial guesses were based upon the values for the CE-1 CHF correlation, Reference 4. The resulting applicable ranges of parameters for the initial KCE-1 CHF correlation were as follows:

INSERT

- System pressure
- Local mass flux
- Local quality

3) As the third step, statistical tests were performed for the indicated CHF elevation data with the CHF statistics for the initial KCE-1 CHF correlation. An outlier test was applied to identify potential test data which could be removed. There was no outlier for the [ ]<sup>TS</sup> elevation data.

[ ]<sup>TS</sup>

4) As the fourth step, an iterative process was then applied by using the initial coefficients of the KCE-1 CHF correlation from the [ ]<sup>TS</sup> elevation for each test section with [ ]<sup>TS</sup>

5) As the fifth step, local fluid conditions were extracted at the minimum DNBR elevation in a channel [ ]<sup>TS</sup> rod. The local fluid conditions at the [ ]<sup>TS</sup> [ ]<sup>TS</sup> rod, if applicable, were extracted for TS101. As stated in section 4.3 and Reference 4,

[ ]<sup>TS</sup>

6) Step 2 was repeated several times with the minimum DNBR data to determine the eight coefficients of the CE-1 CHF correlation formula. After the initial run at the minimum DNBR elevation, the data were examined for outliers. Based upon this outlier test, [ ]<sup>TS</sup> was eliminated, as shown in Table 4-3. [ ]<sup>TS</sup>

[ ]<sup>TS</sup>

- 7) Steps 4 ~ 6 were repeated until the correlation statistics were unchanged with update of the coefficients. Although there is a change in the minimum DNBR elevation for a small number of runs between previous and current runs, if the coefficient change results in essentially no change in the final statistics, the iteration process was completed and the coefficients from the previous run were considered the final.

The data rejected during the correlation development process from the entire [ ]<sup>TS</sup> test data are listed in ~~Table A-2~~ of APPENDIX A.

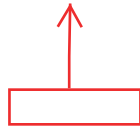
The final coefficients determined and the applicable ranges of parameters for the KCE-1 CHF correlation are presented in Table 4-4. Corresponding data base of KCE-1 CHF correlation is given in ~~Table A-3~~ of APPENDIX A.



**Table 5-5 KCE-1 CHF Correlation Conservatism with Non-Uniform Axial Power Distribution Correction Factor Application**

- Within Applicable Ranges of Parameters

Case	$n$	$\bar{x}_{(M/P)}$	$S_{(M/P)}$
<div style="display: flex; justify-content: space-between; align-items: center;"> <span data-bbox="360 569 375 705" style="font-size: 2em;">{</span> <span data-bbox="1300 569 1325 705" style="font-size: 2em;">}</span> <span data-bbox="1300 569 1325 600" style="margin-left: 5px;">TS</span> </div>			
<div style="display: flex; justify-content: space-between; align-items: center;"> <span data-bbox="383 705 391 741" style="font-size: 2em;">[</span> <span data-bbox="1049 705 1073 741" style="font-size: 2em;">]</span> <span data-bbox="1049 705 1073 741" style="margin-left: 5px;">TS</span> </div>			



**APPENDIX A. DATA FOR KCE-1 CHF CORRELATION DEVELOPMENT**

The raw test data, [ ]<sup>TS</sup> in total, collected from the PLUS7 fuel CHF tests are listed in Table A-1. The [ ]<sup>TS</sup> local fluid conditions excluded during the correlation development process from the local fluid conditions for each test data calculated by the TORC code are listed along with the reason for exclusion in Table A-2. Finally, the KCE-1 CHF correlation database, [ ]<sup>TS</sup> in total, is presented in Table A-3.

Table A-4

Table A-3

Acronyms presented in the subsequent tables:

The initial dataset, [ ]<sup>TS</sup> in total, extracted from the measured CHF location is presented in Table A-2 of APPENDIX A.

INSERT

- TS : test section number
- RUN : run number
- PR : system pressure, *psia*
- TIN : inlet temperature, *°F*
- GIN : inlet mass flux (inlet mass velocity), *Mlbm/hr-ft<sup>2</sup>*
- BAP : bundle average power, *MW*
- HFX : heat flux, *MBtu/hr-ft<sup>2</sup>*
- TC : primary CHF rod and thermocouple number (XX.x)\*
- CT : CHF subchannel type
- M : matrix subchannel
- C : guide thimble corner subchannel
- S : guide thimble side subchannel
- GL : local mass flux (local mass velocity), *Mlbm/hr-ft<sup>2</sup>*
- XL : local quality
- DH : equivalent heated diameter of CHF subchannel, *in.*
- DHM : equivalent heated diameter of matrix subchannel, *in.*
- CHFM : measured CHF, *MBtu/hr-ft<sup>2</sup>*
- CHFP : KCE-1 correlation predicted CHF, *MBtu/hr-ft<sup>2</sup>*

\* XX = Rod number, x = T/C number  
(See Figure 2-5 through Figure 2-7 and Figure 2-9.)

INSERT 1, 2, 3, 4, 5, 6, 7



Page Intentionally Left Blank

Table A-2 KCE-1 CHF Correlation Initial Dataset (1/7)

TS	CT	RUN	PR	GL	XL	hfg	DH	DHM	CHFM
[Empty table body]									

Table A-2 KCE-1 CHF Correlation Initial Dataset (2/7)

TS	CT	RUN	PR	GL	XL	hfg	DH	DHM	CHFM

Table A-2 KCE-1 CHF Correlation Initial Dataset (3/7)

TS	CT	RUN	PR	GL	XL	hfg	DH	DHM	CHFM
----	----	-----	----	----	----	-----	----	-----	------

Table A-2 KCE-1 CHF Correlation Initial Dataset (4/7)

TS	CT	RUN	PR	GL	XL	hfa	DH	DHM	CHFM

Table A-2 KCE-1 CHF Correlation Initial Dataset (5/7)

TS	CT	RUN	PR	GL	XL	hfg	DH	DHM	CHFM

Table A-2 KCE-1 CHF Correlation Initial Dataset (6/7)

TS	CT	RUN	PR	GL	XL	hfg	DH	DHM	CHFM

Table A-2 KCE-1 CHF Correlation Initial Dataset (7/7)

TS	CT	RUN	PR	GL	XL	hfg	DH	DHM	CHFM

Table A-3

~~Table A-2~~ Test Data Groups Excluded during KCE-1 CHF Correlation Development

TS	CT	RUN	PR	GL	XL	hfg	DH	DHM	CHFM	CHFP	M/P	Remark

Table A-4

~~Table A-3~~ KCE-1 CHF Correlation Database (1/8)

TS	CT	RUN	PR	GL	XL	hfg	DH	DHM	CHFM	CHFP	M/P

Table A-4

~~Table A-3~~ **KCE-1 CHF Correlation Database (2/8)**

TS	CT	RUN	PR	GL	XL	hfg	DH	DHM	CHFM	CHFP	M/P

Table A-4

~~Table A-3~~ **KCE-1 CHF Correlation Database (3/8)**

TS	CT	RUN	PR	GL	XL	hfg	DH	DHM	CHFM	CHFP	M/P

Table A-4

~~Table A-3~~ KCE-1 CHF Correlation Database (4/8)

TS	CT	RUN	PR	GL	XL	hfg	DH	DHM	CHFM	CHFP	M/P

Table A-4

~~Table A-3~~ **KCE-1 CHF Correlation Database (5/8)**

TS	CT	RUN	PR	GL	XL	hfg	DH	DHM	CHFM	CHFP	M/P

Table A-4

KCE-1 CHF Correlation

APR1400-F-C-TR-12002-NP Rev.0

~~Table A-3~~ **KCE-1 CHF Correlation Database (6/8)**

TS	CT	RUN	PR	GL	XL	hfg	DH	DHM	CHFM	CHFP	M/P

Table A-4

~~Table A-3~~ **Table A-3 KCE-1 CHF Correlation Database (7/8)**

TS	CT	RUN	PR	GL	XL	hfg	DH	DHM	CHFM	CHFP	M/P

Table A-4

KCE-1 CHF Correlation

APR1400-F-C-TR-12002-NP Rev.0

~~Table A-3~~ KCE-1 CHF Correlation Database (8/8)

TS	CT	RUN	PR	GL	XL	hfg	DH	DHM	CHFM	CHFP	M/P

## RESPONSE TO REQUEST FOR ADDITIONAL INFORMATION

### APR1400 Topical Reports

Korea Electric Power Corporation / Korea Hydro & Nuclear Power Co., LTD

Docket No. PROJ 0782

**RAI No.:** 3-7443 Question 11

**SRP Section:** N/A

**Application Section:** KCE-1 Critical Heat Flux Correlation for PLUS7 Thermal Design  
(APR1400-F-C-TR-12002-NP, Rev.0)

**Date of RAI Issued:** 03/25/2014

**Response Date:** 02/25/2015

---

### **Question 11**

The ratios of measured-to-predicted CHF (M/Ps) of all test data were plotted for system pressure, local mass flux, local quality, and equivalent heated diameter ratio in Figure 5-3 through Figure 5-6, respectively. Figure 4-1 through Figure 4-3 provide similar plots for bundle average heat flux data. However, the topical report does not provide the corresponding plots of the measured CHF data that were used in the KCE-1 correlation coefficient development as well as for the M/P calculations.

- (A) The corresponding plots of the measured CHF data would be needed by the staff to observe any adverse and non-linear trends in the data. Provide these plots and include them in the topical report for future reference.
- (B) Describe in the report the key parameters tabulated in Tables A-1 and A-3; whether and how they were measured, tagged, or computed. This needs describing the data populated on a typical row of these tables and how they are linked with one another or across the tables. For example, explain how HFX is computed from BAP in Table A-1 and how is it linked with TC within the same table and with CHF<sub>M</sub> in Table A-3.
- (C) Include the outlet temperature test data in the topical report to demonstrate their fidelity and facilitate a staff assessment of the heat losses.

### **Response**

- (A) *Corresponding plots of the measured CHF data are given in Figures 11-1 to 11-3 for system pressure, local mass velocity (local mass flux), and equivalent heated diameter ratio,*

respectively. The plot for local quality is presented in the response to Question 10 (Figure 10-1) of RAI 3-7443.

This information will be included in an appropriate section of the topical report as shown in the attached markup.

[

] <sup>TS</sup>.

The trend of measured CHF with respect to system pressure and mass flux is typical, meaning that [

] <sup>TS</sup> without any adverse behavior. The trend of measured CHF with respect to equivalent heated diameter ratio showed no adverse behavior.

Note: Figures 11-1 to 11-3 include all data, as described in the response to Question 10 (the same data listed in Table 10-1) of RAI 3-7443.



*Figure 11-1 Measured CHF vs. Pressure (at CHF location)*



*Figure 11-2 Measured CHF vs. Local Mass Velocity (at CHF location)<sup>1)</sup>*



*Figure 11-3 Measured CHF vs. Equivalent Heated Diameter Ratio (at CHF location)*

(B) Measured values at each CHF data point are tabulated in Appendix Table A-1 of the topical report. On the other hand, the local fluid conditions at MDNBR location are tabulated in Appendix Table A-3 of the topical report. These data were calculated by subchannel code TORC using measured CHF data, presented in Table A-1, as input with the assumptions described in sections 4.2 and 4.3 of the topical report.

The variables in Table A-1 and A-3 of the topical report are explained in page A-1 of the topical report.

In Table A-1, the description of each abbreviation is as follows;

- TS: CHF test section
- RUN: individual data identification number
- PR/TIN/GIN/BAP: Pressure/Inlet Temperature/Inlet Mass Flux/Bundle Power (measured values for each RUN)
- HFX: average heat flux (BAP divided by heat transfer area and multiplied by corresponding unit conversion factor)
- TC: CHF indicated location at each RUN with the convention of XX.x (XX represents the rod identification number as given in Figures 2-5 to 2-7, and x represents the T/C identification number as given in Figure 2-9 of the topical report)

As an example datum from Test Section TS101;

- BAP:  $\left[ \quad \right]_{TS}$
- Bundle heat transfer area:  $39.1652 \text{ ft}^2$  ( $32 \times \pi \times 0.374/12 \times 150/12$ )
- Conversion factor:  $3.413 \text{ (MBtu/hr)/(MW)}$
- HFX:  $\left[ \quad \right]_{TS} \text{ MBtu/hr-ft}^2$  ( $\left[ \quad \right]_{TS} \times 3.413/39.1652$ )
- TC: 23.3 (radially on rod 23 depicted in Figure 2-5 and axially on T/C #3 depicted in Figure 2-9 of topical report)
  - ✓ Rod Power Factor: 1.125 (rod 23)
  - ✓ Axial power Factor: approximately  $\left[ \quad \right]_{TS}$  (at axial elevation of 109.5 inch from BOHL)
- CHF:  $\left[ \quad \right]_{TS} \text{ MBtu/hr-ft}^2$  ( $\left[ \quad \right]_{TS} \times 1.125 \times \left[ \quad \right]_{TS}$ )

In Table A-3 of the topical report, the description of each abbreviation is as follows;

- GL/XL: value at MDNBR location calculated by subchannel code TORC using measured values given in Table A-1 and assumptions described in sections 4.2 and 4.3 of topical report
- CT: the type of subchannel, M/C/S correspond to subchannels, such as 12/19/18 in Figure 2-5 of the topical report
- CHF: local heat flux at MDNBR location calculated by HFX multiplying corresponding rod power factor and axial power factor as shown in Figures 2-5 to 2-

7 and Figure 2-9 of the topical report

The following information will be included in an appropriate subsection of the topical report.

- $HFX$  =  $BAP / \text{bundle heat transfer area} * \text{unit conversion factor}$
- $DH$  =  $4 * \text{flow area} / \text{heated perimeter of the subchannel of interest}$
- $DHM$  =  $4 * \text{flow area} / \text{heated perimeter of the matrix subchannel}$
- $CHFM$  =  $HFX * \text{rod power factor} * \text{axial power factor at the elevation of interest}$

(C) A thermodynamic equilibrium quality value based on inlet fluid condition (inlet mass flux and inlet temperature) and bundle power for PLUS7 CHF data was [

] <sup>TS</sup>. General concerns related to heat loss are addressed in the response to Question 1 of RAI 3-7443.

**Impact on DCD**

N/A

**Impact on Technical/Topical/Environmental Report**

Topical Report APR1400-F-C-TR-12002-NP will be revised as indicated on the attached markups.

- Document Mark-up Cover Sheet : 1 page
- Mark-up for Q11 of RAI 3-7443 : 7 pages

※Remark: Minor formatting, such as numbering figures, tables and references, etc., will be cleaned up before finalizing the topical report.

# Document Mark-up Cover Sheet

1. **Project ID:** *APR1400 NRC DC*
2. **Type of Corresponding Document:**  
 DCD     Topical Report     Technical Report     Other(s) \_\_\_\_\_
3. **Title of Corresponding Document:** *KCE-1 CHF Correlation for PLUS7 Thermal Design  
(APR1400-F-C-TR-12002-NP)*
4. **RAI ID/Question ID:** *3-7443 / Q11*
5. **Page(s) attached:** *7 (Seven)*

For CHF tests using a non-uniform axial power distribution, as in the CHF tests for PLUS7 and for Reference 5, the axial location of CHF occurrence depends on the shape of the axial power distribution and local fluid conditions. Moreover, the surface temperatures of heater rods are measured with ring-typed junction thermocouples installed at various axial positions. In this case, the axial location of a heater rod where CHF occurs can be detected but the subchannel experiencing CHF cannot be identified exactly. Thus, the local fluid conditions for the KCE-1 CHF correlation were extracted with the following basic assumptions:



Therefore, [ ] were extracted per each individual datum from TS101 while [ ]<sup>TS</sup> per datum from TS102.

### 4.3 CORRELATION FORMULA AND ASSUMPTIONS

The functional formula of the KCE-1 CHF correlation is identical to the CE-1 CHF correlation, and is given as follow:

$$q''_{CHF,U} = \frac{B_1(d/d_m)^{B_2} [(B_3 + B_4 P)(G/10^6)^{(B_5 + B_6 P)}]}{(G/10^6)^{(B_7 P + B_8 (G/10^6))}}$$

Figure 4-4 through 4-7 show measured CHF at CHF indication location versus system pressure, local mass flux, local quality and equivalent heated diameter ratio.

↑  
INSERT

- where,  $q''_{CHF,U}$  CHF for uniform axial power distribution, *MBtu/hr-ft<sup>2</sup>*
- $P$  Pressure, *psia*
- $d$  Equivalent heated diameter of subchannel of interest, *inch*
- $d_m$  Equivalent heated diameter of matrix subchannel, *inch*
- $G$  Local mass flux at the CHF location, *lbm / hr-ft<sup>2</sup>*
- $\chi$  Local quality at the CHF location
- $h_{fg}$  Latent heat of vaporization, *Btu/lbm*.

The coefficients of the CE-1 CHF correlation were determined based on the CHF test data with a uniform axial power distribution. Through subsequent CHF tests with a non-uniform axial power distribution, the non-uniform axial power distribution correction factor, Tong factor  $F_C^{(5),(6)}$ , was

INSERT 1, 2, 3, 4



Page intentionally Left Blank

INSERT 1



**Figure 4-4 System Pressure versus Measured CHF at CHF Location**

INSERT 2

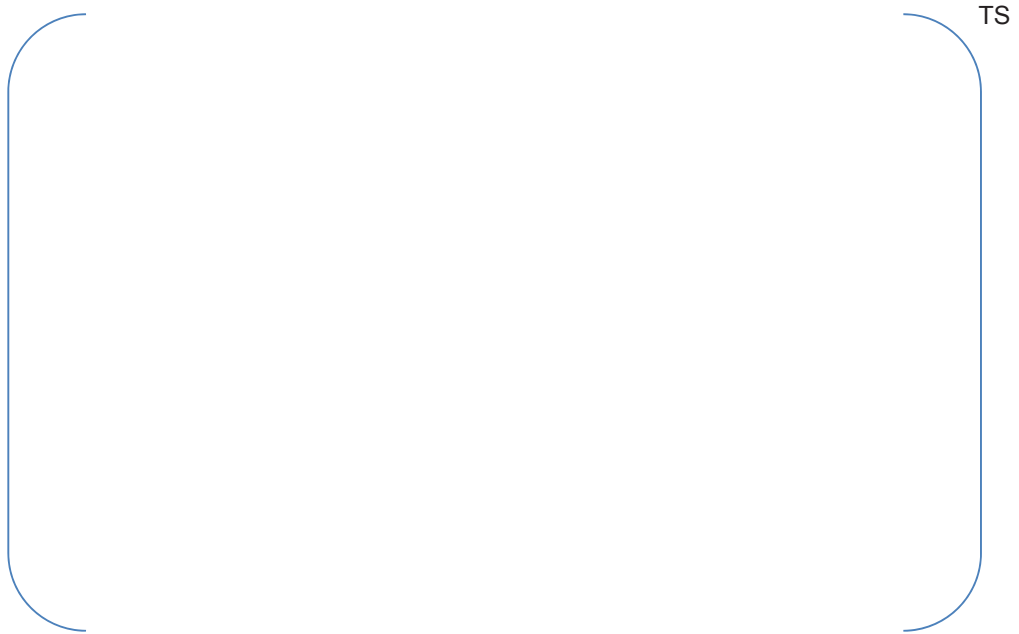


**Figure 4-5 Local Mass Flux versus Measured CHF at CHF Location**

INSERT 3



Figure 4-6 Local Quality versus Measured CHF at CHF Location

INSERT 4



Figure 4-7 Equivalent Heated Diameter Ratio versus Measured CHF at CHF Location

**APPENDIX A. DATA FOR KCE-1 CHF CORRELATION DEVELOPMENT**

The raw test data, [ ]<sup>TS</sup> in total, collected from the PLUS7 fuel CHF tests are listed in Table A-1. The [ ]<sup>TS</sup> local fluid conditions excluded during the correlation development process from the local fluid conditions for each test data calculated by the TORC code are listed along with the reason for exclusion in Table A-2. Finally, the KCE-1 CHF correlation database, [ ]<sup>TS</sup> in total, is presented in Table A-3.

Acronyms presented in the subsequent tables:

- TS : test section number
- RUN : run number
- PR : system pressure, *psia*
- TIN : inlet temperature, °F
- GIN : inlet mass flux (inlet mass velocity), *Mlbm/hr-ft<sup>2</sup>*
- BAP : bundle average power, *MW*
- HFX : heat flux, *MBtu/hr-ft<sup>2</sup>*
- TC : primary CHF rod and thermocouple number (XX.x)\*
- HFX : heat flux (BAP/bundle heat transfer area\*unit conversion factor), *MBtu/hr-ft<sup>2</sup>*
- M : matrix subchannel
- C : guide thimble corner subchannel

DH : equivalent heated diameter of CHF subchannel (4 \* flow area / heated perimeter of the subchannel of interest), *in*

GL : local mass flux (local mass velocity), *Mlbm/hr-ft<sup>2</sup>*

XL : local quality

DH : equivalent heated diameter of CHF subchannel, *in*.

DHM : equivalent heated diameter of matrix subchannel, *in*.

CHF<sub>M</sub> : measured CHF, *MBtu/hr-ft<sup>2</sup>*

DHM : equivalent heated diameter of matrix subchannel (4 \* flow area / heated perimeter of the matrix subchannel), *in*

\* XX = Rod number, x = T/C number  
(See Figure 2-5 through Figure 2-7 and Figure 2-9.)

CHF<sub>M</sub> : measured CHF (HFX \* rod power factor \* axial power factor at the elevation of interest), *MBtu/hr-ft<sup>2</sup>*

---

## RESPONSE TO REQUEST FOR ADDITIONAL INFORMATION

### APR1400 Topical Reports

Korea Electric Power Corporation / Korea Hydro & Nuclear Power Co., LTD

Docket No. PROJ 0782

**RAI No.:** 3-7443 Question 12  
**SRP Section:** N/A  
**Application Section:** KCE-1 Critical Heat Flux Correlation for PLUS7 Thermal Design  
(APR1400-F-C-TR-12002-NP, Rev.0)  
**Date of RAI Issued:** 03/25/2014  
**Response Date:** 02/25/2015

---

### **Question 12**

The testing was conducted with a constant heated length (150 inch) and a constant grid spacing (15.7 inch). During the testing conducted for some other CHF correlations, heated length and grid spacing were also varied and duly accounted for in the resulting correlation using additional terms. The applicant should explain whether the lack of heated length and grid spacing in the KCE-1 correlation would impact its applicability to the actual PLUS7 fuel bundle safety analyses.

### **Response**

*KCE-1 correlation was developed using the CHF data from test sections with the same axial geometry as PLUS7 fuel, as described in Table 2-1 and Figure 2-9 of the topical report.*

*The effect of grid spacing on CHF was included in the measured data, and thus it was inherently reflected to the KCE-1 correlation prediction. For the heated length, as in the case of grid spacing, the effect was reflected in both the measured data and the KCE-1 correlation prediction. KCE-1 correlation is applied to PLUS7 geometry (grid spacing and heated length) only.*

*To confirm the prediction performance of the KCE-1 correlation, M/P versus axial elevation was plotted with and without the assumptions described in section 4.2 of the topical report. KCE-1 correlation shows consistent and reasonable prediction performance according to axial elevation, regardless of assumptions. It means that the assumption applied to the correlation*

*development process does not result in any deficiency on correlation prediction performance according to axial elevation. The plotted data in Figure 12-1 ([ ]<sup>TS</sup> data) and Figure 12-2 ([ ]<sup>TS</sup> data) correspond to Table 5-4 of the topical report.*



*Figure 12-1 M/P Trend with respect to Axial Elevation with assumption  
(all data listed in Table A-3 of topical report)*

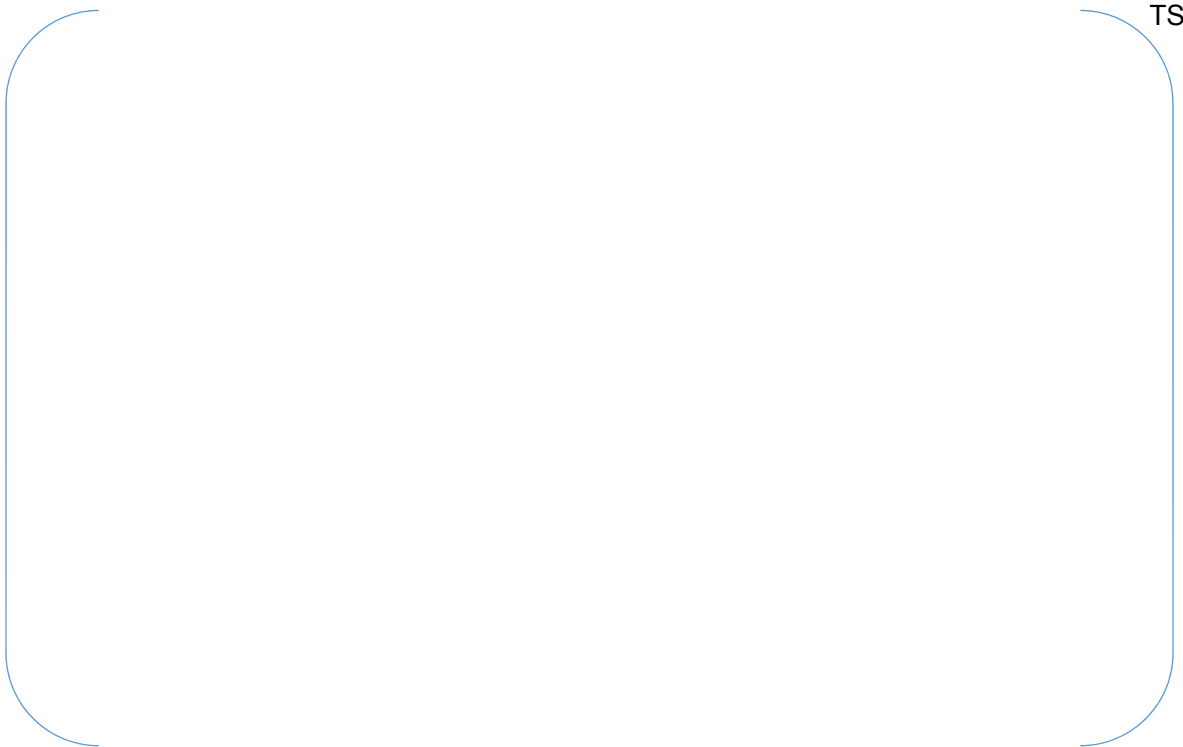


*Figure 12-2 M/P with respect to Axial Elevation without assumption  
(without assumption in section 4.2 of topical report : MDNBR among subchannels)*

---

**Impact on DCD**

N/A

**Impact on Technical/Topical/Environmental Report**

N/A

## RESPONSE TO REQUEST FOR ADDITIONAL INFORMATION

### APR1400 Topical Reports

Korea Electric Power Corporation / Korea Hydro & Nuclear Power Co., LTD

Docket No. PROJ 0782

RAI No.: 3-7443 Question 13  
SRP Section: N/A  
Application Section: KCE-1 Critical Heat Flux Correlation for PLUS7 Thermal Design  
(APR1400-F-C-TR-12002-NP, Rev.0)  
Date of RAI Issued: 03/25/2014  
Response Date: 02/25/2015

---

### **Question 13**

The second paragraph of Section 6 (Correlation Application) of the topical report implies that meeting the 95/95 DNBR limit would also mean meeting the DNB acceptance criterion in SRP Sections 4.2 and 4.4 to provide 95/95 assurance that the hot fuel rod in the core would not experience a DNB or transition condition during AOOs (Anticipated Operational Occurrences). This is not correct. The approval of the topical report for a given 95/95 DNBR limit would not imply its applicability to AOOs that would be separately reviewed under the DCD review of the thermal design and safety analysis. The applicant should either document in the topical report that the applicability of the KCE-1 correlation to AAOs to meet the DNB acceptance criterion will be reviewed separately under the DCD review, or take out the reference to AOOs.

### **Response**

*From the second paragraph of Section 6 of the topical report, the statement*

*“The acceptance criterion is met in thermal design and safety analysis when the MDNBR of the hot rod in the hot channel is above 95/95 DNBR limit of the correlation.”*

*would be changed to*

*“The acceptance criterion is met in thermal design and safety analysis when the MDNBR of the hot rod in the hot channel is above appropriate DNBR limit (Specified Acceptable Fuel Design Limit, SAFDL) which includes 95/95 DNBR limit of the KCE-1 correlation. The results of KCE-1 CHF correlation applying to AOO analysis of APR1400 would be included in the corresponding subsection of the APR1400 Design Control Document (DCD) Section 4.4.”*

*This modification will be included in the corresponding subsection of the topical report as shown in the attached markup.*

*Supporting information is included in a technical report APR1400-F-C-NR-12001 Rev.1, "Thermal Design Methodology". This technical report was submitted with docketing of APR1400 Design Control Document (DCD). (MKD/NW-14-0036L, December 23, 2014)*

**Impact on DCD**

N/A

**Impact on Technical/Topical/Environmental Report**

Topical Report APR1400-F-C-TR-12002-NP will be revised as indicated on the attached markups.

- Document Mark-up Cover Sheet : 1 page
- Mark-up for Q13 of RAI 3-7443 : 1 pages

※Remark: Minor formatting, such as numbering figures, tables and references, etc., will be cleaned up before finalizing the topical report.

# Document Mark-up Cover Sheet

1. **Project ID:** *APRI400 NRC DC*
2. **Type of Corresponding Document:**  
 DCD     Topical Report     Technical Report     Other(s) \_\_\_\_\_
3. **Title of Corresponding Document:** *KCE-1 CHF Correlation for PLUS7 Thermal Design  
(APRI400-F-C-TR-12002-NP)*
4. **RAI ID/Question ID:** *3-7443 / Q13*
5. **Page(s) attached:** *1 (One)*

## 6. CORRELATION APPLICATION

KEPCO Nuclear Fuel uses the KCE-1 CHF correlation for evaluating thermal design of the PLUS7 fuel assembly and the reactor core of APR1400 and OPR1000 in accordance with the CHF or DNB acceptance criteria defined in the Standard Review Plan (SRP)<sup>(7)</sup>.

Sections 4.2 and 4.4 of SRP state that the DNB acceptance criterion provides assurance that there be at least a 95% probability at the 95% confidence level that the hot fuel rod in the core does not experience a DNB or transition condition during normal operation or AOOs (Anticipated Operational Occurrences). ~~The acceptance criterion is met in thermal design and safety analysis when the MDNBR of the hot rod in the hot channel is above 95/95 DNBR limit of the correlation.~~ Establishment of the KCE-1 correlation 95/95 DNBR limit was presented in Chapter 5. The KCE-1 CHF correlation was used only with a computer code that has been used for the correlation development and has been qualified with the 95/95 DNBR limit.

The KCE-1 CHF correlation 95/95 DNBR limit and its supporting M/P statistics with the TORC code is 1.124. The applicable ranges of the parameters, based on database, are given in Table 4.4. Note that the Tong factor  $F_C$  is [ ]<sup>TS</sup> are applied to MDNBR calculation for the design application and safety analyses. The value of Tong factor  $F_C$  depends on the various axial power distribution and local fluid conditions but it is conservatively limited to [ ]<sup>TS</sup>. The application of the KCE-1 CHF correlation with TORC code is in full compliance with the conditions of the Safety Evaluation Report (SER) on the TORC code and modeling for CE-PWRs. The OPR1000 and the APR1400 are CE-PWRs.

The TORC code is used in thermal design and safety analyses to perform detailed modeling of the core and hot assembly and to determine MDNBR in the hot assembly. The CETOP-D code<sup>(8)</sup> is a fast running tool which is used in thermal design and safety analyses to calculate MDNBR in the hot subchannel.

While the TORC code can be applied directly in the thermal analysis and safety analyses, typically the TORC code is used to benchmark the MDNBR results of CETOP-D code such that the CETOP-D results are conservative relative to those of TORC code. The KCE-1 CHF correlation is implemented to both TORC and CETOP-D codes by modifying correlation coefficients only. Note that the functional formula is identical for both KCE-1 and CE-1 CHF correlations, as described in Section 4.3.

Thus, the topical reports described in References 2 and 3 for TORC code and Reference 8 for CETOP-D code will remain valid with the application of KCE-1 CHF correlation. Therefore, the application of KCE-1 CHF correlation with CETOP-D code for OPR1000 and APR1400 is equivalent to its application with TORC code.

Even though a higher value of inverse Peclet number based on the empirically determined thermal diffusion coefficient was used in the TORC model for CHF data analysis and correlation development, the reactor analysis is to be performed with the design inverse Peclet number ( $1/Pe = 0.0101$ ). This is equivalent to the value of the thermal diffusion coefficient ( $TDC = 0.038$ ) applied to the Westinghouse PWR for fuel assembly with "R" mixing vane grid design<sup>(9)</sup>.

The acceptance criterion is met in thermal design and safety analysis when the MDNBR of the hot rod in the hot channel is above appropriate DNBR limit (Specified Acceptable Fuel Design Limit, SAFDL) which includes 95/95 DNBR limit of the KCE-1 correlation. The results of KCE-1 CHF correlation applying to AOO analysis of APR1400 would be included corresponding subsection of the APR1400 Design Control Document (DCD) Section 4.4.

---

## RESPONSE TO REQUEST FOR ADDITIONAL INFORMATION

### APR1400 Topical Reports

Korea Electric Power Corporation / Korea Hydro & Nuclear Power Co., LTD

Docket No. PROJ 0782

RAI No.: 3-7443 Question 14  
SRP Section: N/A  
Application Section: KCE-1 Critical Heat Flux Correlation for PLUS7 Thermal Design  
(APR1400-F-C-TR-12002-NP, Rev.0)  
Date of RAI Issued: 03/25/2014  
Response Date: 02/25/2015

---

### **Question 14**

SRP Section 4.4 Acceptance Criterion#1 deals with experimental uncertainties involved in the CHF measurement. Even though the use of the 95/95 limit for DNBR adequately captures the uncertainty in the prediction of the measured values using the CHF correlation, the origin of each uncertainty parameter, such as fabrication uncertainty, computational uncertainty, or measurement uncertainty have not been identified in the topical report, nor classified as statistical or deterministic, following the acceptance criterion. The topical report should include information about the overall experimental uncertainty, and demonstrate that all the uncertainties in the measured CHF data have been appropriately captured in the 95/95 DNBR limit of the KCE-1 correlation.

### **Response**

*The measured CHF values were calculated based on the voltage and current measurements as described in the response to Question 5 of RAI 3-7443. Thus no computational uncertainties of fluid conditions were involved in the measured CHF.*

[

]TS.

[

]<sup>TS</sup>.

Uncertainties of each measured variable of the CHF test are presented in Table 14-1. The information listed in Table 14-1 and corresponding statements based on the above will be included in Section 3 of the topical report, as shown in the attached markup.

[

]<sup>TS</sup>.

The overall uncertainty in the measured CHF data is as follows (Reference: EPRI-NP 2609 Vol. 1, Sep. 1982). This method has been generally applied to error analysis of measured CHF data on HTRF.

#### 1) Power measurement

- From  $P = V \times I$

$$W_P^2 = \left( W_V \frac{\partial P}{\partial V} \right)^2 + \left( W_I \frac{\partial P}{\partial I} \right)^2$$

$$\frac{W_P}{Power} = [ \quad ]^{TS} \text{ at 3.4 MW (the highest measurement uncertainty, per Table 14-1)}$$

- Converting error from bus to bus V & I to TS: [  $\quad$  ]<sup>TS</sup> (a uncertainty associates with applying a temperature dependent voltage correction factor to convert Bbpwr to Tspwr)

Combination of the above two (2) uncertainties

$$\left( \frac{W_P}{Power} \right)^2 = [ \quad ]^{TS}$$

$$\frac{W_P}{Power} = [ \quad ]^{TS}$$

#### 2) Power at DNB

- Increment step to approaching CHF : [  $\quad$  ]<sup>TS</sup> is maximum (Reference, [  $\quad$  ]<sup>TS</sup>)  
Combination of 'Power Measurement' uncertainty and 'Power at DNB' uncertainty

$$\left( \frac{W_P}{Power} \right)_{at\ DNB}^2 = [ \quad ]^{TS}$$

$$\left( \frac{W_P}{Power} \right)_{at\ DNB} = [ \quad ]^{TS}$$

#### 3) Rod surface area

(Reference: HTRF Tube spec. (generic value))

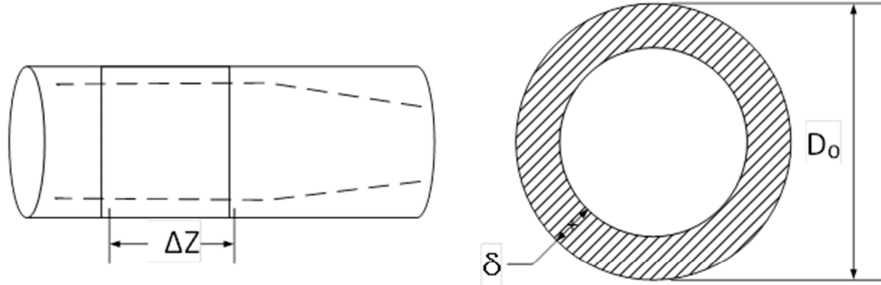
From  $A_r = \sum_{n=1}^{N_{rod}} \pi D_n L_n$

$$\left(\frac{W_{Ar}}{A_r}\right)^2 = \frac{1}{N_{rod}} \left( \left(\frac{W_D}{D}\right)^2 + \left(\frac{W_L}{L}\right)^2 \right) = \frac{1}{36} \left( \left(\frac{0.002}{0.374}\right)^2 + \left(\frac{0.03}{150}\right)^2 \right)$$

$$\frac{W_{Ar}}{A_r} = 0.00089, \frac{W_{Ar}}{A_r} = 0.09\%$$

The rod surface area effect is minor, and it does not change the total measured CHF uncertainty whether it is a test section with a guide tube or not.

4) Tube wall thickness



$$Local\ Heat\ Flux = \frac{\Delta P}{\pi D_o \Delta Z} = \frac{I^2 R_{\Delta Z}}{\pi D_o \Delta Z} \propto R_{\Delta Z} = \left[ \dots \right]^{TS}$$

$$W_R^2 = \left( W_o \frac{\partial R_{\Delta Z}}{\partial D_o} \right)^2 + \left( W_\delta \frac{\partial R_{\Delta Z}}{\partial \delta} \right)^2$$

where, [

$$\left( \frac{W_R}{R_{\Delta Z}} \right)^2 = \left[ \dots \right]^{TS} \quad ]^{TS}$$

For arbitrary rod for CHF indicated T/C locations  
(Reference, [

]^{TS})

- T/C 2 Location : 125.2 inch  
 $W_\delta = [ \dots ]^{TS}, \delta = [ \dots ]^{TS}, \frac{W_R}{R_{\Delta Z}} = [ \dots ]^{TS}$
- T/C 3 Location : 109.5 inch  
 $W_\delta = [ \dots ]^{TS}, \delta = [ \dots ]^{TS}, \frac{W_R}{R_{\Delta Z}} = [ \dots ]^{TS}$
- T/C 4 Location : 93.8 inch  
 $W_\delta = [ \dots ]^{TS}, \delta = [ \dots ]^{TS}, \frac{W_R}{R_{\Delta Z}} = [ \dots ]^{TS}$

5) Total measured CHF uncertainty : [ ]<sup>TS</sup> (maximum)

- T/C 2 Location : 125.2 inch

$$\frac{W_{q_{DNB}}}{q_{DNB}} = [ ]^{TS}$$

- T/C 3 Location : 109.5 inch

$$\frac{W_{q_{DNB}}}{q_{DNB}} = [ ]^{TS}$$

- T/C 4 Location : 93.8 inch

$$\frac{W_{q_{DNB}}}{q_{DNB}} = [ ]^{TS}$$

The overall uncertainty in the measured CHF data is inherently included in the 95/95 DNBR limit, which is determined by the Measured-to-Predicted ratio (M/P) statistics. The conservatism that derives from the application of Tong factor in design analysis, as described in the response to Questions 6 and 9 of RAI 3-7443, can offset the effect of the measurement uncertainty on heat flux.

Table 14-1 Measurement Uncertainties for PLUS7 CHF Tests

<i>Variable</i>	<i>Unit</i>	<i>Range</i>	<i>Uncertainty</i>
<i>Pressure</i>	<i>psi</i>		TS
<i>Mass flux</i>	<i>Mlbm/hr-ft<sup>2</sup></i>		
<i>Inlet Temperature</i>	<i>°F</i>		
<i>Power</i>	<i>MW</i>		

(Reference : [

]<sup>TS</sup>)

**Impact on DCD**

N/A

**Impact on Technical/Topical/Environmental Report**

Topical Report APR1400-F-C-TR-12002-NP will be revised as indicated on the attached markups.

- Document Mark-up Cover Sheet : 1 page
- Mark-up for Q14 of RAI 3-7443 : 9 pages

※Remark: Minor formatting, such as numbering figures, tables and references, etc., will be cleaned up before finalizing the topical report.

# Document Mark-up Cover Sheet

1. **Project ID:** *APRI400 NRC DC*
2. **Type of Corresponding Document:**  
 DCD     Topical Report     Technical Report     Other(s) \_\_\_\_\_
3. **Title of Corresponding Document:** *KCE-1 CHF Correlation for PLUS7 Thermal Design  
(APRI400-F-C-TR-12002-NP)*
4. **RAI ID/Question ID:** *3-7443 / Q14*
5. **Page(s) attached:** *9 (Nine)*

minimal, confirmation of the validity of a CHF point was obtained by observing the temperature decay with power reduction. There was characteristic temperature decay with time as the CHF zone was rewetted. This evidence was considered confirming in cases where the temperature decay pattern was typical. Otherwise, the test would be repeated.

When a CHF point was observed, the following measurements were recorded:

- test section outlet pressure from Heise gauge
- identification number of heater rod experiencing CHF and relevant thermocouple
- test section voltage
- bus-to-bus voltage
- D.C. generator electric current
- inlet temperature
- exit temperature
- exit pressure transducers
- inlet pressure transducers
- turbine flow meter transducer
- Venturi flow meters transducers
- test section pressure drop transducers
- heater rod temperatures

For the above recordings, the first two measurements were recorded manually while other measurements were recorded by the data acquisition system with a HP3852A data acquisition/control unit.

### **3.3 MEASUREMENTS UNCERTAINTIES**

Measurement uncertainties of CHF test data are subject to any inaccuracy of instrumentations and of the techniques for obtaining and processing the data. The uncertainties had been estimated on the basis of instrument specifications, calibration data, electronics of the data acquisition systems, testing procedures, and variations in test section dimensions from specification.

Uncertainties of each measured variable of the CHF test are listed in Table 3-1<sup>(4)</sup>.

INSERT

INSERT 1 at next page

Table 3-1 Measurement Uncertainties for PLUS7 CHF Tests

<i>Variable</i>	<i>Unit</i>	<i>Range</i>	<i>Uncertainty</i>
<i>Pressure</i>	<i>psi</i>		TS
<i>Mass flux</i>	<i>Mlbm/hr-ft<sup>2</sup></i>		
<i>Inlet Temperature</i>	<i>°F</i>		
<i>Power</i>	<i>MW</i>		

## 4. CHF CORRELATION DEVELOPMENT

The KCE-1 CHF correlation was developed using the CHF test data for the PLUS7 fuel obtained from HTRF. This chapter describes the CHF test data, local fluid condition calculation method, the correlation coefficient optimization procedure and applicable range of parameters to the correlation.

### 4.1 CHF TEST DATA

[ ]<sup>TS</sup> test data for the thimble subchannel test section TS101 and [ ]<sup>TS</sup> data for the matrix subchannel test section TS102 were obtained, respectively. The entire [ ]<sup>TS</sup> test data are listed in Table A-1 of APPENDIX A.

Figure 4-1 through Figure 4-3 show average heat fluxes (hence powers) of the test section versus system pressure, inlet temperature and inlet mass flux, respectively. As identified in Figure 4-1, [ ]<sup>TS</sup>

[ ]<sup>TS</sup>

### 4.2 LOCAL FLUID CONDITION CALCULATION

Using the subchannel analysis code, TORC, local fluid conditions for the CHF test data were computed.

The TORC code is an adaptation of the COBRA-IIIC code with modifications including an improved lateral momentum equation and lateral boundary condition capability to simulate actual core behaviors for all flow channels in the core. It is a detailed model code predicting the steady-state thermal hydraulic characteristics of the nuclear reactor cores. The TORC code divides the core into a series of control volumes and solves 3-dimensional conservation equations for each control volume thereby predicting fluid thermal hydraulic local conditions at every position in the core.

The verification of TORC code includes a comparison of subchannel coolant temperature rise and overall pressure drop for CHF test bundles, and full size open core effects of actual operating reactor data.

The TORC code has been approved for use in licensing application of reactor core analyses for steady-state calculations involving unblocked flow channels or subchannels (other than the minimal blockage offered by intact spacer grids). The spacer grid with split type "R" mixing vanes, which was adopted in PLUS7 fuel, did not affect the TORC code applicability to thermal hydraulic analyses of reactor cores as approved by USNRC.

The TORC code models were generated by using subchannel arrangements, radial and axial power distributions and spacer grid locations of each test sections as shown in Figure 2-5 through Figure 2-9. Other main input data are summarized in Table 4-1.

correlation<sup>(5)</sup>

For CHF tests using a uniform axial power distribution, such as the CHF test cases for the CE-1 correlation<sup>(4)</sup> development, CHF always occurs in the upper exit region of the heater rods (end-of-heated-length, EOHL). Hence, surface temperatures of heater rods and subchannels experiencing CHF can be detected by thermocouples installed azimuthally in the EOHL four (4) subchannels surrounding a heater rod.

For CHF tests using a non-uniform axial power distribution, as in the CHF tests for PLUS7 and for Reference 5, the axial location of CHF occurrence depends on the shape of the axial power distribution and local fluid conditions. Moreover, the surface temperatures of heater rods are measured with ring-typed junction thermocouples installed at various axial positions. In this case, the axial location of a heater rod where CHF occurs can be detected but the subchannel experiencing CHF cannot be identified exactly. Thus, the local fluid conditions for the KCE-1 CHF correlation were extracted with the following basic assumptions:



Therefore, [ ] were extracted per each individual datum from TS101 while [ ]<sup>TS</sup> per datum from TS102.

### 4.3 CORRELATION FORMULA AND ASSUMPTIONS

The functional formula of the KCE-1 CHF correlation is identical to the CE-1 CHF correlation, and is given as follow:

$$q''_{CHF,U} = \frac{B_1(d/d_m)^{B_2} [(B_3 + B_4 P)(G/10^6)^{(B_5+B_6P)} - (G/10^6) \chi h_{fg}]}{(G/10^6)^{(B_7 P+B_8(G/10^6))}}$$

- where,  $q''_{CHF,U}$  CHF for uniform axial power distribution,  $MBtu/hr-ft^2$
- $P$  Pressure,  $psia$
- $d$  Equivalent heated diameter of subchannel of interest,  $inch$
- $d_m$  Equivalent heated diameter of matrix subchannel,  $inch$
- $G$  Local mass flux at the CHF location,  $lbm / hr-ft^2$
- $\chi$  Local quality at the CHF location
- $h_{fg}$  Latent heat of vaporization,  $Btu/lbm$ .

The coefficients of the CE-1 CHF correlation were determined based on the CHF test data with a uniform axial power distribution. Through subsequent CHF tests with a non-uniform axial power distribution, the non-uniform axial power distribution correction factor, Tong factor  $F_C^{(6),(6)}$ , was

$F_C^{(6),(7)}$

combined with the CE-1 CHF correlation as follow, and was proven to predict the CHF values conservatively:

$$q''_{CHF,NU} = q''_{CHF,U} / F_C$$

where,  $q''_{CHF,NU}$  CHF for non-uniform axial power distribution,  $MBtu/hr-ft^2$   
 $q''_{CHF,U}$  CHF for uniform axial power distribution,  $MBtu/hr-ft^2$   
 $F_C$  Non-uniform axial power distribution correction factor

The Tong factor  $F_C$  was defined as follow :

$$F_C = \frac{C}{q''_{CHF,NU} (1 - e^{-Cl_{DNB}})} \int_0^{l_{DNB}} q''(z) e^{-C(l_{DNB}-z)} dz$$

$$C = 1.8 (1 - \chi_{DNB})^{4.31} / (G/10^6)^{0.478} f^{-1}$$

where,  $l_{DNB}$  CHF axial location  
 $\chi_{DNB}$  Local quality at the CHF location

Reference 6

According to the SER issued by USNRC shown in the enclosure of ~~Reference 5~~, the 95/95 DNBR (Departure from Nucleate Boiling Ratio) limit of the CE-1 CHF correlation established for the uniform axial power distribution was allowed to be applied to the non-uniform axial power distribution since the CE-1 CHF correlation combined with the Tong factor  $F_C$  predicts the CHF conservatively for the non-uniform axial power distribution.

The CHF test data for the PLUS7 fuel were obtained with a non-uniform axial power distribution, a symmetric cosine with a peak of 1.475. For a conservatism, [

#### 4.4 CORRELATION COEFFICIENTS AND APPLICABLE RANGES OF PARAMETERS

The applicable ranges of parameters for the KCE-1 CHF correlation were determined based on the local fluid conditions at the location of the predicted minimum DNBR. The coefficients of KCE-1 CHF correlation were developed by an iterative process to optimize the coefficients as given below:

- 1) As the first step in the iterative process, the local fluid conditions at the [ ]<sup>TS</sup> elevation were used to determine the initial coefficients for the correlation and to estimate the range of applicability for the correlation. The

selected range used in the initial runs was based upon the range of data at the [ ] elevation.

- 2) The second step was to determine the initial estimate of the eight coefficients of the CE-1 CHF correlation formula by using a nonlinear regression code. To obtain convergence, the initial guesses were based upon the values for the CE-1 CHF correlation, Reference 4. The resulting applicable ranges of parameters for the initial KCE-1 CHF correlation were as follows:

- System pressure
  - Local mass flux
  - Local quality
- } <sup>TS</sup>

Reference 5

- 3) As the third step, statistical tests were performed for the indicated CHF elevation data with the CHF statistics for the initial KCE-1 CHF correlation. An outlier test was applied to identify potential test data which could be removed. There was no outlier for the [ ] <sup>TS</sup> elevation data.

[ ] <sup>TS</sup>

- 4) As the fourth step, an iterative process was then applied by using the initial coefficients of the KCE-1 CHF correlation from the [ ] <sup>TS</sup> elevation for each test section with [ ] <sup>TS</sup>

- 5) As the fifth step, local fluid conditions were extracted at the minimum DNBR elevation in a channel [ ] <sup>TS</sup> rod. The local fluid conditions at the [ ] <sup>TS</sup> rod, if applicable, were extracted for TS101. As stated in section 4.3 and Reference 4,

[ ] <sup>TS</sup>

Reference 5

- 6) Step 2 was repeated several times with the minimum DNBR data to determine the eight coefficients of the CE-1 CHF correlation formula. After the initial run at the minimum DNBR elevation, the data were examined for outliers. Based upon this outlier test, [ ] <sup>TS</sup> was eliminated, as shown in Table 4-3. [ ] <sup>TS</sup>

[ ] <sup>TS</sup>

evaluated by comparing M/P statistics of the database and the results with application of Tong factor  $F_C$  [ ]<sup>TS</sup>.

The average M/P value with [ ]<sup>TS</sup>  
 [ ]<sup>TS</sup>  
 [ ]<sup>TS</sup>, as given in Table 5-5.

This proves that the KCE-1 CHF correlation, which was developed under the assumption of the measured CHF for the non-uniform axial power distribution as that for the [ ]<sup>TS</sup>, has conservatism more than [ ]<sup>TS</sup> in the database and/or more than [ ]<sup>TS</sup> in actual design application, respectively.

### 5.3.5 EFFECT of Measurement Uncertainties

Uncertainties of each measured variable of the CHF test are inherently captured in the 95/95 DNBR limit, which is described in Section 5.2. Also, the conservatism that derives from the application of Tong factor  $F_C$  in design analysis can offset the effect of measurement uncertainties.



## 6. CORRELATION APPLICATION

KEPCO Nuclear Fuel uses the KCE-1 CHF correlation for evaluating thermal design of the PLUS7 fuel assembly and the reactor core of APR1400 and OPR1000 in accordance with the CHF or DNB acceptance criteria defined in the Standard Review Plan (SRP)<sup>(7)</sup>.

(SRP)<sup>(8)</sup>

Sections 4.2 and 4.4 of SRP state that the DNB acceptance criterion provides assurance that there be at least a 95% probability at the 95% confidence level that the hot fuel rod in the core does not experience a DNB or transition condition during normal operation or AOOs (Anticipated Operational Occurrences). The acceptance criterion is met in thermal design and safety analysis when the MDNBR of the hot rod in the hot channel is above 95/95 DNBR limit of the correlation. Establishment of the KCE-1 correlation 95/95 DNBR limit was presented in Chapter 5. The KCE-1 CHF correlation was used only with a computer code that has been used for the correlation development and has been qualified with the 95/95 DNBR limit.

The KCE-1 CHF correlation 95/95 DNBR limit and its supporting M/P statistics with the TORC code is 1.124. The applicable ranges of the parameters, based on database, are given in Table 4.4. Note that the Tong factor  $F_C$  is [ ]<sup>TS</sup> are applied to MDNBR calculation for the design application and safety analyses. The value of Tong factor  $F_C$  depends on the various axial power distribution and local fluid conditions but it is conservatively limited to [ ]<sup>TS</sup>. The application of the KCE-1 CHF correlation with TORC code is in full compliance with the conditions of the Safety Evaluation Report (SER) on the TORC code and modeling for CE-PWRs. The OPR1000 and the APR1400 are CE-PWRs.

code<sup>(9)</sup>

The TORC code is used in thermal design and safety analyses to perform detailed modeling of the core and hot assembly and to determine MDNBR in the hot assembly. The CETOP-D code<sup>(8)</sup> is a fast running tool which is used in thermal design and safety analyses to calculate MDNBR in the hot subchannel.

While the TORC code can be applied directly in the thermal analysis and safety analyses, typically the TORC code is used to benchmark the MDNBR results of CETOP-D code such that the CETOP-D results are conservative relative to those of TORC code. The KCE-1 CHF correlation is implemented to both TORC and CETOP-D codes by modifying correlation coefficients only. Note that the functional formula is identical for both KCE-1 and CE-1 CHF correlations, as described in Section 4.3.

Reference 9

Thus, the topical reports described in References 2 and 3 for TORC code and Reference 8 for CETOP-D code will remain valid with the application of KCE-1 CHF correlation. Therefore, the application of KCE-1 CHF correlation with CETOP-D code for OPR1000 and APR1400 is equivalent to its application with TORC code.

Even though a higher value of inverse Peclet number based on the empirically determined thermal diffusion coefficient was used in the TORC model for CHF data analysis and correlation development, the reactor analysis is to be performed with the design inverse Peclet number ( $1/Pe = 0.0101$ ). This is equivalent to the value of the thermal diffusion coefficient (TDC = 0.038) applied to the Westinghouse PWR for fuel assembly with "R" mixing vane grid design<sup>(9)</sup>.

design<sup>(10)</sup>

## 8. REFERENCES

- (1) APR1400-F-M-TR-12001-P Rev.0, "PLUS7 Fuel Design," November 2012.
- (2) CENPD-161-P-A, "TORC Code, A Computer Code for Determining the Thermal Margin of a Reactor Core," April 1986.
- (3) CENPD-206-P-A, "TORC Code, A Verification and Simplified Modeling Methods," June 1981.

(5) → (4) CENPD-162-P-A, "C-E Critical Heat Flux, Critical Heat Flux Correlation for C-E Fuel Assemblies with Standard Spacer Grids, Part 1 Uniform Axial Power Distribution," September 1976.

(6) → (5) CENPD-207-P-A, "C-E Critical Heat Flux, Critical Heat Flux Correlation for C-E Fuel Assemblies with Standard Spacer Grids, Part 2 Nonuniform Axial Power Distribution," December 1984.

(7) → (6) Tong, L. S., Boiling Crisis and Critical Heat Flux, U. S. Atomic Energy Commission, 1972.

(8) → (7) NUREG-0800, "Standard Review Plan Section 4.2, 'Fuel System Design' Revision 3, and Section 4.4, 'Thermal and Hydraulic Design' Revision 2," March 2007.

(9) → (8) CEN-139(A)-P, "Response to First Round Questions on the Statistical Combination of Uncertainties Program : CETOP-D Code Structure and Modeling Methods," March 1981 and CEN-214(A)-NP, "CETOP-D Code Structure and Modeling Methods for Arkansas Nuclear One –Unit 2," July 1982.

(10) → (9) ML071580898 - Westinghouse AP1000 Design Control Document Rev.16 – Tier 2 "Chapter 4 – Reactor – Section 4.4 Thermal and Hydraulic Design," May 2007.

(4) [ ]<sup>TS</sup>.

## RESPONSE TO REQUEST FOR ADDITIONAL INFORMATION

### APR1400 Topical Reports

Korea Electric Power Corporation / Korea Hydro & Nuclear Power Co., LTD

Docket No. PROJ 0782

**RAI No.:** 3-7443 Question 15  
**SRP Section:** N/A  
**Application Section:** KCE-1 Critical Heat Flux Correlation for PLUS7 Thermal Design  
(APR1400-F-C-TR-12002-NP, Rev.0)  
**Date of RAI Issued:** 03/25/2014  
**Response Date:** 02/25/2015

---

### **Question 15**

The coefficients of the KCE-1 CHF correlation were determined by a non-linear multiple regression analysis of the measured CHF data along with the local fluid conditions calculated by using Westinghouse's subchannel analysis code TORC. The main input data used for TORC are summarized in Table 4-1. However, no discussion of the selection of inputs is provided in the topical report. As using TORC plays an important role in reducing the measured CHF data and generating the KCE-1 correlation coefficients, the applicant is requested to provide justifications and sources for their TORC input selections. For example, the single-phase friction factor that is used in the TORC model is valid for fully-developed turbulent internal flow through a smooth tube for Reynolds numbers greater than 20,000. The applicant needs to demonstrate that using the same friction factor correlation would be valid throughout the application domain of the TORC based CHF data reduction, as a different single-phase friction factor correlation would have to be used for Reynolds number less than 20,000.

### **Response**

*The TORC input parameters, given in Table 4-1 of the topical report, were [*

*]*<sup>TS</sup>.

*As shown in Table 15-1, it is not necessary to justify all input parameters.*

*The following describes the parameters among Table 15-1 that do not require justification and why they do not require justification.*

- *input parameters consistent with design constitutive relations: part of NRC approved TORC subchannel code/method*
- *input parameters specified to the test: consistent value used with test section characteristics*
- *same input parameters consistently applied both on CHF data analysis and design application: the effects of the input parameters are negligible since they have equivalent effects on CHF data analyses and on design application*

*However, three (3) input parameters, thermal diffusion coefficient (TDC), spacer grid loss coefficients ( $K_{Grid}$ ), and turbulent momentum factor, were adjusted to reflect the design characteristics of PLUS7 fuel while maintaining the formula of relationships. The justifications for the above three (3) parameters are provided as follows.*

*TDC of [ ]<sup>TS</sup> or the inverse Peclet number of [ ]<sup>TS</sup> was applied to PLUS7 CHF data analysis. Assessment on the applicability had been performed based on [*

*]<sup>TS</sup>.*

*Generally, [*

*]<sup>TS</sup>. The TDC value for grid spacing of 26 inches was [ ]<sup>TS</sup>. It would be conservatively applicable to PLUS7 CHF data analysis. The mid grid of PLUS7 fuel is an R-type split mixing vane design. The grid spacing of PLUS7 fuel and the CHF test section is 15.7 inches as described in Figure 2-9 of the topical report. A lower value of TDC or an inverse Peclet number would be applied to design and safety analyses, as described in Section 6 of the topical report.*

*$K_{Grid}$ 's were determined by the analytical prediction method for 6x6 CHF test grids (mid grid with mixing vane and non-mixing vane grid, MV and NMV in Figure 2-9 of the topical report) [ ]<sup>TS</sup>. Figure 15-1 shows analytically derived  $K_{Grid}$  for a mid grid with mixing vanes of Test Sections TS101 and TS102 (TS102.0 and TS102.1 were the test sections with the same geometry as described in Subsection 2.2 of the topical report).*

*The turbulent momentum factor is the weighting factor that allows the user to account for uncertainties associated with the formulation of the axial momentum carried by turbulent interchange. For PLUS7 CHF data analysis, the value of [ ]<sup>TS</sup> was used rather than [ ]<sup>TS</sup>. The deviation induced from the turbulent momentum factor is implicitly included in M/P statistics. In design application, the momentum factor of [ ]<sup>TS</sup> would be consistently applied to APR1400 design and safety analyses.*

*Corresponding statements based on the above will be included in subsection 4.2 of the topical report, as shown in the attached markup.*

*For the applicable range of design constitutive relations, corresponding information for TORC analyses was listed in Table 15-2 with ranges of CHF data. Ranges of CHF data were within the applicable range of TORC design constitutive relations. As noted in the footnote of Table 15-1, ranges of some parameters were calculated based on the inlet condition or MDNBR location. However, they are not expected to drastically exceed beyond the applicable ranges of TORC design constitutive relations, even for the case to calculate the parameter range of CHF data at the outlet condition. Moreover, [*

]TS.

Note: KAFD was the project name for PLUS7 development (joint program between Westinghouse Electric Company and KEPCO Nuclear Fuel Company)

Table 15-1 TORC Input data consistency with design constitutive relations

<i>Parameter</i>	<i>Used input data</i>	<i>Consistency with design constitutive relations</i>	<i>Justification</i>
<i>Single Phase friction factor</i>			
<i>Two-phase pressure drop</i>			
<i>Forced flow diversion</i>			
<i>Axial power distribution</i>			
<i>Crossflow resistance relationship</i>			
<i>Diversion crossflow resistance factor(<math>K_{ij}</math>)</i>			
<i>Turbulent momentum factor</i>			
<i>Traverse momentum factor(s/l)</i>			
<i>Number of axial nodes</i>			
<i>Allowable fractional error in flow convergence</i>			
<i>Flow damping factor</i>			
<i>Thermal conduction in the coolant</i>			
<i>Inlet flow option</i>			
<i>Thermal diffusion coefficient</i>			
<i>Tong Factor <math>F_c</math></i>			
<i>Loss Coefficient</i>			

TS

\* No specific input value is presented in Table 4-1 of reference 2 of topical report

Table 15-2 TORC Design Constitutive Relations and Applicable Ranges

<i>Parameter</i>	<i>Constitutive Relation</i>	<i>Applicable Range</i>	<i>CHF Data</i>
<i>Single phase friction factor</i>	<i>McAdams</i>		
<i>Two-phase pressure drop</i>	<i>Sher-Green &amp; modified Martinelli-Nelson</i>		
<i>Two-phase flow model</i>	<i>Homogeneous model</i>		
<i>Quality</i>	<i>Thermodynamic equilibrium quality</i>		
<i>Void fraction</i>	<i>Modified Martinelli-Nelson</i>		
<i>Heat transfer model</i>	<i>Dittus-Boelter (Single-phase forced convection)</i>		
	<i>Jens-Lottes (Two-phase flow)</i>		

\* based on bare-bundle flow area

\*\* based on inlet condition

\*\*\* at the MDNBR location



*Figure 15-1 Grid loss coefficients (mid grids) for CHF tests TS101, TS102*

**Impact on DCD**

N/A

**Impact on Technical/Topical/Environmental Report**

Topical Report APR1400-F-C-TR-12002-NP will be revised as indicated on the attached markups.

- Document Mark-up Cover Sheet : 1 page
- Mark-up for Q15 of RAI 3-7443 : 7 pages

※Remark: Minor formatting, such as numbering figures, tables and references, etc., will be cleaned up before finalizing the topical report.

# Document Mark-up Cover Sheet

1. **Project ID:** *APRI400 NRC DC*
2. **Type of Corresponding Document:**  
 DCD     Topical Report     Technical Report     Other(s) \_\_\_\_\_
3. **Title of Corresponding Document:** *KCE-1 CHF Correlation for PLUS7 Thermal Design  
(APRI400-F-C-TR-12002-NP)*
4. **RAI ID/Question ID:** *3-7443 / Q15*
5. **Page(s) attached:** *7 (Seven)*

## 4. CHF CORRELATION DEVELOPMENT

The KCE-1 CHF correlation was developed using the CHF test data for the PLUS7 fuel obtained from HTRF. This chapter describes the CHF test data, local fluid condition calculation method, the correlation coefficient optimization procedure and applicable range of parameters to the correlation.

### 4.1 CHF TEST DATA

[ ]<sup>TS</sup> test data for the thimble subchannel test section TS101 and [ ]<sup>TS</sup> data for the matrix subchannel test section TS102 were

The TORC input parameters, given in Table 4-1, were [ ]<sup>TS</sup>. Among them, [ ]<sup>TS</sup>.

[ ]<sup>TS</sup>.

TDC of [ ]<sup>TS</sup> or the inverse Peclet number of [ ]<sup>TS</sup> was applied to PLUS7 CHF data analysis. Assessment on the applicability had been performed based on [ ]<sup>TS</sup>.

[ ]<sup>TS</sup>. Generally, [ ]<sup>TS</sup>.

[ ]<sup>TS</sup>. The TDC value for grid spacing of 26 inches was [ ]<sup>TS</sup>.

It would be conservatively applicable to PLUS7 CHF data analysis. The mid grid of PLUS7 fuel is an R-type split mixing vane design. The grid spacing of PLUS7 fuel and the CHF test section is 15.7 inches as described in Figure 2-9 of the topical report. A lower value of TDC or an inverse Peclet number would be applied to design and safety analyses, as described in Section 6 of the topical report.

KGrid's were determined by the analytical prediction method for 6x6 CHF test grids (mid grid with mixing vane and non-mixing vane grid, MV and NMV in Figure 2-9 of the topical report) [ ]<sup>TS</sup>.

Figure 15-1 shows analytically derived KGrid for a mid grid with mixing vanes of Test Sections TS101 and TS102 (TS102.0 and TS102.1 were the test sections with the same geometry as described in Subsection 2.2 of the topical report).

The turbulent momentum factor is the weighting factor that allows the user to account for uncertainties associated with the formulation of the axial momentum carried by turbulent interchange. For PLUS7 CHF data analysis, the value of [ ]<sup>TS</sup> was used rather than [ ]<sup>TS</sup>. The deviation induced from the turbulent momentum factor is implicitly included in M/P statistics. In design application, the momentum factor of [ ]<sup>TS</sup> would be consistently applied to APR1400 design and safety analyses.

minimal blockage offered by intact spacer grids). The spacer grid with split type "R" mixing vanes, which was adopted in PLUS7 fuel, did not affect the TORC code applicability to thermal hydraulic analyses of reactor cores as approved by USNRC.

The TORC code models were generated by using subchannel arrangements, radial and axial power distributions and spacer grid locations of each test sections as shown in Figure 2-5 through Figure 2-9. Other main input data are summarized in Table 4-1.

INSERT

For CHF tests using a uniform axial power distribution, such as the CHF test cases for the CE-1 correlation<sup>(4)</sup> development, CHF always occurs in the upper exit region of the heater rods (end-of-heated-length, EOHL). Hence, surface temperatures of heater rods and subchannels experiencing CHF can be detected by thermocouples installed azimuthally in the EOHL four (4) subchannels surrounding a heater rod.

#### 4. CHF CORRELATION DEVELOPMENT

The KCE-1 CHF correlation was developed using the CHF test data for the PLUS7 fuel obtained from HTRF. This chapter describes the CHF test data, local fluid condition calculation method, the correlation coefficient optimization procedure and applicable range of parameters to the correlation.

##### 4.1 CHF TEST DATA

[ ]<sup>TS</sup> test data for the thimble subchannel test section TS101 and [ ]<sup>TS</sup> data for the matrix subchannel test section TS102 were obtained, respectively. The entire [ ]<sup>TS</sup> test data are listed in Table A-1 of APPENDIX A.

Figure 4-1 through Figure 4-3 show average heat fluxes (hence powers) of the test section versus system pressure, inlet temperature and inlet mass flux, respectively. As identified in Figure 4-1, [ ]<sup>TS</sup>

[ ]<sup>TS</sup>

##### 4.2 LOCAL FLUID CONDITION CALCULATION

Using the subchannel analysis code, TORC, local fluid conditions for the CHF test data were computed.

The TORC code is an adaptation of the COBRA-IIIC code with modifications including an improved lateral momentum equation and lateral boundary condition capability to simulate actual core behaviors for all flow channels in the core. It is a detailed model code predicting the steady-state thermal hydraulic characteristics of the nuclear reactor cores. The TORC code divides the core into a series of control volumes and solves 3-dimensional conservation equations for each control volume thereby predicting fluid thermal hydraulic local conditions at every position in the core.

The verification of TORC code includes a comparison of subchannel coolant temperature rise and overall pressure drop for CHF test bundles, and full size open core effects of actual operating reactor data.

The TORC code has been approved for use in licensing application of reactor core analyses for steady-state calculations involving unblocked flow channels or subchannels (other than the minimal blockage offered by intact spacer grids). The spacer grid with split type "R" mixing vanes, which was adopted in PLUS7 fuel, did not affect the TORC code applicability to thermal hydraulic analyses of reactor cores as approved by USNRC.

The TORC code models were generated by using subchannel arrangements, radial and axial power distributions and spacer grid locations of each test sections as shown in Figure 2-5 through Figure 2-9. Other main input data are summarized in Table 4-1.

correlation<sup>(5)</sup>

For CHF tests using a uniform axial power distribution, such as the CHF test cases for the CE-1 correlation<sup>(4)</sup> development, CHF always occurs in the upper exit region of the heater rods (end-of-heated-length, EOHL). Hence, surface temperatures of heater rods and subchannels experiencing CHF can be detected by thermocouples installed azimuthally in the EOHL four (4) subchannels surrounding a heater rod.

For CHF tests using a non-uniform axial power distribution, as in the CHF tests for PLUS7 and for Reference 5, the axial location of CHF occurrence depends on the shape of the axial power distribution and local fluid conditions. Moreover, the surface temperatures of heater rods are measured with ring-typed junction thermocouples installed at various axial positions. In this case, the axial location of a heater rod where CHF occurs can be detected but the subchannel experiencing CHF cannot be identified exactly. Thus, the local fluid conditions for the KCE-1 CHF correlation were extracted with the following basic assumptions:



Therefore, [ ] were extracted per each individual datum from TS101 while [ ]<sup>TS</sup> per datum from TS102.

**4.3 CORRELATION FORMULA AND ASSUMPTIONS**

The functional formula of the KCE-1 CHF correlation is identical to the CE-1 CHF correlation, and is given as follow:

$$q''_{CHF,U} = \frac{B_1(d/d_m)^{B_2} [(B_3 + B_4P)(G/10^6)^{(B_5+B_6P)} - (G/10^6)\chi h_{fg}]}{(G/10^6)^{(B_7P+B_8(G/10^6))}}$$

- where,  $q''_{CHF,U}$  CHF for uniform axial power distribution, *MBtu/hr-ft<sup>2</sup>*
- $P$  Pressure, *psia*
- $d$  Equivalent heated diameter of subchannel of interest, *inch*
- $d_m$  Equivalent heated diameter of matrix subchannel, *inch*
- $G$  Local mass flux at the CHF location, *lbm / hr-ft<sup>2</sup>*
- $\chi$  Local quality at the CHF location
- $h_{fg}$  Latent heat of vaporization, *Btu/lbm*.

The coefficients of the CE-1 CHF correlation were determined based on the CHF test data with a uniform axial power distribution. Through subsequent CHF tests with a non-uniform axial power distribution, the non-uniform axial power distribution correction factor, Tong factor  $F_C^{(6),(6)}$ , was

$F_C^{(6),(7)}$

combined with the CE-1 CHF correlation as follow, and was proven to predict the CHF values conservatively:

$$q''_{CHF,NU} = q''_{CHF,U} / F_C$$

where,  $q''_{CHF,NU}$  CHF for non-uniform axial power distribution,  $MBtu/hr-ft^2$   
 $q''_{CHF,U}$  CHF for uniform axial power distribution,  $MBtu/hr-ft^2$   
 $F_C$  Non-uniform axial power distribution correction factor

The Tong factor  $F_C$  was defined as follow :

$$F_C = \frac{C}{q''_{CHF,NU} (1 - e^{-Cl_{DNB}})} \int_0^{l_{DNB}} q''(z) e^{-C(l_{DNB}-z)} dz$$

$$C = 1.8 (1 - \chi_{DNB})^{4.31} / (G/10^6)^{0.478} f^{-1}$$

where,  $l_{DNB}$  CHF axial location  
 $\chi_{DNB}$  Local quality at the CHF location

Reference 6

According to the SER issued by USNRC shown in the enclosure of ~~Reference 5~~, the 95/95 DNBR (Departure from Nucleate Boiling Ratio) limit of the CE-1 CHF correlation established for the uniform axial power distribution was allowed to be applied to the non-uniform axial power distribution since the CE-1 CHF correlation combined with the Tong factor  $F_C$  predicts the CHF conservatively for the non-uniform axial power distribution.

The CHF test data for the PLUS7 fuel were obtained with a non-uniform axial power distribution, a symmetric cosine with a peak of 1.475. For a conservatism, [

#### 4.4 CORRELATION COEFFICIENTS AND APPLICABLE RANGES OF PARAMETERS

The applicable ranges of parameters for the KCE-1 CHF correlation were determined based on the local fluid conditions at the location of the predicted minimum DNBR. The coefficients of KCE-1 CHF correlation were developed by an iterative process to optimize the coefficients as given below:

- 1) As the first step in the iterative process, the local fluid conditions at the [ ]<sup>TS</sup> elevation were used to determine the initial coefficients for the correlation and to estimate the range of applicability for the correlation. The

selected range used in the initial runs was based upon the range of data at the [ ] elevation.

- 2) The second step was to determine the initial estimate of the eight coefficients of the CE-1 CHF correlation formula by using a nonlinear regression code. To obtain convergence, the initial guesses were based upon the values for the CE-1 CHF correlation, Reference 4. The resulting applicable ranges of parameters for the initial KCE-1 CHF correlation were as follows:

- System pressure
  - Local mass flux
  - Local quality
- } TS

Reference 5

- 3) As the third step, statistical tests were performed for the indicated CHF elevation data with the CHF statistics for the initial KCE-1 CHF correlation. An outlier test was applied to identify potential test data which could be removed. There was no outlier for the [ ]<sup>TS</sup> elevation data.

[ ]<sup>TS</sup>

- 4) As the fourth step, an iterative process was then applied by using the initial coefficients of the KCE-1 CHF correlation from the [ ]<sup>TS</sup> elevation for each test section with [ ]<sup>TS</sup>

- 5) As the fifth step, local fluid conditions were extracted at the minimum DNBR elevation in a channel [ ]<sup>TS</sup> rod. The local fluid conditions at the [ ]<sup>TS</sup> rod, if applicable, were extracted for TS101. As stated in section 4.3 and Reference 4,

[ ]<sup>TS</sup>

Reference 5

- 6) Step 2 was repeated several times with the minimum DNBR data to determine the eight coefficients of the CE-1 CHF correlation formula. After the initial run at the minimum DNBR elevation, the data were examined for outliers. Based upon this outlier test, [ ]<sup>TS</sup> was eliminated, as shown in Table 4-3. [ ]<sup>TS</sup>

[ ]<sup>TS</sup>

## 6. CORRELATION APPLICATION

KEPCO Nuclear Fuel uses the KCE-1 CHF correlation for evaluating thermal design of the PLUS7 fuel assembly and the reactor core of APR1400 and OPR1000 in accordance with the CHF or DNB acceptance criteria defined in the Standard Review Plan (SRP)<sup>(7)</sup>.

(SRP)<sup>(8)</sup>

Sections 4.2 and 4.4 of SRP state that the DNB acceptance criterion provides assurance that there be at least a 95% probability at the 95% confidence level that the hot fuel rod in the core does not experience a DNB or transition condition during normal operation or AOOs (Anticipated Operational Occurrences). The acceptance criterion is met in thermal design and safety analysis when the MDNBR of the hot rod in the hot channel is above 95/95 DNBR limit of the correlation. Establishment of the KCE-1 correlation 95/95 DNBR limit was presented in Chapter 5. The KCE-1 CHF correlation was used only with a computer code that has been used for the correlation development and has been qualified with the 95/95 DNBR limit.

The KCE-1 CHF correlation 95/95 DNBR limit and its supporting M/P statistics with the TORC code is 1.124. The applicable ranges of the parameters, based on database, are given in Table 4.4. Note that the Tong factor  $F_C$  is [ ]<sup>TS</sup> are applied to MDNBR calculation for the design application and safety analyses. The value of Tong factor  $F_C$  depends on the various axial power distribution and local fluid conditions but it is conservatively limited to [ ]<sup>TS</sup>. The application of the KCE-1 CHF correlation with TORC code is in full compliance with the conditions of the Safety Evaluation Report (SER) on the TORC code and modeling for CE-PWRs. The OPR1000 and the APR1400 are CE-PWRs.

code<sup>(9)</sup>

The TORC code is used in thermal design and safety analyses to perform detailed modeling of the core and hot assembly and to determine MDNBR in the hot assembly. The CETOP-D code<sup>(8)</sup> is a fast running tool which is used in thermal design and safety analyses to calculate MDNBR in the hot subchannel.

While the TORC code can be applied directly in the thermal analysis and safety analyses, typically the TORC code is used to benchmark the MDNBR results of CETOP-D code such that the CETOP-D results are conservative relative to those of TORC code. The KCE-1 CHF correlation is implemented to both TORC and CETOP-D codes by modifying correlation coefficients only. Note that the functional formula is identical for both KCE-1 and CE-1 CHF correlations, as described in Section 4.3.

Reference 9

Thus, the topical reports described in References 2 and 3 for TORC code and Reference 8 for CETOP-D code will remain valid with the application of KCE-1 CHF correlation. Therefore, the application of KCE-1 CHF correlation with CETOP-D code for OPR1000 and APR1400 is equivalent to its application with TORC code.

Even though a higher value of inverse Peclet number based on the empirically determined thermal diffusion coefficient was used in the TORC model for CHF data analysis and correlation development, the reactor analysis is to be performed with the design inverse Peclet number ( $1/Pe = 0.0101$ ). This is equivalent to the value of the thermal diffusion coefficient (TDC = 0.038) applied to the Westinghouse PWR for fuel assembly with "R" mixing vane grid design<sup>(9)</sup>.

design<sup>(10)</sup>

**8. REFERENCES**

- (1) APR1400-F-M-TR-12001-P Rev.0, "PLUS7 Fuel Design," November 2012.
- (2) CENPD-161-P-A, "TORC Code, A Computer Code for Determining the Thermal Margin of a Reactor Core," April 1986.
- (3) CENPD-206-P-A, "TORC Code, A Verification and Simplified Modeling Methods," June 1981.

(5) → (4) CENPD-162-P-A, "C-E Critical Heat Flux, Critical Heat Flux Correlation for C-E Fuel Assemblies with Standard Spacer Grids, Part 1 Uniform Axial Power Distribution," September 1976.

(6) → (5) CENPD-207-P-A, "C-E Critical Heat Flux, Critical Heat Flux Correlation for C-E Fuel Assemblies with Standard Spacer Grids, Part 2 Nonuniform Axial Power Distribution," December 1984.

(7) → (6) Tong, L. S., Boiling Crisis and Critical Heat Flux, U. S. Atomic Energy Commission, 1972.

(8) → (7) NUREG-0800, "Standard Review Plan Section 4.2, 'Fuel System Design' Revision 3, and Section 4.4, 'Thermal and Hydraulic Design' Revision 2," March 2007.

(9) → (8) CEN-139(A)-P, "Response to First Round Questions on the Statistical Combination of Uncertainties Program : CETOP-D Code Structure and Modeling Methods," March 1981 and CEN-214(A)-NP, "CETOP-D Code Structure and Modeling Methods for Arkansas Nuclear One –Unit 2," July 1982.

(10) → (9) ML071580898 - Westinghouse AP1000 Design Control Document Rev.16 – Tier 2 "Chapter 4 – Reactor – Section 4.4 Thermal and Hydraulic Design," May 2007.

(4) [ ]<sup>TS</sup>.

INSERT

## RESPONSE TO REQUEST FOR ADDITIONAL INFORMATION

### APR1400 Topical Reports

Korea Electric Power Corporation / Korea Hydro & Nuclear Power Co., LTD

Docket No. PROJ 0782

**RAI No.:** 3-7443 Question 16  
**SRP Section:** N/A  
**Application Section:** KCE-1 Critical Heat Flux Correlation for PLUS7 Thermal Design  
(APR1400-F-C-TR-12002-NP, Rev.0)  
**Date of RAI Issued:** 03/25/2014  
**Response Date:** 02/25/2015

---

### **Question 16**

As a TORC model was used to analyze the CHF test data, it is logical that the resulting KCE-1 CHF correlation can be implemented in TORC to perform the PLUS7 fuels thermal design and safety analyses, as it would use the same fluid properties database and compute the same local fluid conditions. However, the topical report mentions that the correlation can also be used in the CETOP-D code. The applicant should justify it by relating it to how the two codes calculate the local fluid conditions and whether they use the same fluid properties database. At a minimum, the use of the KCE-1 correlation in the CETOP-D code should be dependent on CETOP-D being an approved methodology for the OPR-1000 and APR1400 designs. It is not clear from the topical report what CETOP-D methodology is being referenced. Please submit the topical report for the CETOP-D methodology which will be used with OPR-1000 and APR1400, otherwise take out the reference to CETOP-D.

### **Response**

*A reference to the CETOP-D computer code and corresponding statements in the topical report (APR1400-F-C-TR-12002) will be deleted.*

*The sections of the topical report with statements on CETOP-D are ;*

#### **○ ABSTRACT**

...

The KCE-1 CHF correlation can be applied to the thermal design and safety analyses with TORC and **CETOP-D** codes for the OPR1000 and the APR1400, in which PLUS7 fuels are loaded.

○ 6. CORRELATION APPLICATION

...

The TORC code is used in thermal design and safety analyses to perform detailed modeling of the core and hot assembly and to determine MDNBR in the hot assembly. The **CETOP-D** code<sup>(8)</sup> is a fast running tool which is used in thermal design and safety analyses to calculate MDNBR in the hot subchannel.

While the TORC code can be applied directly in the thermal analysis and safety analyses, typically the TORC code is used to benchmark the MDNBR results of **CETOP-D** code such that the **CETOP-D** results are conservative relative to those of TORC code. The KCE-1 CHF correlation is implemented to both TORC and **CETOP-D** codes by modifying correlation coefficients only. Note that the functional formula is identical for both KCE-1 and CE-1 CHF correlations, as described in Section 4.3.

Thus, the topical reports described in References 2 and 3 for TORC code and Reference 8 for **CETOP-D** code will remain valid with the application of KCE-1 CHF correlation. Therefore, the application of KCE-1 CHF correlation with **CETOP-D** code for OPR1000 and APR1400 is equivalent to its application with TORC code.

...

○ 7. CONCLUSION

...

The KCE-1 CHF correlation can be applied to the thermal design and safety analysis with the Westinghouse thermal hydraulic design codes TORC and **CETOP-D** for the OPR1000 and the APR1400, which PLUS7 fuels are loaded.

○ 8. REFERENCES

...

- (8) CEN-139(A)-P, "Response to First Round Questions on the Statistical Combination of Uncertainties Program : **CETOP-D** Code Structure and Modeling Methods," March 1981 and CEN-214(A)-NP, "**CETOP-D** Code Structure and Modeling Methods for Arkansas Nuclear One –Unit 2," July 1982.

...

*Modifications to the above statements in the topical report would be;*

○ ABSTRACT

...

The KCE-1 CHF correlation can be applied to the thermal design and safety analyses with the TORC code for OPR1000 and APR1400, in which PLUS7 fuel is loaded.

○ 6. CORRELATION APPLICATION

...

The TORC code is used in thermal design and safety analyses to perform detailed modeling of the core and hot assembly and to determine MDNBR in the hot assembly.

The KCE-1 CHF correlation is implemented to the TORC code by modifying correlation coefficients only. Note that the functional formula is identical for both KCE-1 and CE-1 CHF correlations, as described in Section 4.3.

Thus, the topical reports described in References 2 and 3 for the TORC code will remain valid with the application of KCE-1 CHF correlation.

...

○ 7. CONCLUSION

...

The KCE-1 CHF correlation can be applied to the thermal design and safety analysis with the Westinghouse thermal hydraulic design code TORC for OPR1000 and APR1400, in which PLUS7 fuel is loaded.

○ 8. REFERENCES

...

(8) Deleted.

*The modifications above will be included in the topical report as shown in the attached markup.*

*A description of the CETOP-D computer code model and applicability to APR1400 reactor cores (PLUS7 fuel) are addressed in a technical report of APR1400-F-C-NR-12001 Rev.1, "Thermal Design Methodology". The technical report was submitted with docketing of APR1400 Design Control Document (DCD). (MKD/NW-14-0036L, December 23, 2014)*

**Impact on DCD**

N/A

**Impact on Technical/Topical/Environmental Report**

Topical Report APR1400-F-C-TR-12002-NP will be revised as indicated on the attached markups.

- Document Mark-up Cover Sheet : 1 page
- Mark-up for Q16 of RAI 3-7443 : 4 pages

※Remark: Minor formatting, such as numbering figures, tables and references, etc., will be cleaned up before finalizing the topical report.

# Document Mark-up Cover Sheet

1. **Project ID:** *APRI400 NRC DC*
2. **Type of Corresponding Document:**  
 DCD     Topical Report     Technical Report     Other(s) \_\_\_\_\_
3. **Title of Corresponding Document:** *KCE-1 CHF Correlation for PLUS7 Thermal Design  
(APRI400-F-C-TR-12002-NP)*
4. **RAI ID/Question ID:** *3-7443 / Q16*
5. **Page(s) attached:** *4 (Four)*

## ABSTRACT

The Critical Heat Flux (CHF) tests for PLUS7 fuel were conducted at Columbia University's Heat Transfer Research Facility (HTRF) in New York City, New York. The objective of the tests was to obtain the data to develop an applicable CHF correlation for PLUS7 fuel.

The CHF tests were performed with two test sections simulating with and without a guide thimble tube, respectively. Each test section was composed of 6x6 heater rods with a heated length of 150 inches and a grid span of 15.7 inches, in accordance with the PLUS7 fuel geometry. The tests were performed with a cosine non-uniform axial power distribution and the radial power split between hot and cold rods was approximately 1 : 0.82.

The functional formula of the KCE-1 CHF correlation is identical to the Westinghouse CE-1 CHF correlation. The coefficients of the KCE-1 CHF correlation were determined by a non-linear multiple-regression analysis for the measured CHF data with local fluid conditions calculated by using the subchannel analysis code TORC (T<sub>h</sub>ermal h<sub>y</sub>draulics Of a Reactor Core).

The correlation DNBR (Departure from Nucleate Boiling Ratio) limit was determined with a 95% probability and at a 95% confidence level (95/95 DNBR limit). The statistical results and the applicable ranges of parameters for the KCE-1 CHF correlation are given below.

- Statistical results

Number of Data	$\bar{x}_{(M/P)}$	$S_{(M/P)}$	Correlation DNBR Limit (95/95 DNBR Limit)
225	0.9866	0.05304	1.124

- Applicable ranges of parameters

Parameter	British Unit	SI Unit
System Pressure	1395 ~ 2415 <i>psia</i>	9.62 ~ 16.65 <i>MPa</i>
Local Mass Flux	0.85 ~ 3.15 <i>Mlbm/hr-ft<sup>2</sup></i>	1153 ~ 4272 <i>kg/s-m<sup>2</sup></i>
Local Quality	-0.150 ~ 0.275	

The test data analysis for the correlation development, its results, the CHF test facility and test procedure for the PLUS7 fuel are described in this report. The CHF test data, the statistical methods applied to the correlation development and verification are provided in the appendices.

The KCE-1 CHF correlation can be applied to the thermal design and safety analyses with TORC and ~~CETOP-D~~ codes for the OPR1000 and the APR1400, in which PLUS7 fuels are loaded.

## 6. CORRELATION APPLICATION

KEPCO Nuclear Fuel uses the KCE-1 CHF correlation for evaluating thermal design of the PLUS7 fuel assembly and the reactor core of APR1400 and OPR1000 in accordance with the CHF or DNB acceptance criteria defined in the Standard Review Plan (SRP)<sup>(7)</sup>.

Sections 4.2 and 4.4 of SRP state that the DNB acceptance criterion provides assurance that there be at least a 95% probability at the 95% confidence level that the hot fuel rod in the core does not experience a DNB or transition condition during normal operation or AOOs (Anticipated Operational Occurrences). The acceptance criterion is met in thermal design and safety analysis when the MDNBR of the hot rod in the hot channel is above 95/95 DNBR limit of the correlation. Establishment of the KCE-1 correlation 95/95 DNBR limit was presented in Chapter 5. The KCE-1 CHF correlation was used only with a computer code that has been used for the correlation development and has been qualified with the 95/95 DNBR limit.

The KCE-1 CHF correlation 95/95 DNBR limit and its supporting M/P statistics with the TORC code is 1.124. The applicable ranges of the parameters, based on database, are given in Table 4.4. Note that the Tong factor  $F_C$  is [ ]<sup>TS</sup> are applied to MDNBR calculation for the design application and safety analyses. The value of Tong factor  $F_C$  depends on the various axial power distribution and local fluid conditions but it is conservatively limited to [ ]<sup>TS</sup>. The application of the KCE-1 CHF correlation with TORC code is in full compliance with the conditions of the Safety Evaluation Report (SER) on the TORC code and modeling for CE-PWRs. The OPR1000 and the APR1400 are CE-PWRs.

The TORC code is used in thermal design and safety analyses to perform detailed modeling of the core and hot assembly and to determine MDNBR in the hot assembly. ~~The CETOP-D code<sup>(8)</sup> is a fast running tool which is used in thermal design and safety analyses to calculate MDNBR in the hot subchannel.~~

~~While the TORC code can be applied directly in the thermal analysis and safety analyses, typically the TORC code is used to benchmark the MDNBR results of CETOP-D code such that the CETOP-D results are conservative relative to those of TORC code. The KCE-1 CHF correlation is implemented to both TORC and CETOP-D codes by modifying correlation coefficients only. Note that the functional formula is identical for both KCE-1 and CE-1 CHF correlations, as described in Section 4.3.~~

~~Thus, the topical reports described in References 2 and 3 for TORC code and Reference 8 for CETOP-D code will remain valid with the application of KCE-1 CHF correlation. Therefore, the application of KCE-1 CHF correlation with CETOP-D code for OPR1000 and APR1400 is equivalent to its application with TORC code.~~

Even though a higher value of inverse Peclet number based on the empirically determined thermal diffusion coefficient was used in the TORC model for CHF data analysis and correlation development, the reactor analysis is to be performed with the design inverse Peclet number ( $1/Pe = 0.0101$ ). This is equivalent to the value of the thermal diffusion coefficient ( $TDC = 0.038$ ) applied to the Westinghouse PWR for fuel assembly with "R" mixing vane grid design<sup>(9)</sup>.

## 7. CONCLUSION

The CHF tests were performed with two test sections simulating with and without a guide thimble tube, respectively. Each test section was composed of 6x6 heater rods with a heated length of 150 inches and a grid span of 15.7 inches, in accordance with the PLUS7 fuel geometry. The tests were performed with a non-uniform cosine axial power shape and the radial power split between hot and cold rods was approximately 1 : 0.82.

The KCE-1 CHF correlation was developed based on the CHF test data of the PLUS7 fuel. The functional formula of the KCE-1 CHF correlation is the same as the CE-1 CHF correlation. The correlation coefficients were optimized by performing a non-linear multiple-regression analysis for the measured CHF data along the local fluid conditions calculated by a subchannel analysis code, TORC. During the development stage, the non-uniform axial power distribution correction factor, the Tong factor  $F_C$ , was [

of nuclear power plants. The optimized correlation coefficients are presented in Table 4-4.

Based on the statistical analysis of the test data groups used for the correlation development and for the correlation DNBR limit establishment, the most conservative DNBR limit for the test sections was established as the 95/95 DNBR limit of the KCE-1 CHF correlation. Based on the local fluid conditions used for the correlation development, the applicable ranges of parameters for the KCE-1 CHF correlation were determined. The results are summarized in the following table.

- Statistical results for KCE-1 CHF Correlation

Number of Data	$\bar{x}_{(M/P)}$	$s_{(M/P)}$	Correlation DNBR Limit (95/95 Limit)
225	0.9866	0.05304	1.124

- Applicable ranges of parameters for KCE-1 CHF Correlation

Parameter	British Unit	SI Unit
System Pressure	1395 ~ 2415 <i>psia</i>	9.62 ~ 16.65 <i>MPa</i>
Local Mass Flux	0.85 ~ 3.15 <i>Mlbm/hr-ft<sup>2</sup></i>	1153 ~ 4272 <i>kg/s-m<sup>2</sup></i>
Local Quality	-0.150 ~ 0.275	

The data groups used for the correlation development were generated conservatively and any adverse trend was not observed against the correlation DNBR limit (95/95 DNBR limit). Thus, the validity of the CHF correlation and the established correlation DNBR limit were confirmed.

The KCE-1 CHF correlation can be applied to the thermal design and safety analysis with the Westinghouse thermal hydraulic design codes TORC and ~~CETOP-D~~ for the OPR1000 and the APR1400, which PLUS7 fuels are loaded.

**8. REFERENCES**

- (1) APR1400-F-M-TR-12001-P Rev.0, "PLUS7 Fuel Design," November 2012.
- (2) CENPD-161-P-A, "TORC Code, A Computer Code for Determining the Thermal Margin of a Reactor Core," April 1986.
- (3) CENPD-206-P-A, "TORC Code, A Verification and Simplified Modeling Methods," June 1981.
- (4) CENPD-162-P-A, "C-E Critical Heat Flux, Critical Heat Flux Correlation for C-E Fuel Assemblies with Standard Spacer Grids, Part 1 Uniform Axial Power Distribution," September 1976.
- (5) CENPD-207-P-A, "C-E Critical Heat Flux, Critical Heat Flux Correlation for C-E Fuel Assemblies with Standard Spacer Grids, Part 2 Nonuniform Axial Power Distribution," December 1984.
- (6) Tong, L. S., Boiling Crisis and Critical Heat Flux, U. S. Atomic Energy Commission, 1972.
- (7) NUREG-0800, "Standard Review Plan Section 4.2, 'Fuel System Design' Revision 3, and Section 4.4, 'Thermal and Hydraulic Design' Revision 2," March 2007.
- ~~(8) GEN 139(A) P, "Response to First Round Questions on the Statistical Combination of Uncertainties Program: CETOP-D Code Structure and Modeling Methods," March 1981 and CEN 214(A) NP, "CETOP-D Code Structure and Modeling Methods for Arkansas Nuclear One Unit 2," July 1982.~~
- (9) ML071580898 - Westinghouse AP1000 Design Control Document Rev.16 – Tier 2 "Chapter 4 – Reactor – Section 4.4 Thermal and Hydraulic Design," May 2007.

## RESPONSE TO REQUEST FOR ADDITIONAL INFORMATION

### APR1400 Topical Reports

Korea Electric Power Corporation / Korea Hydro & Nuclear Power Co., LTD

Docket No. PROJ 0782

**RAI No.:** 3-7443 Question 17

**SRP Section:** N/A

**Application Section:** KCE-1 Critical Heat Flux Correlation for PLUS7 Thermal Design  
(APR1400-F-C-TR-12002-NP, Rev.0)

**Date of RAI Issued:** 03/25/2014

**Response Date:** 02/25/2015

### Question 17

In the development of a correlation, the potential for overfitting exists in which the correlation can predict the data used to develop the correlation well, but lacks in predictive capability on other data not used in the development of the correlation. It is not clear from the topical report whether some test data were initially excluded from the KCE-1 correlation coefficient generation and were used later as additional points for independent correlation validation. The applicant should address the potential for overfitting in the KCE-1 correlation.

The applicant should also resolve the inconsistencies among the number of data points reported in various parts of the report. During the PLUS7 fuel CHF tests, [ ]<sup>TS</sup> test data for the thimble subchannel test section Test Section 101 and [ ]<sup>TS</sup> data for the matrix subchannel test section Test Section 102 were collected, respectively. The [ ]<sup>TS</sup> test data points are listed in Table A-1 of APPENDIX A. Table A-2 lists [ ]<sup>TS</sup> test data points that were rejected during the correlation development process. The applicant needs to explain how this data processing has led to an overall KCE-1 CHF correlation database of [ ]<sup>TS</sup>.”

The two hundred and twenty-five (225) data points cited in the abstract as well as in Section 5.2 of the report are also confusing.

Also provide clear descriptions identifying the following:

- (A) The total number of test points for each test
- (B) The total number of test points which were used for generating the coefficients of the correlation for each test.

- (C) The total number of test points which were excluded from calculating the coefficients of the correlation for each test.
- (D) The validation statistics (similar to that provided in the first table of Table 5-4) for both (B) and (C) above. Statistics should be provided for each test.

### **Response**

*Potential for overfitting is not expected in the KCE-1 CHF correlation prediction because;*

- *Four (4) variables for flow condition, pressure, local mass flux, local quality, and latent heat of vaporization are the minimum essential basic variables to characterize CHF phenomena in flowing water. One (1) variable, equivalent heated diameter ratio, is used to characterize the effect of the unheated guide tube on CHF.*
- *Corresponding eight (8) coefficients represented by five (5) basic variables and a combination of them make a simple functional formula.*
- *The functional form and the variables in the KCE-1 correlation are not brand new, but are the same as the CE-1 correlation (Reference: CENPD-162-P-A, reference 4 of topical report). CE-1 correlation is proven technology.*
- [

*]TS due to the higher CHF performance in PLUS7 fuel with mixing vanes (KCE-1 correlation prediction) than that of Guardian fuel without mixing vanes (CE-1 correlation prediction).*

*The prediction trends of both correlations are compared in Figures 17-1 to 17-3 for quality, pressure, and mass flux, respectively. [*

*]TS.*

*In the response to (D) of Question 17 of RAI 3-7443, the results of detailed analysis with applying cross-validation technique to KCE-1 CHF correlation data are discussed.*

*To provide a clear description identifying the number of data, corresponding information is listed, as requested, below.*

(A) The total number of test points for each test:

- [ ]TS test points for Test Section TS101 (or [ ]TS)
- [ ]TS test points for Test Section TS102

*and*

- [ ]<sup>TS</sup> test points: listed in Table A-1 of the topical report
  - [ ]<sup>TS</sup> test points: listed in Table 10-1 of the response to RAI 3-7443  
Question 10
- (B) The total number of test points that were used for generating the coefficients of the correlation for each test:
- [ ]<sup>TS</sup> test points for Test Section TS101 (or [ ]<sup>TS</sup>)
  - [ ]<sup>TS</sup> test points for Test Section TS102
- (C) The total number of test points that were excluded when calculating the coefficients of the correlation for each test:
- [ ]<sup>TS</sup> test points for Test Section TS101 (or [ ]<sup>TS</sup>):  
excluded due to [ ]<sup>TS</sup>
  - [ ]<sup>TS</sup> test points for Test Section TS102: excluded due to [ ]<sup>TS</sup>
  - Excluded data listed in Table A-2 of the topical report per the types of subchannel. Out of [ ]<sup>TS</sup> listed in Table A-2 of the topical report, [ ]<sup>TS</sup>.
- (D) The validation statistics (similar to that provided in the first table of Table 5-4) for both (B) and (C) above. Statistics should be provided for each test:
- Corresponding M/P statistics for the above (B) and (C) are given in Tables 17-1 and 17-2, respectively.
  - To estimate the potential of overfitting, cross validation was performed on the KCE-1 CHF correlation based on the  $k$ -fold method ( $k = 2 \sim 5$ ). In the  $k$ -fold cross-validation, the original sample is randomly partitioned into  $k$  equal sized subsamples. Of the  $k$  subsamples, a single subsample is retained as the validation data for testing the model, and the remaining  $k-1$  subsamples are used as training data. The cross-validation process is then repeated  $k$  times (the folds), with each of the  $k$  subsamples used exactly once as validation data. The analyses were performed using a free software, R programming (available at <http://www.r-project.org/>).
- Before cross validation for various data splits was performed, the process using R programming was verified with 100% data for training, same as when the KCE-1 correlation was developed. Same values of the initial guess for correlation coefficients were assumed to all cases, as described in section 4.4 of the topical report. The Levenberg-Marquardt method was applied to non-linear regression analysis using R programming. The estimated coefficients and the M/P statistics of the correlation using the R programming process were very close to those of the original KCE-1 correlation, as given in Tables 17-3 and 17-4, respectively. Ranges of correlation variables, such as pressure, mass flux, and quality, were comparable to those of the KCE-1 correlation. Therefore, subsequent  $k$ -fold cross-validation was performed with the verified R programming process.*

Among each of the  $k$ -folds results, the results with maximum MAPE (mean absolute percent error) value for validation data are summarized in Table 17-4. MAPE is a measure of the accuracy of a model defined by,

$$MAPE(\%) = \frac{1}{n} \sum_i^n \left| \frac{M_i - P_i}{M_i} \right|$$

where ;

$n$  = number of data  
 $M$  = measured value  
 $P$  = predicted value

Therefore, the results in Table 17-4 are the worst case for each  $k$ -folds.

M/P statistics of training data and validation data were similar for all cases. 95/95 DNBR limits for each case were calculated using the relations given in Appendix B.4.1 of the topical report based on the results of normality and poolability tests for both training and validation data for each  $k$ -folds, as given in Table 17-5. Poolability tests were performed using the parametric method (F-test for variance and t-test for mean) benchmarked with the non-parametric method of Wilcoxon-Mann-Whitney test. [

]TS.

[

]TS.

Therefore, it is concluded that a potential for overfitting, if any, would not lead to any adverse effects on KCE-1 CHF correlation application to APR1400 thermal design and safety analyses with [

]TS.

*Table 17-1 M/P Statistics for (B)*

<i>Test Section</i>	<i>n</i>	$\bar{x}_{(M/P)}$	$S_{(M/P)}$
101			
102			

*Table 17-2 M/P Statistics for (C)*

<i>Test Section</i>	<i>n</i>	$\bar{x}_{(M/P)}$	$S_{(M/P)}$
101			
102			

*Table 17-3 Comparison of coefficients for Process Verification*

<i>Coeff.</i>	<i>KCE-1 (original)</i>	<i>Refit (100% Data)</i>
B1		
B2		
B3		
B4		
B5		
B6		
B7		
B8		

Table 17-4 M/P Statistics for Cases with max. MAPE for each k-folds

Case	Group	<i>n</i>	$\bar{x}_{(M/P)}$	$S_{(M/P)}$	MAPE (%)	System Pressure (psia)	Local Quality	Local Mass Flux (Mlbm/hr-ft <sup>2</sup> )	95/95 Limit
5-folds (80% / 20%)	Training								
	Validation								
	All								
4-folds (75% / 25%)	Training								
	Validation								
	All								
3-folds (67% / 33%)	Training								
	Validation								
	All								
2-folds (50% / 50%)	Training								
	Validation								
	All								
Refit (100%/0%)	All								

TS

Table 17-5 Poolability Check Results

Case	Test		Statistics	P-Value	Test Result
80% / 20%	Normality	Training			
		Validation			
		All			
	F-test				
	T-test				
	Wilcoxon-Mann-Whitney				
75% / 25%	Normality	Training			
		Validation			
		All			
	F-test				
	T-test				
	Wilcoxon-Mann-Whitney				
67% / 33%	Normality	Training			
		Validation			
		All			
	F-test				
	T-test				
	Wilcoxon-Mann-Whitney				
50% / 50%	Normality	Training			
		Validation			
		All			
	F-test				
	T-test				
	Wilcoxon-Mann-Whitney				

TS

\* For normality test, the Kolmogorov-Smirnov method was applied.

\*\* 5% of risk level was applied to all test statistics.



*Figure 17-1. Comparison of CHF Prediction : KCE-1 and CE-1 Correlations (for Local Quality)*

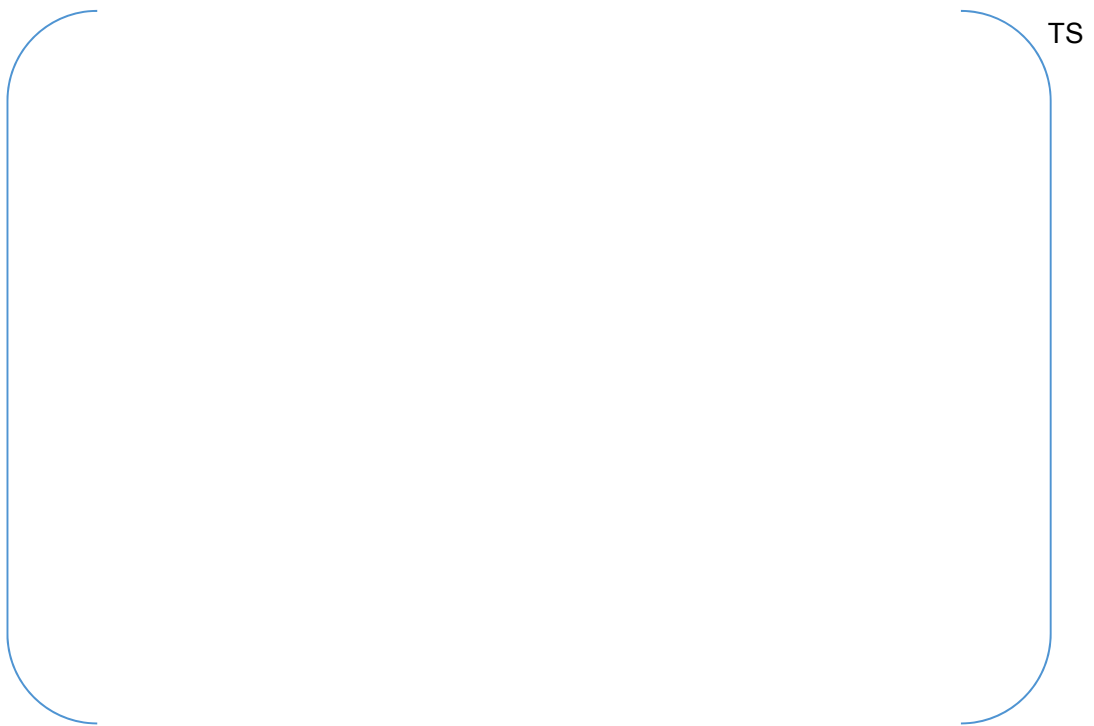


*Figure 17-2. Comparison of CHF Prediction : KCE-1 and CE-1 Correlations (for Pressure)*



Figure 17-3. Comparison of CHF Prediction : KCE-1 and CE-1 Correlations (for Mass Velocity)

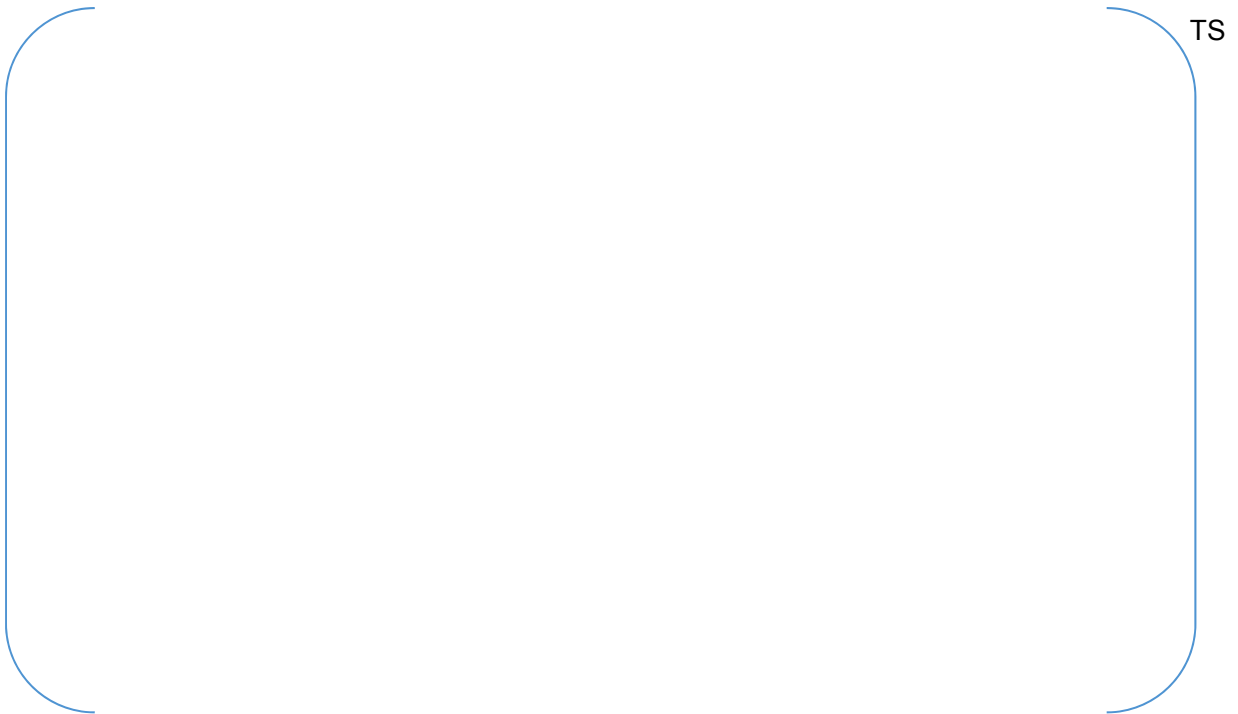
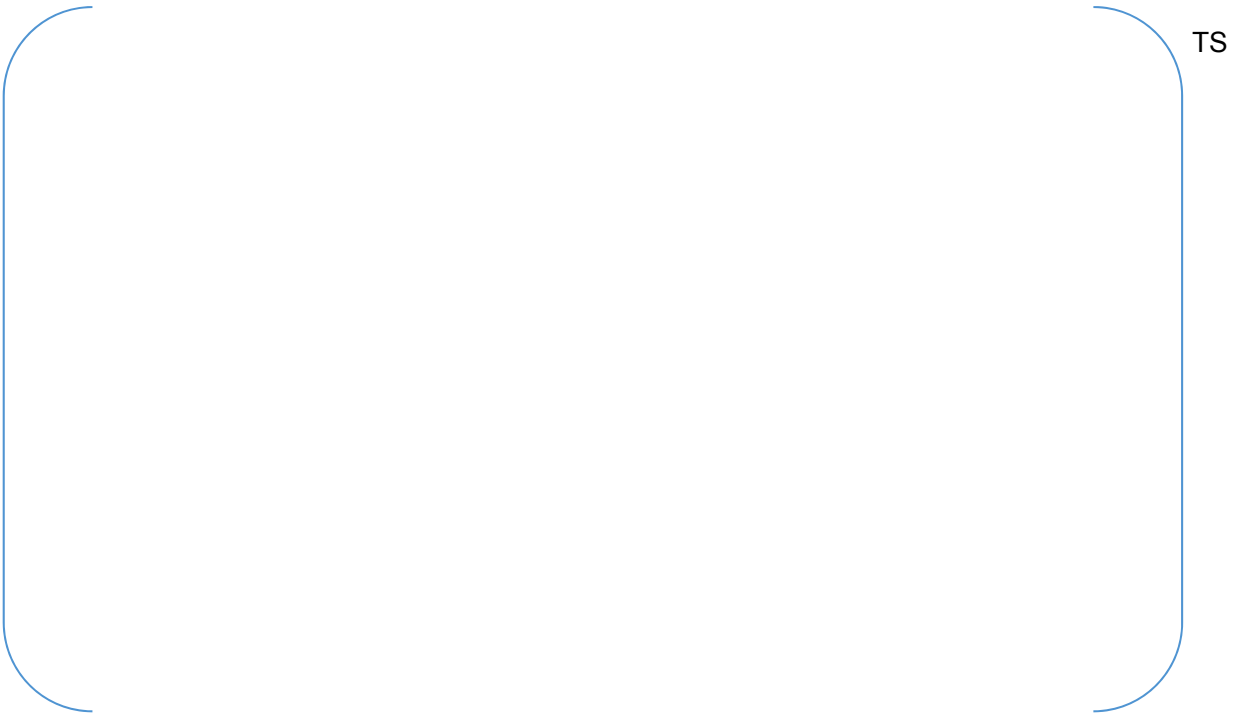


Figure 17-4. Distribution of M/P vs. System Pressure (most limiting case)



*Figure 17-5. Distribution of M/P vs. Local Mass Flux (most limiting case)*



*Figure 17-6. Distribution of M/P vs. Local Quality (most limiting case)*



*Figure 17-7. Distribution of M/P vs. Equivalent Heated Diameter Ratio (most limiting case)*



*Figure 17-8. Predicted CHF vs. Measured CHF (most limiting case)*

---

**Impact on DCD**

N/A

**Impact on Technical/Topical/Environmental Report**

N/A

## RESPONSE TO REQUEST FOR ADDITIONAL INFORMATION

### APR1400 Topical Reports

Korea Electric Power Corporation / Korea Hydro & Nuclear Power Co., LTD

Docket No. PROJ 0782

RAI No.: 3-7443 Question 18

SRP Section: N/A

Application Section: KCE-1 Critical Heat Flux Correlation for PLUS7 Thermal Design  
(APR1400-F-C-TR-12002-NP, Rev.0)

Date of RAI Issued: 03/25/2014

Response Date: 02/25/2015

### **Question 18**

As identified in Figure 4-1, [

effectively reduced the application domain of the KCE-1 correlation to a maximum 2415 psia pressure and 3.15 Mlbm/hr-ft<sup>2</sup> inlet mass flux. The applicant should explain the technical bases for selecting the upper limits on the tested system pressure and inlet mass flux ranges, and whether the applicant envisions the actual PLUS7 design exceeding these ranges in any circumstances. ]<sup>TS</sup>.

### **Response**

*The design analysis range of APR1400 is shown in Table 18-1 together with the applicable range of KCE-1 correlation. All design/safety analyses are performed within the applicable range of KCE-1 correlation at the MDNBR location. The process of checking variable range would be applied to APR1400 design analyses with respect to the applicable range of KCE-1 correlation. Therefore, data with variable values higher than those in Table 18-1 were excluded based on the fact that [ ]<sup>TS</sup>, as discussed in Section 4.1 of the topical report.*

*Among the variables included in Table 18-1, the inlet temperature is not an issue for the applicable range of KCE-1 correlation because it is not the variable in the functional form of a*

*correlation. For pressure and local quality, the APR1400 design analysis range is within the applicable range of KCE-1 correlation. For inlet mass flux, the upper limit of the KCE-1 correlation range is slightly lower than the APR1400 design analysis range. However, the local mass flux at the location of MDNBR in actual core analyses is a value within the applicable range of KCE-1 correlation. It is generally true caused from a higher pressure drop due to higher power and higher quality of the hot subchannel force to redistribute flow from the hot subchannel to surrounding subchannels. Redistribution of flow reduces the flowrate of the hot subchannel where calculated DNBR is the minimum.*

*Even though those data were [*

*] <sup>TS</sup>, the M/P behavior is comparable/conservative to data within the applicable range, as shown in Figures 18-1 and 18-2 for pressure and mass flux, respectively.*

*Table 18-1 Range of AOO Design Analysis for APR1400*

<i>Parameter</i>	<i>Design Analysis Range (AOO)</i>	<i>KCE-1 Correlation Applicable Range</i>
<i>Core Inlet Temperature, °F</i>	<i>500 ~ 595</i>	<i>N/A</i>
<i>Pressurizer Pressure, psia</i>	<i>1785 ~ 2415</i>	<i>1395 ~ 2415</i>
<i>Mass Flux, Mlbm/hr-ft<sup>2</sup></i>	<i>1.91 ~ 3.20 (inlet)</i>	<i>0.85 ~ 3.15 (local)</i>
<i>Local Quality</i>	<i>-0.150 ~ 0.275</i>	<i>-0.150 ~ 0.275</i>



*Figure 18-1 M/P Trend vs. System Pressure  
(with Excluded Data due to [ ]<sup>TS</sup>)*



*Figure 18-2 M/P Trend vs. Local Mass Flux  
(with Excluded Data due to [ ]<sup>TS</sup>)*

**Impact on DCD**

N/A

**Impact on Technical/Topical/Environmental Report**

N/A

**Non-Proprietary**

**SECTION D**

**Non-Proprietary**

Page intentionally left blank



**KHNP**

**KOREA HYDRO & NUCLEAR POWER CO., LTD**

70-1312-gil, Yuseong-daero, Yuseong-gu, Daejeon, 305-343, KOREA

Tel: +82-42-870-5740 / Fax: +82-42-870-5779

<http://www.khnp.co.kr>

October 9, 2015  
Document Control Desk  
U.S. Nuclear Regulatory Commission  
Washington, DC 20555-0001

Attention: Mr. Jeff Ciocco  
Division of New Reactor Licensing

Docket No. 52-046 (PROJ 0782)  
MKD/NW-15-0189L / MT-15-144-P

**Subject: Revised Response to RAI 3-7443 on Questions 6, 7, 9, and 17**

**References: 1) NRC Request for Additional Information 3-7443, dated March 25, 2014**  
**2) KHNP Letter MKD/NW-15-0002L, Revised Response to RAI 3-7443, dated March 2, 2015**

KHNP is hereby submitting the revised response to the RAI 3-7443 on topical report “KCE-1 Critical Heat Flux Correlation for PLUS7 Thermal Design”, APR1400-F-C-TR-12002-P/NP, Rev.0, as discussed with the NRC staff during the public meeting held on September 3, 2015. The response addresses questions 6, 7, 9, and 17.

Enclosure 1 contains a copy of the associated affidavit (KHNP). Enclosure 2 contains a copy of the associated affidavit (Westinghouse). Enclosure 3 provides the revised response to RAI 3-7443 on questions 6, 7, 9, and 17 (Proprietary). Enclosure 4 provides the revised response to RAI 3-7443 on questions 6, 7, 9, and 17 (Non-Proprietary).

If additional information or clarification is required, please contact Daegeun Ahn, Director of KHNP Washington DC Center at [ahn.daeguen@khnp.co.kr](mailto:ahn.daeguen@khnp.co.kr) or 703-388-0592.

Sincerely,

---

Jae-yong Lee  
Project Manager  
Advanced Reactors Development Laboratory  
Korea Hydro and Nuclear Power Co., Ltd

Enclosures:

1. Affidavit KAW-15-0189
2. Affidavit CAW-15-4304
3. Revised Response to RAI 3-7443 on Questions 6, 7, 9, and 17 (Proprietary)
4. Revised Response to RAI 3-7443 on Questions 6, 7, 9, and 17 (Non-Proprietary)

**Non-Proprietary**

Page intentionally left blank

Non-Proprietary

Page intentionally left blank

**Non-Proprietary**

Page intentionally left blank

Non-Proprietary

Page intentionally left blank

Non-Proprietary

Page intentionally left blank

**Non-Proprietary**

Page intentionally left blank

**Enclosure 4**

Revised Response to RAI 3-7443 on Questions 6, 7, 9, and 17

(Non-Proprietary)

October 9, 2015

---

---

## RESPONSE TO REQUEST FOR ADDITIONAL INFORMATION

### APR1400 Topical Reports

Korea Electric Power Corporation / Korea Hydro & Nuclear Power Co., LTD

Docket No. 52-046 (PROJ 0782)

**RAI No.:** 3-7443 Question 6

**SRP Section:** N/A

**Application Section:** KCE-1 Critical Heat Flux Correlation for PLUS7 Thermal Design  
(APR1400-F-C-TR-12002-NP, Rev.0)

**Date of RAI Issued:** 03/25/2014

**Response Date:** 10/09/2015

---

### Question 6

The CHF test data for the PLUS7 fuel geometry were obtained by using a non-uniform axial power distribution, a symmetric cosine power profile shape with a peak of 1.475. The applicant should explain the appropriateness of testing a single axial profile and why the inlet/bottom or outlet/top peaked power profiles were not included in the test matrix. The applicant should describe how well the tested power distribution represents the actual profile experienced during the operation of the PLUS7 fuel.

### Response

*A symmetric cosine axial power distribution is a typical axial power shape resulting from two (2) dimensional neutron diffusion equation for finite cylinder geometry in Table 6-2 of the corresponding reference (Reference : J.R. Larmarsh & A.J. Baratta, "Introduction to Nuclear Engineering 3 e/d," Prentice-Hall 2001). A cosine axial power distribution with a high peaking factor is typically used as a reference power shape in reactor DNB analyses, and it is supplemented with top-skewed and bottom-skewed axial power distributions to cover the design range of the axial power variations. Representative axial power shapes from sample plant operation and protection system analyses are shown in Figure 6-1.*

*Effect of nonuniform axial power distribution on Critical Heat Flux (CHF) or DNB is accounted for through the Tong factor ( $F_c$ ) that reduces the predicted CHF or DNB Ratio (DNBR) margin relative to the uniform axial power distribution. Similar to other DNB correlations, DNBR for the KCE-1 correlation is calculated as:*

$$DNBR = \frac{KCE - 1 \text{ CHF Prediction (Uniform Axial Shape)}}{\text{Actual (Measured) heat Flux}} \cdot \left(\frac{1}{F_c}\right)$$

The cosine shape is preferred to CHF tests for non-uniform axial power distribution [

]TS,(a,c). The range of  $F_c$  in the KCE-1 CHF correlation application using the PLUS7 tested cosine shape is [ ]TS as shown in Figure 6-2. The Tong factor range from the KCE-1 cosine tests is [ ]TS,(a,c) the range covered in previous CE-1 CHF tests with several different axial power shapes (CENPD-207-P-A, Reference 5 of the ToR).

A non-cosine axial power shape can be more DNB limiting than the cosine shape, as shown in Figure 6-3. However, the  $F_c$  factor values at the MDNBR elevations (solid symbols) of such DNB-limiting shape are [

]TS,(a,c), as illustrated in Figure 6-4. The PLUS7 CHF tests using the cosine shape provides a good representation of effects of the nonuniform axial power distributions on DNB through the Tong factor encountered in plant safety analysis and operation using the PLUS7 fuel. As explained in the topical report, the KCE-1 coefficients were conservatively generated by [

]TS,(a,c), but KCE-1 is then applied with the Tong factor for DNB calculations in plant applications.



*Figure 6-1 Axial Power Shapes for Sample Analysis*



*Figure 6-2 Distribution of M/P versus Tong Factor Fc (Application Database)*



*Figure 6-3 Axial Behavior of KCE-1 DNBR for each Power Shape*



*Figure 6-4 Axial Behavior of Fc for each Power Shape*

**Impact on DCD**

N/A

**Impact on PRA**

N/A

**Impact on Technical Specification**

N/A

**Impact on Technical/Topical/Environmental Report**

N/A

---

---

## RESPONSE TO REQUEST FOR ADDITIONAL INFORMATION

### APR1400 Topical Reports

Korea Electric Power Corporation / Korea Hydro & Nuclear Power Co., LTD

Docket No. 52-046 (PROJ 0782)

**RAI No.:** 3-7443 Question 7

**SRP Section:** N/A

**Application Section:** KCE-1 Critical Heat Flux Correlation for PLUS7 Thermal Design  
(APR1400-F-C-TR-12002-NP, Rev.0)

**Date of RAI Issued:** 03/25/2014

**Response Date:** 10/09/2015

---

### Question 7

As no testing was conducted with uniform axial power distribution, no “non-uniform axial power distribution correction factor, Tong factor  $FC$ ,” could be developed for the KCE-1 CHF correlation for the tested PLUS7 fuel geometry. Such an optimization of Tong factor for the PLUS7 fuel split vane mixing grid geometries would require testing both uniform and non-uniform axial power distributions with and without guide thimbles, but it was not done for the tested PLUS7 fuel geometry. However, the applicant plans to conservatively use the Tong factor along with the KCE-1 correlation to predict the CHF in the design analyses. The applicant should justify using the CE-1 Correlation Tong factor not developed for the tested PLUS7 fuel geometry. Other CHF correlations generally use Tong factor developed by the test data taken with both uniform and non-uniform axial power profiles.

### Response

*Since no CHF test with uniform axial power shape was performed for the PLUS7 fuel design, the original Tong factor ( $F_c$ ) without any adjustment or optimization is applied to the KCE-1 correlation. The original Tong factor ( $F_c$ ) was developed based on single tube and annuli data. It has been shown to be conservative for rod bundle data in the CE-1 topical report (CENPD-207-P-A, Reference 5 of the ToR) and in the WNG-1 topical report (WCAP-16766-P-A).*

- *The CE-1 CHF correlation was developed with CHF data from axially uniformly heated rod bundles ( $F_c = 1$ ) for various spacer grid designs and pitch to rod diameter ratios (CENPD-162-P-A, Reference 4 of the ToR).*

*When CE-1 was used with the standard Tong factor,  $F_c$ , for several axially non-uniformly heated rod bundles, the resultant M/P values were very conservatively high (CENPD-207-P-A, Reference 5 of ToR) as shown in the table below.*

Axial Power Shape	CE-1 M/P Statistics			Peak
	N	Average	Standard Deviation	
Top Peaked	74	1.119	0.106	1.68
Bottom Peaked	82	1.287	0.130	1.68
Cosine	107	1.236	0.122	1.46
Top Peaked	106	1.254	0.083	1.47

- The WNG-1 correlation was developed with both uniform and non-uniform data, and its validation database included data from a PLUS7 test (Test 102). The optimized value for  $F_{OPT}$  was calculated with the expression:

$$F_{OPT} = [ \dots ]^{(a,c)}$$

where:  $F_{OPT}$  = Optimized non-uniform axial shape factor  
 $F_C$  = Non-uniform shape factor computed with Tong empirical coefficients  
 $B$  = Constant fit with nonlinear regression analysis  
 [ ... ]<sup>(a,c)</sup> of WCAP-16766-P-A

For fuel designs with mixing grid spacers, the optimized  $F_{OPT}$  [ ... ]<sup>(a,c)</sup>  
 for the nonuniform axial power shapes. For the PLUS7 geometry, [ ... ]<sup>TS,(a,c)</sup>.

Without the CHF data from a test using the uniform axial power shape, the KCE-1 CHF correlation was developed with a conservative process described in section 4.3 of topical report: [ ... ]

[ ... ]<sup>TS</sup> for the correlation coefficient generation. Then the KCE-1 correlation is applied to safety analysis with the original Tong factor for nonuniform axial power shapes. The conservative process resulted in a minimum [ ... ]<sup>TS</sup> DNBR margin in the 95/95 DNBR limit of 1.124, or a [ ... ]<sup>TS</sup> lower (conservative) DNBR prediction than the M/P average of [ ... ]<sup>TS</sup>.

The KCE-1 correlation under-predicted the cosine CHF data by [ ... ]<sup>TS</sup>, because of  $q''_{CHF,NU} < q''_{CHF,U}$  ( $F_C > 1$ ) with the definition of Tong factor ( $F_C$ ) as;

$$q''_{CHF,NU} = \frac{q''_{CHF,U}}{F_C} \quad \text{or} \quad q''_{CHF,U} = q''_{CHF,NU} \times F_C$$

The Tong factor ( $F_C$ ) accounts for “memory effect” of non-uniform axial power shape on CHF. As addressed in the response to Question 3 of RAI 3-7443, all PLUS7 CHF data showed consistency with known physical phenomenon as CHF occurred [ ... ]<sup>TS</sup>. Since it was developed with [ ... ]<sup>TS</sup> for a non-uniform axial power test (cosine), the KCE-1 correlation is more conservative than CE-1 or WNG-1 for CHF data with uniform axial power distribution. CE-1 and WNG-1 predict uniform data well, but KCE-1 under-predicts uniform data by its design.

- To estimate the under-prediction of the uniform heat flux with KCE-1, a comparison of the calculated uniform heat flux with KCE-1 and WNG-1 was made. As stated above, test section TS102 was a validation data set for the WNG-1 correlation. The WNG-1 correlation has both uniform and non-uniform CHF data, and the optimized Tong factor  $F_{OPT}$  based on those data. The M/P statistics at MDNBR for TS102 of both correlations are ;

Correlation	M/P Statistics			Remark
	N	Average	Standard Deviation	
WNG-1	94	[ ] <sup>(a,c)</sup>	[ ] <sup>(a,c)</sup>	w/ Optimized Fc
KCE-1	[ ] <sup>TS</sup>	[ ] <sup>TS</sup>	[ ] <sup>TS</sup>	Table 5-4 of topical report, w/ [ ] <sup>TS</sup>

Both correlations predict the test data well as shown in the above statistics, but the KCE-1 correlation under-predicts the CHF from  $q''_{KCE-1u}$  by [ ]<sup>TS</sup>. For Test 102, the average ratio of  $q''_{WNG-1U} / q''_{KCE-1u}$  is [ ]<sup>TS,(a,c)</sup>, or KCE-1 under-predicts  $q''_{KCE-1u}$  by about [ ]<sup>TS,(b,c)</sup> as compared to WNG-1.

Effect of the Tong factor on KCE-1 prediction (and the corresponding DNBR) is illustrated in Figures 7-1 and 7-2. As shown in Figure 7-1, the Tong factor ( $F_c$ ) starts to increase ( $F_c > 1$ ) after peak power elevation. As shown in Figure 7-2, KCE-1 prediction (PCHF) with  $F_c > 1$  results in a reduction in the MDNBR which occurred at [ ]<sup>TS</sup>.

For this example, elevation of MDNBR is [ ]<sup>TS</sup>. Therefore local fluid conditions, especially for quality, are different between the two MDNBRs [ ]<sup>TS</sup>. Per the range of correlation variables for data given in Table 7-1, [ ]<sup>TS</sup>

as shown in Table 7-3 and Figures 7-3 to 7-5. Although KCE-1 CHF predictions with  $F_c$  are conservative at the higher quality, the applicable quality range (27.5% maximum) in the topical report remains unchanged for design applications. There are no adverse M/P trends with respect to pressure, local flow and local quality in Figures 7-3 through 7-5. The predicted CHF values are conservative with respect to the 95/95 DNBR limit line of 1.124, as shown in Figure 7-6.

- The standard/original Tong factor is applied to KCE-1 prediction for design and safety analyses on PLUS7 cores. The application database is based on MDNBR (KCE-1 prediction) with the Tong factor. The M/P statistics and 95/95 DNBR for the application database are provided below for the tested axial power cosine shape:



Since KCE-1 also under-predicts the uniform heat flux, the application of KCE-1 with Fc is conservative for all axial power shapes in design analysis.

In addition to the conservatism due to correlation development with [ ]<sup>TS</sup> and application with Fc, the DNBR limit of 1.124 was conservatively derived based on the development database. The development database has [

]<sup>TS</sup>, as described in section 4.2 of the topical report. This led to [ ]<sup>TS</sup>. As

a result, the DNBR limit of 1.124 was [ ]<sup>TS</sup>. The KCE-1 MDNBR (hence the maximum M/P) for each data point of TS101 occurred at the subchannel [ ]<sup>TS</sup> described in Table A-3 of the topical report. The M/P statistics, based on the MDNBR of the test bundle in the lower part of Table 5-4 of the topical report (ToR), indicated a 95/95 DNBR value lower than 1.124 .

Test Section	M/P Statistics			95/95 DNBR	Remark
	N	Average	Standard Deviation		
101					
102					
All					

The application database of KCE-1 with Fc consists of [ ]<sup>TS</sup> data points as listed in Table 7-1. [ ]<sup>TS</sup>. The excluded data points are listed in Table 7-2. Similar to the points in Table A-2 of the topical report, [ ]<sup>TS</sup> were excluded. [

]<sup>TS</sup> were excluded. The information is to be added in Tables in APENDIX A (for both the excluded data similar to Table A-2 and the database for application

TS

similar to Table A-3 of the topical report, respectively) of the topical report. Table 5-5 of the topical report will be replaced by the Table above (Table with [ ]<sup>TS</sup> data points). Corresponding M/P trend plots will be added to the topical report, as the attached markups.

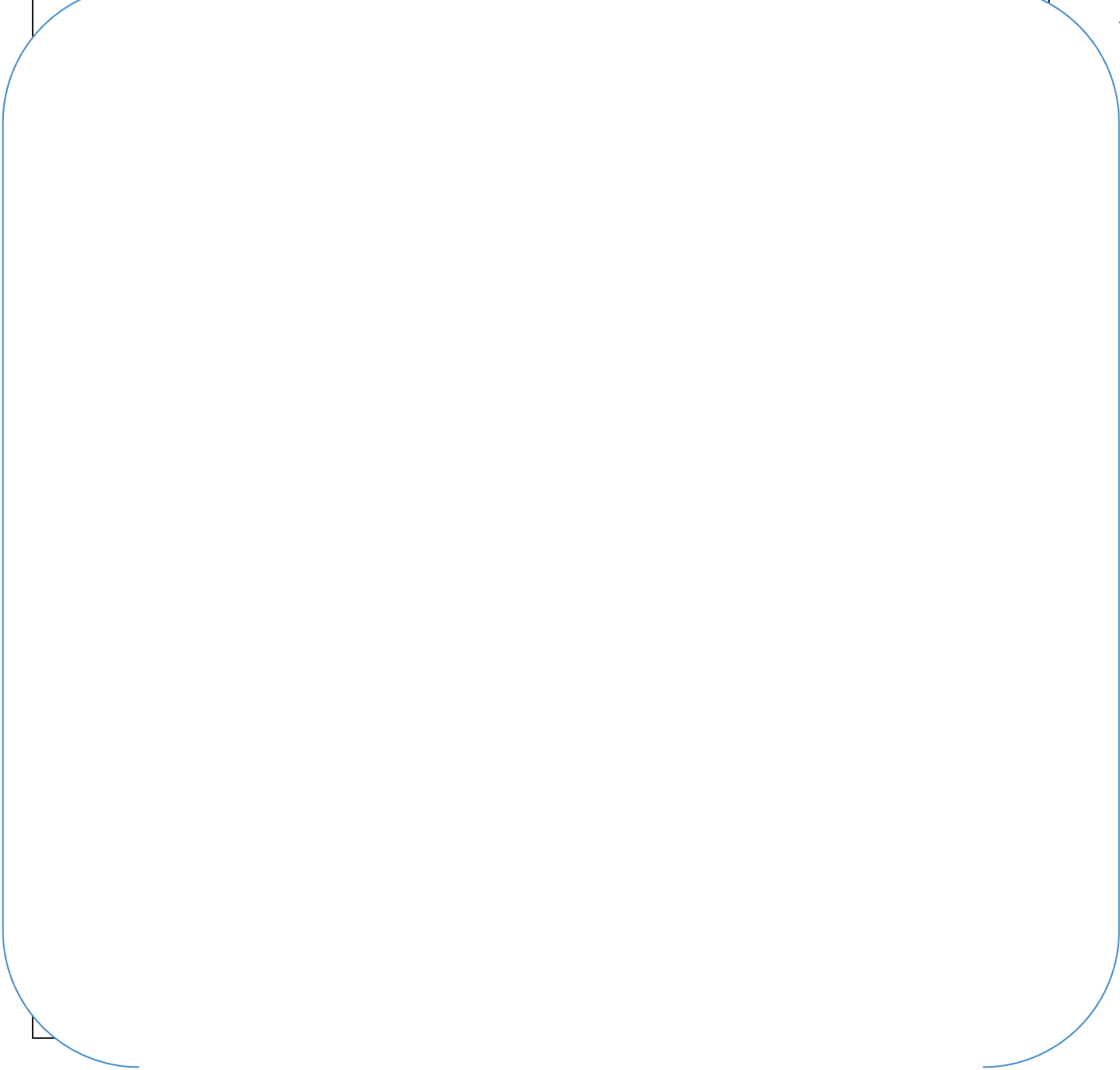
The conservatism in the KCE-1 correlation development [ ]<sup>TS</sup> for the cosine data can also be reflected from a lesson learned in the Westinghouse WRB-2M correlation adjustment due to lack of uniform test data. In contrast to the KCE-1 development, the WRB-2M correlation (WCAP-15025-P-A) was developed with the original Tong factor based on the cosine data only. When compared to the data from uniform power distribution tests for a similar fuel design later, the WRB-2M correlation over-predicted the uniform CHF by about [ ]<sup>(a,c)</sup>, or the M/P CHF average ratio was about [ ]<sup>(a,c)</sup>. As a result, an adjustment was made to the WRB-2M correlation to correct the potentially non-conservative predictions for nearly uniform axial power shapes (NRC Letter, February 2006). The WRB-2M experience showed that without any uniform test data, optimization of DNB correlation coefficients using the original Tong factor from cosine test data could result in non-conservative CHF predictions when applied to uniform CHF data. On the other hand, the KCE-1 coefficients generated from the cosine data [ ]<sup>TS</sup> are conservative when applied to [ ]<sup>TS</sup>.

*Reference:*

- 1) WCAP-16766-P-A / WCAP-16766-NP-A, "Westinghouse Next Generation Correlation (WNG-1) for Predicting Critical Heat Flux in Rod Bundles with Split Vane Mixing Grids," February 2010.
- 2) WCAP-15025-P-A, "Modified WRB-2 Correlation, WRB-2M, for Predicting Critical Heat Flux in 17x17 Rod Bundles with Modified LPD Mixing Vane Grids," April 1999.
- 3) Letter from D. S. Collins (NRC) to J.A. Gresham (Westinghouse), "Modified WRB-2 Correlation in 17x17 Rod Bundles with Modified LPD Mixing Vane Grids," February 2006.

*Table 7-1 KCE-1 CHF Correlation Database for Application (1/5)*

TS	RUN	PR	CHFM	HL	GL	XL	CH.	hfg	Fc	DH	DHM	DNBR	M/P
----	-----	----	------	----	----	----	-----	-----	----	----	-----	------	-----



TS

*Table 7-1 KCE-1 CHF Correlation Database for Application (2/5)*

TS	RUN	PR	CHFM	HL	GL	XL	CH.	hfg	Fc	DH	DHM	DNBR	M/P
----	-----	----	------	----	----	----	-----	-----	----	----	-----	------	-----

TS

*Table 7-1 KCE-1 CHF Correlation Database for Application (3/5)*

TS	RUN	PR	CHFM	HL	GL	XL	CH.	hfg	Fc	DH	DHM	DNBR	M/P
----	-----	----	------	----	----	----	-----	-----	----	----	-----	------	-----



TS

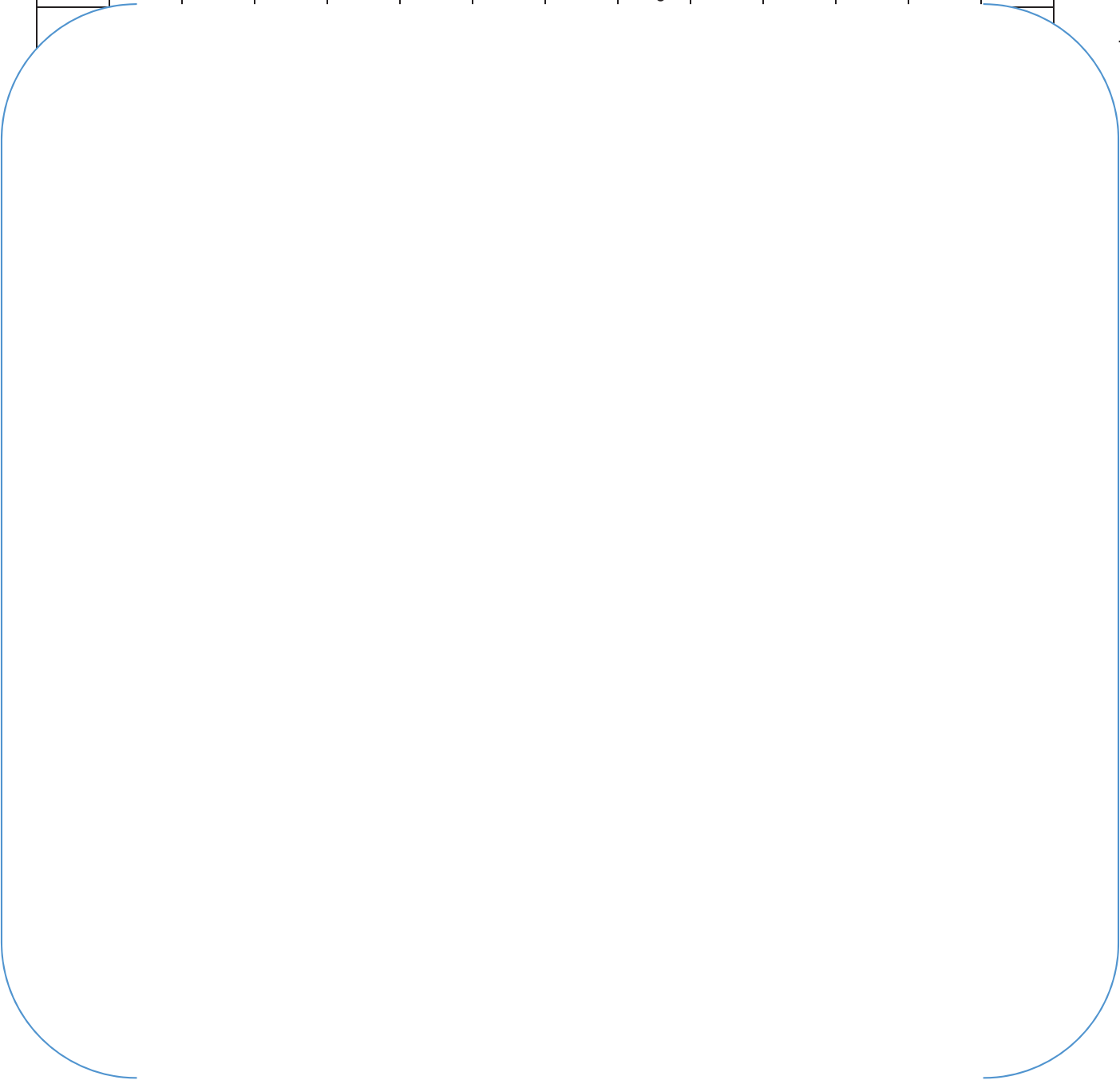
*Table 7-1 KCE-1 CHF Correlation Database for Application (4/5)*

TS	RUN	PR	CHFM	HL	GL	XL	CH.	hfg	Fc	DH	DHM	DNBR	M/P
----	-----	----	------	----	----	----	-----	-----	----	----	-----	------	-----

TS

*Table 7-1 KCE-1 CHF Correlation Database for Application (5/5)*

TS	RUN	PR	CHFM	HL	GL	XL	CH.	hfg	Fc	DH	DHM	DNBR	M/P
----	-----	----	------	----	----	----	-----	-----	----	----	-----	------	-----



TS

*Table 7-2 Data Excluded from Database for Application*

TS	RUN	PR	CHFM	HL	GL	XL	CH.	hfg	Fc	DH	DHM	DNBR	M/P	Remark
----	-----	----	------	----	----	----	-----	-----	----	----	-----	------	-----	--------

TS

Table 7-3 Variables Range of Database for Application

Case	Pressure (psia)	Local Mass Flux (Mlbm/hr-ft <sup>2</sup> )	Local quality * (fraction)
[ ] <sup>TS</sup>	[ ] <sup>TS</sup>	[ ] <sup>TS</sup>	[ ] <sup>TS</sup>
KCE-1 (Topical Report)	1395 ~ 2415	0.85 ~ 3.15	-0.150 ~ 0.275

\* Local quality range of the Topical Report is remained unchanged.



Figure 7-1 Axial Distribution of Fc ( [ ]^TS )

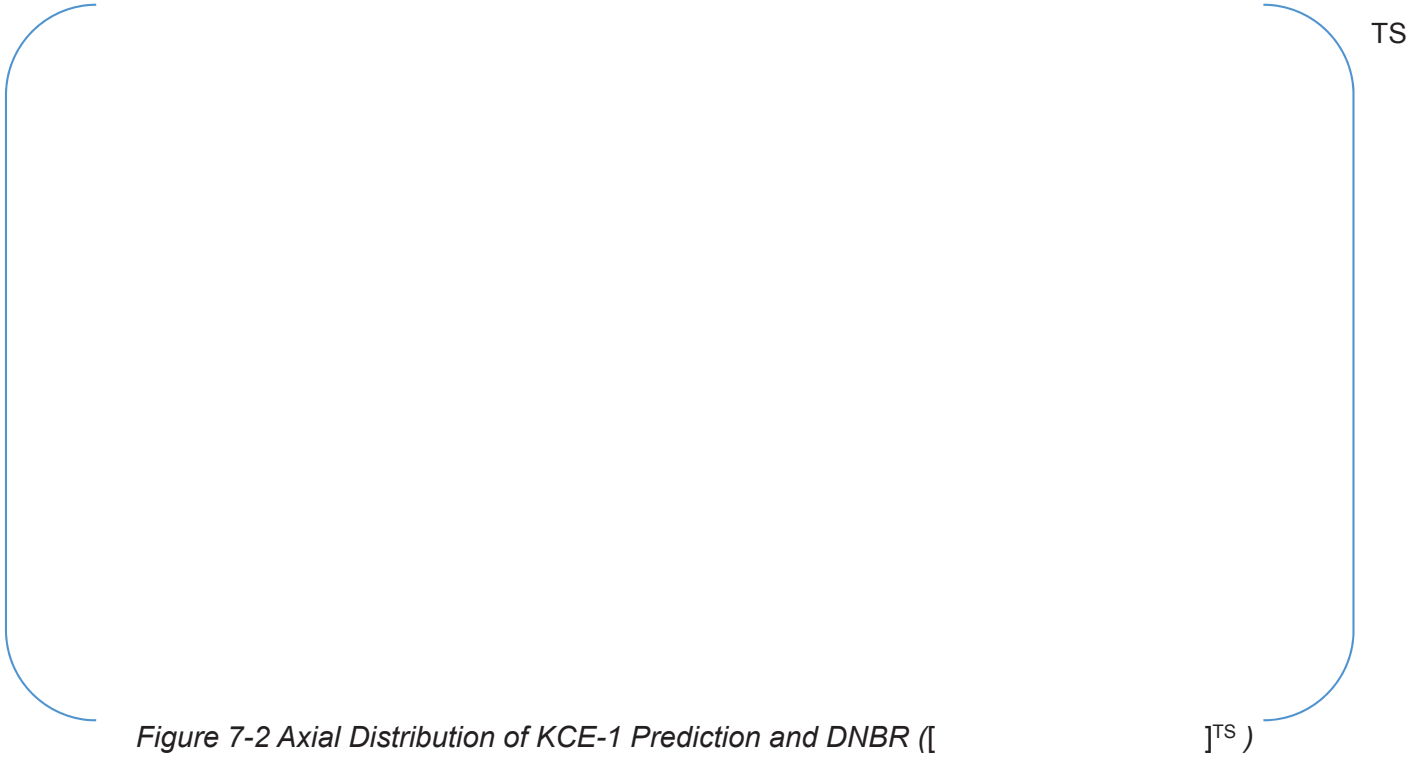


Figure 7-2 Axial Distribution of KCE-1 Prediction and DNBR ( [ ]^TS )



*Figure 7-3 Distribution of M/P (M/P Trend) versus System Pressure for Application Database*



*Figure 7-4 Distribution of M/P (M/P Trend) versus Local Mass Flux for Application Database*



TS

*Figure 7-5 Distribution of M/P (M/P Trend) versus Local Quality for Application Database*



TS

*Figure 7-6 KCE-1 Prediction versus Measured CHF for Application Database*

**Impact on DCD**

N/A

**Impact on PRA**

N/A

**Impact on Technical Specification**

N/A

**Impact on Technical/Topical/Environmental Report**

Topical Report APR1400-F-C-TR-12002-NP will be revised as indicated on the attached markups.

- Document Mark-up Cover Sheet : 1 page
- Mark-up for Q7 of RAI 3-7443 : 36 pages

※ Remark: Minor formatting, such as numbering figures, tables and references, etc., will be cleaned up before finalizing the topical report.

# Document Mark-up Cover Sheet

1. **Project ID:** *APR1400 NRC DC*
2. **Type of Corresponding Document:**  
 DCD     Topical Report     Technical Report     Other(s) \_\_\_\_\_
3. **Title of Corresponding Document:** *KCE-1 CHF Correlation for PLUS7 Thermal Design  
(APR1400-F-C-TR-12002-NP)*
4. **RAI ID/Question ID:** *3-7443 / Q7*
5. **Page(s) attached:** *36 (Thirty Six)*

## 1. INTRODUCTION

The PLUS7 fuel has been developed with the advanced “R” mixing vane grid design<sup>(1)</sup>. The split mixing vanes attached to the top of the grid strap improve the heat transfer between the coolant and fuel rods and increase the thermal margin. To verify the thermal performance of the PLUS7 fuel, critical heat flux (CHF) tests were conducted at Columbia University’s Heat Transfer Research Facility (HTRF) in New York City, New York and the KCE-1 CHF correlation was developed by using the measured CHF data.

This report describes the test data analysis for the correlation development, its results, the CHF test facility and test procedure for the PLUS7 fuel including configurations of the test section.

A description of CHF tests supporting KCE-1 CHF correlation is described in Chapters 2 and 3. Chapter 4 describes the test data evaluation and development of the KCE-1 CHF correlation. The test data were evaluated by using Westinghouse thermal-hydraulic code, TORC<sup>(2),(3)</sup>. TORC code was used to calculate the local fluid condition for the CHF test sections. Chapter 5 summarizes the statistical analysis to determine the 95/95 DNBR limit and the results of verification and validation of the KCE-1 CHF correlation. Discussion on the correlation application to thermal design and safety analyses is described in Chapter 6.

The CHF test data and the statistical methods applied to the correlation development are described in the appendices.



, correlation database

- 7) Steps 4 ~ 6 were repeated until the correlation statistics were unchanged with update of the coefficients. Although there is a change in the minimum DNBR elevation for a small number of runs between previous and current runs, if the coefficient change results in essentially no change in the final statistics, the iteration process was completed and the coefficients from the previous run were considered the final.

The data rejected during the correlation development process from the entire [ ]<sup>TS</sup> test data are listed in Table A-2 of APPENDIX A.

The final coefficients determined and the applicable ranges of parameters for the KCE-1 CHF correlation are presented in Table 4-4. Corresponding ~~data base~~ of KCE-1 CHF correlation is given in Table A-3 of APPENDIX A.

development database

**Table 4-4 KCE-1 CHF Correlation Coefficients and Applicable Ranges of Parameters**

- $DNBR = \frac{q''_{KCE-1}}{q''_{measured}}$

INSERT

- $q''_{KCE-1} = q''_{KCE-1,U} / F_C$

- Functional Formula of KCE-1 CHF Correlation

$$q''_{CHF} = \frac{B_1 (d / d_m)^{B_2} [(B_3 + B_4 P)(G / 10^6)^{(B_5 + B_6 P)} - (G / 10^6) \chi h_{fg}]}{(G / 10^6)^{(B_7 P + B_8 (G / 10^6))}} \left[ \frac{1}{F_C} \right]$$

DELETE

$q''_{KCE-1,U}$

where,  $q''_{CHF,U}$  Critical Heat Flux, MBtu/hr-ft<sup>2</sup>

INSERT

$q''_{KCE-1,U}$  Predicted CHF by KCE-1 correlation for uniform axial power distribution, MBtu/hr-ft<sup>2</sup>

$q''_{measured}$  Actual measured CHF, MBtu/hr-ft<sup>2</sup>

$PP$  Pressure, psia

$dd$  Equivalent heated diameter of subchannel of interest, inch

$d_m d$  Equivalent heated diameter of matrix subchannel, inch

$GG$  Local mass flux, lbm/hr-ft<sup>2</sup>

$\chi \chi$  Local quality

$h_{fg} h$  Latent heat of vaporization, Btu/lbm.

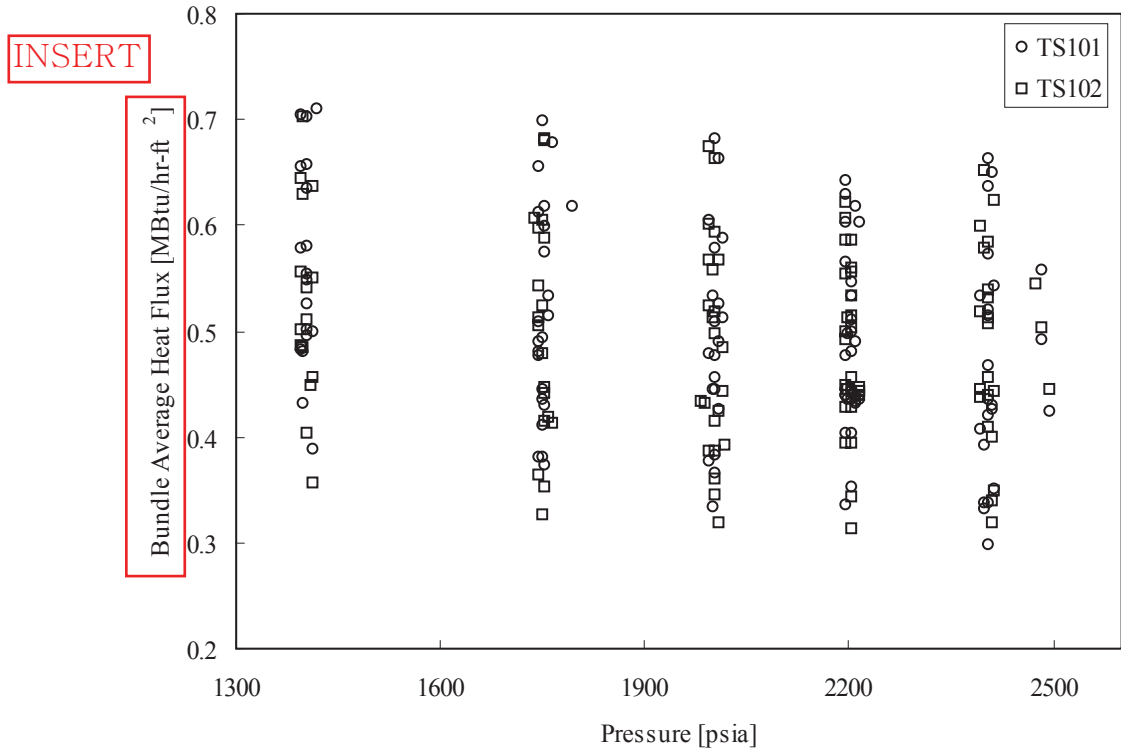
$F_C F$  Tong's non-uniform axial power distribution correction factor.

- KCE-1 CHF Correlation Coefficients

B <sub>1</sub>	( ) <sup>TS</sup>	B <sub>5</sub>	( ) <sup>TS</sup>
B <sub>2</sub>		B <sub>6</sub>	
B <sub>3</sub>		B <sub>7</sub>	
B <sub>4</sub>		B <sub>8</sub>	

- Applicable Ranges of Parameters for KCE-1 CHF Correlation

Parameter	British Unit	SI Unit
System Pressure	1395 ~ 2415 psia	9.62 ~ 16.65 MPa
Local Mass Flux	0.85 ~ 3.15 Mlbm/hr-ft <sup>2</sup>	1153 ~ 4272 kg/s-m <sup>2</sup>
Local Quality	-0.150 ~ 0.275	



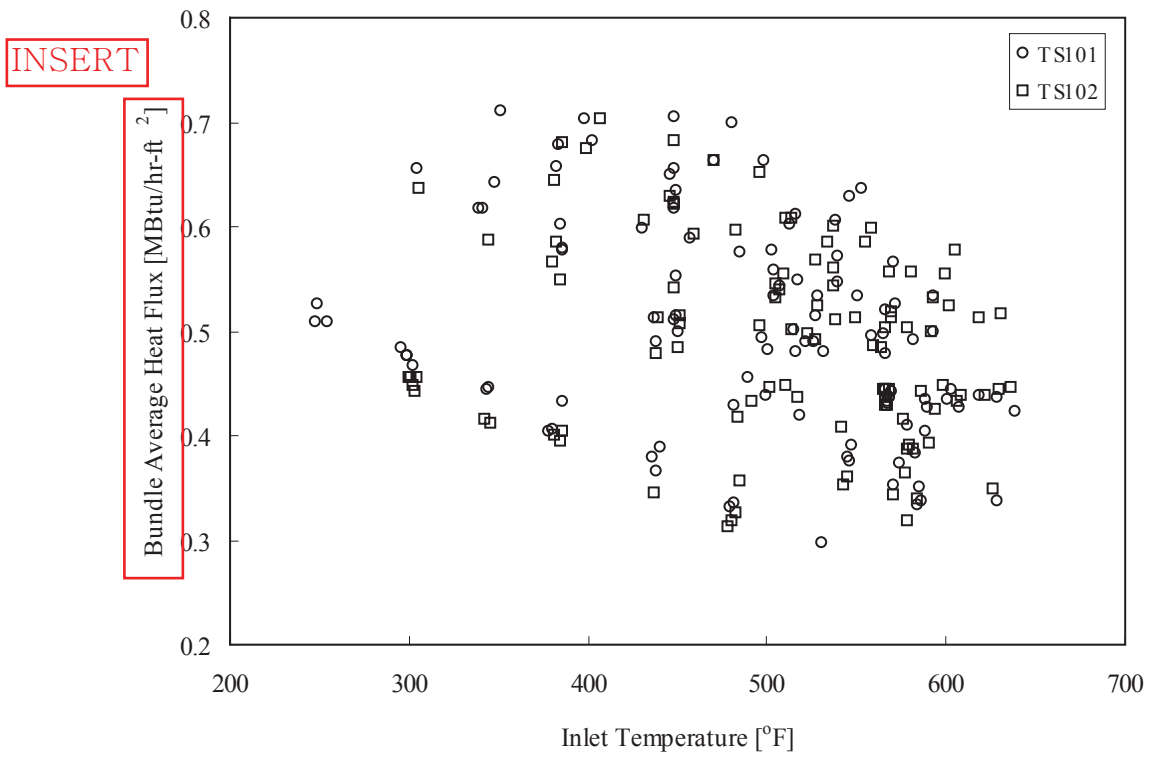


Figure 4-2 Inlet Temperature versus Average Heat Flux of Test Section

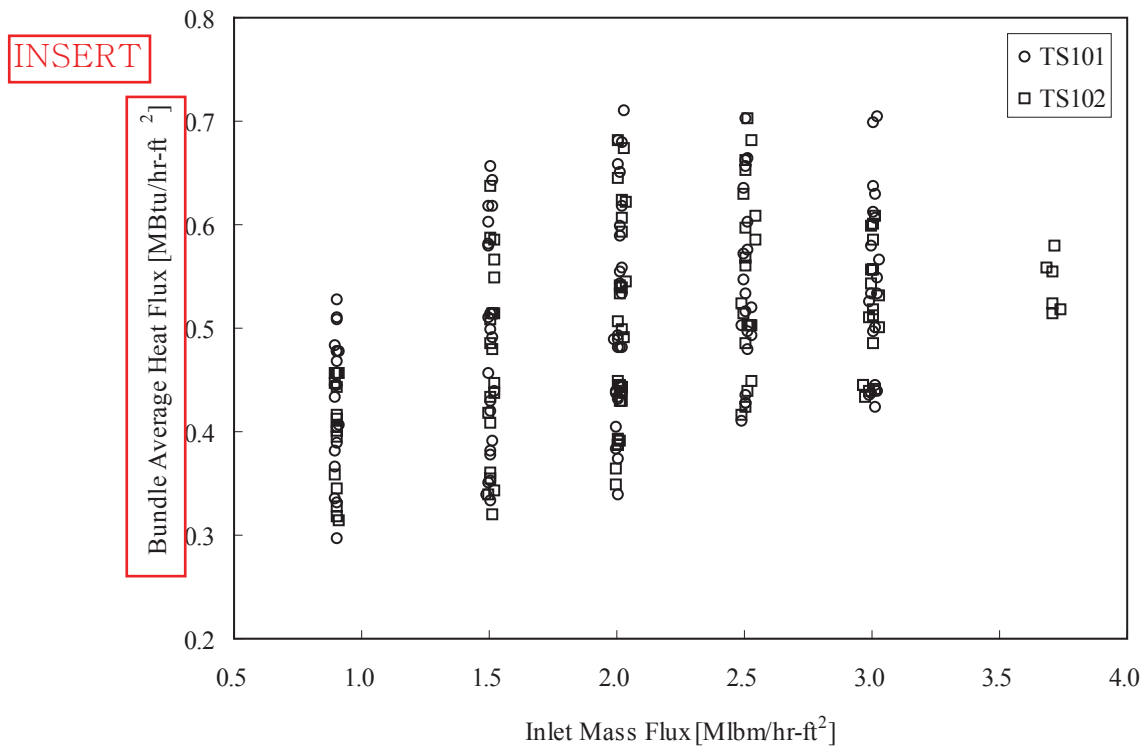


Figure 4-3 Inlet Mass Flux versus Average Heat Flux of Test Section

**5. CORRELATION DNBR LIMIT**

DEVELOPMENT DATABASE

This chapter describes the process for determining the 95/95 DNBR limit (DNBR limit with a 95% probability and a 95% confidence interval) of the KCE-1 CHF correlation developed in Chapter 4 and the statistical tests applied to the process.

**5.1 STATISTICAL ANALYSIS FOR DATA BASE**

for development database

To determine the 95/95 correlation DNBR limit, each data group used for the correlation development must be checked whether these groups could be pooled. For this purpose, a normality test and homogeneity tests for variances and means were performed. The brief description of these statistical tests is provided in sections B.2 and B.3 of APPENDIX B.

The normality test was performed using the D' test and the test results are provided in Table 5-1.

	TS
	TS
	TS

**5.2 ESTABLISHMENT OF CORRELATION DNBR LIMIT**

[ ] →

APPENDIX B.

according to the method described in section B.4 of

TS

	TS
--	----

Number of Data	$\bar{x}_{(M/P)}$	$S_{(M/P)}$	Correlation DNBR Limit (95/95 DNBR Limit)
225	0.9866	0.05304	1.124

### 5.3 VALIDATION AND VERIFICATION

the conservatism of

The validities of the local condition extraction method, which was used to generate the test data groups for the correlation development, and the 95/95 DNBR limit were verified as follows.

#### 5.3.1 Validity for Local Fluid Condition Extraction

The validity of the method for extracting the local fluid conditions, described in section 4.2, was verified via comparison of the M/P statistics between the cases with and without the assumption of [ ]. For the case without the assumption, [ ]<sup>TS</sup> was considered where calculated DNBR was the minimum regardless of [ ]<sup>TS</sup>.

As shown in Table 5-4, the former (with the assumption) led to more conservative results than the latter (without assumption) with respect to the 95/95 DNBR limit. Hence, the assumption for extracting the local fluid conditions applied to develop the KCE-1 CHF correlation is valid.

#### 5.3.2 Graphical Test for Correlation DNBR Limit

for development database

After the determination of the 95/95 DNBR limit for the correlation, scatter plots were then generated for all of the variables in the correlation to examine the correlation for trends or regions of non-conservatism. The Measured-to-Predicted CHF ratio (M/P) was plotted as a function of fluid parameters such as pressure, local mass flux, local quality and geometric parameter (equivalent heated diameter ratio,  $d/d_m$ ). The 95/95 DNBR limit ( $DNBR_{95}$ ) is also shown on these plots to show the number of tests points that fall below the limit and the location of those points.

Figure 5-2 shows the predicted and measured values for each test point. The M/Ps of all test data were plotted for system pressure, local mass flux, local quality and equivalent heated diameter ratio in Figure 5-3 through Figure 5-6, respectively. When the lines of each figure corresponding to the correlation DNBR limit are compared with those M/Ps, any adverse trend is not observed against them.

The numbers of data out of 95/95 DNBR limit are [ ]<sup>TS</sup> for test sections TS101 and TS102, respectively, which correspond to less than [ ]<sup>TS</sup> of the total number of data for each group.

(development database)

for development database

#### 5.3.3 Evaluation of Prediction Performance for Axial Location of CHF

To evaluate the accuracy of the KCE-1 CHF correlation in predicting the axial location (or elevation) of indicated CHF, the actual indicated CHF elevation were compared with the elevations of the minimum DNBR predicted by the KCE-1 CHF correlation. As shown in Figure 5-7, approximately [ ]<sup>TS</sup> of the entire test data are included within [ ]<sup>TS</sup> of the heated length with respect to the indicated CHF elevation. Thus the prediction performance for the elevation of CHF is acceptable.

based on Application Database

#### 5.3.4 Evaluation for Conservatism of Non-Uniform Axial Power Distribution Correction Factor Application

During the KCE-1 CHF correlation development process, the CHF test data for the non-uniform axial power distribution were not [ ]<sup>TS</sup>. However, the non-uniform axial power distribution correction factor (Tong factor  $F_C$ ) should be applied to the actual design calculation. Therefore, the conservatism of the correlation could be

development, application database

evaluated by comparing M/P statistics of the database and the results with application of Tong factor  $F_c$  [ ]<sup>TS</sup>.

The average M/P value with [ ]<sup>TS</sup>  
 [ ]<sup>TS</sup>  
 [ ]<sup>TS</sup>, as given in Table 5-5.

This proves that the KCE-1 CHF correlation, which was developed under the assumption of the measured CHF for the non-uniform axial power distribution as that for the [ ]<sup>TS</sup>, has conservatism more than [ ]<sup>TS</sup> in the database and/or more than [ ]<sup>TS</sup> in actual design application, respectively.

[ ]<sup>TS</sup> for 95/95 DNBR limit

[ ]<sup>TS</sup> for DNBR

The average M/P value is [ ]<sup>TS</sup>, as given in Table 5-5.

For the application database, [ ]<sup>TS</sup>.

[ ]<sup>TS</sup>. Corresponding application database is given in Table A-5 of APPENDIX A with excluded data in Table A-4 of APPENDIX A. Frequency diagram of M/P for the application database is similar to that for the development database, as shown in Figure 5-8.

Graphical tests, corresponding Figures 5-2 to 5-6 for the development database, show no adverse trend [ ]<sup>TS</sup> current 95/95 DNBR limit (1.124 based on development database), as shown in Figures 5-9 to 5-13 for the application database. No adverse trend shows with respect to Tong factor  $F_c$  as shown in Figure 5-14 for the application database.

Prediction performance for axial location of CHF, corresponding to Figure 5-7 for the development database, shows that similar results as shown in Figure 5-15 for the application database.

(Development Database)

Table 5-1 D' Normality Test

TS	<i>n</i>	$\bar{x}_{(M/P)}$	$S_{(M/P)}$	S	T	D' Calculated	D' P=0.025	D' P=0.975	Test
101									
102									
All									

(Development Database)

Table 5-2 Statistical Tests for Each Data Group

- KCE-1 CHF Correlation Data Groups

Test Section	Bundle Array	Rod Diam. [ in ]	Heated Length [ in ]	Grid Spacing [ in ]	Guide Thimble	Axial Power Distribution	$n$	$\bar{x}_{(M/P)}$	$S_{(M/P)}$
101	6x6	0.374	150.0	15.7	Yes	1.475 Cosine			
102	6x6	0.374	150.0	15.7	No	1.475 Cosine			
All									

- Bartlett Test Results

TS	$n$	$\bar{x}_{(M/P)}$	$S_{(M/P)}$	$K$	$M/C$	$\chi^2_{0.95}$	Test
101							
102							
All							

- Unpaired  $t$  Test Results

TS	$n$	$\bar{x}_{(M/P)}$	$S_{(M/P)}$	$\bar{x}_1 - \bar{x}_2$	$s_0$	$t$	$t_{0.025,319}$	Test
101								
102								
All								

- Wilcoxon-Mann-Whitney Test Results

TS	$N$	$W$	$\mu_{W_1}$	$\sigma_{W_1}^2$	$z$	$z_{0.95}$	Test
101							
102							
All							

**Table 5-3 95/95 DNBR Limits for Each Data Group**

(Development Database)

- 95/95 DNBR Limit calculated with [ ]<sup>TS</sup>

TS	$\bar{x}_{(M/P)}$	$S_{(M/P)}$	$n$	$K$	95/95 DNBR Limit (DNBR <sub>95</sub> )
[ ] <sup>TS</sup>					

- [ ]<sup>TS</sup> 95/95 DNBR Limit

TS	$\gamma$	$P$	$n$	$m^*$	Value	95/95 DNBR Limit (DNBR <sub>95</sub> )
[ ] <sup>TS</sup>						

\* Ranking of Data

Run	M/P	Rank( $m$ )
[ ] <sup>TS</sup>		1
		2
		3
		4
		5
		6
		7
		8

**Table 5-4 KCE-1 CHF Correlation Statistical Data per Local Fluid Condition**

**Extraction Method**

(Development Database)

- [ ]<sup>TS</sup> (minimum DNBR per each [ ]<sup>TS</sup> )

TS	<i>n</i>	$\bar{x}_{(M/P)}$	$S_{(M/P)}$	95/95 DNBR Limit (DNBR <sub>95</sub> )
101	[ ] <sup>TS</sup>			
102				
All				

- Regardless of [ ]<sup>TS</sup> (minimum DNBR [ ]<sup>TS</sup> )

TS	<i>n</i>	$\bar{x}_{(M/P)}$	$S_{(M/P)}$	95/95 DNBR Limit (DNBR <sub>95</sub> )
101	[ ] <sup>TS</sup>			
102				
All				

based on Application Database

**Table 5-5 KCE-1 CHF Correlation Conservatism with Non-Uniform Axial Power Distribution Correction Factor Application**

• Within Applicable Ranges of Parameters

Case	$n$	$\bar{x}_{(M/P)}$	$S_{(M/P)}$

} TS

} TS

**DELETE**

**INSERT**

TS	$n$	$\bar{x}_{(M/P)}$	$S_{(M/P)}$	Min. M/P	95/95 DNBR	Remark
101						
102						
All						

} TS

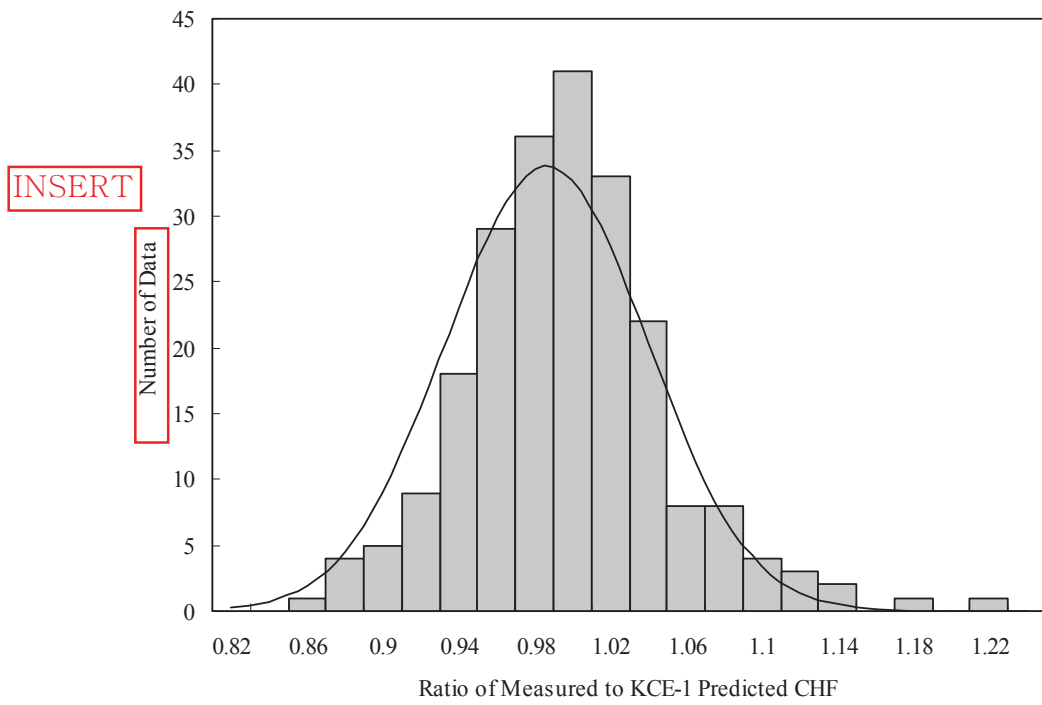


Figure 5-1 Frequency Diagram of M/P for Test Section TS101

(Development Database)

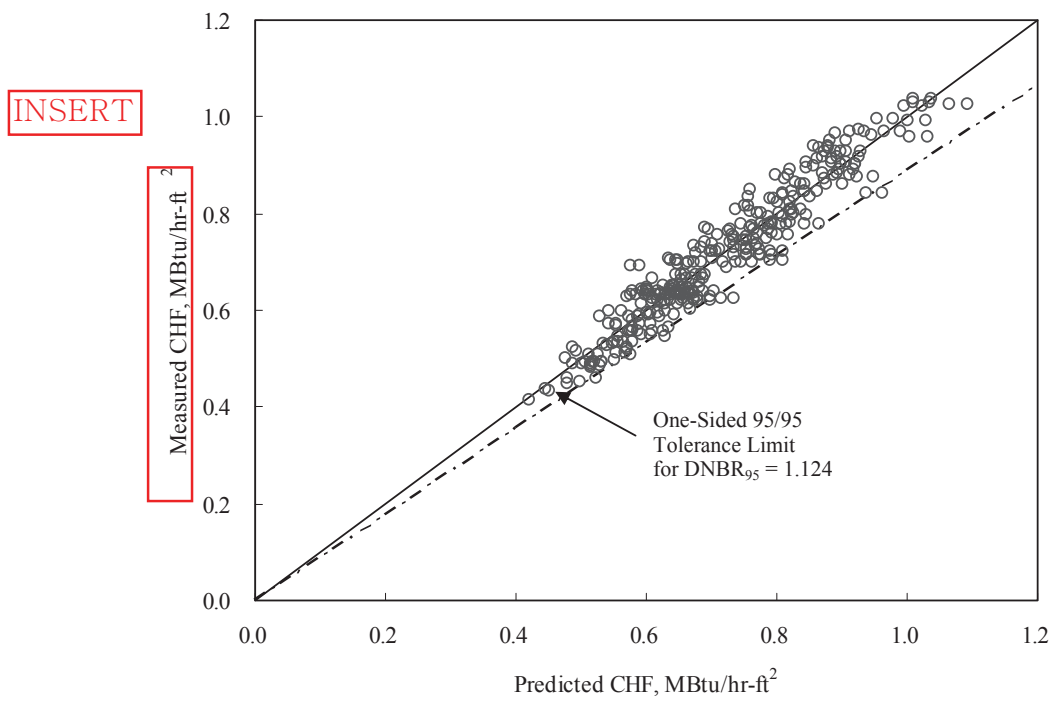


Figure 5-2 KCE-1 CHF Correlation Predicted CHF versus Measured CHF

(Development Database)

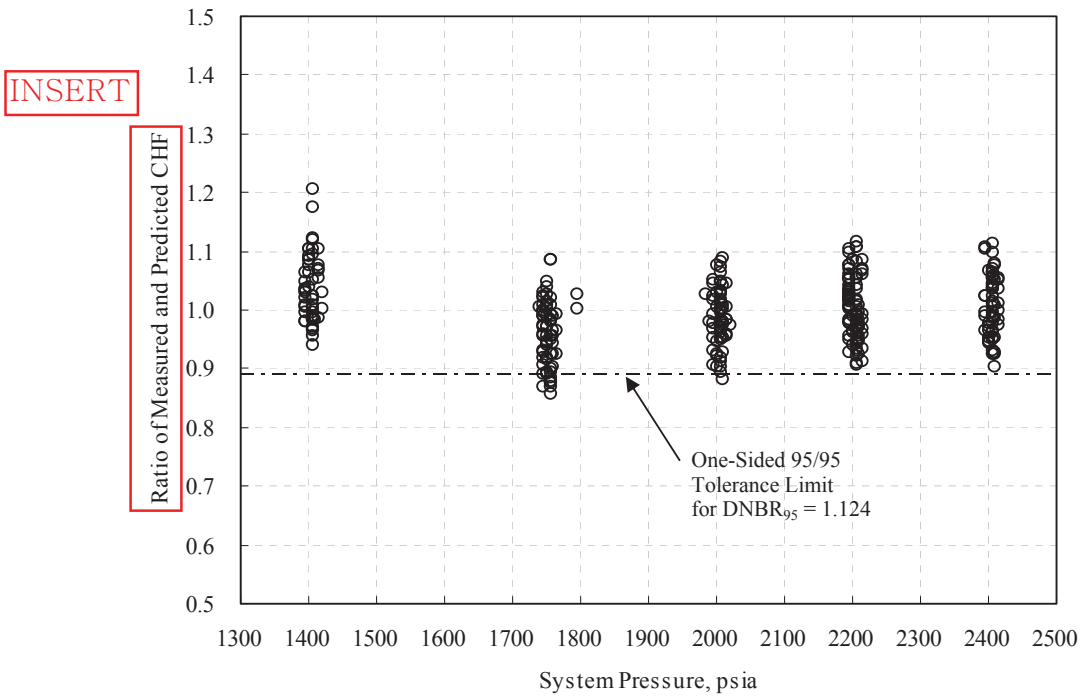


Figure 5-3 Distribution of M/P versus System Pressure

(Development Database)

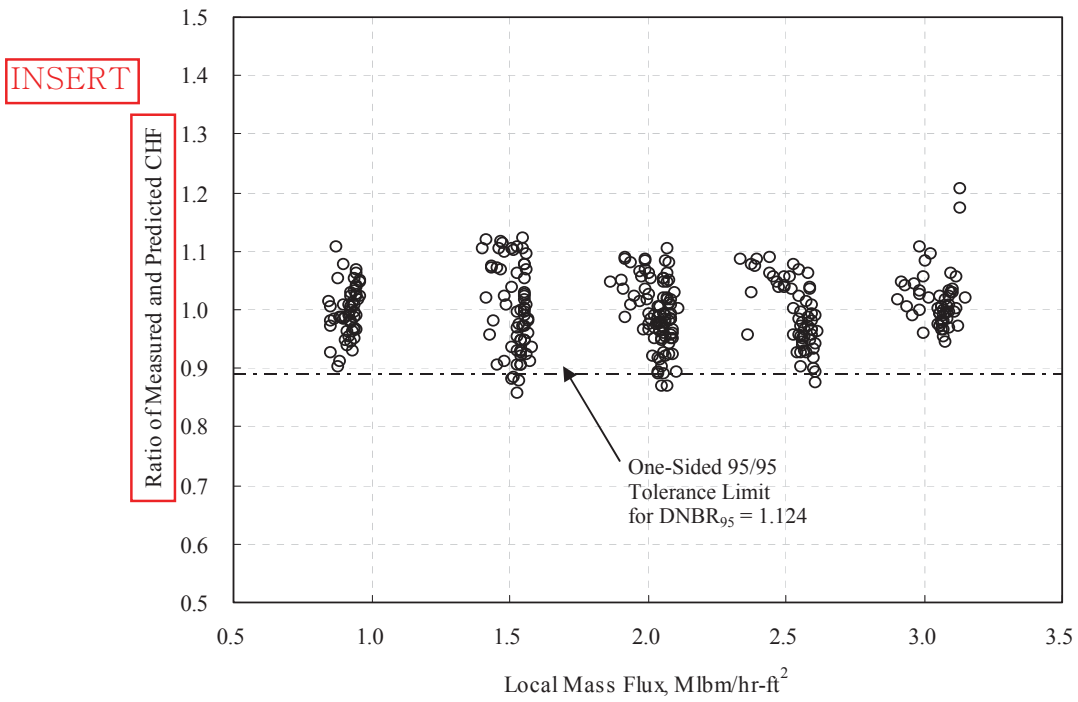


Figure 5-4 Distribution of M/P versus Local Mass Flux

(Development Database)

INSERT

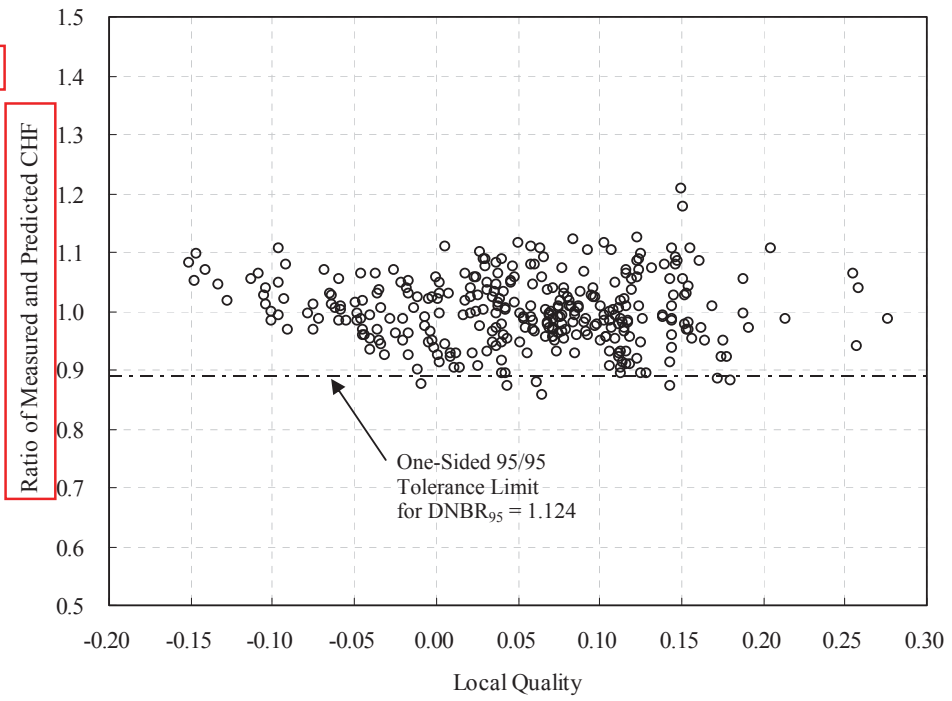


Figure 5-5 Distribution of M/P versus Local Quality

(Development Database)

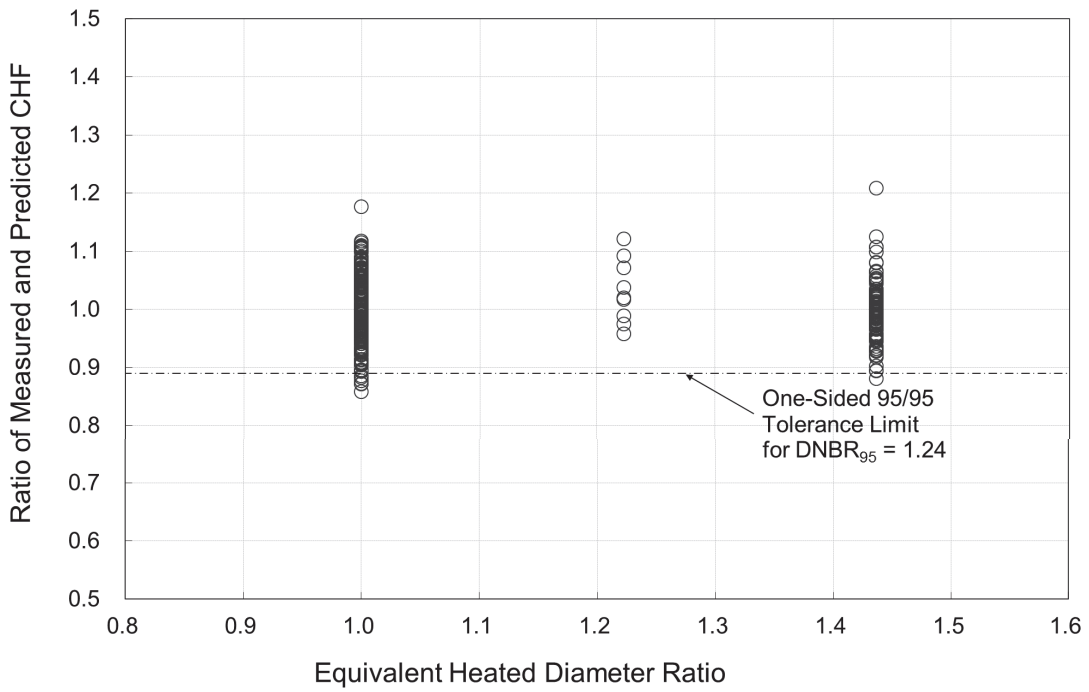
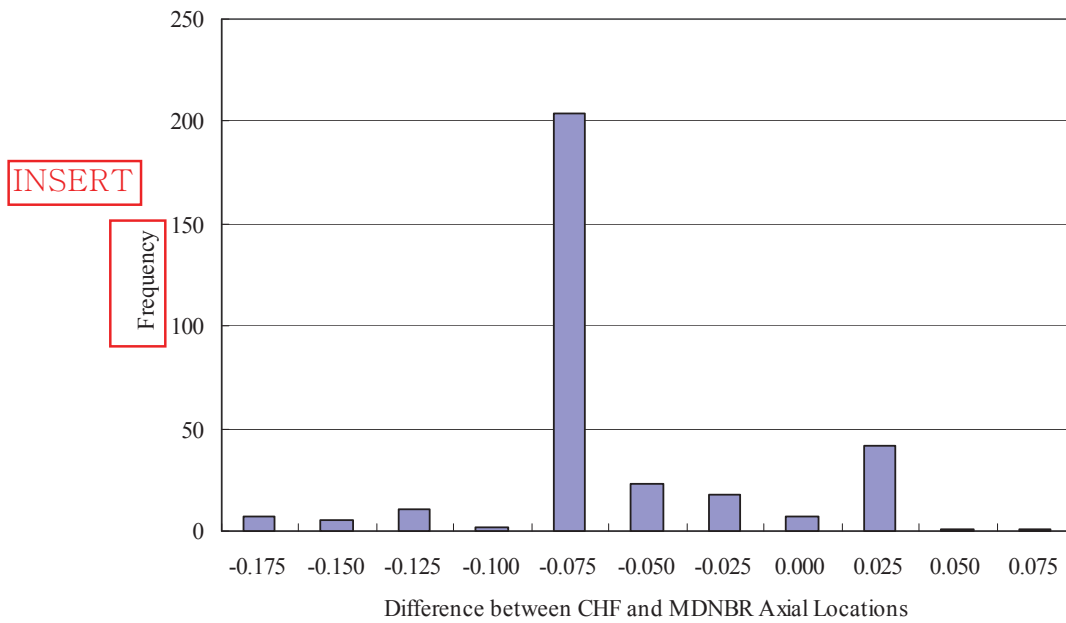


Figure 5-6 Distribution of M/P versus Equivalent Heated Diameter Ratio

(Development Database)





$$Difference = \frac{(MDNBR \text{ Axial Location}) - (CHF \text{ Axial Location})}{Heated \text{ Length}}$$

**Figure 5-7 Prediction Accuracy of KCE-1 CHF Correlation for CHF Axial Location**

(Development Database)

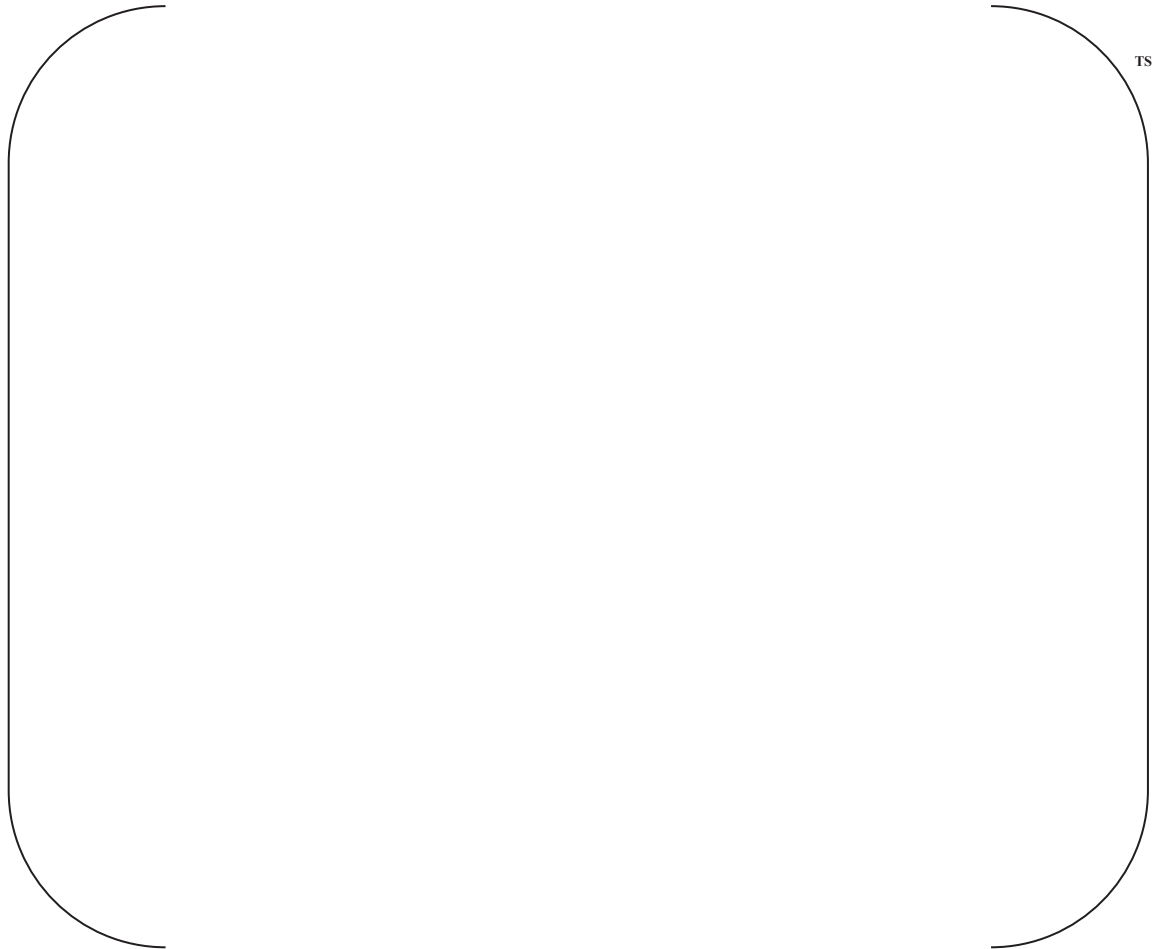


**Figure 5-8 Frequency Diagram of M/P for Test Section TS101 for Application Database**



**Figure 5-9 KCE-1 CHF Correlation Predicted CHF versus Measured CHF for Application Database**

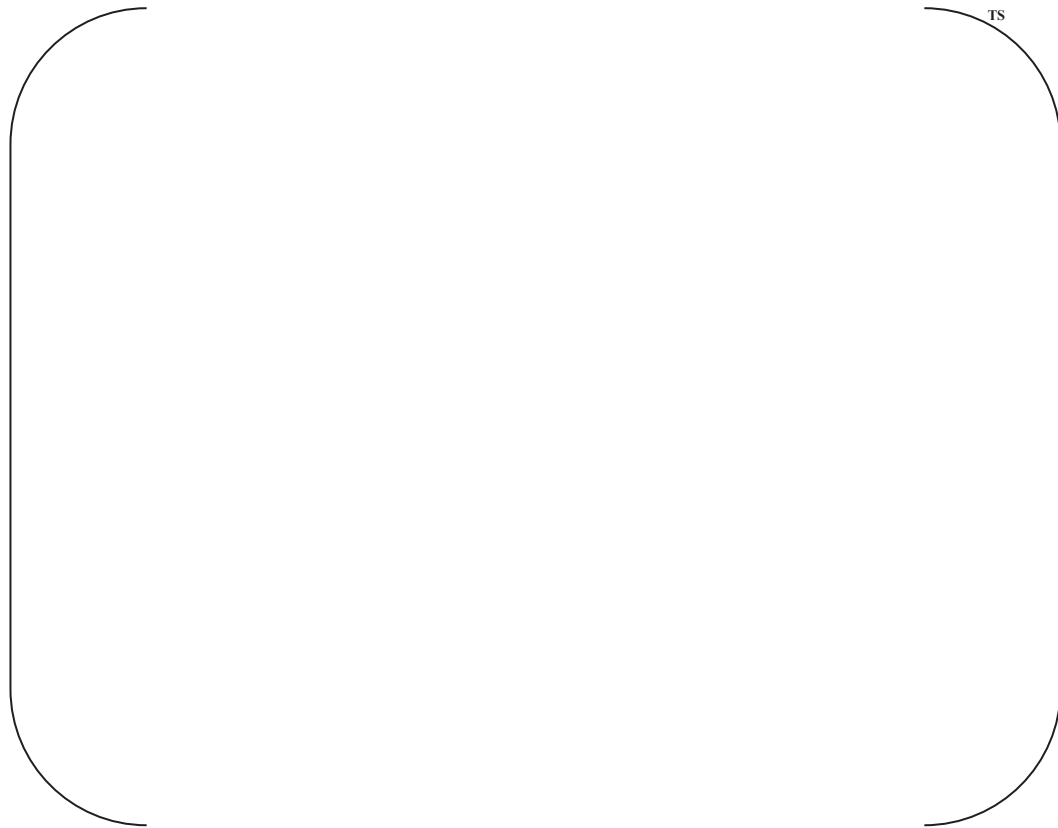


**Figure 5-10 Distribution of M/P versus System Pressure for Application Database**



**Figure 5-11 Distribution of M/P versus Local Mass Flux for Application Database**



**Figure 5-12 Distribution of M/P versus Local Quality for Application Database**

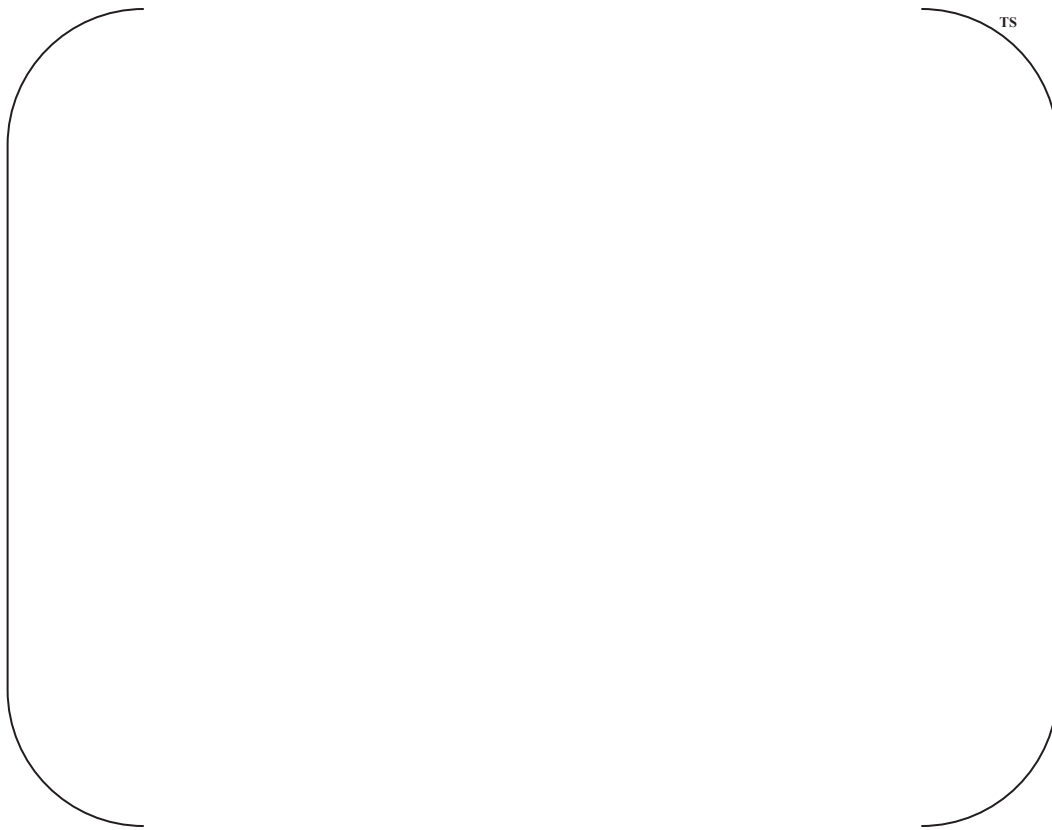


**Figure 5-13 Distribution of M/P versus Equivalent Heated Diameter Ratio for Application Database**

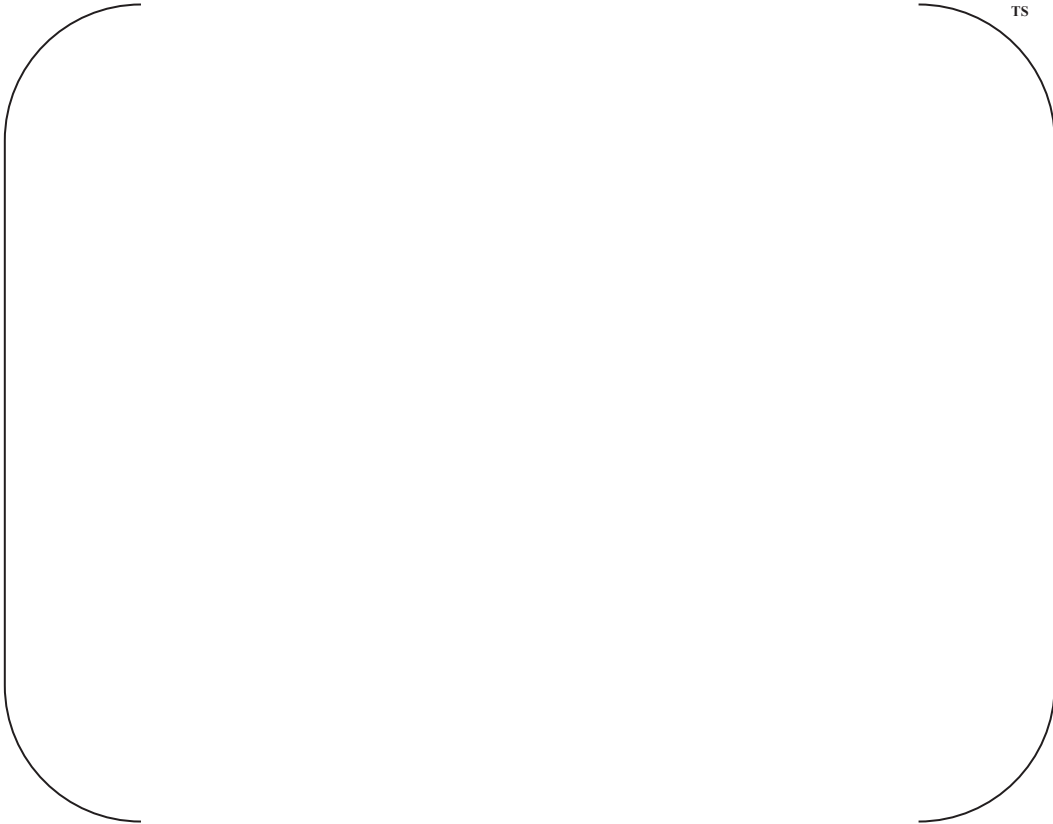


**Figure 5-14 Distribution of M/P versus Tong Factor for Application Database**



$$\text{Difference} = \frac{(\text{MDNBR Axial Location}) - (\text{CHF Axial Location})}{\text{Heated Length}}$$

**Figure 5-15 Prediction Accuracy of KCE-1 CHF Correlation for CHF Axial Location for Application Database**

/APPLICATION

**APPENDIX A. DATA FOR KCE-1 CHF CORRELATION DEVELOPMENT**

The raw test data, [ ]<sup>TS</sup> in total, collected from the PLUS7 fuel CHF tests are listed in Table A-1. The [ ]<sup>TS</sup> local fluid conditions excluded during the correlation development process from the local fluid conditions for each test data calculated by the TORC code are listed along with the reason for exclusion in Table A-2. Finally, the KCE-1 CHF correlation database, [ ]<sup>TS</sup> in total, is presented in Table A-3.

development

Acronyms presented in the subsequent tables:

TS	:	test section number
RUN	:	run number
PR	:	system pressure, <i>psia</i>
TIN	:	inlet temperature, °F
GIN	:	inlet mass flux (inlet mass velocity), <i>Mlbm/hr-ft<sup>2</sup></i>
BAP	:	bundle average power, <i>MW</i>
HFX	:	heat flux, <i>MBtu/hr-ft<sup>2</sup></i>
TC	:	primary CHF rod and thermocouple number (XX.x)*
CT	:	CHF subchannel type
M	:	matrix subchannel
C	:	guide thimble corner subchannel
S	:	guide thimble side subchannel
GL	:	local mass flux (local mass velocity), <i>Mlbm/hr-ft<sup>2</sup></i>
XL	:	local quality
DH	:	equivalent heated diameter of CHF subchannel, <i>in.</i>
DHM	:	equivalent heated diameter of matrix subchannel, <i>in.</i>
CHFM	:	measured CHF, <i>MBtu/hr-ft<sup>2</sup></i>
CHFP	:	KCE-1 correlation predicted CHF, <i>MBtu/hr-ft<sup>2</sup></i>

Application database of the KCE-1 CHF correlation, [ ]<sup>TS</sup>, is presented in Table A-5 with excluded data in Table A-4.

\* XX = Rod number, x = T/C number  
(See Figure 2-5 through Figure 2-7 and Figure 2-9.)

Fc : Tong factor  
HL : length from BOHL, *in.*  
CH : subchannel number  
hfg : latent heat of vaporization, *Btu/lbm*  
DNBR : departure from nucleate boiling ratio  
M/P : ratio of measured CHF to predicted CHF

**Table A-4 Data Excluded from Application Database**

TS	RUN	PR	CHFM	HL	GL	XL	CH.	hfg	Fc	DH	DHM	DNBR	M/P	Remark

**Table A-5 KCE-1 CHF Correlation Application Database (1/5)**

TS	RUN	PR	CHFM	HL	GL	XL	CH.	hfg	Fc	DH	DHM	DNBR	M/P	TS
----	-----	----	------	----	----	----	-----	-----	----	----	-----	------	-----	----

**Table A-5 KCE-1 CHF Correlation Application Database (2/5)**

TS	RUN	PR	CHFM	HL	GL	XL	CH.	hfg	Fc	DH	DHM	DNBR	M/P
----	-----	----	------	----	----	----	-----	-----	----	----	-----	------	-----

TS

**Table A-5 KCE-1 CHF Correlation Application Database (3/5)**

TS	RUN	PR	CHFM	HL	GL	XL	CH.	hfg	Fc	DH	DHM	DNBR	M/P
----	-----	----	------	----	----	----	-----	-----	----	----	-----	------	-----

--	--	--	--	--	--	--	--	--	--	--	--	--	--

**Table A-5 KCE-1 CHF Correlation Application Database (4/5)**

TS	RUN	PR	CHFM	HL	GL	XL	CH.	hfg	Fc	DH	DHM	DNBR	M/P
----	-----	----	------	----	----	----	-----	-----	----	----	-----	------	-----

--	--	--	--	--	--	--	--	--	--	--	--	--	--

**Table A-5 KCE-1 CHF Correlation Application Database (5/5)**

TS	RUN	PR	CHFM	HL	GL	XL	CH.	hfg	Fc	DH	DHM	DNBR	M/P	TS
----	-----	----	------	----	----	----	-----	-----	----	----	-----	------	-----	----

---

---

## RESPONSE TO REQUEST FOR ADDITIONAL INFORMATION

### APR1400 Topical Reports

Korea Electric Power Corporation / Korea Hydro & Nuclear Power Co., LTD

Docket No. 52-046 (PROJ 0782)

**RAI No.:** 3-7443 Question 9

**SRP Section:** N/A

**Application Section:** KCE-1 Critical Heat Flux Correlation for PLUS7 Thermal Design  
(APR1400-F-C-TR-12002-NP, Rev.0)

**Date of RAI Issued:** 03/25/2014

**Response Date:** 10/09/2015

---

### Question 9

Detailed investigation of the test data, conducted by the staff, has revealed a potentially nonconservative subregion at pressures near 1750 psia, qualities near 0.1, and local mass fluxes near 2 Mlbm/hr-ft<sup>2</sup>. This subregion contains a higher than expected number of M/P values which were below the 95/95 statistic than can be explained by random chance. Provide justification for the use of the KCE-1 correlation in this subregion, and the surrounding empty subregions.

### Response

*The number of M/P values below the 95/95 DNBR limit in pressure near 1750 psia was based on the correlation development database [ ]<sup>TS</sup>. The number of M/P values below the 95/95 DNBR limit is reduced when [ ]<sup>TS</sup> are considered as shown in the lower part of Table 5-4 of the topical report (ToR). Furthermore, when Fc is incorporated into the KCE-1 CHF predictions, the M/P versus pressure plot in Figure 9-1 (attached) shows no M/P data point below the M/P value associated with the 95/95 DNBR limit of 1.124, and no obviously non-conservative subregion with respect to pressure.*

*It is certainly conservative to limit the applicable pressure range of KCE-1 above 1700 psia.*



*Figure 9-1 M/P versus Pressure with Tong factor Fc*

**Impact on DCD**

N/A

**Impact on PRA**

N/A

**Impact on Technical Specification**

N/A

**Impact on Technical/Topical/Environmental Report**

N/A

## RESPONSE TO REQUEST FOR ADDITIONAL INFORMATION

### APR1400 Topical Reports

Korea Electric Power Corporation / Korea Hydro & Nuclear Power Co., LTD

Docket No. 52-046 (PROJ 0782)

**RAI No.:** 3-7443 Question 17

**SRP Section:** N/A

**Application Section:** KCE-1 Critical Heat Flux Correlation for PLUS7 Thermal Design  
(APR1400-F-C-TR-12002-NP, Rev.0)

**Date of RAI Issued:** 03/25/2014

**Response Date:** 10/09/2015

### Question 17

In the development of a correlation, the potential for overfitting exists in which the correlation can predict the data used to develop the correlation well, but lacks in predictive capability on other data not used in the development of the correlation. It is not clear from the topical report whether some test data were initially excluded from the KCE-1 correlation coefficient generation and were used later as additional points for independent correlation validation. The applicant should address the potential for overfitting in the KCE-1 correlation.

The applicant should also resolve the inconsistencies among the number of data points reported in various parts of the report. During the PLUS7 fuel CHF tests, [ ]<sup>TS</sup> test data for the thimble subchannel test section Test Section 101 and [ ]<sup>TS</sup> data for the matrix subchannel test section Test Section 102 were collected, respectively. The [ ]<sup>TS</sup> test data points are listed in Table A-1 of APPENDIX A. Table A-2 lists [ ]<sup>TS</sup> test data points that were rejected during the correlation development process. The applicant needs to explain how this data processing has led to an overall KCE-1 CHF correlation database of [ ]<sup>TS</sup>.”

The two hundred and twenty-five (225) data points cited in the abstract as well as in Section 5.2 of the report are also confusing.

Also provide clear descriptions identifying the following:

- (A) The total number of test points for each test
- (B) The total number of test points which were used for generating the coefficients of the correlation for each test.

- (C) The total number of test points which were excluded from calculating the coefficients of the correlation for each test.
- (D) The validation statistics (similar to that provided in the first table of Table 5-4) for both (B) and (C) above. Statistics should be provided for each test.

### Response

No test data were initially separated from the database used for the KCE-1 coefficient generation as the validation data set. However, any potential for overfitting the KCE-1 coefficients is low during the KCE-1 CHF correlation development because;

- Four (4) variables for flow condition, pressure, local mass flux, local quality, and latent heat of vaporization are the minimum essential basic variables to characterize CHF phenomena in flowing water. One (1) variable, equivalent heated diameter ratio, is used to characterize the effect of the unheated guide tube on CHF.
- Corresponding eight (8) coefficients represented by five (5) basic variables and a combination of them make a simple functional formula.
- The functional form and the variables in the KCE-1 correlation are not new, but are the same as the CE-1 correlation (Reference: CENPD-162-P-A, reference 4 of topical report). CE-1 correlation is a proven technology.
- [

]TS due to the higher CHF performance in PLUS7 fuel with mixing vanes (KCE-1 correlation prediction) than that of Guardian fuel without mixing vanes (CE-1 correlation prediction).

The prediction trends of both correlations are compared in Figures 17-1 to 17-3 for quality, pressure, and mass flux, respectively. As expected, the general prediction behavior of the KCE-1 correlation is comparable to that of the CE-1 correlation. Predicted CHF decreased as quality and pressure increased, as shown in Figures 17-1 and 17-2, respectively. Predicted CHF increased as mass flux increased, as shown in Figure 17-3. Behaviors of the predicted CHF of KCE-1 correlation show consistency with the measured CHF. Behavior of measured CHF was discussed in the response to Question 11 of RAI 3-7443.

Results of an impact assessment of the data partitioning for correlation development and validation show [ ]TS above the KCE-1 limit of 1.124 based on the development database [ ]TS. Any potential effect of coefficient overfitting without a validation data set is much less than the conservatism of [ ]TS in the KCE-1 correlation with the Tong factor  $F_c$ . The detailed impact assessment is attached.

A clarification on the number of data points in the KCE-1 data tables is provided below.

- (A) The total number of test points for each test:

- [ ]TS test points for Test Section TS101 ([ ]TS)  
Some test points of the thimble test bundle (TS101) included DNBR and local fluid

conditions from [ ]<sup>TS</sup>, as indicated in the topical report.

- [ ]<sup>TS</sup> test points for Test Section TS102

and

- [ ]<sup>TS</sup> test points: listed in Table A-1 of the topical report
- [ ]<sup>TS</sup> test points: listed in Table 10-1 of the response to RAI 3-7443 Question 10.

(B) The total number of test points that were used for generating the coefficients of the correlation for each test:

- [ ]<sup>TS</sup> test points for Test Section TS101 ( [ ]<sup>TS</sup> )
- [ ]<sup>TS</sup> test points for Test Section TS102

(C) The total number of test points that were excluded when calculating the coefficients of the correlation for each test:

- [ ]<sup>TS</sup> test points for Test Section TS101 ( [ ]<sup>TS</sup> ): excluded due to [ ]<sup>TS</sup>
- [ ]<sup>TS</sup> test points for Test Section TS102: excluded due to [ ]<sup>TS</sup>
- Excluded data listed in Table A-2 of the topical report per the types of subchannel. Out of [ ]<sup>TS</sup> listed in Table A-2 of the topical report, [ ]<sup>TS</sup>.

(D) The validation statistics (similar to that provided in the first table of Table 5-4) for both (B) and (C) above. Statistics should be provided for each test:

- The corresponding M/P statistics for the above (B) and (C) are given in Tables 17-1 and 17-2, respectively.
- There was no validation data set separated from the correlation development database.
- The KCE-1 M/P statistics with the Tong factor  $F_c$  incorporated, consistent with the intended applications in the safety analysis, are given in Table below (replica of Table in the response to Question 7 of RAI 3-7443).



### **Assessments to Estimate the Potential for Overfitting**

Below is the detail of the assessment results for cross-validation to estimate the potential of overfitting.

- The assessments were performed on the KCE-1 CHF correlation based on the 5-fold method and the repetitive cross-validation by 1000 times with data splitting (80% for training and 20% for validation). To make apple-to-apple comparison, the same data used to KCE-1 development given in Table A-3 of the topical report are considered (with [ ]<sup>TS</sup>).

In the 5-fold cross-validation, the original sample is randomly partitioned into 5 equal sized subsamples. Of the 5 subsamples, a single subsample is retained as the validation data for testing the model, and the remaining 4(= 5-1) subsamples are used as training data. The cross-validation process is then repeated 5 times (the folds), with each of the 5 subsamples used exactly once as validation data.

In the repetitive cross-validation, determination of correlation coefficients based on each training data and assessment to the correlation to validation data had performed for each of 1000 randomly split training (80%) and validation (20%) data set.

The analyses were performed using a free software, R programming (available at <http://www.r-project.org/>).

- Before cross validation for various data splits was performed, the process using R programming was verified with 100% data for training (0% data for validation), the same as when the KCE-1 correlation was developed. Same values of the initial guess for correlation coefficients were assumed to all cases, as described in section 4.4 of the topical report. The Levenberg-Marquardt method was applied to non-linear regression analysis using R programming. The estimated coefficients and the M/P statistics of the correlation using the R programming process were very close to those of the original KCE-1 correlation, as given in Tables 17-3 and 17-4, respectively. Ranges of correlation variables, such as pressure, mass flux, and quality, were comparable to those of the KCE-1 correlation. Therefore, subsequent cross-validations were performed with the verified R programming process (with the same values of initial guess for the correlation coefficients as described above).
- Results of 5-folds : [ ]<sup>TS</sup>

M/P statistics of training data and validation data were similar for subset(case) of 5-folds, as given in Table 17-4. 95/95 DNBR values for each case were calculated using the relations given in Appendix B.4.1 of the topical report based on the results of normality and poolability tests for both training and validation data, as given in Table 17-5. Poolability tests were performed using the parametric method (F-test for variance and t-test for mean) benchmarked with the non-parametric method of Wilcoxon-Mann-Whitney test. [ ]

]<sup>TS</sup>. Therefore [  
]<sup>TS</sup>, worst case for each subset of 5-folds  
(maximum MAPE (mean absolute percent error) value for validation data). MAPE is  
a measure of the accuracy of a model defined by,

$$MAPE(\%) = \frac{1}{n} \sum_i^n \left| \frac{M_i - P_i}{M_i} \right|$$

where ;

- $n$  = number of data
- $M$  = measured value
- $P$  = predicted value

○ Results of repetitive Cross-Validation : [  
]<sup>TS</sup>

To avoid any coincidental bias due to sampling (data splitting), a repetitive cross-validation has performed for thousand times with each randomly split training data (80%) and validation (20%) data. That is, 1000 CHF correlations had developed and validated with CE-1 functional formula (and hence KCE-1 functional formula).

Table 17-6 shows M/P statistics for a thousand 80%/20% subgroups. Five classifications are categorized by the following meaning. "Training" means the data that are used in fitting CHF correlation's coefficients. "Validation" means the data that are not used in developing CHF correlation. [  
]

]<sup>TS</sup>. Figure 17-4 shows average M/P distribution of five classifications for Table 17-6. Average M/Ps for 4 classifications are well distributed. But, the average M/Ps for [  
]<sup>TS</sup> classification are separated around the [  
]<sup>TS</sup>.

Table 17-7 shows 95/95 DNBR statistics for thousand 80%/20% subgroups. The average 95/95 DNBR values are [  
]

]<sup>TS</sup>, is the most probable effect of data partitioning on 95/95 DNBR limit. Compared to current 95/95 DNBR limit, the effect is [  
]<sup>TS</sup>. The average of 95/95 DNBR of [  
]<sup>TS</sup> of five classifications. Even for the worst/rare-case, the effect is [  
]<sup>TS</sup>. The average 95/95 DNBR value of [  
]<sup>TS</sup>. Figure 17-5 shows 95/95 DNBR distribution of five classifications

for Table 17-7. However, 95/95 DNBR values for [ ]<sup>TS</sup> classification are distributed continuously, different from the average M/Ps distribution. The reason is that 95/95 DNBR value is determined by the combination of average M/P, its standard deviation and Owen's factor or rank.

Best representative 95/95 DNBR value can be derived based on the [ ]<sup>TS</sup> for the resulting distribution of 1000 95/95 DNBRs.[

] <sup>TS</sup> among 1000 cases.

When this tolerance based on [

] <sup>TS</sup> with respect to current 95/95 DNBR limit of 1.124.

Table 17-8 shows M/P statistics of [ ]<sup>TS</sup> out of one thousand 95/95 DNBRs. Average M/P and standard deviation for training data ([ ]<sup>TS</sup> data) are similar compared to all data of KCE-1 correlation in Table 5-4 of the topical report. [

] <sup>TS</sup>. Table 17-9 shows poolability check between training data and validation data of [ ]<sup>TS</sup> out of one thousand 95/95 DNBRs. Table 17-10 shows results of normality test using D'Agostino test. All passed. Table 17-11 shows range of variables for [ ]<sup>TS</sup> out of one thousand 95/95 DNBRs, training data and validation data. Variable ranges are similar between the training data and the validation data, and those of KCE-1 correlation (Section 7 of the topical report). [

] <sup>TS</sup>.

Data of [ ]<sup>TS</sup> are listed in Tables 17-12 and 17-13 for training and validation, respectively.

Table 17-1 M/P Statistics for (B)

Test Section	<i>n</i>	$\bar{x}_{(M/P)}$	$S_{(M/P)}$
101			
102			

TS

Table 17-2 M/P Statistics for (C)

Test Section	<i>n</i>	$\bar{x}_{(M/P)}$	$S_{(M/P)}$
101			
102			

TS

Table 17-3 Comparison of coefficients for Process Verification

Coeff.	KCE-1 (original)	Refit (100% Data)
B1		
B2		
B3		
B4		
B5		
B6		
B7		
B8		

TS

Table 17-4 M/P Statistics for 5-folds

Case	Group	<i>n</i>	$\bar{x}_{(M/P)}$	$S_{(M/P)}$	MAPE (%)	System Pressure (psia)	Local Quality	Local Mass Flux (Mlbm/hr-ft <sup>2</sup> )	95/95 DNBR
5-1	Training								
	Validation								
	All								
5-2	Training								
	Validation								
	All								
5-3	Training								
	Validation								
	All								
5-4	Training								
	Validation								
	All								
5-5	Training								
	Validation								
	All								
Refit 100%/0%	All								

TS

Table 17-5 Poolability Check Results for 5-folds

Case	Test*		Statistics	P-Value	Test Result
5-1	Normality	Training			TS
		Validation			
		All			
	F-test				
	T-test				
	Wilcoxon-Mann-Whitney				
5-2	Normality	Training			
		Validation			
		All			
	F-test				
	T-test				
	Wilcoxon-Mann-Whitney				
5-3	Normality	Training			
		Validation			
		All			
	F-test				
	T-test				
	Wilcoxon-Mann-Whitney				
5-4	Normality	Training			
		Validation			
		All			
	F-test				
	T-test				
	Wilcoxon-Mann-Whitney				
5-5	Normality	Training			
		Validation			
		All			
	F-test				
	T-test				
	Wilcoxon-Mann-Whitney				

\* For normality test, the Kolmogorov-Smirnov method was applied.  
5% of risk level was applied to all test statistics.

Table 17-6 M/P statistics for 1000 cases (Five classifications)

Distribution of $\bar{x}_{(M/P)}$	Group	No. of Case	Average	S.D.	Remark

Table 17-7 95/95 DNBR statistics for 1000 cases (Five classifications)

Distribution of 95 / 95 DNBR	Group	No. of Case	Average	S.D.	Remark

Table 17-8 M/P statistics of [ ]<sup>TS</sup> out of 1000 95/95 DNBRs.

Group	n	Average	S.D.	95/95 DNBR
Training				
Validation				
All				
KCE-1 (topical report)				

Table 17-9 Result of poolability of [ ]<sup>TS</sup> out of 1000 95/95 DNBRs.

Case	Test	Statistics	P-Value	Test Result

Table 17-10 Results of D'Agostino normality test of [ ]<sup>TS</sup> out of 1000 95/95 DNBRs

Group	N	D'Agostino Test					Normality
		T	S	D'	Lowest	Highest	
Training							} TS
Validation							
All							

Table 17-11 Range of variables for [ ]<sup>TS</sup> out of 1000 95/95 DNBRs

Group	Pressure (psia)	Local Mass Flux (Mlbm/hr-ft <sup>2</sup> )	Local Quality
Training			
Validation			
KCE-1 (topical report)	1395 ~2415	0.85 ~3.15	-0.150 ~0.275

} TS

Table 17-12 Data of [ ]<sup>TS</sup> out of 1000 95/95 DNBRs – Training (1/7)

TS

Table 17-12 Data of [

]TS out of 1000 95/95 DNBRs – Training (2/7)

TS

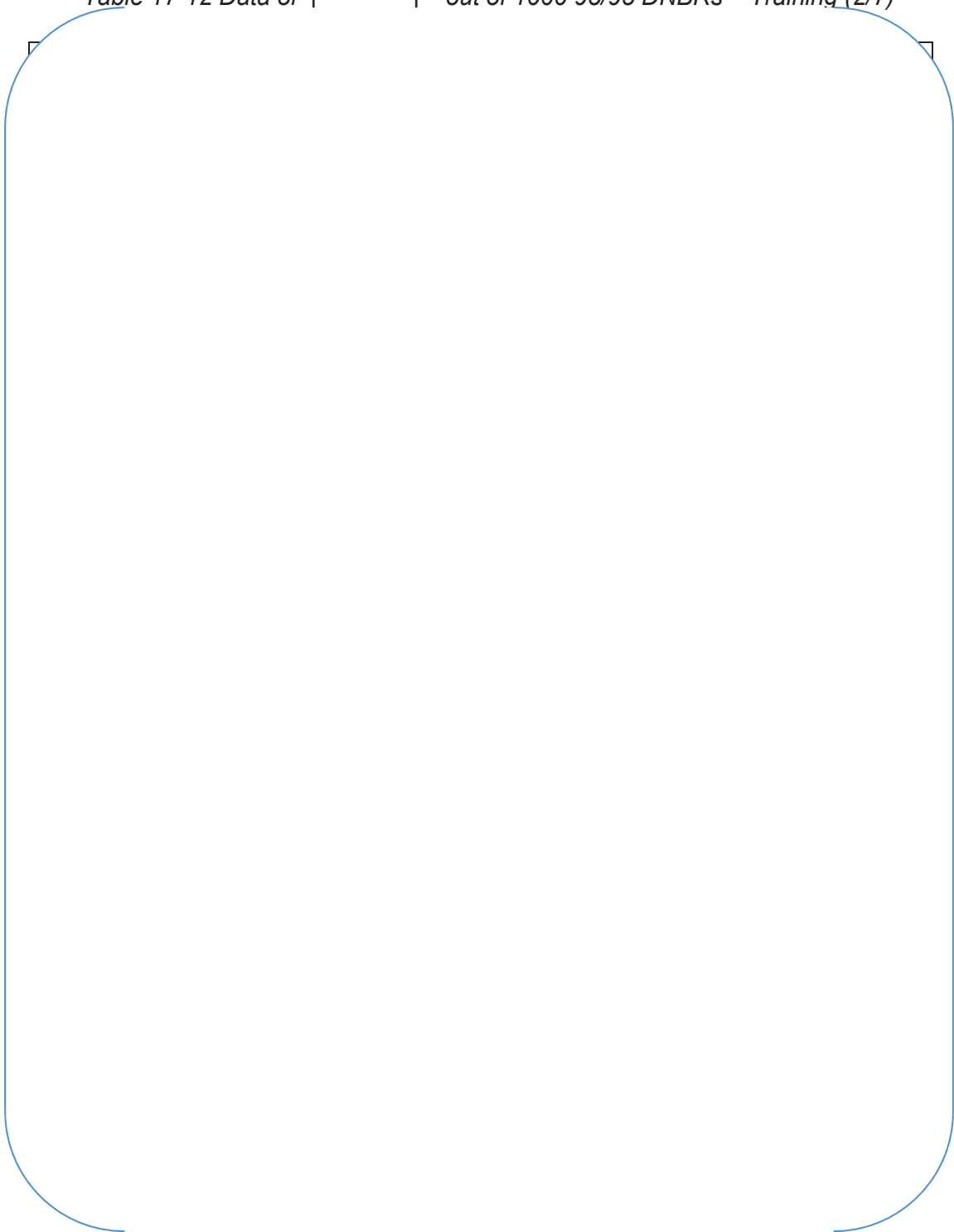


Table 17-12 Data of [ ]<sup>TS</sup> out of 1000 95/95 DNBRs – Training (3/7)

TS

Table 17-12 Data of [ ]<sup>TS</sup> out of 1000 95/95 DNBRs – Training (4/7)

TS

*Table 17-12 Data of [ 39<sup>th</sup> rank ]<sup>TS</sup> out of 1000 95/95 DNBRs – Training (5/7)*

TS

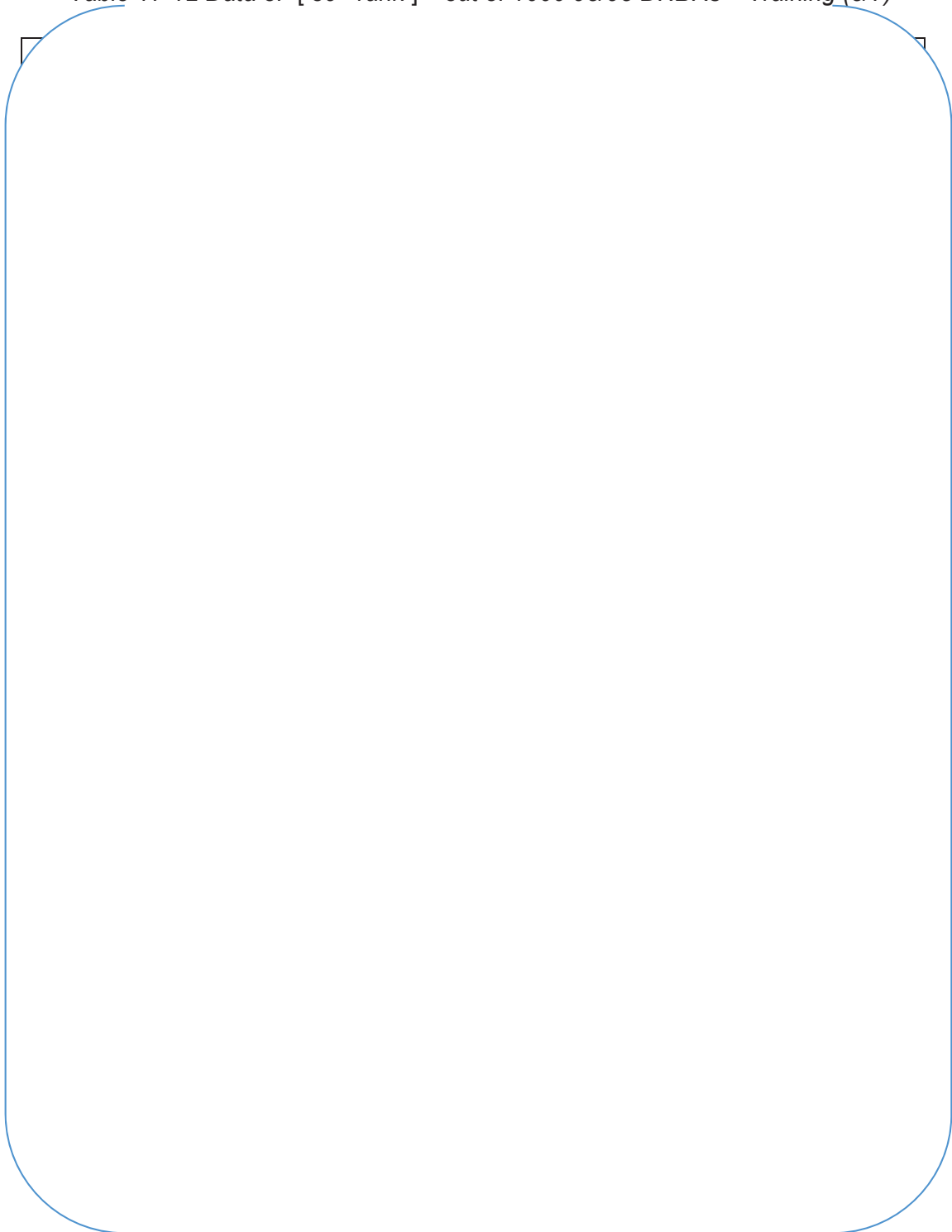


Table 17-12 Data of [ ]<sup>TS</sup> out of 1000 95/95 DNBRs – Training (6/7)

TS

Table 17-12 Data of [ ]<sup>TS</sup> out of 1000 95/95 DNBRs – Training (7/7)

TS

Table 17-13 Data of [ ]<sup>TS</sup> out of 1000 95/95 DNBRs – Validation (1/2)

TS

Table 17-13 Data of [ ]<sup>TS</sup> out of 1000 95/95 DNBRs – Validation (2/2)

TS

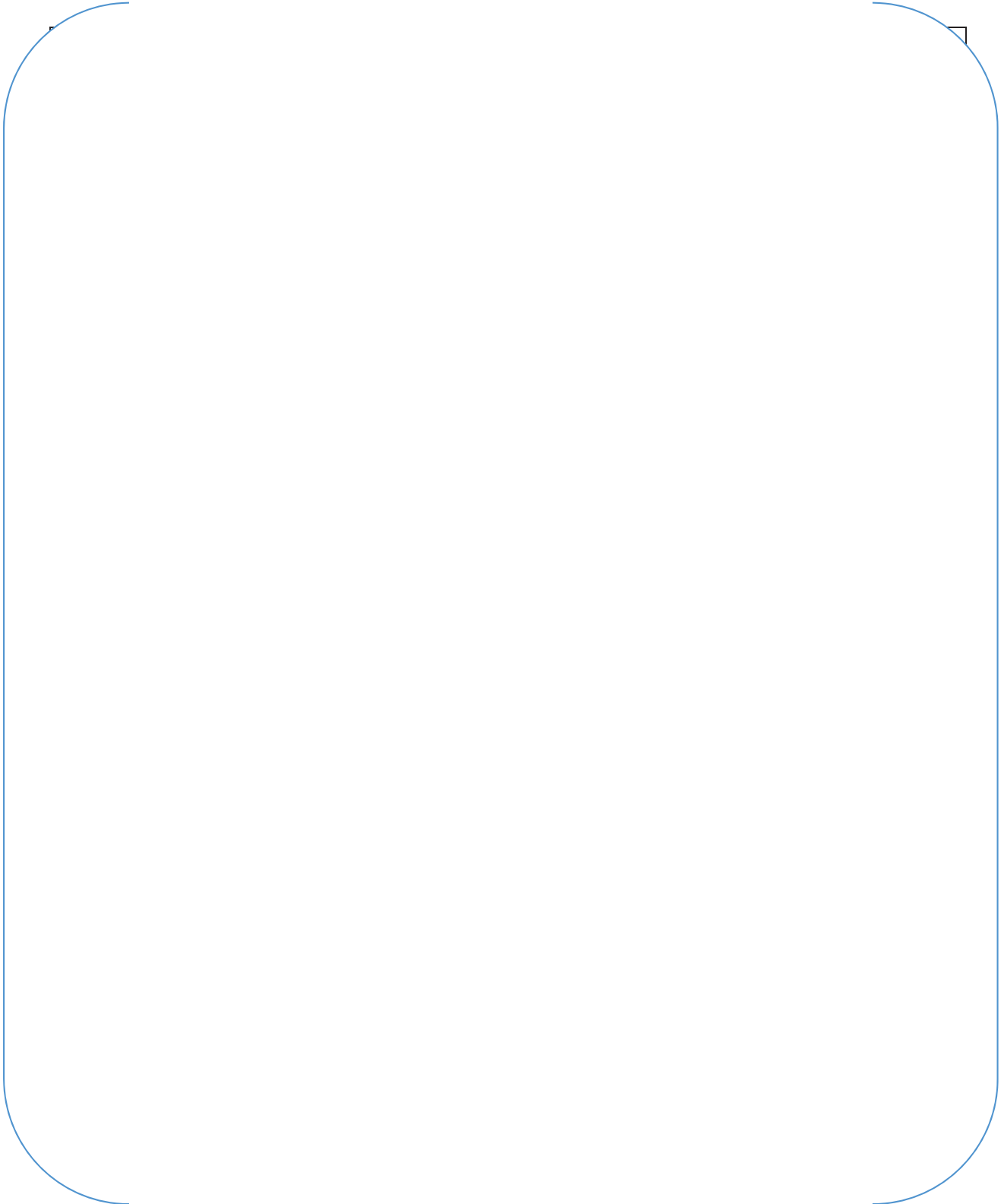




Figure 17-1. Comparison of CHF Prediction : KCE-1 and CE-1 Correlations (for Local Quality)

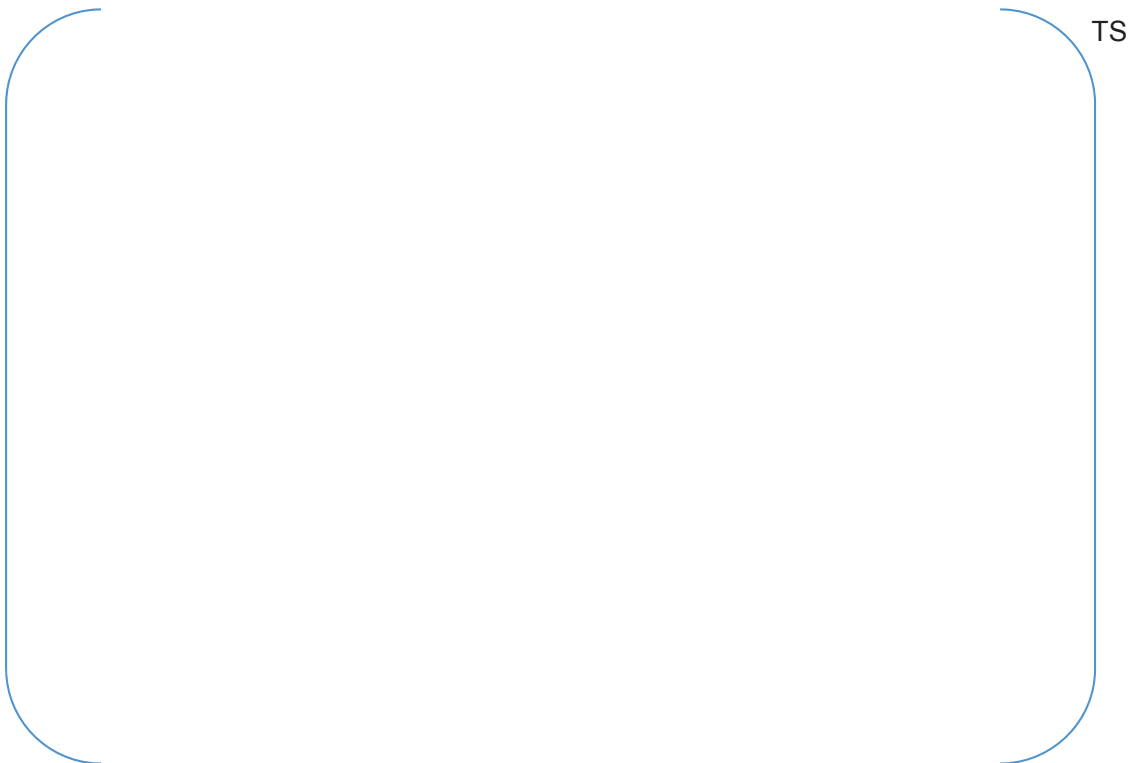


Figure 17-2. Comparison of CHF Prediction : KCE-1 and CE-1 Correlations (for Pressure)



Figure 17-3. Comparison of CHF Prediction : KCE-1 and CE-1 Correlations (for Mass Velocity)



Figure 17-4. Distribution of M/P for 1000 cases (Five classifications)



Figure 17-5. Distribution of 95/95 DNBRs for 1000 cases (Five classifications)



Figure 17-6. Distribution of M/P vs. System Pressure ([ ]<sup>TS</sup>)



Figure 17-7. Distribution of M/P vs. Local Mass Flux ( $[ ]^{TS}$ )



Figure 17-8. Distribution of M/P vs. Local Quality ( $[ ]^{TS}$ )



TS

Figure 17-9. Distribution of M/P vs. Equivalent Heated Diameter Ratio ([

]TS)



TS

Figure 17-10. Predicted CHF vs. Measured CHF ([

]TS)

---

**Impact on DCD**

N/A

**Impact on PRA**

N/A

**Impact on Technical Specifications**

N/A

**Impact on Technical/Topical/Environmental Report**

N/A